DEVELOPMENT AND EVALUATION OF CETUXIMAB ANCHORED RESVERATROL LOADED MULTIWALLED CARBON NANOTUBES FOR THE TREATMENT OF COLORECTAL CANCER

Thesis Submitted for the Award of the Degree of

DOCTOR OF PHILOSOPHY

in

Pharmaceutics

By

NEHA SHARMA

Registration Number: 41800791

Supervised By

Prof. (Dr.) Vijay Mishra (20352)

Professor

School of Pharmaceutical sciences, Lovely

Professional University

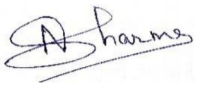


LOVELY PROFESSIONAL UNIVERSITY, PUNJAB

2025-2026

DECLARATION

I, hereby declared that the presented work in the thesis entitled " **DEVELOPMENT AND EVALUATION OF CETUXIMAB ANCHORED RESVERATROL LOADED MULTIWALLED CARBON NANOTUBES FOR THE TREATMENT OF COLORECTAL CANCER** " in fulfilment of degree of **Doctor of Philosophy (Ph. D.)** is outcome of research work carried out by me under the supervision of **Prof. (Dr.) Vijay Mishra**, working as **Professor**, in School of Pharmaceutical sciences, of Lovely Professional University, Punjab, India. In keeping with general practice of reporting scientific observations, due acknowledgements have been made whenever work described here has been based on findings of other investigator. This work has not been submitted in part or full to any other University or Institute for the award of any degree.



(Signature of Scholar)

Name of the scholar: Neha Sharma

Registration No.: 41800791

Department/school: School of Pharmaceutical Sciences

Lovely Professional University,

Punjab, India

CERTIFICATE

This is to certify that the work reported in the Ph. D. thesis entitled "**DEVELOPMENT AND EVALUATION OF CETUXIMAB ANCHORED RESVERATROL LOADED MULTIWALLED CARBON NANOTUBES FOR THE TREATMENT OF COLORECTAL CANCER"** submitted in fulfillment of the requirement for the award of degree of **Doctor of Philosophy (Ph.D.)** in the Pharmaceutics Department of School of Pharmaceutical Sciences, is a research work carried out by Neha Sharma, Registration No. 41800791, is Bonafide record of his/her original work carried out under my supervision and that no part of thesis has been submitted for any other degree, diploma or equivalent course.



(Signature of Supervisor)

Prof. (Dr.) Vijay Mishra

Designation: Professor

Department/school: School of Pharmaceutical Sciences

Lovely Professional University,

Punjab, India

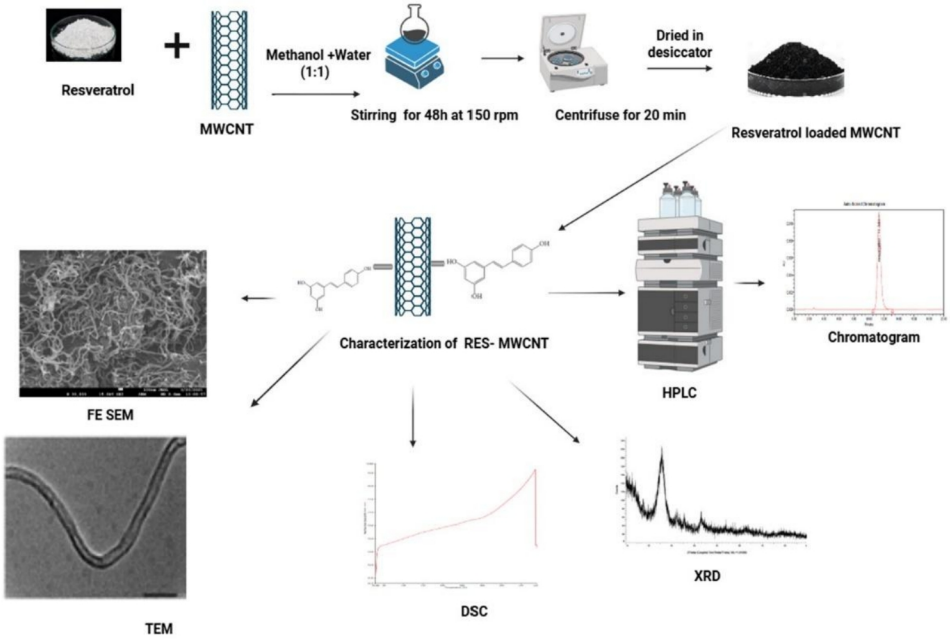
(Signature of Co-Supervisor)

Name of Co-Supervisor:

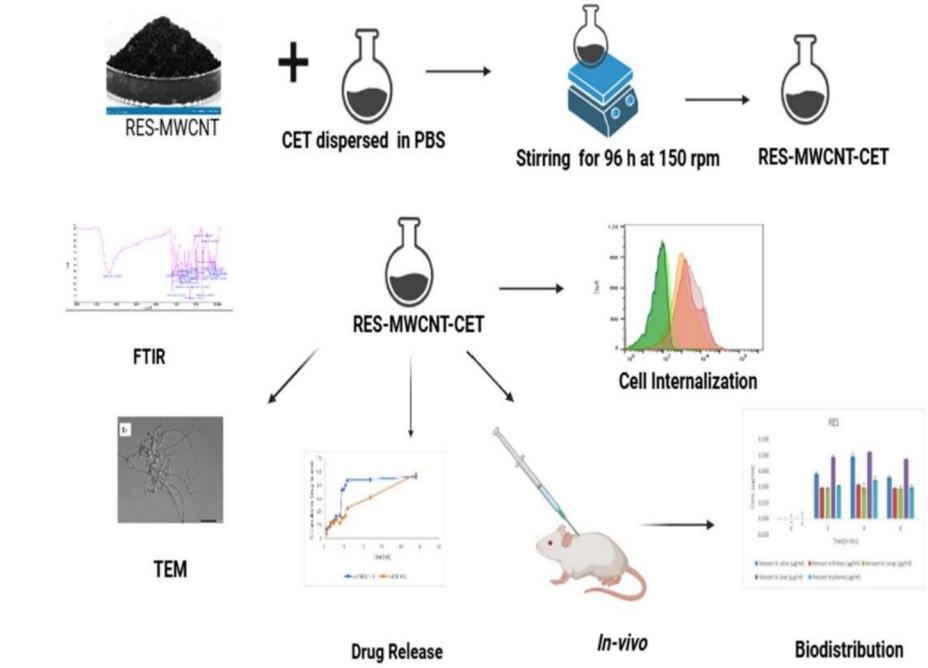
Designation: NA

Department/school: NA

Formulation of RES-MWCNT



Formulation of RES-MWCNT- CET



Abstract

Objective:

Globally, colorectal cancer (CRC) continues to be a major cause of cancer-related morbidity and death. Poor specificity, unfavourable side effects, and the development of medication resistance are the main limitations of current CRC diagnostic and treatment approaches. To improve treatment efficacy and reduce systemic toxicity, a tailored, biocompatible, and effective drug delivery platform is desperately needed. The current study set out to create a cetuximab-conjugated carbon nanotube-based nanocarrier system for the targeted administration of resveratrol (t-Res), a polyphenolic molecule with demonstrated anticancer potential in order to enhance treatment outcomes for colorectal cancer (CRC).

Scope:

In this work, multi-walled carbon nanotubes (MWCNTs) functionalised with resveratrol and conjugated with cetuximab (RES-MWCNT-CET) are synthesised, characterised, and evaluated as a possible drug delivery strategy for colorectal cancer. The compatibility, structural characteristics, and drug loading efficiency of resveratrol and carbon nanotubes were evaluated by extensive Preformulation investigations. The formulation was subjected to stringent physicochemical, analytical, and biological assessments using spectroscopy, chromatography, microscopy, and in vitro/in vivo experiments to investigate safety, stability, drug release kinetics, cytotoxicity, biodistribution, and histopathological compatibility.

Status and Purpose:

The proposed RES-MWCNT-CET system has undergone complete formulation, characterisation, and initial biological testing as part of its development status. The purpose of the study was to confirm the hypothesis that conjugating resveratrol-loaded CNTs with cetuximab, a monoclonal antibody that targets epidermal growth factor receptors (EGFR), would improve therapeutic efficacy, decrease off-target toxicity, and greatly increase the anticancer agent's selective delivery to colorectal tumours. The incorporation of cetuximab

was intended to target CRC cells that overexpress EGFR preferentially by taking advantage of receptor-mediated endocytosis pathways.

Hypothesis:

The following hypothesis was put forth:

1. Functionalised MWCNTs might efficiently encapsulate resveratrol and enable its prolonged release.
2. Combination with cetuximab might improve the specificity of targeting for colorectal cancer cells that overexpress EGFR.
3. The nanocarrier method would decrease systemic toxicity and adverse effects by increasing medication absorption in the colon and minimising distribution to non-target organs.
4. Resveratrol, cetuximab, and CNTs would all work together to increase cytotoxicity against colorectal cancer cells while still being hemocompatible and histologically safe for key organs.

Results:

In contrast to the smooth walls of pristine MWCNTs, functionalisation (COOH and NH_2) caused surface roughness and opened the nanotube caps, which is a sign that functional groups were successfully introduced and defect sites were successfully generated. Three different particle sizes were measured: Carboxylated (279.9 nm), amino-functionalized (241.4 nm), and virgin (182.4 nm). Functionalised CNTs and resveratrol were found to be compatible by FTIR, DSC, and XRD. Drug entrapment efficiencies for the four resveratrol-loaded MWCNT formulations (RES-MWCNT 1–4) that were created ranged from 73.83% to 96.29%. The best characteristics of RES-MWCNT 2 were the maximum drug loading (96.29%), smallest hydrodynamic diameter (289.6 nm), lowest PDI (0.070), and highest zeta potential (-18.8 mV), all of which indicated good dispersion stability.

Cetuximab Conjugation and Final Formulation (RES-MWCNT-CET)

RES-loaded MWCNTs had their inner cavities physically mixed with cetuximab. With a Z-average particle diameter of 730 nm and a zeta potential change of -11.9 mV, the resultant RES-MWCNT-CET indicated a stable structure despite aggregation tendencies. Following

conjugation, morphological examination verified that MWCNTs' tubular shape and nanostructure remained unaltered.

Drug Release Studies

The in vitro release of RES from RES-MWCNT-CET demonstrated effective pH-sensitive drug release appropriate for tumour microenvironments, reaching 96.58% at pH 5 and 92.73% at pH 7.4 during a 48-hour period. Limited leakage and drug encapsulation were also verified.

Cytotoxicity and Cellular Uptake Studies

MWCNTs demonstrated greater cytotoxicity than RES-MWCNT-CET; however, encapsulation in the RES-MWCNT-CET complex increased the cytotoxic effect of resveratrol by more than 3.2 times. Compared to pure RES (MIF = 59.4) or RES-MWCNT (MIF = 2420), the CET-conjugated formulation had significantly higher maximum inhibitory factor (MIF) values (MIF = 5404), suggesting a synergistic effect of drug transport and targeting. At lower concentrations, cell viability stayed higher, suggesting dose-dependent effectiveness.

Pharmacokinetics and Tissue Distribution

High linearity was established by the RES calibration curve ($R2 = 0.9989$) in plasma, and RES recovery surpassed 95% with RSD < 2%. When compared to RES-MWCNT and plain RES, biodistribution tests showed that RES-MWCNT-CET transported considerably more medication to the colon ($p<0.0001$ at 1, 4, and 8 hours). Off-target buildup in the liver, lungs, kidneys, and plasma was also reduced by RES-MWCNT-CET.

Biocompatibility and Toxicity Assessment

Haemolysis experiments showed that adding nanotubes decreased haemolytic activity. With RES alone showing 30.75% haemolysis, RES-MWCNT showing 14.92%, and RES-MWCNT-CET showing only 4.03%, there appears to have been a 7.5-fold decrease in haemolysis, indicating improved hemocompatibility. Histopathological examinations of the kidney, liver, colon, and lung after RES-MWCNT-CET treatment showed no appreciable structural damage, confirming the systemic safety of the treatment.

Conclusion:

The development and assessment of cetuximab-conjugated resveratrol-loaded carbon nanotubes (RES-MWCNT-CET) showed great promise as a targeted nanocarrier system for the treatment of colorectal cancer. The nanocarrier solved several drawbacks of traditional CRC treatment by means of structural alterations, effective drug loading, targeted transport, and pH-responsive release mechanisms. Its therapeutic potential is confirmed by improved drug retention in the colon, less systemic toxicity, and increased cytotoxicity against cancer cells. These results confirm the initial theory and provide compelling evidence for the RES-MWCNT-CET system's ongoing advancement as a targeted, safe, and efficient treatment for colorectal cancer. Clinical translation initiatives, long-term toxicity investigations, and a thorough in vivo pharmacodynamic evaluation will all be part of future research.

Acknowledgement

With deep humility and devotion, I begin by offering my heartfelt thanks to Radha Rani and Lord Shiva, whose divine presence has been my constant source of strength, clarity, and grace throughout this transformative journey. Their blessings have illuminated my path and sustained my spirit in moments of challenge and triumph.

I extend my sincere gratitude to ***Prof. (Dr.) Monica Gulati****, Dean, School of Pharmaceutical Sciences, Lovely Professional University, for her visionary leadership and unwavering support, which laid the foundation for my academic growth.*

I am deeply indebted to ***Prof. (Dr.) Vijay Mishra****, whose mentorship has been a cornerstone of my doctoral journey. His unwavering commitment to academic excellence, coupled with his calm demeanour and insightful feedback, helped me navigate the most complex phases of my research with confidence. He not only guided me with scholarly precision but also empowered me to think independently, challenge assumptions, and grow as a researcher. His belief in my potential gave me the courage to persevere, and his integrity continues to inspire my own professional values.*

A special and heartfelt thank you to ***Dr. Yachana Mishra****, an exceptional teacher and a truly beautiful human being. Her wisdom, empathy, and unwavering support have been like that of a guardian—always present, always uplifting. She has guided me not only academically but also emotionally, helping me navigate the complexities of this journey with grace and resilience.*

I am grateful to ***Prof. (Dr.). Bimlesh Kumar****, for his consistent encouragement, and to* ***Dr. Neelam Sharma****, (Pharmacy Bela college) whose timely help and generous support were crucial during the most demanding phases of my work.*

To my ***husband****, whose love, patience, and belief in me have been my anchor—I owe this achievement to his quiet strength and unwavering support. He has stood beside me through sleepless nights, endless revisions, and emotional highs and lows, never once letting me feel alone. His sacrifices and encouragement have been the silent force behind every*

milestone I have reached. His ability to balance his own responsibilities while lifting me through mine is nothing short of extraordinary. He is my partner in every sense—my strength, my calm, and my greatest cheerleader.

*To my **mother-in-law**, whose kindness, wisdom, and nurturing presence have been a blessing—I am deeply grateful for her unwavering support and understanding. She has been my pillar at home, ensuring that I could focus on my research without worry. Her quiet sacrifices and loving encouragement have made this journey smoother and more meaningful. Her belief in me has been a source of strength, and her presence has brought peace to the most chaotic days.*

*To **my children**, Aadish and Aadya, whose innocent smiles have been my greatest stress relievers—thank you for bringing joy and light into my life even during the most challenging times. Their laughter, hugs, and boundless energy reminded me daily of life's true purpose and beauty. They have unknowingly taught me resilience, patience, and the art of finding happiness in small moments. This thesis is as much theirs as it is mine.*

*To my brother **Rohit**, my unwavering backbone, and **to my father and mother**, the pillars of my life—your love, sacrifices, and belief in me have shaped the person I am today. I am forever indebted to you.*

*I gratefully acknowledge **Manoj Sir** for his technical assistance in the laboratory, which greatly supported the practical aspects of my research.*

*Finally, I thank my friends and co-workers, especially **Navdeep Kaur**, for their moral support, companionship, and encouragement throughout this journey.*

This thesis is not just a scholarly document—it is a testament to the collective love, strength, and wisdom of all those who have walked this path with me. Thank you for being part of my story.

Table of Contents

1. Introduction **1**

1.1 Colorectal cancer 1

1.1.1 Etiology 1

1.1.2 Risk Factors 2

1.1.3 Epidemiology 3

1.1.4 Pathophysiology 4

1.1.5 Stage of the colon cancer 5

1.1.6 Colorectal Cancer Development 7

1.1.8 Preventive Strategies 8

1.1.9 Treatment Strategies 9

1.2 Applications of Nanotechnology 13

1.3 Carbon nanotube 14

1.3.1 Classification of CNTs 15

1.3.2 Functionalization 16

1.3.4 Polymer functionalized CNTs 18

1.3.6 The role of carbon nanotubes in cancer diagnosis 19

1.3.7 **Advantage of Carbon Nanotubes Over Other Nanocarriers** 21

1.4 Resveratrol 22

1.4.1 Sources 23

1.4.2 Chemistry of Resveratrol 23

1.4.3 Properties 24

Chemical formula: 24

Appearance: 24

Melting point: 24

Solubility in water: 24

UV-vis (λ_{max}) : 24

Molecular weight: 24

1.4.4 Pharmacokinetic of resveratrol 24

1.4.5 Mechanisms of Resveratrol in Cancer Prevention 25
1.5 Cetuximab 27
1.5.1 Chemical and physical data 27
1.5.2 Mechanism of Action 28
1.5.3 Administration 28
1.5.4 Adverse Effects 29
1.5.5 Indications 29
1.6 Research Gap **30**
2. Review of literature **32**
2.1 Review of literature related to colorectal cancer 32
2.2 Review of literature related to Current treatment for colorectal cancer 34
2.3 Review of literature related to Nanotechnology for colon cancer treatment 37
2.3 Review of literature related to Carbon nanotube for cancer treatment 39
2.4 Review of literature related to Cetuximab in treatment of colorectal cancer 47
2.5 Cetuximab mechanism of action in colorectal cancer 48
3. Hypothesis **51**
3.1 Aim 55
3.2 Objective 55
4.Experimental work **60**
4.1 Preformulation study of resveratrol 60
4.1.1 Melting point 60
4.1.2 UV calibration plot 60
4.1.2.1 Determination of absorption maxima 60
4.1.2.2 Preparation of standard plot in water 60
4.1.2.3 Preparation of standard plot in Phosphate Buffer Saline (PBS) 7.4 61
4.1.3 Partition coefficient 61
4.1.4 Differential Scanning Calorimetry (DSC) 62
4.1.5 Fourier Transform Infrared Spectroscopy (FTIR) spectra 62

4.1.6 Field Emission Scanning Electron Microscope (FE- SEM) 62
4.1.7 X-Ray Diffraction (XRD) 62
4.1.8 Development of HPLC Methods 63
4.1.8.1 Chromatographic Conditions and Instrumentation 63
4.1.8.2 Safety measures 63
4.1.8.3 Identification of retention time 63
4.1.8.3.1 Preparation stock solution 63
4.1.8.3.2 Preparation working solution 64
4.1.8.4 Method Validation 64
4.1.8.4.1 System Suitability 64
4.1.8.4.2 Limit of Detection and Limit of Quantification 65
4.1.8.4.3 Range and Linearity 65
4.1.8.4.4 Accuracy 66
4.1.8.4.5 Precision 66
4.1.8.4.6 Robustness 67
4.1.8.4.7 Force Degradation Studies 67
4.2 Preformulation study of carbon nanotube 68
4.2.1 Physical appearance 68
4.2.2 Fourier Transform Infrared Spectroscopy (FTIR) spectra 68
4.2.3 Field Emission Scanning Electron Microscope (FE- SEM) 68
4.2.4 X-Ray Diffraction (XRD) 68
4.2.5 Zeta Size and Potential 69
4.3 Formulation of Resveratrol loaded Carbon Nanotubes 69
4.4 Characterization of Resveratrol loaded Carbon Nanotubes 70
4.4.1 Uv spectroscopy 70
4.4.2 Fourier Transform Infrared Spectroscopy (FTIR) spectra 70
4.4.3 X- Ray Diffraction (XRD) 70
4.4.4 Percentages entrapment of resveratrol to the carbon nanotube 70
4.4.5 Particle size and Zeta Potential 71

4.4.6 ^{1}H and ^{13}CNMR NMR studies 71
4.4.7 Raman spectroscopy 71
4.4.8 Differential Scanning Calorimetry (DSC) 71
4.4.*9 In vitro* Release 72
4.5. Development of RES-CNT-CET formulation 72
4.6. Characterization of RES-CNT-CET formulation 72
4.6.1 Raman spectroscopy 72
4.6.2 Particle size and Zeta Potential 72
4.6.3 ^{1}H and ^{13}CNMR NMR studies 73
4.6.4 FTIR 73
4.6.5 TEM 73
4.6.6 Percentages entrapment of resveratrol to the carbon nanotube 73
4.6.7 Drug Release 74
4.6.8 Release Kinetics 74
4.6.9 Stability study 74
4.6.10 MTT Assay 75
4.6.11 Cell Internalization 75
4.6.12 *In-vivo* studies 76
4.6.13.1 Development of Bio analytical method 77
4.6.13.2 Safety Measures 77
4.6.13.3 Procurement of blood and separation of plasma 77
4.6.13.4 Blank Plasma Sample Preparation 77
4.6.13.5 Standard Stock Solution Preparation 77
4.6.13.6 Internal Standard (IS) Preparation 78
4.6.13.7 Method specificity 78
4.6.13.8 Standard calibration curve development 79
4.6.13.9 Accuracy 79
4.6.13.10 Precision 80
4.6.13.11 Limit of Detection and Quantification 81

4.6.13.12 System Suitability 81
4.6.13.13 Stability studies 82
4.6.14 Biodistribution studies 83
4.6.15 Haematological studies 84
4.6.15.1 Hemolytic toxicity studies 84
4.6.15.2 Haematological and Histopathological study 84
5. Results and discussion 86
5.1 Preformulation study of t-RES 86
5.1.1 Melting point 86
5.1.2 Establishment of UV standard linearity curve 86
5.1.2.1 Determination of the absorption maxima 86
5.1.2.2 Standard calibration curve in water solvent 86
5.1.3 Partition coefficient 88
5.1.4 Differential Scanning Calorimetry (DSC) 89
5.1.5 Fourier Transform Infrared Spectroscopy (FTIR) spectra 90
5.1.6 Field Emission Scanning Electron Microscope (FE- SEM) 91
5.1.7 X-Ray Diffraction (XRD) 91
5.1.8 Development of HPLC Methods 92
5.1.8.1 Identification of retention time 92
5.1.8.2 Method Validation 93
5.1.8.2.3 System Suitability 93
5.1.8.2.4 Range and Linearity 94
5.1.8.2.5 Accuracy 95
5.1.8.2.6 Precision 95
5.1.8.2.7 Robustness 97
5.1.8.2.8 Force degradation Studies 97
5.2 Preformulation study of carbon nanotube 100
5.2.1 Fourier Transform Infrared Spectroscopy (FTIR) spectra 100
5.2.2 Field Emission Scanning Electron Microscope (FE- SEM) 102

5.2.3 X-Ray Diffraction (XRD) 104
5.2.4 Zeta Size and Potential 105
5.3 Formulation of t-RES loaded Carbon Nanotubes 109
5.4 Characterization of t-RES loaded Carbon Nanotubes 110
5.4.1 Uv spectroscopy 110
5.4.2 Fourier Transform Infrared Spectroscopy (FTIR) spectra 110
5.4.3 X- Ray Diffraction (XRD) 113
5.4.4 Percentage drug entrapment of t-RES to the carbon nanotube 115
5.4.5 Particle size and Zeta Potential 116
5.4.6 ^{1}H and ^{13}CNMR NMR studies 117
5.4.7 Raman spectroscopy 121
5.4.8 Differential scanning calorimetry (DSC) 123
5.4.*9 In vitro* Release 124
5.5 Development of RES-CNT-CET formulation 126
5.6 Characterization of RES-CNT-CET formulation 126
5.6.1 Raman Spectra 126
5.6.2 Zeta potential and Particle size 127
5.6.3 ^{1}HNMR and ^{13}CNMR studies 129
5.6.4 FTIR 131
5.6.5 TEM 132
5.6.6 Percentage drug entrapment 133
5.6.7 Drug Release 133
5.6.8 Drug release kinetics 135
5.6.9 Stability study 139
5.6.9.1 Physiochemical characterization 139
5.6.9.2 Drug leakage 140
5.6.10 MTT Assay 140
5.6.11 Cell Internalization 142
5.6.12 In-vivo studies 144

5.6.13 Development of Bio analytical method using HPLC 144
5.6.13.1 Specificity studies 144
5.6.13.2 Calibration curve Development 145
5.6.13.3 Accuracy studies 146
5.6.13.4 Precisions 147
5.6.13.5 LOQ and LOD 155
5.6.13.6 System suitability 155
5.6.13.7 Stabilities studies of plasma samples 156
5.6.14 Biodistribution studies 166
5.6.15 Hemolytic toxicity studies 170
5.6.16 Haematological studies 174
5.6.17 Histopathology 176
Summary 183
Future Aspects **186**
Bibliography 187

List of Tables

Sr. No	Tables Name	Page No
1.1	Stage systems	6
4.1	List of materials utilized.	57
4.2	List of instruments and equipment utilized.	58-59
4.3	Different parameter for drug optimization	69
4.4	Details of different animal groups	76
5.1	Melting Point of t-RES	86
5.2	Standard calibration curve of t-RES in water	87
5.3	Standard calibration curve of t-RES in Phosphate Buffer Saline (PBS) 7.4	88
5.4	Partition coefficient Absorbance of t-RES	89
5.5	Partition coefficient of drug	89
5.6	FTIR Peaks of t-RES	90
5.7	Retention time, area and theoretical plates	93
5.8	System suitability parameters	94
5.9	Standard calibration curve	95
5.10	Results of accuracy study	96
5.11	Results of precision	96-97
5.12	Results of robustness study	98
5.13	Results of stressed studies performed	99
5.14	FTIR spectra of amine-functionalized multi-walled carbon nanotubes	102
5.15	Percentage drug loading of the t-RES in carbon nanotube	117
5.16	Drug release profile of t- RES from RES-MWCNT-CET	127-128
5.17	Cumulative drug release of t-RES from RES-MWCNT-CET	135-136
5.18	Drug release kinetics of RES showing R^2 value in RES-CNT-CET	137
5.19	Physiochemical characterization of RES-MWCNT and RES-MWCNT-CET at different storage condition	140
5.20	% Drug leakage of RES-MWCNT and RES-MWCNT-CET at different storage condition	141
5.21	Evaluating the cytotoxicity of various formulations in HT-29 cancer cells using the MTT assay	142

5.22	**Cell uptake studies by using FACS**	144
5.23	**Standard calibration curve of t-RES in plasma**	147
5.24	**Accuracy Result of t-RES in plasma**	148
5.25	**Precision Result of t-RES in plasma**	149-156
5.26	**System Suitability Parameter**	157
5.27	**Stability Studies**	157-166
5.28	**Biodistribution studies of t-RES from pure drug, RES- MWCNT and RES- MWCNT-CET at 1hr**	168
5.29	**Biodistribution studies of t-RES from pure drug, RES-MWCNT2 and RES- MWCNT-CET at 4hr**	169
5.30	**Biodistribution studies of t-RES from pure drug, RES-MWCNT2 and RES- MWCNT-CET at 8hr**	170
5.31	**Haematological parameters**	175

List of Figure

Sr. No	Figure Name	Page No
1.1	Estimated age-standardized incidence rate for colorectal cancer	4
1.2	Demonstration of application of various nano size range formulation in CRC	14
1.3	Image of various carbon nanostructure	15
1.4	Various applications of CNT in cancer therapy	21
1.5	Sources of resveratrol	23
1.6	Resveratrol chemical structure	24
1.7	Main effects of resveratrol in tumour cells	26
2.1	Imaged of single-walled carbon nanotubes (SWCNT).	40
2.2	Image of multi-walled carbon nanotubes (MWCNT)	40
2.3	Different mechanism of action of resveratrol in the treatment of colorectal cancer	45
4.1	Process of the preparation of samples for biodistribution study	84
4.2	Process of the Haematological studies	85
5.1	UV spectra of t-RES	86
5.2	Standard calibration curve of t-RES in water	87
5.3	Standard calibration curve of drug in Phosphate Buffer Saline (PBS) 7.4	88
5.4	DSC thermogram of t-Res.	89
5.5	FTIR spectra of t-Res	90
5.6	FE-SEM of t-Res	91
5.7	XRD of t-Res	91

5.8	**HPLC chromatogram of the A) Blank B) Sample working solution 2µg/mL**	93
5.9	**Calibration curve of t-RES**	95
5.10	**Chromatogram of (A) Untreated sample, (B) Acid treatment, (C) Alkali treatment, (D) Light exposure, (E) H_2O_2 Treatment, and (F) Thermal treatment**	100
5.11	**FTIR spectra of Pristine Multi-Wall Carbon Nanotubes**	101
5.12	**FTIR spectra of amine-functionalized Multi-Walled Carbon Nanotubes**	101
5.13	**FTIR spectrum of COOH-MWCNT**	102
5.14	**FE-SEM of Pristine Multi-Walled Carbon Nanotubes.**	103
5.15	**FE-SEM of NH_2-MWCNT**	104
5.16	**FE-SEM of COOH-MWCNT**	104
5.17	**XRD of Pristine Multi-Walled Carbon Nanotubes**	105
5.18	**XRD of Amine-Functionalized Multi-Walled Carbon Nanotubes.**	106
5.19	**XRD pattern of COOH-MWCNT.**	106
5.20	**Zeta Size of Pristine Multi-walled carbon nanotubes**	107
5.21	**Zeta Potential of Pristine Multi-walled carbon nanotubes**	108
5.22	**Zeta Size of Amine Multi-walled carbon nanotubes**	108

5.23	**Zeta potential of Amine Multi-Walled Carbon Nanotubes.**	109
5.24	**Zeta Size of Carboxylic Acid Multi-Walled Carbon Nanotubes**	109
5.25	**Zeta potential of Carboxylic Acid Multi-Walled Carbon Nanotubes**	110
5.26	**UV Spectroscopy of a) t-RES b) RES-MWCNT-4 c) RES-MWCNT-3 d) RES-MWCNT-2 e) RES-MWCNT-1 f) NH2-MWCNT 4 g) COOH-MWCNT**	112
5.27	**FTIR spectrum of Formulation RES-MWCNT 1.**	112
5.28	**FTIR spectrum of Formulation RES-MWCNT 2.**	113
5.29	**FTIR spectrum of Formulation RES-MWCNT 3.**	113
5.30	**FTIR Spectrum of Formulation RES-MWCNT 4.**	114
5.31	**XRD pattern of RES-MWCNT 1.**	115
5.32	**XRD pattern of RES-MWCNT 2**	115
5.33	**XRD pattern of RES-MWCNT 3**	116
5.34	**XRD pattern of RES-MWCNT-4.**	116
5.35	**Percentage drug entrapment of t-RES in carbon nanotube**	117
5.36	**Particle size of RES-MWCNT 2**	118
5.37	**Zeta Potential of RES-MWCNT 2**	119
5.38	**^{1}H NMR spectra of t-RES**	119
5.39	**^{1}H NMR spectra of carboxylic CNT**	120

5.40	**^{1}H NMR spectra of RES-MWCNT 2**	120
5.41	**Chemical structure of t-RES**	121
5.42	**^{13}C NMR spectra of t-RES**	121
5.43	**^{13}C NMR spectra of MWCNT**	122
5.44	**^{13}C NMR spectra of RES-MWCNT 2.**	122
5.45	**Raman spectra of (A) t-RES (B) COOH-MWCNT (C) RES-MWCNT 2**	123-124
5.46	**DSC thermogram of [A] t-RES, [B] Carboxylated MWCNTs, and [C] RES-MWCNT 2**	125-126
5.47	**Percentage Cumulative drug release of RES from RES-MWCNT 2 at pH 5 and pH 7.4.**	128
5.48	**Raman spectra of RES-MWCNT-CET**	129
5.49	**Zeta Potential of RES-MWCNT-CET**	130
5.50	**Particle Size of RES-MWCNT-CET**	130
5.51	**^{1}H NMR spectra of RES-MWCNT-CET**	131
5.52	**^{13}C NMR spectra of RES-CNT-CET**	131
5.53	**^{13}C NMR spectra of RES-CNT-CET**	132
5.54	**FTIR spectrum of CET**	133
5.55	**FTIR spectrum of RES-MWCNT-CET**	133
5.56	**TEM image of (A) MWCNT, (B) RES-MWCNT (C) RES-MWCNT-CET.**	134
5.57	**Percentage Cumulative drug release of RES from RES-MWCNT-CET at pH 5 and pH 7.4**	136

5.58	**First Order Release kinetics**	137
5.59	**Zero Order Release kinetics**	138
5.60	**Korsmeyer Peppas release kinetics**	138
5.61	**Higuchi release kinetics**	139
5.62	**Hixson Crowell kinetics**	139
5.63	**Percent cell growth inhibition by Free RES, COOH-MWCNTs, RES-MWCNT2, CET and RES-MWCNT-CET formulations.**	142
5.64	**Combine cellular uptake studies graph by using FACS**	144
5.65	**Cellular uptake studies graph by using FACS (A) control (B) RES (C) MWCNT (D) RES-MWCNT2 (E) CET (F) RES-MWCNT-CET**	144
5.66	**Chromatogram of RES and Caffeine in Mobile Phase**	145
5.67	**Chromatogram of Blank Plasma**	146
5.68	**Chromatogram of t-RES and Caffeine in Plasma**	146
5.69	**Calibration curve of t-RES in Plasma**	147
5.70	**Amount of t-RES from pure drug, RES- MWCNT2 and RES- MWCNT-CET at 1hr**	168
5.71	**Amount of t-RES from pure drug, RES- MWCNT2 and RES- MWCNT-CET at 4hr**	169

5.72	**Amount of t-RES from pure drug, RES- MWCNT2 and RES- MWCNT-CET at 8hr**	170
5.73	**Hemolytic studies of different formulation**	171
5.74	**Homolysis of images of Water, Saline, t-RES, MWCNT, RES-MWCNT, RES-MWCNT-CET.**	172
5.75	**Histopathological images of vehicle control.**	177
5.76	**Histopathological images of t-RES treated group.**	178
5.77	**Histopathological images of MWCNT treated group.**	179
5.78	**Histopathological images of RES-MWCNT treated group**	180
5.79	**Histopathological images of RES-MWCNT-CET treated group**	181

1. Introduction

1.1 Colorectal cancer

Among cancer-related death rates, colorectal cancer comes third in the US (Siegel et al., 2023). In the US and around the world, the malignancy associated with the colon and rectal rated as second dominant source of cancer-associated deaths (Sung et al., 2020). The widespread use of colonoscopy screening has been primarily responsible for the decline in incidence rates in Western countries. However, the issue is increasingly affecting younger people (Stoffel et al., 2020).

Genetic alterations that are inherited account for about 5% of colon cancers. Most cases of colon cancer occur at random. The transformation of the healthy colon epithelium cells to malignant cells took several years and is identified by a series of genetic changes, adenoma development (Xiao et al., 2019; Gajendran et al., 2019; Sokic-Milutinovic to 2019; Fabregas et al., 2022).

It is recommended to screen for colon cancer, and there are several methods for doing so. Organisations' rules on the start and continuation of screenings vary (Smith et al., 2019). For most patients with invasive cancer, chest and abdominal computed tomography (CT) scans are required (Benson and others, 2021).

For initially localized colon cancer, surgery is the main therapy option. Following treatment, surveillance is crucial for detecting metastatic disease and local recurrences, both are manageable with multimodality therapy. (Drago, 2019; Ven Fong et al., 2019).

1.1.1 Etiology

Mutation of genes leads to develop a Colorectum malignancy similar to the other malignancy. The genes like Oncogenes, tumour suppressor genes are sensitive to the alteration (Fearon and Vogelstein, 1990). The three types of colorectal carcinomas include familial, hereditary, and sporadic, depending on where the mutation originated. Point mutations only influence the health of single cells and their progeny. They occur during life.

Approximate 70% of colorectal cancers are sporadic malignancy originated due to point mutations (Fearon and Vogelstein, 1990). However, most of the cases accompany the specific sequence of mutations result into a specific morphological sequence, initiating the

origin adenoma followed by the carcinoma state. At initial stage of the mutation a non-malignant tumour was developed, which was further transformed into the malignant tumour. TP53, KRAS, and DCC mutations follow this APC mutation (Fearon and Vogelstein, 1990).

Lynch syndrome is the most prevalent syndrome, accounting for 2% to 3% of all colorectal cancer cases (Lynch, 2003; Umar et al., 2004). Although inherited mutations are the cause of about 25% of cases of familial colorectal cancer, these malignancies are not considered hereditary cancers in and of themselves because they are not categorized in inherited cancer variants (Stoffel et al., 2014).

1.1.2 Risk Factors

Around 4-5% of humans worldwide get colorectum malignancy. A lot of individual characteristics or behaviours are regarded as risk factors. Age is major factor which indicate the origin of colorectum cancer. The people who have crossed the 50 years are more sensitive to develop a colorectum cancer and the peoples who are less than 50 years of age are less sensitive to the colorectum cancer (Levin et al., 2008). Age is just one of several innate risk factors that are unchangeable.

Furthermore, the other factor which play major role in the development of the colorectum cancer is personal history of colorectum malignancy or 'inflammatory bowel disease' (IBD), patients suffered from the ulcerative colitis and Crohn's disease have a 3.7% and 2.5% increased risk (Eaden et al., 2001; Canavan et al., 2006). Dysplasia indicated by the is an anomalous cell growth, associated with IBD, transformed into the anaplastic followed by mass of tumour. The history of the colorectum cancer in the family also increases the risk of the colorectum cancer during the diagnosis.

Environmental factors or genetic mutations may contribute to an elevated risk resulting from family history (Johns and Houlston 2001). Making little lifestyle adjustments in terms of eating and exercise patterns can help lower some other risk variables that are linked to lifestyle. For example, the sedative lifestyle having less exercise are more sensitive to the colorectum cancer while the lifestyle including the exercise, increasing the metabolic process and lower blood pressure result in less risk to the colorectum cancer (Robertson 2012).

1.1.3 Epidemiology

As per the sources observation of Surveillance and Epidemiology, and End Results (SEER) database, about 153,000 new patients suffered from colorectum cancer was diagnosed in 2023. It has been ranked the third number in the list of the common cancer in united state. Rectal tumours make up the remaining percentage of these cancers, with colonic cancers accounting for over 70%. Men are 53 percent more likely than women to get colorectal cancer, and they do so at an earlier age (68 vs. 72 years). The incidence of the disorder has been progressively reducing, but the rate of decline has slowed recently. A rising proportion of newly diagnosed cancer cases are in those under the age of 55. On the other side, the proportion of colon and rectal cancers has also increased.

The incidence and prognosis are significantly influenced by racial and socioeconomic disparities, with Asian Americans and Alaska Natives having the greatest rates. Globally, colorectal cancer rates vary significantly by socioeconomic status, race, and population, with the highest rates found in more developed countries.

As per the database shared by International Agency for Research on Cancer (IARC) the colorectum cancer has been identified as second number sources for the cancer related death globally about 935,172. Europe had the highest estimated ASMR of CRC (12.3), Africa had the lowest (5.6), and the eastern Mediterranean region (EMRO) had the lowest (5.3).

Lung and breast cancers were the most common malignancies worldwide in 2020, with colorectal cancer coming in third. Europe (30.4), Oceania (29.8), and North America (26.2) were found to have the highest ASRs (Figure 1).

According to research, countries with extremely larger human development indices (29.4) and high HDIs (20.4) and those with medium HDIs (6.1) and less HDIs (7.4) have comparable incidence rates of colorectal cancer (CRC) (Roshandel et al., 2024).

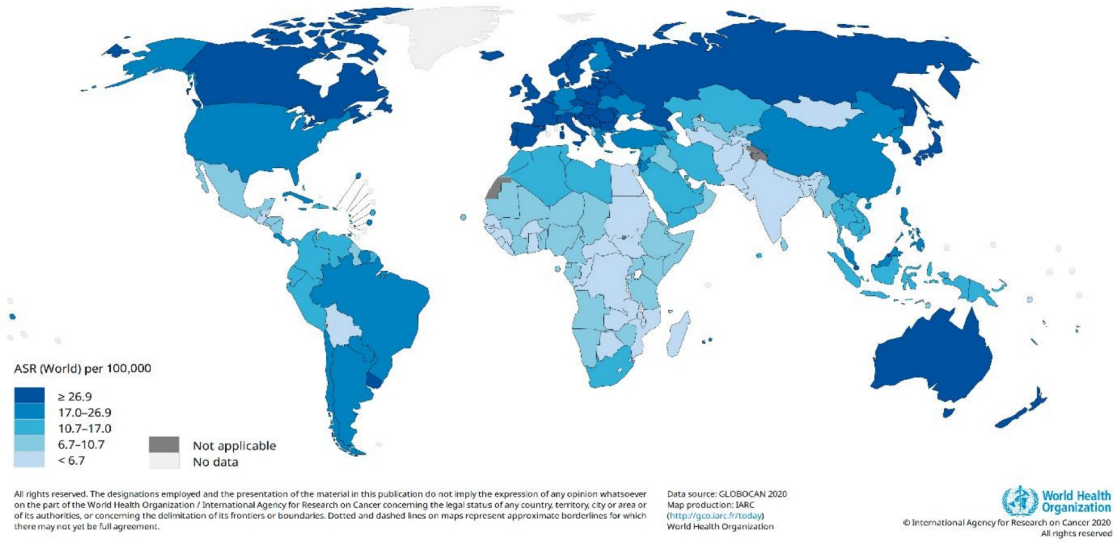


Figure 1.1: Estimated age-standardized incidence rate for colorectal cancer (Roshandel et al., 2024)

1.1.4 Pathophysiology

Effective treatment includes understanding of pathophysiology, just as prevention of the disease depends on knowledge of its aetiology.

It could be useful to briefly review normal cellular proliferation and bowel wall histology when talking about the pathophysiology of colorectal cancer. The intestine comprises of four layers namely the mucosa, submucosa, muscularis, and serosa. Between the mucosal and submucosal layers, the muscularis mucosa acts as a barrier (Sordelett, 1982). In the colon, the crypts of Lieberstein are the site of a continual and quick process of cellular reproduction.

Typically, the proliferative zone occupies the lower 2/3 area of the crypt, while cellular differentiation takes place in the upper third. This results in the continuous production of new undifferentiated cells in the lower 2/3 area of the crypt, which subsequently move along the crypt walls to the upper part followed by mature and further expel out of the crypt towards the mucosal surface and finally extruded or shed. In healthy people, the mucosa maintains a constant level of cells migration, production, and loss.

The malignancy impacts the replicating ability of the crypt's cells. Fewer surviving cells heal with normal DNA repair, whereas remaining can be called initiated cells since

they repair their DNA with errors. The typical migration-extrusion route will gradually eradicate the generated cells if they are merely dispersed and the carcinogenic stimulus is not repeated. These cells populate one or more crypts if there are numerous transformed cells or if multiple carcinogenic exposures occur. The differentiation of these cells can be incomplete, flawed, or non-existent. These cells have the potential to become cancerous and susceptible to different stimulating factors. Then, early neoplastic lesions are produced by the altered cells (Chang, 1984).

Neoplasms proliferate in different direction at various rate and transform into the polyp or a flat discoid lesion. The proliferation of neoplastic lesions turns on the intrinsic elements. These alterations take place in benign adenomatous lesions and do not, by themselves, signify cancer.

The characteristic that distinguishes benign neoplasms from malignant ones is their invasive behaviour, or downward growth. A malignant lesion begins in the mucosa and spreads lower, finally entering the submucosa through the muscularis mucosa.

It is evident that the lesion is malignant once it has penetrated the submucosa. The cytological characteristics of the cells themselves gradually alter in tandem with the development of malignant tumours. Both downhill progression and increased cytological deviation are linked to malignant lesions (Chang, 1984).

1.1.5 Stage of the colon cancer

The staging system defined by American Joint Committee on Cancer (AJCC) employed for colorectum cancer. However, alternative staging systems are still in use, such the Astler-Coller (Bomme et al., 2001) and Dukes (Bomme et al., 1988) systems. The TNM method (Weiser et al., 2011) is more accurate than these outdated approaches (Table 1).

In the AJCC system, the three letters stand for the following:

T indicates the extent of the initial tumour's growth into the intestinal wall and if it has migrated to neighbouring regions; N indicates the degree of dissemination to neighbouring (regional) lymph nodes. Lymph nodes comprise of bunches of immune system cells contribute a major part in the defence mechanism against infections. M word denoted the spreading nature of malignancy to other part of the body.

Table 1.1: Stage systems

	AJCC/TNM	Dukes	Astler-Coller
Stage 0	Tis, N0, M0	-	-
Stage I	T1-T2, N0, M0	A,	A, B1
Stage IIA	T3, N0, M0	B	B2
Stage IIB	T4a, N0, M0	B	B2
Stage IIC	T4b, N0, M0	B	B3
Stage IIIA	T1-T2, N1, M0 N2a, M0	C	C1
Stage IIIB	T3-T4a, N1, M0 T2-T3, N2a, M0 T1-T2, N2b, M0	C	C1, C2
Stage III	T4a, N2a, M0 T3-T4, N2b, M0 T4b, N1-N2, M0	C	C2, C3
Stage IV	Any T, Any N, M1a Any T, Any N, M1b	-	D

Tis: Denoted by earliest stage of malignancy and indicate the involvement of mucosa only. The stage indicates rolling out to only muscularis mucosa.

T1: This stage when malignant cells extend through the muscularis mucosa to submucosa.

T2: The stage denoted when the malignant cells enlarge through the submucosa and roll out into the muscularis propria.

T3: This stage denoted when the malignant cells enlarge through the muscularis propria and extend into the outermost layers of the colon or rectum.

T4a: The stage is denoted by enlarging the malignant cells and extend through the serosa.

T4b: The stage is denoted when malignant cells transferred to the colon or rectum's wall

Nx: Incomplete information prevents a description of lymph node involvement.

N0: There is no malignancy in the lymph nodes nearby.

N1: One to three neighbouring lymph nodes contain cancer cells.

N1a: One neighbouring lymph node contains cancer cells.

N1b: Two to three neighbouring lymph nodes contain cancer cells.

N1c: Areas of fat close to lymph nodes have tiny accumulations of cancer cells, while the lymph nodes themselves do not.

N2: Four or more neighbouring lymph nodes contain cancer cells.

N2a: Four to six neighbouring lymph nodes contain cancer cells.

N2b: At least seven neighbouring lymph nodes contain cancer cells.

M0: No evidence of distant spread.

M1a: Malignancy impacted one single organ or a group of distant lymph nodes

M1b: The malignancy affected and roll out to the peritoneum or to more than one distant organ

The cancer's grade is another feature that is utilised to analyse survival (Ried et al., 2007). Under a microscope, the cancer's grade describes how closely it resembles healthy colon tissue. A colorectal cancer is graded on a scale from G_1 (where it resembles normal colon tissue) to G4 (where it is highly aberrant). In the middle are the grades G_2 and G_3.

1.1.6 Colorectal Cancer Development

The development of colorectum malignancy is dule to the genetic variations and comprise of several of definite processes. As per the sources the colorectum cancer has been categorized in two types 'Hypermutated' and non-hypermutated depending on the quantity of soma clonal mutations.

Additionally, concurrent attempts have been made to categorized the colorectum cancer based on the arrangement of the gene expression, consequently creation of a novel categorisation system. These categorify has been revised time to time based on the data collected from arrangement of gene expression patterns and tumour genotypes (Testa et al., 2018). The benign adenoma that develops from these fast-growing cells can transformed to the malignancy and transfer through a various rout like serrated neoplasia, chromosomal instability, and microsatellite instability (MSI, 2020; Nguyen and Duong, 2018; Vogelstein et al., 1988). One phrase used to characterise the course of cancer is adenoma–carcinoma sequence.

The large no. of metastasis of colorectum cancer is created due to the conventional pathway. Before developing into cancer, a tiny adenoma first grows into a giant adenoma. The National Cancer Institute estimates that 11-14% of sporadic colorectal cancers are caused by this model. It is distinguished by the transformation of healthy cells into sessile serrated adenomas, hyperplastic polyps, consequently malignancy. Usually, this mechanism responsible for the creation of the inflammation-related CpG island methylator phenotype (CIMP)-high subtype. Normal cells develop indeterminate dysplasia as a result of the ongoing inflammation, which then develops into low-grade dysplasia, high-grade dysplasia, and finally malignancy (Keum and Giovannucci, 2019).

1.1.8 Preventive Strategies

1.1.8.1. Primary Prevention

Incidence rates may drop much more if risk factor reduction accelerates. Risk factor adjustment is possible for many malignancies; however, it typically leads to a long-term decrease in incidence rates rather than a short-term one. Because of this, monitoring and assessing how shifts in the number of colorectum malignancy risk variables affect number of patients takes a long time (Cronin et al., 2001).

The studies based on the Epidemiological have been find a number of modifiable characteristics, which offers both opportunities and obstacles for primary prevention. Less intake of alcoholic beverages (Bagnardi et al., 2015), smoking of cigarette (Botteri et al., 2008), high body weight (Freisling et al., 2017), and higher intake processed meat (Vieira et al., 2017) to prevent colorectal cancer. The incidence of colorectum malignancy can be hampered, through continuous consumption of aspirin (Cao et al., 2016), hormone replacement treatment (Green et al., 2012), and physical activity (Boyle et al., 2012). Eating whole grains and milk may also help prevent colorectal cancer, according to some research.

1.1.8.2. Secondary Prevention

Unlike other cancers, colorectal cancer usually progresses gradually over years to decades once the normal colon epithelium transforms into an adenoma (Brenner et al., 2013). Because colonoscopy can detect and remove adenomas, it can diagnose colorectal cancer (CRC) at an earlier stage, which is often a viable method for secondary prevention

of CRC due to the slow evolution of the adenoma–carcinoma sequence. In addition, receiving treatment makes it possible to prevent secondary deaths more successfully. Screening methods most frequently include stool tests examinations of the large intestine through endoscope, and colonoscopy. Though computed tomography (CT), blood or urine tests, capsule endoscopy, and other stool-based (including DNA-based) diagnostics have been proposed, their usage has been restricted due to concerns regarding their high cost and diagnostic effectiveness. Moreover, CT is known to have negative effects. However, scientists worldwide are searching for novel biomarkers, like as markers in the blood which could greatly expand range of minimally invasive or non-invasive CRC screening tests now available (Reddy et al., 2007).

1.1.8.3. Tertiary Prevention

Numerous elements have an impact on result associated to colorectum malignancy, according to mounting epidemiological evidence. This suggests that there may be several opportunities for tertiary prevention. Although it is known that it can be challenging to convince people to change unhealthy lifestyle factors, a cancer diagnosis, for example, is thought to offer a useful teachable moment employed to motivate patients to make the urgent lifestyle adjustments. Smoking cigarettes and heavy drinking are common risk element for colorectal cancer (CRC). The above both elements participate to decrease the no. of incidence of survival in colorectum cancer (Walter et al., 2016; Ordóñez-Mena et al., 2018; Walter et al., 2015), Though the process behind this relating these risk elements to these outcomes not established, it is thought that lower survival rates are caused by larger incidence of surgical complications, less than optimal outcome to chemo and radio therapy, and smoking induced suppression of cancer cell apoptosis (Sharma et al., 2013; Dinicola et al., 2013).

1.1.9 Treatment Strategies

For many years, surgery and later chemotherapy are the common treatment option for the patient suffer from the malignancy. However, people with colorectal cancer who have metastatic disease typically have a poor prognosis. Colorectal cancer survival has increased due to advancements in primary and adjuvant treatment. To fully remove the tumour, surgery is typically required (Messersmith, 2019; Keum and Giovannucci, 2019).

Notably, chemotherapy or radiation therapy may be employed either with the surgery or after the surgery process leading to shrink or stabilise the tumour. The chemotherapy treatment comprises of single molecule, mostly fluoropyrimidine (5-FU), and combined therapy, including oxaliplatin (OX), capecitabine, and irinotecan (IRI). The most widely used first-line treatment regimens are still CAPIRI, XELOX or CAPOX, FOXFIRI (5-FU + IRI), and FOLFOX (5-FU + OX). For patients who have little chance of declining or doing poorly, single-agent therapy is recommended. Only the adverse effects appear to differ, suggesting that the effectiveness of choosing additive medicines is similar (Xie et al., 2020). Inadequate response rates, systemic toxicity, are some of its long-term drawbacks.

1.1.9.1. Targeted Therapy

One innovative new strategy that attributed augment overall endurance in cases with colorectal cancer is targeted therapy. An unusual rate of checkpoint development is being caused by the increasing effectiveness of novel medications that block various immune pathways, ex. bevacizumab and cetuximab agent (Xie et al., 2020). Cetuximab, the first targeted treatment for colorectal cancer, was approved by the FDA in 2004. Subsequently, several have been approved.

1.1.9.2. Gene Therapy

It employed the use of genetic element to treat cancer and other illnesses. The genetic comprise element like DNA or RNA, play a vital role in modification and maintenance of affected genes. The therapy comprise the use of the genetic element can also be enrolled to activate a response through the immune system or as carrier itself.

Gene mutations could be able to prevent colorectal cancer by making correction in the sequence, composition and working of these affected genes and avoiding overexpression of the genes. Colon cancer is caused by a variety of gene alterations. Malignancy can be triggered by ‘point mutations’, oncogene production, proto-oncogene deregulation or deletion, and suppressor-oncogene activity loss (Armaghany et al., 2012).

The main edge of the therapy based on the genetic element is its ability to deliver particular genes to targeted tumour cells, which prevents the mutant gene's aberrant function and slows the tumour’s growth, is the main advantage of gene therapy.

1.1.9.3. Immunotherapy

Researchers are interested in tumour immunotherapy. Because of its great potential as a treatment for colorectal cancer. In previous and recent investigation, several studies are going on related to the clinical activity of these immunotherapies in curing the treatment of patient suffer from colorectum malignancy (Zahavi and Weiner, 2020).

1.1.9.3.1. Monoclonal Antibody Therapy

This treatment uses humanised antibodies, likes cetuximab and panitumumab, that specifically directed towards the epidermal growth factor receptor (EGFR) to cure metastatic colorectal cancer. The mAbs for colorectal cancer (CRC) that are now undergoing clinical trials include pemtumomab against mucins, labetuzumab against carcinoembryonic antigen (CEA) (Hu et al., 2018).

1.1.9.3.3. Cancer Vaccines

Cancer vaccine act by transmitting the antigen-to-antigen presenting cells consequently trigger activity of antigen-specific T- or B-cell activity against malignancy, such as dendritic cells (DCs). Vaccine components like OncoVAX and the DC vaccination are also designed to stimulate the dendritic cells which direct the antigens to the lymph node (Hu et al., 2018).

DC Vaccine

DCs vaccines act by demonstrating the affinity towards the CEA peptides or CEA mRNA because CEA antigen overexpressed over the most colorectal malignancies (CRCs). Most patients with advanced colorectal cancer (CRC) who received DC vaccine demonstrated the response triggered due CEA-specific T-cell (Lesterhuis et al., 2006).

OncoVAX

This was created to boost the immune system against tumours and prevent colon cancer from recurring after surgery by using the cancer cells of patients in combination with an immune-stimulating adjuvant. Targeted immunotherapy with surgery dominantly augments the lifespan of patient (Fong et al., 2001; Orsini et al., 2013).

1.1.9.4. Adoptive T-Cell Therapy

The therapy augments the efficacy of the vaccine and immunity against the malignant cells. The desired antigen receptors have been the aim of recent research (Wu et al., 2015).

1.1.9.5. Complement Inhibition

The immune system relies heavily on complement. The immune surveillance response to colorectal cancer depends critically on complement activation. The innate and adaptive immune systems both use complement, which is made up of about 30 protein fragments. Complement inhibitors like venom of cobra and recombinant Staphylococcus aureus superantigens has been investigated in rat model with colon cancer cell. It can be applied as a component of a program of combination immunotherapy (Downs-Canner et al., 2016).

1.1.9.6. Cytokine Therapy

The leads the development of the malignancy through the inflammation and immunogenic responses. Cytokines trigger the activation of nuclear factor-B, inducer of transcription 3 (STAT3), and other malignancy causing protein result in development of resistance against apoptosis (West et al., 2015).

1.1.9.7. Natural Products as Therapy

A variety of well-known compounds and natural resources are available for first-line therapy to treat a variety of critical disorders (Hossain et al., 2016; Urbi et al., 2015). According to estimates, 75–80% of individuals globally use traditional medicinal systems as their first option of treatment because they lack access to treatment facilities and are worried about the therapeutic efficacy and toxicity of synthetic medications (Hossain et al., 2014; Hossain et al., 2021).

Natural products have demonstrated the beneficial effect and have been employed to treat colorectal cancer (CRC) and other disease conditions. The treatment of colorectal cancer still faces significant challenges due to resistance against active molecule and toxicity.

Currently a unique approach has been utilized for the curing of colorectum cancer. That approach involves the application of synthetic drug molecule with the herbal molecule to augment the sensitivity of the synthetic drug molecule against the cancer cells. Patient suffered from the metastasis colorectal cancer has been received the synthetic molecule like oxaliplatin, 5-fluorouracil, and leucovorin to augment the no. of treated patient and quality of life. Additionally, a network meta-analysis found that they reduced peripheral neurotoxicity (III-IV) (Ge et al., 2016). The technique increases potency while reducing side effects.

1.2 Applications of Nanotechnology

The application of the nano size range technology in the diagnosis and therapeutic application has been used in the past 40 years (Fortina et al., 2007). Technology comprise of nao size range particles has been advance and emerged a vital option for the screening, detection, diagnosis and treatment several diseases (Upendra et al., 2016). It is essential for the creation and effective administration of medications with specific actions at predetermined locations. The nano size range formulations include lipid-based vesicles, dendrimers, silica nanoparticles, gold nanoparticles, quantum dots, nano size range emulsion has been used as drug delivery carrier for the delivery of the therapeutic drug molecules at the target site (Bose et al., 2015; Yallapu et al., 2015).

It has been established that there are several important nanotechnological benefits in cancer biology, such as early cancer detection and screening and the creation of innovative treatment approaches that are not achievable with the present standard practices (Laroui et al., 2013). For the detection, staging, and therapy of colorectal cancer, nanoparticles of varying sizes and constitution have been identified a vital and promising approaches (Figure 1.2) (Dong et al., 2016). Early detection and screening for colorectal cancer (CRC), which can impact a patient's long-term survival, is the main solution to the challenges.

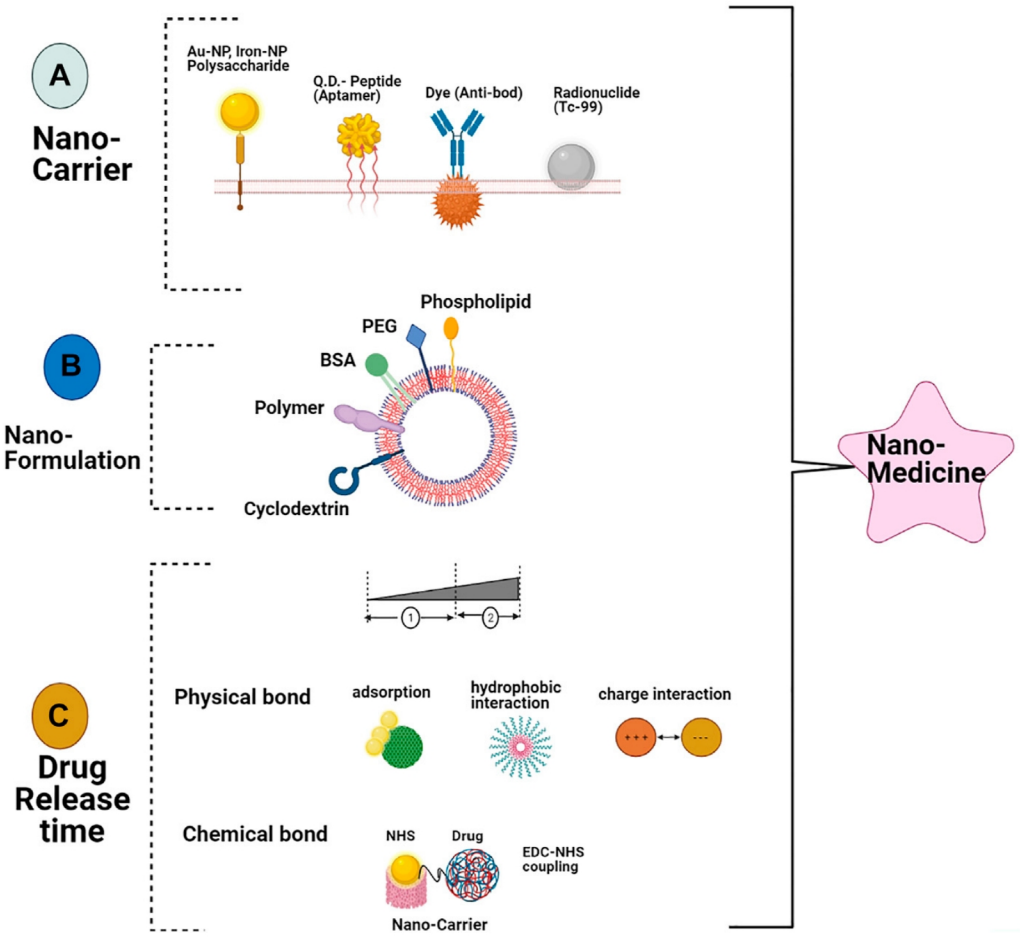


Figure 1.2: Demonstration of application of various nano size range formulation in CRC (Dong et al., 2016).

1.3 Carbon nanotube

Carbon nanotube also termed as smart nanocarriers or nanostructures composed completely of carbon. The nanostructures employed as targeting drug delivery carrier and offer a wide group of potential benefits, including the encapsulation of both hydrophobic and hydrophilic molecules. They also improve medication stability and enable site-specific delivery. Among the many different geometries and structures that could be produced are nano size range particles, tubes, disk, shell, buds, sp^3 hybridised crystalline carbon flakes, and wires (Kumari et al., 2010; Bao et al., 2013; Cheung et al., 2010). A type of nanostructure known as carbon nanotubes (CNTs) has a high aspect ratio and other

remarkable characteristics, including as its size at the nanoscale (Cheung et al., 2010; Rathod et al., 2019; Anzar et al., 2020). In addition to carbon nanotubes (CNTs), Figure.1.3 shows how other carbon nanostructures comprise of fullerene, nanobuds, carbon black, graphene, nanodots, and nanohorns, share properties and serve distinct purposes (Rezaee et al., 2018).

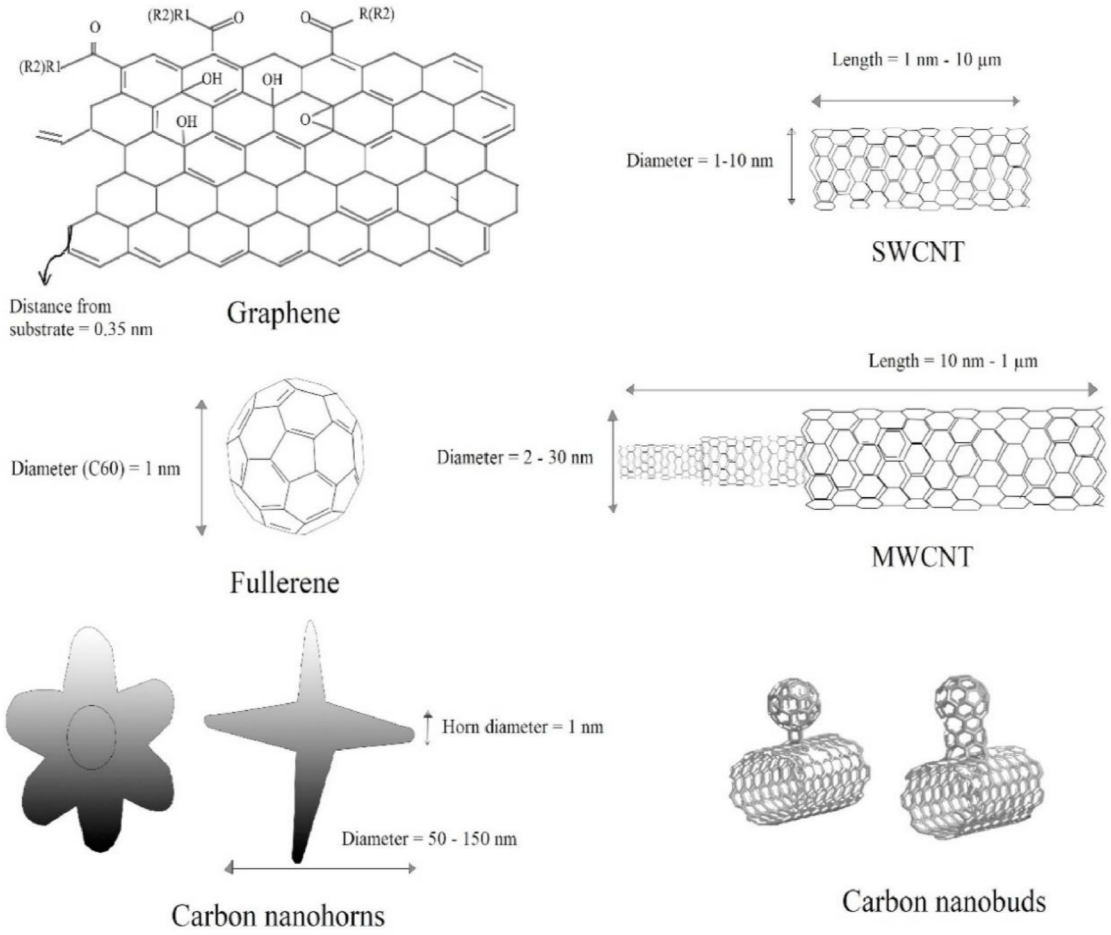


Figure1.3: Image of various carbon nanostructure (Rezaee et al., 2018).

1.3.1 Classification of CNTs

Depending on how many graphene sheets they include, nanotubes can be divided into a variety of categories. Consequently, these are further separated into:

1.3.1.1 Single-walled CNTs (SWCNTs)

Graphene sheet orientation makes up single-walled carbon nanotubes. It requires the synthesis of a catalyst. It also doesn't have a complex structure. Twisting the material is easy (Aqel et al., 2012). They can occasionally appear bright and metallic and are either granular or black and fluffy (Beg et al., 2011). Due to this order, depending on chirality and diameter, SWCNTs may exhibit characteristics more akin to a specific semiconducting, metallic (Dresselhaus et al., 2004).

1.3.1.2 Multi-walled CNTs (MWCNTs)

The number of tubes in the coiled sheets, possess diameter ranging from 1 to 50 nm, determines the size of CNTs, which are composed of several layers of graphene rolled on top of one another (Ajayan, 2003). A catalyst is not necessary for its synthesis. MWCTs possess high purity and complex architectures. It is not easily twistable. These tubes have layers that are about 0.34 nm apart (Ding et al., 2001; Tang et al., 2001). They typically take the form of a frothy, granular black powder.

1.3.1.3 Double-walled CNTs (DWCNTs)

In addition to this, another type of CNT shares structural similarities with SWCNTs. These nanotubes were composed of an inner cylindrical tube enclosed by two outer concentric layers (Aqel, 2012).

1.3.2 Functionalization

Nanotubes primary issue is that they can collect because of lower intermolecular interactions, which makes it more difficult to disperse them in different solvents and into the right polymeric media. In order to improve their dispersion in polymeric materials and solvents, they are functionalised to inhibit bundle formation and aggregation (Georgakilas et al., 2002). One significant technological barrier for biological and biomedical applications has been the limited solubility of carbon nanotubes (CNTs) in aqueous media (Yang et al., 2001).

The functionalisation process defined as the of attaching unique chemical groups to the side chains or terminals of carbon nanotubes is known as functionalisation (Georgakilas et al., 2002). In addition to increasing the CNTs' solubility, this will render them more hydrophilic and fundamentally alter their biocompatibility profile (Lacerda et al., 2006). It has been demonstrated to enhance biological compatibility, decrease toxic

effects, and improve aqueous solubility. It also provides the capability of loading drug molecules, genes, or proteins into functionalised carbon nanotubes for efficient delivery systems.

1.3.2.1. Non-covalent functionalization

The foundation of the non-covalent functionalisation is van der Waals forces. Non-covalent functionalisation is important and crucial because it wouldn't substantially alter or change the arrangement of CNT (Hirsch, 2002). This is an additional method for modifying the nanotubes' interfacial characteristics. The aromatic structure of nanotubes and, thus, their electrical properties are preserved due to their non-covalent dispersion in the solution. Ultrasonic dispersion, filtration, and centrifugation are generally simple and quick processes. Numerous substances, including efficiently adhered to the surface of carbon nanotubes using the physical adsorption technique that makes use of the π-π stacking interaction (Paloniemi et al., 2005; Wu et al., 2008; Zhang et al., 2006). Numerous cationic, anionic, and non-ionic surfactants have already been suggested for use in the surface modification of nanotubes. Polymers, for instance, are good alternative in the solubilisation of CNT, even if they lack a greater dispersion efficiency.

1.3.2.2 Covalent functionalization

In the functionalisation process described above, the groups of interest are adhered to the surface of the CNTs' walls or tips. The outermost layer or the ends of the nanotubes have been joined to several chemical groups, such auxiliary dichloro-carbon groups, fluorine carboxylic groups, and p-aminobenzoic acid. The two primary benefits of chemical functionalisation are its ability to form covalent bonds with polymeric materials and its ease of dissolution in a variety of solvents (Kim and Min, 2010). According to Mallakpour and Soltanian (2016), there are two kinds of covalently functionalised carbon nanotubes.

1.3.2.2.1 Oxidation of CNTs

The prevalent approach for functionalisation of surface through the chemical group is the application of several oxidising agents, like nitric acid (HNO_3), which produces hydrophilic or carboxylic groups that are usually present on the walls, surfaces, and end of the carbon nanotubes (CNTs) (Tour et al., 2007). According to Zeng et al. (2008), SP_3 carbon atoms undergo oxidation to form SWCNTs, which facilitate or participate in the

surface modification process with other molecules such as proteins or amino acids. Oxidization of CNTs makes them more soluble, but it also makes them more prone to aggregation. Presence of salt tend to aggregate the Oxidised CNTs, which could be due to charge screening. The presence of different salts in the biological fluid makes the CNTs unstable in vivo. This aggregation problem is addressed by the oxidised CNTs, which are also coated with a hydrophilic polymer, like polyethylene glycol (PEG), making them stable and soluble (Schipper et al., 2008). It has been shown that oxidation of carbon nanotubes is a practical functionalisation technique that may be utilised to produce functionalised CNTs on an industrial scale in addition to being ideal for small-scale manufacture.

1.3.3.2.2 Cycloaddition reaction

This process not similar to previous reaction, accompanied next to the sides functional group of the carbon nanotube instead of its ends or flaws. This covalent functionalisation technique is also widely used. This response can be divided into three categories: A photo-chemical reaction involving azides is known as photoinduced cyclo addition (Lee et al., 2008; Moghaddam et al., 2004); Bingal reaction yields carbenes in the presence of a strong base. (3) Also referred to as the [2 + 1] cycloaddition process, the 1,3dipolar cycloaddition reaction is currently prevalent reaction for the functionalisation of CNTs (Umeyama et al., 2007; Tagmatarchis and Prato, 2004).

1.3.3 Reaction with acyl peroxides or sulfoxides

This process involves functionalization of CNTs over their surface, attaching functional group to their side walls and ends via covalent bonds without producing structural damage or flaws like oxidised CNTs do. Acid peroxide possesses terminal groups for further functionalisation due to the formation of carbon-centered radicals. The same function as acyl peroxides is served by sulfoxides (Khabashesku et al., 2006).

1.3.4 Polymer functionalized CNTs

The functionalization of carbon nanotube with polymer molecules leads to enhance the dispersion and impart the new features to the carbon nanotube. Chemical attachment (sometimes called "grafting to") and physical adsorption are the two primary techniques for altering CNTs using polymers, according to Mallakpour and Soltanian (2016). In the

presence of initiators, the polymer attached to the CNT surface through in-situ monomer polymerisation (Sahoo et al., 2010).

1.3.5 Characterization of CNTs

Raman spectroscopy

It may be used for accurate screening of SWCNT. It is a rapid, straightforward, and accurate characterization method. According to Joio et al. (2003), the equipment is widely accessible to a range of people and may be utilised at ambient temperature and pressure (Eklund et al., 1995).

Transmission electron microscopy (TEM)

The evaluation of thin specimens by projecting an image via the electron way is replaced by this microscopy. TEM is comparable to the conventional (compound) light microscope in many aspects (Branca et al., 2004). It permits a comprehensive determined the nano size range structure. Through TEM, only qualitative data like surface artifacts, morphology, and size range sample's non-CNT impurities and carbonaceous components can be acquired.

Scanning electron microscopy (SEM)

Though less sensitive to sample homogeneity and preparation than TEM, it provides an information regarding the constituent parts of the test samples. The form of carbon nanotubes is often assessed in advance using this method. SEM is probably the only method that can provide information regarding the morphology and metallic impurity content of carbon nanotubes (CNTs) (Abdulkareem et al., 2007).

Proton NMR

Utilising this, the development of CNT functionalisation is being investigated. No. of proton would likewise be predicted by existence of distinct peaks that result from the alteration of the magnetic field. Proton NMR was employed to investigate the preparation and surface modification of the carbon nano tube (Yinghuai et al., 2005).

Thermogravimetric analysis

The objective of this evaluation is to quantify the amount of carbonaceous and non-carbonaceous components and thermal stability of CNTs (Itkis et al., 2005).

1.3.6 The role of carbon nanotubes in cancer diagnosis

The properties like electrical, mechanical and thermal of carbon nano size range tube make them a viable option for the diagnosis and identification of protein element expressed over the surface of the malignancy at early stage (Coleman et al., 2006). Currently, the imaging technique including Raman imaging (Yu et al., 2021a), fluorescence imaging (FI) (Zhou and Jokerst, 2020), and photoacoustic imaging (PAI) (Kang et al., 2022). With their strong absorption of near-infrared (NIR) light, carbon nano size range tube demonstrated benefits in photoacoustic imaging as a contrast agent through by augmenting imaging signals (Gao et al., 2022). According to Yaghoubi and Ramazani (2020), single-walled carbon nanotubes have unique excitation and emission wavelengths that enable multicolour fluorescence imaging.

The single walled carbon nao size range tube surface modified using the isotopic (Gong et al., 2013) demonstrated facts related to the constitution of cells and tissues (Ijaz et al., 2023) and enables multicolour Raman imaging of different cancer cells. These outcomes attributed the vital application and benefits of carbon size range tube in imaging and early-stage malignancy diagnosis. As per previous researchers make a lot of efforts and create method to detect a malignancy by combining quantum defect-functionalized nanotube arrays with machine learning techniques.

1.3.6 Carbon nanotubes in cancer therapy

Tumour cells and their surroundings are the focus of several oncology therapeutic approaches nowadays. The tumour parenchyma can be removed directly and effectively by focussing on the tumour cells. Conversely, targeting the tumour microenvironment (TME) stops tumour cells from multiplying and spreading by interfering with their basic survival conditions, so indirectly killing the tumour cells. CNTs' properties, drug-carrying surfaces, and tumour-penetration capacities have made them vital option for curing of the various malignancy in a variety of biomedical fields (Figure 1.4). This provides a multimodal approach to cancer treatment by addressing both the intracellular regions of tumour cells and the exterior components of TME (Gao et al., 2024).

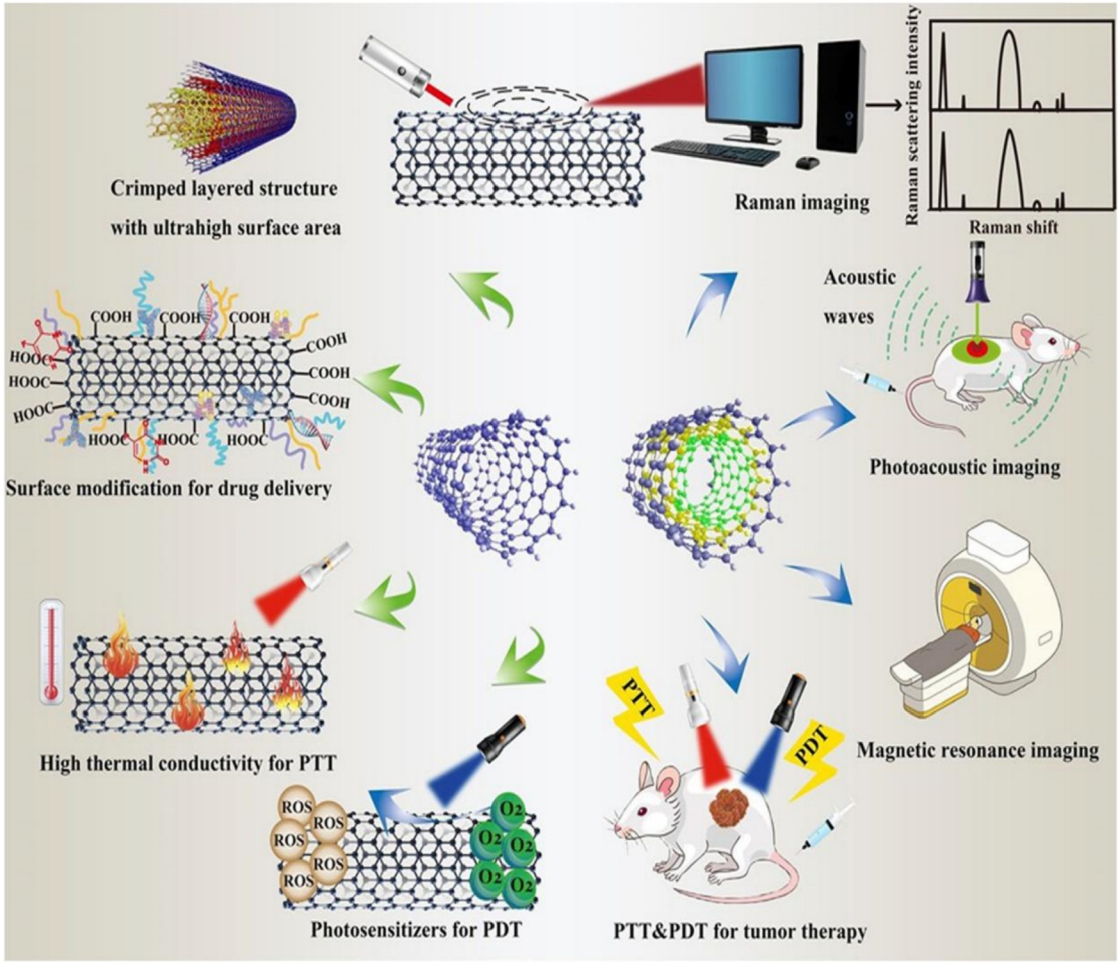


Figure 1.4: Various applications of CNT in cancer therapy (Gao et al., 2024)

1.3.7 **Advantage of Carbon Nanotubes Over Other Nanocarriers**

MWCNT represent a significant advancement in nanotechnology due to its exceptional physicochemical properties that exceed those of traditional carriers including micelles, liposomes, and polymeric nanoparticles. Carbon nanotubes possess a significant aspect ratio and a considerably greater surface area than spherical nanoparticles, which facilitates drug loading by π–π stacking, covalent bonding, and encapsulation within their hollow structure. This structural benefit enables CNTs to concurrently encapsulate both hydrophilic and hydrophobic pharmaceuticals, a constraint frequently encountered in liposomes or micelles. Additionally, CNTs possess exceptional mechanical strength,

electrical conductivity, and optical responsiveness, making them suitable for drug delivery as well as multifunctional theragnostic applications like imaging, biosensing, and photothermal therapy (Balaji et al., 2026).

An additional significant advancement is their potential for functionalization. Carbon nanotubes can undergo chemical functionalization with polymers, antibodies, peptides, or ligands to enhance solubility, biocompatibility, and targeted delivery. This flexibility enables CNTs to surmount the challenges of aggregation and inadequate dispersibility frequently associated with pure CNTs. Liposomes are typically prone to instability and leakage, whereas polymeric nanoparticles face challenges with consistency and scalability. CNTs facilitate medication release in reaction to stimuli like pH, temperature, or light, enabling accurate targeting of treatments inside the tumor microenvironment. The controlled release systems in traditional nanocarriers exhibit inefficiency and may undermine effectiveness due to early drug leakage or sudden release (R et al., 2026).

In summary, carbon nanotubes (CNTs) exhibit significant potential as advanced nanocarriers owing to their elevated drug loading capacity, multifunctional properties, structural integrity, and exceptional targeting capabilities. The difficulties of toxicity and regulation are significant challenges; yet, ongoing research into surface functionalization and biocompatibility is progressively addressing these concerns, positioning CNTs as a transformative platform in nanomedicine compared to conventional formulations (R et al., 2026).

1.4 Resveratrol

In 1940, resveratrol separated through the extraction process from the roots of white hellebore, and later on in 1963, it was obtained from the roots of Polygonum cuspidatum. The current poly phenol was exhibited in the more than 70 plant species It is also present in low quantity in red wines and a variety of foods consumed by humans. Vitis vinifera's reaction to fungal infection may be the reason for the high amounts found in grapes. Resveratrol functions in plants as a phytoalexin that is produced in reaction to fungal invasions, UV radiation, and mechanical damage. Saccharomyces cerevisiae yeasts are

typically used to produce resveratrol for industrial use through chemical or biotechnological synthesis (Aggarwal et al., 2004).

1.4.1 Sources

Common sources of RV nowadays include peanut skins, red grapes, mulberries, soybeans, pomegranates, cranberries, soy, dark chocolate, pistachios, and Polygonum cuspidatum (Japanese knotweed). Because of their high concentrations of RV, these foods are frequently used in RV supplements (Aggarwal et al., 2004).

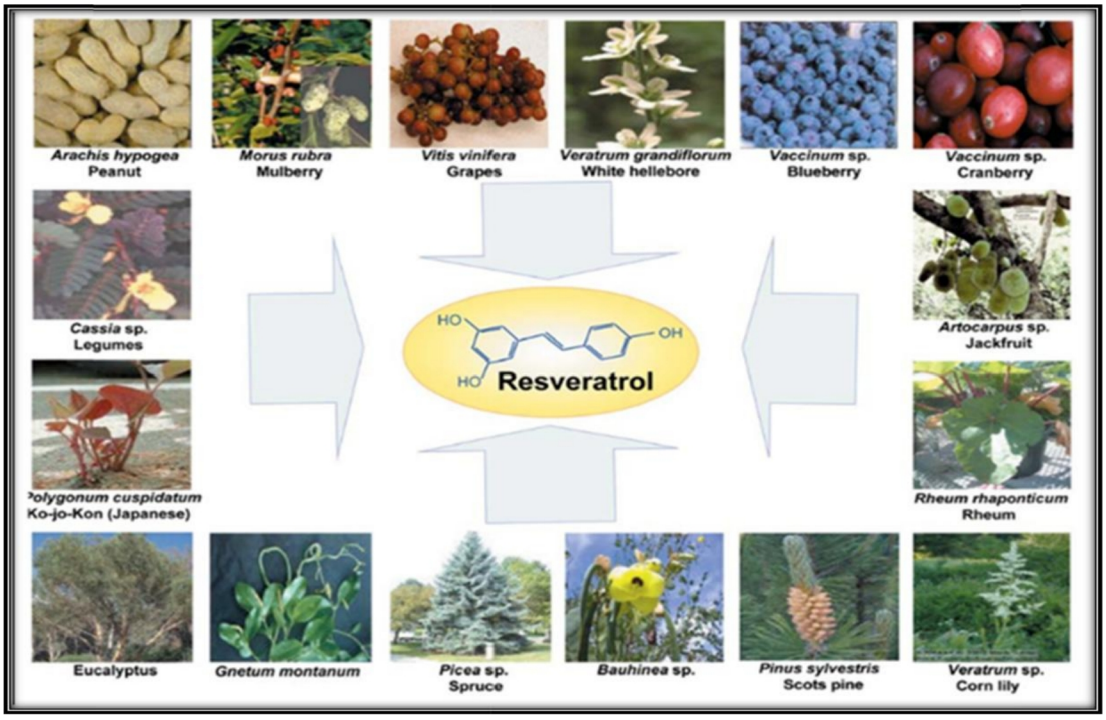
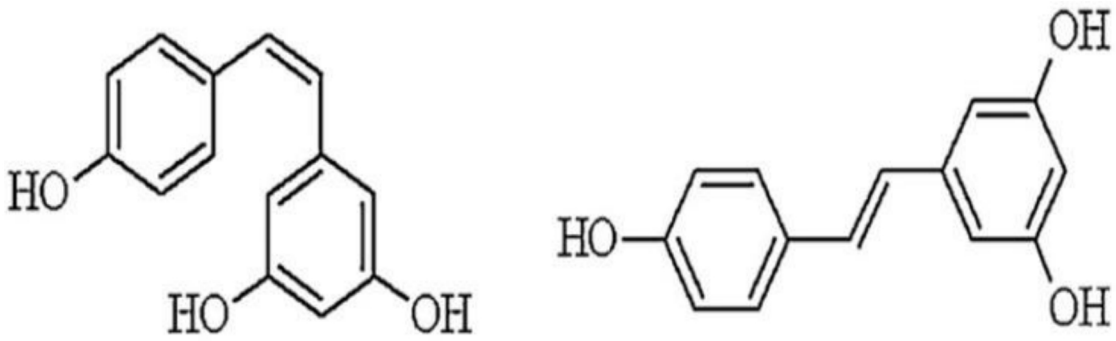


Figure 1.5: Sources of resveratrol (Aggarwal et al., 2004).

1.4.2 Chemistry of Resveratrol

Resveratrol comprises of two phenol rings covalently attached with each other by an ethylene bridge. The two isomeric forms of resveratrol (trans-3,5,4′-trihydroxystilbene), cis- and trans-resveratrol, are distinguished by their chemical structures (Figure 1.6). According to various biological activities, trans form is dominant in terms of its prevalence. These activities include enhancing the anti-proliferation of cancer cells and triggering cellular responses (Akinwumi et al., 2018; Anisimova et al., 2011; Orallo, 2006).



cis-Resveratrol *trans*-Resveratrol

Figure 1.6: Resveratrol chemical structure (Akinwumi et al., 2018; Anisimova et al., 2011; Orallo, 2006).

IUPAC name: *E*-5-(4-hydroxystyryl) benzene-1,3-diol.

Polymeric form: There are two geometric isomers of it: trans-(E) and cis-(Z).

1.4.3 Properties

Chemical formula:	$C_{14}H_{12}O_3$
Appearance:	white powder with slight yellow cast
Melting point:	261 to 263 °C (502 to 505 °F; 534 to 536 K) (Camont et al., 2008)
Solubility in water:	0.03 g/L
UV-vis (λ_{max}) :	304nm (trans-resveratrol, in water) 286nm (cis-resveratrol, in water) (Camont et al., 2008)
Molecular weight:	228.25 g/mol (Crozier et al., 2009)

1.4.4 Pharmacokinetic of resveratrol

Absorption

The absorption of resveratrol is impacted by its low water solubility (<0.05 mg/mL) due to its molecular nature. It can be made more soluble by using organic solvents or ethanol (50 mg/mL). The intestinal absorption of resveratrol occurs through passive diffusion or the formation of complexes with membrane transporters, including integrins.

There are basically three types of resveratrol in the bloodstream: glucuronide, sulphate, or free.

Metabolism

Resveratrol or its metabolites undergo phase II metabolism in the liver. Some cycles may return to the small intestine as a result of enterohepatic transit in bile (Crozier et al., 2009). Additionally, resveratrol can stimulate its own metabolism, which raises the activity of enzymes that detoxify the liver in phase II (Lanc et al., 2005). Due to its high metabolism, resveratrol produces conjugated sulphates and glucuronides, which still have some biological activity (Wang et al., 2004). The urine can contain up to five different metabolites, including resveratrol mono-sulphate, two isomeric forms of resveratrol monoglucuronide, mono-sulphate di-hydro resveratrol, and monoglucuronide di-hydro resveratrol. But because of interindividual variability, the type and amount of these metabolites can vary from one subject to another (Walle et al., 2004; Cottart et al., 2010).

Bioavailability

Resveratrol has a high absorption rate because of its lipophilic properties. Note that the type of food consumed and the manner of consumption can affect the absorption of resveratrol (Vitaglione et al., 2005). Resveratrol's low bioavailability is one element that could lessen its effectiveness.

1.4.5 Mechanisms of Resveratrol in Cancer Prevention

Resveratrol has garnered significant attention as an anti-cancer agent with a variety of uses, partly due to its capacity to specifically modify a number of significant cellular pathways implicated in tumour progression (Amini et al., 2023; Gielecińska et al., 2023; Karkon-Shayan et al., 2023; Kumar et al., 2022; Song et al., 2023). In numerous experimentally induced tumour models, including skin, lung, gastric, colon, liver, pancreas, prostate, bladder, breast, ovarian, esophagus, thyroid, etc., resveratrol proved to have a chemo preventive effect (Amini et al., 2023; Gielecińska et al., 2023; Karkon-Shayan et al., 2023; Kumar et al., 2022; Song et al., 2023).

Exposure to resveratrol caused differentiation in canine oral mucosal melanoma cells, boosting the mRNA expression of melanoma differentiation markers such microphthalmia-associated transcription factor (MITF) and making the cells more sensitive

to cisplatin (Fukuoka et al., 2022). Resveratrol's suppression of JNK signalling, as demonstrated by inhibitor studies and a reduction in JNK activity, was credited with this differentiation impact (Fukuoka et al., 2022). 17β-estradiol increased neuroglobin levels in estrogen receptor α-positive breast cancer cells, which helped the cells survive (Montalesi et al., 2023). Resveratrol may block this route, but its effectiveness was hampered by its quick metabolism. As a result, conjugating resveratrol with gold nanoparticles may increase its bioactivity and open the door to targeted breast cancer treatments (Montalesi et al., 2023). Resveratrol targeted the β1-integrin/HIF-1α signalling pathway, altered the tumour microenvironment, and made colorectal cancer cells more sensitive to 5-fluorouracil through β1-integrin receptors. According to Brockmueller et al. (2023), this interaction may be crucial in the tactics used to overcome 5-fluorouracil resistance in advanced colorectal cancer therapy.

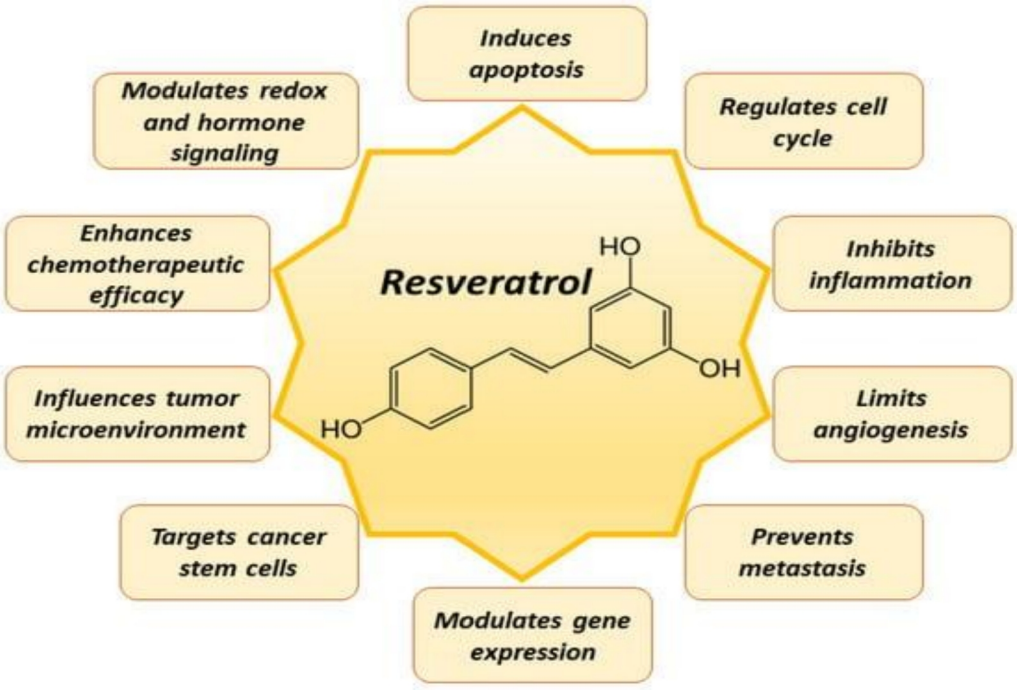


Figure 1.7: Main effects of resveratrol in tumour cells (Amini et al., 2023; Gielecińska et al., 2023; Karkon-Shayan et al., 2023; Kumar et al., 2022; Song et al., 2023).

Programmed cell death mechanisms in tumour cells are triggered by resveratrol. Many cancer cells have been shown to have increased nuclear transcription factor NF-κB, which promotes tumour cell survival, proliferation, and metastasis (Xia et al., 2018). Through the $SIRT_1$ signalling pathway, resveratrol suppresses NF-κB phosphorylation, which is connected to its effects (Buhrmann et al., 2017). By inhibiting the expression of β-catenins and targeting the genes c-Myc, MMP-7, and surviving in multiple myeloma cells, resveratrol has been demonstrated to decrease the migration, invasion, and proliferation of cancer cells (Geng et al., 2018). The reduction of vascular endothelial growth factor (VEGF) and hypoxia-inducible factor (HIF)-1 generation is linked to resveratrol's effects on angiogenesis (Talib et al., 2020).

1.5 Cetuximab

The FDA has approved cetuximab, an epidermal growth factor receptor (EGFR) inhibitor, for the treatment of colorectal cancer, metastatic cancer, KRAS wild-type (without mutation), and squamous cell head and neck cancer. EGFR-expressing, advanced, squamous cell skin cancer, colorectal cancer, and non-small cell lung cancer (NSCLC) are among the non-FDA-approved uses. Regarding the treatment of individuals with cancers for which cetuximab is prescribed, this activity goes over the drug's mechanism of action, adverse event profile, toxicity, dosage, pharmacodynamics, and monitoring.

Human IgG1 heavy and kappa light chain constant regions are combined with the Fv regions of a mouse anti-EGFR antibody to form cetuximab. Hemoglobulin G1, anti-(human epidermal growth factor receptor), dimer, disulfide with human-mouse monoclonal C225 kappa-chain (Beljanski, 2007).

1.5.1 Chemical and physical data

Physical properties:	Cetuximab is a sterile, clear, colourless liquid of pH 7.0–7.4,
Formula:	$C_{6484}H_{10042}N_{1732}O_{2023}S_{36}$
Molar mass:	145781.92 g·mol^{-1}

Solubility: Cetuximab is supplied as an aqueous solution with concentration of 2 mg/mL in a preservative-free solution containing 8.48 mg/mL sodium chloride, 1.88 mg/mL sodium phosphate dibasic heptahydrate, 0.42 mg/mL sodium phosphate monobasic monohydrate (Beljanski, 2007).

1.5.2 Mechanism of Action

Cetuximab, a human/mouse IgG1 monoclonal antibody also termed as recombinant chimeric antibody that attaches to the receptor of epidermal growth factor (EGFR) and competitively prevents the binding of EGF and other ligands. One of the receptors in the ErbB family is EGFR. When EGFR is not in use, it is a monomer; however, when it is bound by TGF-alpha or epidermal growth factor, it can form homodimers or heterodimers with other receptors in the ErbB family. Autophosphorylation and a series of intracellular processes are triggered when dimerization activates the EGFR's intracellular tyrosine kinase region. Cancer cells exhibit dysregulation of the EGFR signalling system, which controls angiogenesis, migration, apoptosis, proliferation, and differentiation of cells. By binding to EGFR with more specificity and affinity than either TGF-alpha or epidermal growth factor, cetuximab prevents EGFR from being phosphorylated by ligands. In experimental systems, cetuximab also improves the results of radiation and irinotecan. Activating mutations in exon 2 can affect K-ras, a minor G-protein downstream of EGFR and an essential part of the EGFR signalling cascade. This can isolate the pathway from EGFR's influence and make EGFR inhibitors ineffective (Park et al., 2019; Agarwal et al., 2019)

1.5.3 Administration

The drug is administered by intravenous infusion, with a weekly maintenance dosage lasting one hour and a loading dose lasting more than two hours. Don't give it as a bolus or IV push. Don't dilute or shake. Use a syringe pump or an infusion pump to administer. An observation period of one hour is advised after the infusion; a longer observation period may be required after an infusion reaction. While premedication with an antihistamine alone is permissible, people who live in high-incidence areas may find it sensible to add a glucocorticoid. For colorectal cancer, metastatic, KRAS wild-type

(without mutation), and head and neck cancer, the recommended dosage is 400 mg/m^2 infused over 120 minutes for the initial loading dose and 250 mg/m^2 infused over 60 minutes for the maintenance dose (Zenda et al., 2019; Qiu et al., 2019).

1.5.4 Adverse Effects

Adverse effects include the following based on body systems: Central nervous system: Fatigue (91%), malaise (73% or less), pain (59%), peripheral sensory neuropathy (45%; grades 3/4: 1%), headache (19% to 38%), insomnia (27%), confusion (18%), chills (16% or less), rigors (16%or less), anxiety (14%), depression (14%).

Dermatologic: Desquamation (95%), acneiform eruption (15% to 88%; grades 3/4: 1% to 18%), radiodermatitis (86%), xeroderma (14% to 57%), pruritus (14% to 47%), skin rash (28% to 44%), changes in nails (31%), acne vulgaris (14% to 22%), paronychia (20%), palmar-plantar erythrodysesthesia (19%), skin fissure (19%), alopecia (12%).

Endocrine & metabolic: Weight loss (15% to 84%), hypomagnesemia (6% to 55%), dehydration (13% to 25%), hypocalcaemia (12%), hypokalaemia (12%).

1.5.5 Indications

Cetuximab is an epidermal growth factor receptor (EGFR) inhibitor utilized to treat the following:

1.5.5.1 FDA-Approved Uses

Cetuximab retains quality-of-life metrics for patients with colorectal cancer when other treatments have failed and increases overall and progression-free survival in cases of metastatic, colorectal cancer, and KRAS wild-type (without mutation) cancer. The usage is restricted. Patients with tumour-bearing wild-type K-ras benefited from cetuximab, while those with colorectal tumour-bearing mutant K-ras did not. Patients with metastatic colorectal cancer should not receive anti-EGFR antibody therapy if a KRAS mutation in either codon 12 or 13 is found.

Head and neck cancer (squamous cell): Treatment of locoregionally advanced head and neck cancer with cetuximab and concurrent high-dose radiation improves locoregional control and reduces mortality without exacerbating the typical toxic side effects of head and neck radiation. The combination of cetuximab and platinum-fluorouracil chemotherapy, when administered as the initial treatment for patients with recurrent or

metastatic head and neck squamous-cell carcinoma, increased overall survival (Zenda et al., 2019; Park et al., 2019).

Non-FDA-Approved Uses (Qiu et al., 2019; Agarwal et al., 2019)

Colorectal cancer, advanced, biweekly administration

Non-small cell lung cancer (NSCLC), EGFR-expressing, advanced.

1.6 Research Gap

Some commonly researched nanocarrier systems for colorectal cancer treatment include liposomes as well as polymeric particles due to their ability to encapsulate chemotherapeutic agents and enhance drug bioavailability. However, both techniques present several issues, including the untimely release of medications and inadequate retention inside the colon, which significantly reduce their therapeutic effectiveness. Liposomes exhibit instability in gastrointestinal conditions, whereas polymeric nanoparticles often demonstrate burst release properties, limiting their use in prolonged drug delivery (Firoz et al., 2026; Yang et al., 2026). These limitations highlight the requirement for alternative nanocarrier systems to facilitate controlled release and targeted drug localization.

In this scenario, multiwalled carbon nanotubes (MWCNTs) have garnered significant attention as promising candidates due to their remarkably high surface area and unique physicochemical properties. Their ability to undergo various functionalization techniques (both covalent and non-covalent) can lead to improved solubility, biocompatibility, and targeted delivery. Moreover, π–π stacking interactions promote the steady integration of phytochemicals, rendering MWCNTs appealing for controlled release applications in cancer treatment (Priyanka et al., 2026; Thakur et al., 2023). These attributes render MWCNTs superior substitutes for traditional nanocarriers. Nonetheless, their potential for antibody-facilitated phytochemical transport remains little explored.

Antibody attachment in nanocarrier systems offers an additional degree of specificity, particularly in colorectal cancer characterized by the overexpression of epidermal growth factor receptor (EGFR). Cetuximab is a monoclonal antibody that inhibits EGFR and has shown clinical significance in the treatment of colorectal malignancies. Nonetheless,

thorough studies integrating antibody anchoring and phytochemical delivery with MWCNTs are lacking. Although the potential of nano-delivery systems utilizing phytochemicals has been investigated, the synergistic capabilities of antibody-phytochemical conjugation remain largely unexplored (Unnikrishnan et al., 2026). This disparity underscores the necessity to investigate antibody-functionalized MWCNTs for enhanced tumour-specific absorption and less off-target toxicity.

Resveratrol, a naturally occurring polyphenol, has demonstrated anticancer properties and the ability to enhance the sensitivity of colorectal cancer cells to Cetuximab by modulating Akt signalling pathways. Resveratrol selectively enhances the expression of Connexin 43, which inhibits Akt activity and mitigates resistance to Cetuximab (Wang et al., 2020). Nonetheless, comprehensive studies regarding its incorporation into antibody-functionalized nanocarriers like MWCNTs have yet to be conducted. Rectifying this deficiency may pave the way for an innovative treatment strategy that utilizes the bioactive properties of phytochemicals alongside antibody-mediated targeting, resulting in enhanced drug retention, reduced systemic toxicity, and improved management of colorectal cancer (Thirumalaisamy et al., 2026).

2. Review of literature

2.1 Review of literature related to colorectal cancer

The deadliest of the most common malignancies, cancer occupies in colorectum, highly rated second among the all cancer for the deaths in women and the third dominating death causing cancer in men globally (Huyghe and coworker 2020). Global risk and mortality rate of cancer occupies in colorectum is predicted to augmented by 61% by 2030, referring published reports (Brand and coworkers, 2017; Huyghe and coworkers, 2020). Colorectal cancer is removed from patients using time-consuming, invasive procedures that have unanticipated side effects under the present diagnosis and treatment approaches. To improve the specificity and affectivity of a new detection technique, more study is required (Bray and colleague, 2019).

Li and coworker (2024) looked into the many signalling mechanisms that lead to colon cancer. Deregulation of all pathways of the signal mechanism in body, consequently the epithelial cells of the colon acquired properties of malignancy, is a clear pathophysiological feature of colorectal cancer. Their goals were to elucidate the general ideas behind the genesis and metastasis of neoplasms and to examine the basic signalling pathways associated with colorectal cancer (CRC). Specifically, they looked at the genetic, epigenomic, and microbiological aspects of colorectal cancer (CRC). They also investigated their ramification on the clinical environment while showcasing the introduction of immunological and targeted therapy for colorectal cancer. In order to identify effective markers within these networks which pharmacologically exploited, a fuller understanding of oncogenic signalling has guided the development of these medicines. They also highlighted their involvement in personalised medicine and talked about how AI might be used to increase the precision of therapy targeting and patient classification.

Roshandel and coworker (2024) investigated prevention, risk factors, and epidemiology. The epidemiology of colorectal cancer (CRC) varies across population, most likely because of variations in living style and environments condition to CRC. For the regulation of the cancer occupies in colon the recommended method is precaution and prevention. First category of prevention added identifying and impeding factors related to dietary beverages, and smoking. and other factors related to the consumption to aspirin. More investigation necessities to clarify the connection between subjection to various and the prevalence of colorectal cancer, Precancerous lesions can also be found and removed to help control colorectal cancer. The development and

enactment of initial screening study related to CRC should take into account a variety of factors like patient preferences, screening method, costs, advantages, and toxic effect. Health policymakers should consider the best option for establishing the screening procedures and the starting age of the target population.

Al-Joufi and Coworker (2022) described the pathogenesis of Colorectal Can at the molecular level and also explored the biomarkers responsible for the origin of cancer occupies in colon. A sequence of alterations related to the genetic and metabolic in the function and structure of the epithelial cells of colon result in the origin of malignant adenoma of colorectal. In-depth research on the mechanisms associated to genetic and metabolic pathway underlying the initiation, progression, and metastasis of sporadic colorectal malignancy has led to the discovery of signature molecules that may be utilised to assess the character and prognosis outside of staging and impact treatment choices.

Al-Joufi and coworkers (2022) examined the biomarkers linked to colorectal cancer pathophysiology and offered a molecular account of the disease's progression. In-depth investigations into the genetic and epigenetic mechanisms underlying the onset, progression, and metastasis of sporadic colorectal cancer have yielded biomarkers that may be utilised to inform treatment choices and forecast behaviour and prognosis beyond staging. Using signature molecules that are variably revealed over the malignant cells, surface modified nano size range particles may deliver lethal drugs. By using different molecules as ligands on the surface of nanoparticles, it becomes easier to engage with malignant cells and deliver anticancer drugs efficiently.

Hossain and coworker (2022) investigated colorectal cancer's carcinogenesis, global epidemiology, present issues, and risk factors. The prevalence and impermanence rate of cancer occupies in the colorectum are increasing in low-income countries, even though the disease accounts for a disproportionately high number of deaths in high-income countries. Colorectal cancer can be totally treated with surgery and medication if detected early. However, recurrence is highly likely, and resistance to cancer medications increases treatment failure. Immediate identification at early stage of colorectal cancer is fairly feasible in industrialised countries in order to increase survival rates. But similar facilities are rarely found in developing countries.

Brar and coworkers (2021) illustrated how nanotechnology employed for accurate diagnosis and cure of cancer occupies in colorectal. They investigated the fact that cancer occupies

in colorectum is the third rated prevalent tumour in people. Adeno-carcinomatous colorectal cancers (CRCs) account for the majority of cases originated as a small polyp through the inner wall of the colon or rectum followed by transformed to malignancy. Whilst colorectal cancer (CRC) has limited treatment options, early detection may be essential for both preventive and therapeutic actions meant to reduce the death rate. Several molecular markers found in colorectal cancer (CRC)-affected tissues may be utilised as a new strategy to develop more sophisticated disease treatment strategies.

2.2 Review of literature related to Current treatment for colorectal cancer

The initial therapy for removable colorectal cancer is surgical excision; immunotherapy, chemotherapy, and radiation therapy are common therapies for nonresectable colorectal cancer. However, some of these treatments' drawbacks include their cytotoxicity to healthy cells and non-specificity, which might lead to further issues (Schuell and colleague 2005). Depending on the extent and progression of colorectal cancer, combinations of these treatments may be employed. However, about 50% of patients relapse into CRC that has established acquired multidrug resistance while receiving combination therapies (Zhou and coworkers 2021).

As per the 2021 statistics, the number of deaths of patients suffering from colorectal cancer is increasing, even with significant improvement in surgical approach, treatment options, and screening approaches. The development of new CRC therapies is necessary to increase the susceptibility of resistant tumours to chemotherapeutic drugs. It has recently been demonstrated that cytokine therapy, immune checkpoint inhibitors, chimeric antigen receptor T cell therapy, and, T cell receptor., mutations are effective treatments for colorectal cancer. Additionally, recent research has demonstrated promising outcomes in the treatment of colorectum malignancy with natural products, RNA-based therapies, microRNA, and RNA aptamer (Liu and coworker 2020), probiotics (Ding and coworker 2020), and oncolytic viral therapies (Fukuhara and coworker 2016). However, there is still a serious problem with survival in patients suffering from an advanced stage. The goal of research into the pathophysiology of colorectal cancer (CRC) is to enhance current therapies like immunotherapy, chemotherapy, endoscopic resection, radiation therapy, and targeted therapy.

Gmeiner and coworkers (2024) investigated an advanced approaches to colorectal malignancy treatment. The use of biomarkers for mCRC stratification enables precision therapy

based on distinct tumour mutational profiles. The colorectum cancer originated due to mutation in the RAS/RAF/MAPK pathway followed by downstream of EGFR signalling increasing the application of EGFR-targeted treatments. But in several extremely deadly mCRC subtypes (like BRAF-mutant), survival rates are rising due to the application of anti-RAS and anti-RAF treatments as well as improved methods to inhibit compensatory signalling pathways. In order to increase the survival, rate the therapy based on the fluoropyrimidine have been used. The advancements in precision oncology must be positioned in respect to future developments in mCRC treatment.

Maurya and coworkers (2024) investigated colorectal cancer's current and targeted therapies. Colorectal cancer (CRC) has historically been treated with three primary options: radiation therapy, chemotherapy, and surgery. However, the investigation of new approaches is required because of their low therapeutic success rates. Patients suffered from the metastatic colorectal cancer possess poor prognosis. Recent efforts to understand the evolution of colorectum malignancy have led to discoveries of key regulatory genes implicated in colorectal cancer and improvements in CRC care. Immunotherapeutic molecule such as 'immune checkpoint inhibitors' and 'CAR T cell-based therapies' have been identified as a result of the complex interaction between the tumour microenvironment and the origination of colorectum malignancy

Pathak and coworker (2024) investigated colorectal cancer management options. Recent advances in molecular characterisation have fundamentally changed their understanding of the heterogeneity within colorectal malignancies, particularly with regard to tumour sidedness. Tumour sidedness, or whether the original tumour is in the left or right colon, is one of the most significant variables influencing prognosis and treatment results in metastatic colorectal cancer. The identification of tumour DNA as a prognostic and predictive tool represents a possible advancement in the screening and regulation of colorectal cancer.

Fadlallah and coworkers (2024) presented a variety of cutting-edge colorectal cancer management techniques. Nowadays, radiotherapy, chemotherapy, and immunotherapy, as well as their combination, are used to treat CRC. Surgery is used to treat cases of the cancer that can be removed. Despite the availability of these alternatives, 50% of CRC cases remain incurable. Due to significant improvements in research methodology, CRC therapy approaches are constantly being updated, resulting in the availability of novel medications and therapeutic approaches.

Adebayo and coworkers (2023) investigated the therapeutic diagnosis and treatment option of colorectal cancer. Prospects for the future and available treatment options. The continuous advancement has been made in the treatment approaches of colorectum cancer. The treatment option includes surgery, chemotherapy, cryotherapy, and radiation therapy. For the treatment of advanced-stage colorectum cancer, chemotherapy is necessities. Examples of this include 5-fluorourecil, irinotecan, oxaliplatin, and leucovorin. The monoclonal antibodies namely vascular endothelial growth factor inhibitors and epidermal growth factor receptor inhibitors have been authenticated by the FDA for the treatment of colorectum cancer. Toxic side effects, off-target effects, and the decrease of efficacy of monoclonal antibodies are the main serious problems that still plague these medications.

Li and coworkers (2023) investigated the different modern and cutting-edge methods of treating colorectal cancer. The main option for individualised and comprehensive CRC treatment is now targeted therapy, thanks to the development of novel targeted drugs. They demonstrated the targeted therapies including the Anti-vascular endothelial growth factor and its receptor, multi-target kinase inhibitors, and epidermal growth factor receptor most prevalent for the treatment of the colorectal cancer. The growing of the application of second-generation sequencing (NGS) technology and advancements in precision diagnosis are leading to the discovery of rare targets such as the KRAS mutation, the BRAF V600E mutation, the HER2 overexpression/amplification, and the MSI-H/dMMR in metastatic colorectal cancer (mCRC). In addition, a great deal of research is being conducted on new therapeutic drugs that specifically target these mutations.

Kumar and coworkers (2023) illustrated several current and developing treatment modalities for colorectal cancer were illustrated. Surgery, a conventional and traditional therapy for removable colorectum malignancy; for unresectable CRC, the combined regimen includes immunotherapy, chemotherapy, and radiation. Despite these tactics, over 50% of individuals have recurring, incurable colorectal cancer. Cancer cells become resistant to the therapeutic efficacy of chemo-based drugs molecule through no. of processes, like drug inactivation, remodelling in influx and efflux process of drug molecule, and overexpression of the 'ATP-binding cassette transporter'. These curb necessities the development of innovative target-specific therapeutic strategies. There are some merging therapies including Probiotics, natural products, oncolytic viral therapies and

non-coding RNA-based therapeutics, and biomarker-driven medications have demonstrated optimum results in preclinical and clinical trials.

Xie and coworker (2020) investigated targeted treatments for colon cancer. Chemotherapy and surgery were the first choices for cancer patients for a long time. The therapies based on the targeting approach has been emerged to augment the survival rate in the patient of CRC. New medications that block numerous critical pathways and immunological checkpoints are emerging at a never-before-seen rate since the anti-EGFR medications cetuximab and bevacizumab proven effective. The increasing number of high-quality clinical trials and the recommended targeted medications are reflected in the ongoing updates to global guidelines.

2.3 Review of literature related to Nanotechnology for colon cancer treatment

Previous research and application of nanotherapeutics leads the development of the various carrier based on the nanoparticles with improved therapeutic and diagnostic application. However, efficacy of the nanotherapeutics in clinical studies impose challenges because of their tedious pharmacokinetics. NPs can further our knowledge of the physiological and biochemical foundations of a number of diseases and their treatments (Siddique and Chow, 2020; Rosado-de-Castro and coworkers 2018). Persistent luminescence nanoparticles have also been used to take use of the long-lasting near-infrared luminescence in optical imaging systems as a unique optical nanoprobe (Lecuyer and colleague 2016). Because of this effect, optical imaging can operate without continuous autofluorescence and excitation (Liu and coworker 2019).

The NPs possess less size, high sensitivity and unique composition which make them a suitable diagnostic agent. NPs, which are also commonly employed to treat cancer, are no different. It improves pharmacological effect and reduces detrimental toxicity by augmenting the accumulation and delivery of pharmacologically active molecules at the diseased location. Moreover, Current studies confirmed that the NPs possess the ability the Co-administered the both pharmacological active molecule and diagnostic compounds which can be easily administer and easily deliver the molecule at diseased location (Siddique and Chow, 2020). Furthermore, research indicated that theragnostic NPs employed in customised nano-medicine to augment the therapeutic efficacy (Baetke and coworker 2015).

The development of multifunctional NPs using a range of functional materials will improve the theragnostic, or simultaneous diagnosis and therapy (Kim and colleague 2017). The application

of nanomedicine as a carrier method for curing of colorectal cancer was examined by Singh and coworker in 2024. In order to treat a range of diseases, including colorectal cancer, numerous developments in nanomedicine have been produced recently, including biological agents, immunotherapeutic agents, and chemotherapeutic drugs.

Wang and coworkers (2024) showed techniques to utilize nanomaterials to ministrations colorectum malignancy orally. The investigation discussed main issues with colorectal cancer treatment, physiological and environmental factors, and necessities for a new oral colon-targeted drug delivery system (OCDDSs). By delivering therapeutic compounds to the location of colonic disease, the OCDDSs can increase bioavailability, reduce systemic adverse effects, and ministrates colorectum malignancy and 'inflammatory bowel disease'.

Freitas and coworkers (2023) presented a nanotechnology that combines therapy including photo and radiation to ministrates colorectum malignancy. Nanomedicine is likely the answer to this issue since it enhances restorative and symptomatic abelites. The 'plasmonic' nano size range particles demonstrate high capabilities because of their application as radiosensitizers in radiotherapy and photothermal treatment agents. Binary function, superior biocompatibility, simple functionalisation, and ability to target enable the efficient induction of cancer cell death with minimal adverse consequences. Application of nano size range particles as radiosensitizers to make malignant tissues more sensitive to radiation has been studied in recent years. Metal-oxide-based, bimetallic, and metallic nanoparticles have all attracted a lot of attention.

Nanomedicine is likely answer to this issue since it augments pharmacological effect and distinctive capacities. Plasmonic nano size range particles demonstrated great dormant because of its binary namely as radiosensitizers in radiotherapy and photothermal treatment agents. Binary function, superior biocompatibility, simple functionalisation, and ability to target enable the efficient induction of cancer cell death with minimal adverse consequences. The application nano size range particles as radiosensitizers to make malignant tissues more sensitive to radiation has been studied in recent years. Metal-oxide-based, bimetallic, and metallic nanoparticles have all attracted a lot of attention. Because tumour in large size is more complicated, phototherapy might not be a suitable treatment on its own for complete tumour eradication without recurrence. Researchers are now investigating various applications of phototherapy in conjunction with other treatments in order to profit from its advantages at the same time.

Gogoi and coworkers (2022) illustrated how nanotechnology can be employed to identify and cure colorectum malignancy. Nanotechnology crucial part of cancer treatment because it can deliver targeted chemotherapy to cancer cells directly and selectively. The simultaneous use of nanoparticles for diagnostic and treatment is one potential use case. Researchers from all over the world have been interested in learning how nanoparticles' fascinating properties might be applied to the initial diagnosis and curing of colorectal cancer.

Carbon nanotubes (CNTs) represent a distinctive and specialized category of nanotechnology-driven drug delivery systems. In contrast to conventional nanocarriers, CNTs possess unique structural and physicochemical characteristics, including a high aspect ratio, elongated form, and exceptionally large surface area, which enhance drug loading efficiency and enable direct cellular infiltration. Its capability for diverse functionalization (both covalent and non-covalent) enhances solubility, biocompatibility, and targeted distribution (Mody et al., 2014). Consequently, the extensive section on nanotechnology must describe the basic fundamentals of nanotechnology drug delivery, whereas the subsequent discourse on CNTs should be confined to their distinctive characteristics and uses.

2.3 Review of literature related to Carbon nanotube for cancer treatment

Since its discovery in 1976 by Oberlin, the carbon fibre structure has captivated significant attentiveness globally because of dormant to revolutionise all facets of nano-based technology (Takakura and collaborators 2019). The three main processes for creating carbon nanotubes are arc discharge, thermal and plasma chemical vapour deposition, and laser ablation. Iijima Sumio made the discovery of carbon nanotubes in 1991 (Naik and coworker 2021). Carbon nanotubes categorized in single-walled (SWCNTs) and multi-walled (MWCNTs). SWCNTs termed as rolled nano size range tubes because MWCNTs possess supplementary carbon nano size range tube encircling the core. Carbon nanotubes are depicted in Figure 1 (He and coworker 2020). Carbon nanotubes with one wall are depicted in Figure 2. A structure resembling fullerene usually covers these tubular structures. Their diameter lies in nanometre while the length lies in centimetres. As per the previous research the carbon nano size range tube possesses the rivet-like properties and this will help to open the new ways for materials research (Song and coworkers 2020). In comparison to diamond, which has a modulus of elasticity of 1.21 TPa's, carbon nanotubes have an extraordinarily high modulus of elasticity of >1 TPa, based on both theoretical and experimental

evaluations (Zhang and coworker 2019a). It is reportedly 10–100 times stronger per unit weight than the strongest steel (Norizan and counterparts 2020).

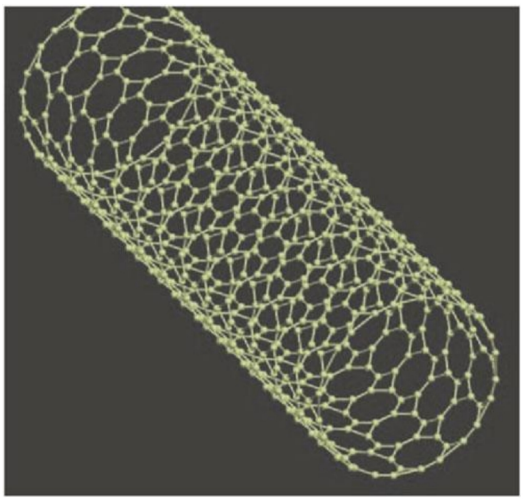


Figure 2.1: Imaged of single-walled carbon nanotubes (SWCNT).

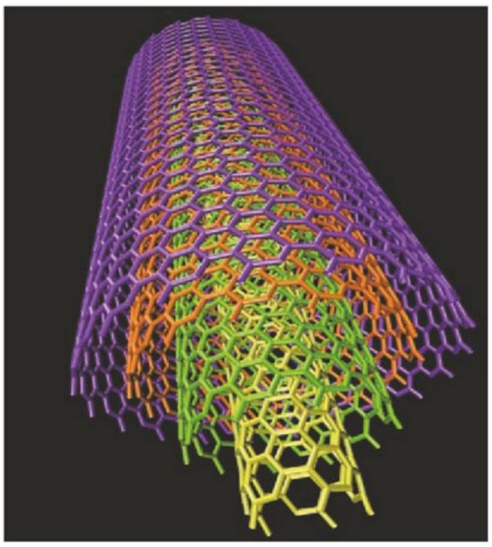


Figure 2.2: Image of multi-walled carbon nanotubes (MWCNT).

These days, many oncology therapy approaches centre on tumour cells and their surroundings. The tumour parenchyma can be successfully and quickly eliminated by focussing on the tumour cells. By interfering with the tumour cells' basic survival needs, targeting the

malignant cell function and its environment, inhibits the growth and spread of malignant cells. As per previous literature carbon nanotube possess the properties like surface for modification, loading of drug, capacity to permeate through the malignant cells therefor it has been emerged a vital candidate for the treatment of the various diseases in a variety of biomedical domains, such as drug delivery carrier, screening and diagnostic agent (Gao and coworkers 2024).

Kumar and coworkers (2025) explored into the supplication of nanotubes in treatment of the malignant cells. These days, carbon nanotubes (CNTs) are cutting-edge instruments that provide novel solutions to problems in diagnosis and treatment. across a range of cancer types. CNTs function as imaging agents for early detection using fluorescence, CT, and MRI. Using biosensors that identify cancer biomarkers for an early diagnosis, they deliver accurate results. CNTs are excellent at accurately administering drugs, increasing their bioavailability, and reducing side effects when it comes to cancer treatment. Their proficiency in photothermal therapy eliminates cancer cells exclusively. Notwithstanding these obstacles, studies on CNT continue to show its revolutionary potential, which may eventually result in more precise diagnosis, more potent treatment, and individualised cancer treatment for a variety of tumours in clinical settings.

Gao and coworkers (2024) explored the use of nanotubes as a nanotechnology technique for cancer treatment. In the last decades researchers took interest in carbon nanotubes as a potential therapeutic candidate in nanomedicine because of its exceptional mechanical, electrical, and physicochemical characteristics. Imaging, drug delivery, and combination therapy are just a few of the numerous possible uses for carbon nanotubes in curing of malignancy. Active ingredient employed in treatment of malignancy can be delivered employing carbon nanotubes, which enable tailored delivery with augment efficacy and lessen toxicity. To completely remove cancer, carbon nanotubes can also be utilised in combination with additional therapeutic treatment approaches like photo-therapy and radio-therapy.

Farani and coworkers (2024) investigated the application of carbon nanomaterials in the ministrations of colorectum malignancy. Nanoparticles are special because they exploit the differences between malignant and healthy cells. Therefore, they can minimally damage healthy tissue while selectively inflicting severe cytotoxicity on cancer cells. The rigid structural properties, biocompatibility, and post-chemical modification capabilities of carbon nanomaterials, including graphene oxide (GO), carbon nanotubes, and nanodiamonds, have prompted a great deal

of research. GO has demonstrated remarkable potential as a cancer therapy material. A number of novel nanoparticle-based therapies, the majority of which contain GO, are currently in clinical trials.

Xie et al., (2024) prepared carbon nanotubes coated with nano-titanium oxide for use in photothermal therapy to treat colorectal cancer. First, TiO_2 nanosheets on the surface are modified to produce nano-TiO_2-coated MCNTs. After that, nano-TiO_2-coated MCNTs are tested for cell compatibility and found to be safe at concentrations between 0 and 200 µg / mL. It's intriguing to observe that nano-TiO_2-coated MCNTs effectively destroy CRC cells when subjected to near-infrared (NIR) laser radiation.

Randive et al., (2023) developed and characterized the surface modified single-walled carbon nanotube for delivery of the oxaplatin in treatment of colon cancer. The current work aimed to adding the folic acid, chitosan, and oxaliplatin to surface modified nano size range carbon tube tidy to capture folate receptors on colon malignant cells. With the use of ultrasonic technology, single-walled carbon nanotubes were under purification steps employing acid digestion process. The obtained compound was subjected to various spectroscopy thermal, morphological and in vitro dissolution tests. SRB and MTT tests were employed to evaluate the in vitro cytotoxicity of active molecules and test formulation against the 'HT29' and 'COLO320DM' cell lines. Additionally, the cell internalization and apoptosis properties of the formulation was accessed employing the progress of apoptosis in cells was examined using flow cytometry.

Naief and coworkers (2023) explored the application of the carbon nano size range tube as the photothermal and photodynamic therapy for the ministrates of colorectum malignancy. The special optical characteristics of carbon nanostructures allow them to transformed the light source into the heat. By inducing surface plasmons, or collective electron oscillations, it augments temperature in local tissue. Numerous treatment modalities have been explored due to the rapid growth of nanomedicine.

Since phototherapy has excellent tumour selectivity, low toxicity, limited invasiveness, and remarkable spatial/temporal controllability, it has attracted a lot of interest. The phototherapy categorized in two types namely photodynamic therapy (PDT) and photothermal therapy (PTT). In PDT, when the tumour cells are exposed to light, reactive oxygen species kill them.

Photothermal agents produce localised hyperthermia when exposed to light, which kills tumours in PTT.

Jin and coworkers (2021) created a carbon nanotube that can administer CpG immunotherapy intratumorally in order to cure colon cancer. According to their research, CNT causes mice's colon cancer cells to absorb more CpG. Only CpG with CNT conjugation was found to strongly activate the NF-κB signal. Also, intratumor injection of CNT-CpG successfully suppressed liver metastasis and local xenograft tumour development. CNT-CpG therapies reduced the frequency of liver metastases from colon cancer cells, significantly extended survival periods, and prevented the formation of local tumours in 75% of animals. They used the human colon cancer cell line HCT116 to demonstrate that CNT-CpG significantly suppressed cell proliferation. CNT-CpG therapy stopped the epithelium from changing into mesenchymal tissue (EMT). In vitro and In vivo colon cancer cells isolated and analysed for EMT marker mRNA levels with and without CNT-CpG therapy. The findings demonstrated a consistent rise in the expression of the epithelial marker E-cadherin by CNT-CpG.

Shejawal and coworkers (2021) developed and described a functionalized carbon nanotube to deliver lycopene to patients with colorectal cancer. Polyvinylpyrrolidone K30 and phosphatidylcholine were used to ensure system stability. It was also assessed for other factors, such as loading efficiency and in vitro release. Several tests were used to investigate cytotoxicity against HT29 and COLO320DM. The system was made, placed in a gelatine capsule coated with enteric, and examined using in vivo roentgenography and drug release parameters. Lycopene demonstrated a loading capacity of 90 ± 0.256% and a 93.81% release at 60 minutes. The in vitro cytotoxicity assessment of the devised system against COLO320DM and HT 29 was found to be superior to that of pure lycopene. By the twelfth hour, batch F2 had an 81% release

Review of literature related to Resveratrol for colorectal cancer

The most common contributing factor to cause colon malignancy is inflammation. Therefore, anti-inflammatory medications may be useful in the management of colorectum malignancy. Previous research demonstrated that resveratrol, a multifunctional component, possess the ability to inhibit inflammation and progress of cancer cell in in colorectal cancer.

Liang and coworker (1999) Pro-inflammatory signalling pathways like NF-kB, pro-inflammatory enzymes like iNOS and COX-2, and TNF-α and IL-1β are all decreased by

resveratrol. Recent studies have demonstrated the downfall of NF-κB-dependent signalling pathways through resveratrol. Resveratrol also boosted apoptotic factors like cleaved caspase-3 and impede TNF-β and TNF-α, which enhanced CRC cell survival, according to another study (Albini and coworkers 2011).

Resveratrol act by impeding the signalling pathways for MMP-9 and vascular endothelial growth factor (VEGF). By blocking MMP-9 and VEGF, resveratrol prevents angiogenesis and metastasis (Boghossian et al., 2012; Kimura et al., 2008).
In carcinomas, integrin-mediated signalling through focal adhesion has been shown to reorganise the cytoskeleton and stimulate tumour development, invasion, and metastasis (Hynes 2002). By boosting the activity of Sirt1, lowering the NF-κB-mediated inflammatory pathway, and impeding the activity of focal adhesion kinase (FAK), resveratrol prevents colorectal cancer cells from growing and invading. As a result, apoptosis rises and focal adhesion molecules fall (Buhrmann and coworker 2017).

Additionally, resveratrol inhibited cell proliferation, β1-Integrin expression, progress of cancer cells, and FAK activation of cells. Resveratrol decreases the sensitivity of NF-kB, which in turn inhibited the end products of NF-κB-dependent genes linked to invasion, metastasis, and mortality (Buhrmann and coworker 2017).

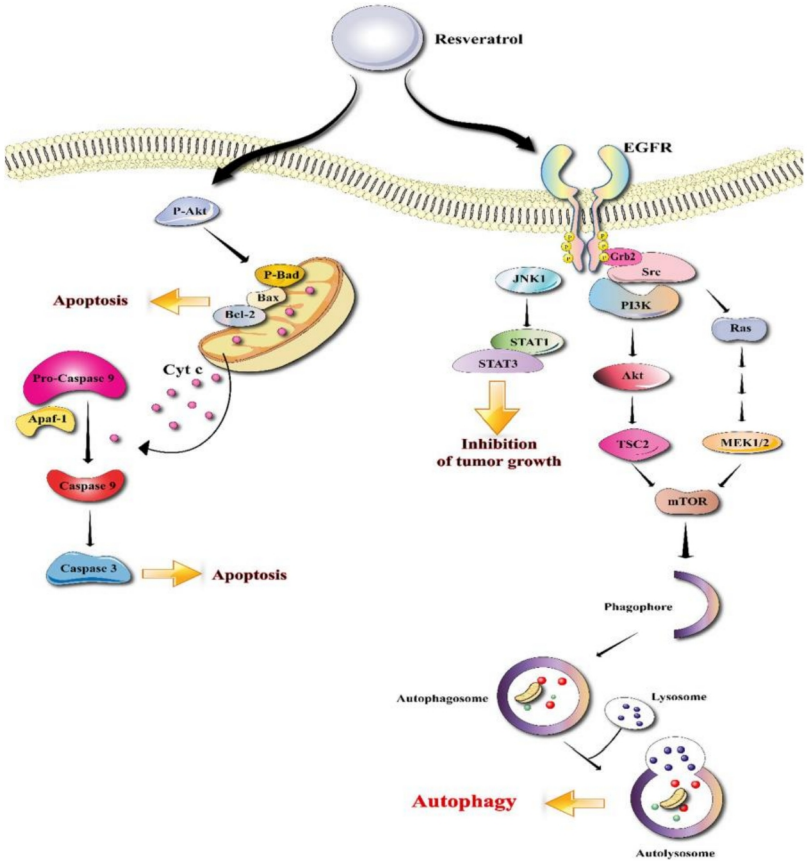


Figure 2.3: Different mechanism of action of resveratrol in the treatment of colorectal cancer

Brockmueller and coworker (2024) demonstrated the application of resveratrol in colorectum malignancy progress. Resveratrol is a naturally occurring polyphenolic phytoalexin that is present in many fruits and vegetables, such as peanuts, berries, and red grapes. Resveratrol effectively chemosensitizers colorectal cancer cells to chemotherapeutic drugs when paired with standard treatments, according to numerous in vitro and in vivo studies. The resveratrol revered the resistance of cells by impeding the several pathways, like transcription factors, proliferation, metastasis, angiogenesis, cell cycle, and apoptosis. The resveratrol capability to alter a number of intracellular pathways that may impede malignant cells plasticity and chemoresistance reversal is essential to comprehending its anti-cancer actions.

Rena and coworkers (2021) demonstrated the way resveratrol can be used to treat cancer. Their objective was to determine the reasons behind the lack of utilisation of resveratrol in cancer treatment. Further development of resveratrol as an anticancer medication is further hampered by

nephrotoxicity that occurs in patients with multiple myeloma. To expedite the journey from bench to bedside, new ideas and tactics have been put forth. Meanwhile, the most promising approach is to use novel formulations to make resveratrol more bioavailable. As an alternative, stronger resveratrol analogues might be created to boost the anticancer effects of the compound.

Moutabian and coworkers (2022) investigated the therapeutic application of combining 5-fluorouracil with resveratrol for the treatment of colorectum malignancy. The groups treated with 5-FU showed more decreasing the proliferation of colorectum malignant cells than the untreated groups, according to the in vitro data. Additionally, the cytotoxicity generated by 5-FU was greatly increased when resveratrol was administered concurrently. According to the in vivo findings, mice given 5-FU showed less tumour growth than the untreated group, and when resveratrol and 5-FU were given together, there was a notable decrease. Furthermore, it was demonstrated that 5-FU, both alone and in conjunction with resveratrol, might control cell cycle colorectum malignant cells

Sudha and coworker (2020) investigated the role of resveratrol. and its nano size range formulation in the curing of the colorectum cancer that are orthotopic and xenograft. Both RSV and NP-RSV dramatically decreased tumour growth and the haemoglobin content of the tumour mass, despite NP-RSV's higher bioavailability and efficiency.

Honari and coworker (2019) demonstrated the role of resveratrol in the treatment of colorectal cancer. The pharmacologic characteristics of the polyphenolic molecule resveratrol include lipid-lowering, hypoglycaemic, anti-inflammatory, and anti-cancer effects. According to several studies, resveratrol may also have a chemo preventive effect on colorectal cancer.

Huang and coworkers (2019) investigated that resveratrol affected chemotherapy-induced drug resistance in colon cancer. Flow cytometry employed to investigate the effects of 5-FU and resveratrol on the growth and proliferation of LoVo and SW480 cells while the western blot employed the investigate the proteins associated with colon cancer were determined. LoVo cell line CD133+ and SW480 proportions were 95.8% and 97.5%, respectively, after flow sorting. The in vitro-cultivated cells differentiated and proliferated more quickly. According to the MTT experiment, the cells with the 5FU group had a lower survival rate ($P < 0.05$) than the blank group LoVo and CD133+ LoVo cells.

Colon cancer cells respond best to a combination of resveratrol and 5-FU; the sorted CD133+ cells are more drug-resistant, and the sorted colon cancer cells have dry stem cells. Early

studies on the drug's mechanism of action suggest that 5-FU and resveratrol cooperate to modulate the BAX gene, which controls apoptosis in CD133+ colon cancer stem cells, while other, more complex mechanisms may be involved.

2.4 Review of literature related to Cetuximab in treatment of colorectal cancer

In 2009, cetuximab was developed as an immunoglobulin monoclonal antibody which can be employed to capture epidermal growth factor receptor (EGFR) (Goldstein and coworkers, 2017). In 2004, cetuximab was accredited from the regulatory agency European Medicines Agency (EMA) and the Food and Drug Administration (FDA). It is also called chimeric monoclonal IgG1 antibody and created from the mammalian cell line (Sp2 /0). It acts by inhibiting the process of the phosphorylation and activation of the receptor-associated kinases (MAPK and PI3K/Akt)' followed by binding to the EGFR receptor, consequently inhibit the growth of the cells, increase apoptosis, and decrease the proliferation of the malignant cells. It also acts by inhibiting the angiogenesis process by reduction of vascular endothelial growth factor production, cetuximab also prevents the development of new blood vessels. However, mutations in particular RAS genes cetuximab is ineffective. Cetuximab is recommended for the curing of metastatic RAS, a wild type colorectal cancer. By inhibiting EGFR signalling, cetuximab may potentially increase radiation cytotoxicity (Farjami and coworker 2019)

Mechanism of Action in cancer

The cetuximab, a IgG1 monoclonal, comprises of the recombinant chimeric antibody, isolated from human/mouse attach to EGFR and inhibit the attachment of the markers like EGF. EGFR, a belong to the ErbB receptor family. In inactivation stage it is occurred as a monomer state, however as it is attached through the transforming growth factor-alpha (TGF-alpha) or epidermal growth factor, it modified to the homodimers or heterodimer with other ErbB receptors. Cancer cells show dysregulation of the EGFR signalling system, which controls cell growth, spreading, proliferation, migration, angiogenesis, and apoptosis.

Cetuximab binds to EGFR more specifically and affinitive than either TGF-alpha or epidermal growth factor, preventing the ligand-induced phosphorylation; of EGFR. Cetuximab also augment the outcomes of irinotecan and radiation in scientific research. When activating mutations are obtained in exon 2 of K-ras, a minor G-protein downstream of EGFR and a crucial

component of the EGFR signalling cascade, EGFR inhibitors lose their effectiveness (Gurdal and coworkers 2019; Agarwal and coworkers 2019).

2.5 Cetuximab mechanism of action in colorectal cancer

Inhibition of EGFR signalling transduction by cetuximab

All mesenchymal and epithelial cells express EGFR, however in different amounts. Numerous examples of EGFR overexpression or deregulation in human malignancies have been made (Nicholson and coworker 2001; Arteaga 2002). The majority patient suffered from head and neck cancer and about 51% of CRC patient demonstrated positive EGFR' tests (Mendelsohn 2001; Mendelsohn 2003). By selectively and selectively binding to EGFR, cetuximab can impede EGFR signalling (Kim and coworker 2001). Additionally inhibiting cell cycle at G1 phase and apoptosis (Prewett and coworker 1996; Fan and coworkers 1997), its dose-dependently impede the proliferation of multiple tumour cell lines (Goldstein and coworkers 1995; Mutsaers and coworkers 2009).

TA-targeted cellular immunity and antitumour activity

Cetuximab contains human immunoglobulin G1 backbones, and it has been demonstrated that chimeric immunoglobulin G1 antibodies efficiently increase the ADCC process of human effector cells, like monocytes, macrophages, and NK cells. Cetuximab-mediated ADCC activity only needs low levels of EGFR expression to have anticancer effects, according to Kurai et al. (2007). Using DC-mediated cross-priming of antigens from cetuximab adhered cancer cells, Correale and coworker (2011) found that this elicited an anticancer response from cytotoxic lymphocytes (CTLs). NK cell–DC cross-talk can also enhance antitumour efficacy when both NK cells and DCs are attracted to the inflammatory areas caused by malignancy (Lee and coworker 2011), potentially lowering the number and activity of immunosuppressive regulatory T cells (Toi and coworker 2010).

Alhajj and coworker (2024) investigated the treatment cost of cetuximab in the curing of colorectum cancer. Its cost-effectiveness in comparison to bevacizumab or other chemotherapy regimens such as FOLFIRI or FOLFOX is being debated. There are disparities in the perceived worth of anti-EGFR drugs like cetuximab in relation to their costs concerning overall survival. Weighing the financial implications against these clinical advantages should be the focus of future research.

Rastin and coworkers (2024) investigated the function and application of immunotherapy in the curing of colorectum malignancy. In current years they Figure out that immunotherapy has originated a very interesting and prevalent cancer treatment option. This innovative approach has effectively established as an emerging cancer treatment pillar by providing new opportunities for treating solid tumours. The creation of new drugs that target immunological checkpoints has great potential as a promising and perhaps revolutionary treatment for colorectal cancer (CRC). Immunotherapy for colorectal cancer has made great strides, yet limitations and obstacles still exist. The immune system is suppressed by the tumour microenvironment (TME) of patients with colorectal cancer (CRC), which leads to a poor response to therapy.

Saoudi González and coworker (2024) explored the ability of cetuximab as a targeted therapy for metastatic colorectal cancer. Cetuximab expands the therapeutic choices and offers hope to patients with mCRC who are not responding to conventional treatments when used in conjunction with immunotherapy and other targeted medications. As new cetuximab-based treatment techniques are discovered through ongoing clinical studies, patients with mCRC have a brighter future.

Zhang and coworkers (2024) examined the application of cetuximab in preventing the development of colorectum malignancy by inhibiting the Wnt/β-catenin pathway and modifying the expression of 'PLCB$_3$'. They investigated how cetuximab treatment affected PLCB$_3$, a potential oncogene of colorectal cancer. They extracted genes that were differently expressed from the GSE140973 and discovered 151 genes associated with the Wnt/β-Catenin signalling pathway. Then, bioinformatics analysis was used to identify the hub gene. During the investigation, 26 overlapping genes were discovered. Higher expression of PLCB$_3$ was linked to a worse prognosis. PLCB3 emerged as a significant oncogene associated with patient outcomes.

In vitro, it was demonstrated that cetuximab cytotoxically affected colorectal cancer cells, whereas PLCB$_3$ knockdown inhibited the proliferation of CRC cells. Additionally, cetuximab treatment decreased the expression of PLCB$_3$ and β-catenin while increasing that of E-cadherin. These outcomes demonstrated that PLCB$_3$ boosted cetuximab inhibition of Wnt/β-catenin signalling. Cetuximab administered in combination with PLCB$_3$ and a Wnt activator (IM12) attributed suppression of CRC invasion, migration, and proliferation.

Zhou and coworkers (2021) examined anti-EGFR treatment resistance in metastatic colorectal cancer. They also investigated the reverse procedure. Cetuximab can add 8.2 months to the life expectancy of those with RAS wild-type (WT) mCRC. Unfortunately, targeted therapy resistance limits its clinical application and efficacy. Tumour resistance mechanisms include both external and intrinsic alterations. There are several well-researched therapy techniques that have been used to combat anti-EGFR mAb resistance.

Microsatellite instability, RAS/RAF/PI3K gene changes, EGFR ligand overexpression, EGFR change, metabolic remodelling, autophagy, and ERBB2/MET/IGF-1R activation are some of the intrinsic pathways. EGFR-targeted inhibitors, metabolic regulators, and a mixture of multitargeted inhibitors are the main treatments for intrinsic processes.

Extrinsic changes mostly interfere with the tumour microenvironment, particularly with angiogenesis, immune cells, and cancer-associated fibroblasts (CAFs). Suppression of CAFs and anti-VEGFR drugs, as well as immune cell modification or activation, are among the instruction.

Wang and coworkers (2020) chose the resveratrol dosages based on safety and mechanistic factors. A concentration of 5 µg/ml was employed for in vitro tests, which successfully inhibited colorectal cancer cell growth while reducing cytotoxicity. By upregulating connexin 43 and preventing Akt phosphorylation, resveratrol has been demonstrated to make cells more sensitive to cetuximab. A daily intraperitoneal dose of 1 mg/kg resveratrol and 2 mg/kg cetuximab was selected in in vivo models to maximize biological activity and minimize systemic toxicity, indicating resveratrol's synergistic effects in the treatment of colon cancer without the interference of high-dose toxicity.

Despite extensive research on nanocarriers for colorectal cancer, the majority rely on traditional methods that exhibit issues with stability and drug release. Limited analyses have compared them with carbon nanotubes, particularly with phytochemical transport associated with antibodies. The lack of such analysis leads to our research on cetuximab-conjugated resveratrol-encapsulated MWCNTs.

3. Hypothesis

Colorectal cancer is the second most common cause of cancer-related deaths globally and accounts for around 10% of all cancer cases, making it the third most common cancer globally. It was anticipated that there were over 1.9 million new cases of colorectal cancer and over 930,000 deaths from the disease globally in 2020. Significant regional differences in the rates of occurrence and death were noted. Colorectal cancer will cause 3.2 million new cases year (a 63% rise) and 1.6 million deaths annually (a 73% increase) by 2040. The bulk of instances occur in those 50 years of age and beyond, primarily affecting the elderly. Colorectal cancer is caused by a number of lifestyle factors, including a sedentary lifestyle, obesity, smoking, excessive alcohol use, a high intake of processed meats, and a poor intake of fruits and vegetables. When there are few therapeutic options, colorectal cancer is frequently discovered at an advanced stage (WHO, 2023).

Limitation of current treatment option for treatment of colorectal cancer

Surgery, radiation, chemotherapy, targeted therapy, and immunotherapy are currently the main treatment methods for colorectal cancer, which makes its management more complicated (Arafat et al., 2022). The patient's age, immune system condition, lifestyle, and tumour stage all affect the therapy decision for colorectal cancer. Considering all of these aspects, a number of traditional treatments have been investigated for the treatment of colorectal cancer (CRC), including surgery, radiation therapy, chemotherapy, herbal and synthetic medications, gene therapy, and cellular therapies (Kamal et al., 2024). They do, however, come with certain restrictions. For instance, surgery works well for cancer that is in its early stages but is ineffective for cancer that has progressed or spread. Some postoperative consequences have also been noted, including anaesthesia-related problems, haemorrhage, and infection. While radiation therapy is less harmful to healthy tissues and has a potent effect on in situ cancers, it can be difficult to precisely identify early metastases and may also result in sexual and bladder disorders. As a result, postoperative chemotherapy is still required to lower the chance of recurrence. For the majority of cases that neither surgery nor radiation therapy can resolve, chemotherapy is still the best option. First, palliative chemotherapy can reduce the growth of colorectal

cancer in individuals with advanced disease, extending and improving their quality of life. As a neoadjuvant or adjuvant therapy, chemotherapy is also an essential treatment for preventing colorectal cancer from reoccurring and spreading (Chen et al., 2024).

The Food and Drug Administration has licensed a number of chemotherapy medications, such as 5-fluorouracil (5-FU), irinotecan (IRI), oxaliplatin (OXA), and capecitabine, for the treatment of colorectal cancer (CRC) (Matos et al., 2019). Unfortunately, limiting factors like drug resistance, nontargeted drug delivery, the unfavourable systemic side effects of conventional chemotherapy, and the poor water solubility of some chemotherapeutics still resulted in poor clinical benefits and negatively impacted patient acceptance and quality of life (Chen et al., 2024). Combination therapy has been employed as an alternate therapeutic strategy to cancer monotherapy in order to solve these shortcomings. In addition to overcoming medication resistance, combining therapeutic drugs with distinct mechanisms of action has shown significant promise for obtaining synergistic therapeutic benefits with fewer side effects (Bayat Mokhtari et al., 2017). In the clinical treatment of colorectal cancer (CRC), a number of combination chemotherapy regimens are often employed, including FOLFIRI (folinic acid, 5-FU, and IRI), XELOX/CAPOX (OXA and capecitabine), and FOLFOX (folinic acid, 5-FU, and OXA) (Moradi-Marjaneh et al., 2019). However, even with ongoing efforts to improve chemotherapy for colorectal cancer, the prognosis remains poor, especially for patients with metastatic CRC (Ginghină et al., 2021).

Application of resveratrol in treatment of colorectal cancer

Resveratrol (trans-3, 4′, 5-trihydroxystil bene), a phenolic molecule derived from the stilbene family, is found in nuts, pines, berries, and especially the skin of red grapes (Rotelli et al., 2015). According to Shankar et al. (2007), resveratrol has anti-oxidant, anti-inflammatory, and vasodilatory properties because it prevents lipid peroxidation and thrombocyte aggregation. Resveratrol was recently discovered to trigger autophagy in cancer cells (Wang et al., 2018). Resveratrol has been shown to increase immune cells' production of a number of pro-inflammatory cytokines, which ultimately increases cytotoxicity against cancer (Trung, 2018). There is evidence linking this safe and

multitargeted natural chemical to the inhibition of cancer cell invasion and survival (Buhrmann et al., 2018).

Application of the Cetuximab in colorectal cancer

An IgG_1 monoclonal antibody called cetuximab, which is designed to target EGFR, works by preventing tyrosine kinase (TK) activity after EGFR binding. This contact causes intracellular signal transduction pathways to be disrupted, which has a variety of effects, including an increase in cell death, a decrease in matrix metalloproteinase synthesis, and a suppression of cancer cell growth. By directly targeting EGFR, cetuximab can produce a variety of antitumour effects that can enhance the effectiveness of conventional chemotherapy, which is why it plays such a significant role in the treatment of colorectal cancer. A more customized and targeted therapeutic strategy can be given to patients with metastatic colorectal cancer by physicians by incorporating cetuximab into treatment regimens. Such integration is expected to reduce treatment-related toxicity and improve survival results (Zhang et al., 2024).

Application of Cetuximab decorated resveratrol loaded nanotube for treatment of colorectal cancer.

Chemotherapy alone or in combination is limited by its poor solubility, short half-life, rapid metabolism of anticancer drugs, lack of tumour site selectivity, non-specific biodistribution, and consequent failure to achieve effective therapeutic concentrations at the action sites (Entezar-Almahdi et al., 2020; Arshad et al., 2020). The pharmacokinetics, metabolism, and toxicity of resveratrol have been evaluated in cancer patients as well as healthy individuals (Patel et al., 2011). Resveratrol breaks down quickly, mostly into conjugates of glucuronide and sulfate, which are subsequently excreted in the urine. Because resveratrol has a fast metabolism and a low bioavailability, researchers have used high dosages (up to 5 g/day). Studies have indicated that this polyphenolic molecule appears to be well tolerated and safe. However, taking more than 1 g of resveratrol per day was associated with negative side effects, including diarrhoea, nausea, and stomach pain (Patel et al., 2011). Consequently, this dose limitation is being investigated in clinical trials

(Patel et al., 2011; Chow et al., 2010). Because of its low bioavailability, resveratrol's effects on humans are difficult to extrapolate, and many strategies have been explored to improve its bioavailability. The existing approaches for early detection and treatment of colorectal cancer (CRC) are imprecise, have side effects, and cause cancer cells to become resistant. In this context, nanoparticles can be helpful since they are efficient therapeutic and diagnostic tools that also lessen negative effects by making medications more soluble when placed into structured sequences. Nanoparticles that have a limited ability to accumulate in off-target organs like the liver, kidney, or spleen can be used to specifically target tumour cells. Therefore, a lot of thought needs to be given to nanomedicine in order to treat CRC. Because of their inherent qualities—such as their large surface area, flexible structure for cargo contacts and effective loading, superior stability, biocompatibility, and the ability to release drugs at specific sites thanks to their nanoneedle morphology—carbon nanotubes (CNTs) have been regarded as appealing candidates for both drug delivery and nanomedicine. Due to these characteristics, CNTs are widely used in imaging, diagnostics, drug release monitoring, and the development of biosensors for associated medical applications. According to the previously stated properties, carbon nanotubes (CNTs) are utilized in lab-on-a-chip systems because they can also convert near-infrared radiation into heat (Ma et al., 2023). To optimize drug delivery to tumour tissues and reduce toxicity in healthy tissues, novel platforms have been created. Targeted therapy for colorectal cancer may be possible with the coupling of a ligand, especially monoclonal antibody (mAb), to a drug delivery system. The Food and Drug Administration (FDA) approved cetuximab as an anticancer monoclonal antibody in 2004 (Falahzadeh et al., 2024). The use of cetuximab, particularly cetuximab scFv, in a variety of nano formulations for targeted drug delivery has improved therapeutic potential for the treatment of many cancer types, according to the field of nanomedicine. There have also been a few documented instances of cetuximab–CNT conjugates that have strong targeting capabilities against cells that overexpress EGFR. To the best of our knowledge, however, there has never been a documented instance of resveratrol delivery using cetuximab-labelled carbon nanotubes.

Utilizing this Mba's remarkable targeting effectiveness to guide filled CNTs to colorectal tissue piqued our curiosity (Spinato et al., 2016).

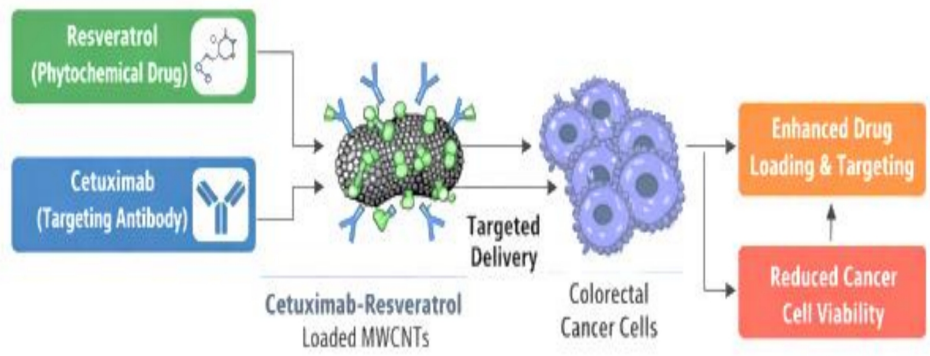


Figure 3.1 Conceptual model illustrating the hypothesis

3.1 Aim

Development And Evaluation of Cetuximab Anchored Resveratrol Loaded Multi Walled Carbon Nanotubes for The Treatment of Colorectal Cancer.

3.2 Objective

- To develop Resveratrol and Cetuximab loaded multi-walled carbon nanotubes formulations.
- To determine the toxicity of drug-loaded multi-walled carbon nanotubes formulations.
- To perform stability studies
- To estimate the anticancer potential of developed multi-walled carbon nanotubes formulations.

❖ **Elaboration of each objective respectively**

- ✓ For efficient drug loading and antibody conjugation, surpassing traditional carriers like polymeric nanoparticles or liposomes owing to their extensive surface area and easily modified surface.
- ✓ Demonstrating their diminished off-target effects and their ability to protect RES from deterioration.

- ✓ for understanding physiological and storage condition parameters for physicochemical integrity, colloidal stability and efficacy of antibody conjugation.
- ✓ Highlighting the role of MWCNTs in enhancing therapeutic efficacy by increasing penetration into tumour cells.

Table 4.1. List of Materials Utilized

Material	**Source**
Acetic acid	S.D fine chemicals, India
Acetone	Loba Chemie Private Limited, India
Methanol (HPLC grade)	Rankem, India Limited., India
Buffer capsules pH 7.0 ± 0.05	Qualigens fine chemicals, India
Chloroform	Loba Chemie Private Limited, India
COOH-MWCNTs	Adnano Technologies Pvt Ltd, India
Cetuximab	Lupin Limited
Dialysis membrane-110 (LA395)	Himedia Lab Private limited, India
Formaldehyde	Loba Chemie Private Limited, India
Formic acid	Qualigens Fine Chemicals, India
Hydrochloric acid	Loba Chemie Private Limited, India
Millipore water	Bio-Age Equipment Ltd., India
n-octanol	Loba Chemie Private Limited, India
NH_2-MWCNTs	Adnano Technologies Pvt Ltd, India
Potassium dihydrogen orthophosphate anhydrous purified	Central Drug House Pvt. Ltd., India
Sodium chloride 99.5% extra pure	Loba Chemie Private Limited, India
Sodium hydroxide	Loba Chemie Private Limited, India
Sodium acetate	S.D fine chemicals, India
Sodium phosphate dibasic anhydrous 98% Purified	Loba Chemie Private Limited, India
t- Resveratrol	Changsha Huir Biological-Tech Co.,Ltd

Table 4.2. List of instruments and equipment utilized

Instruments/equipment	**Model/Manufacturer details**
Analytical balance	AX200 Shimadzu Analytical Pvt. Ltd., India
Atomic force microscopy	Veeco (XE100), Plainview, New York, United States
Differential scanning calorimetry	Perkin Elmer, Waltham, Massachusetts, United States
Digital ultrasonic cleaner	LMUC-4 Labman Scientific Instruments Serial No: L10321, India
Diode array detector	SPD-M20A Shimadzu, Japan
FTIR spectroscopy	Perkin Elmer, Waltham, Massachusetts, United States
Hot air oven	Q-5247, Navyug, India
HPLC	Waters, USA
Nylon membrane filter (0.45 µm)	Millipore, Germany
Nylon syringe filter (0.22 µm)	Millipore, Germany
Nanoparticle size analyzer	Malvern Zetasizer, Nano ZS90, Malvern Panalytical Ltd., UK
NMR spectroscopy	Avance NEO 500mhz, FT-NMR spectrophotometer, Bruker, Switzerland
Optical microscope	KYOWA, Getner Instruments Pvt. Ltd., Japan
pH meter	Phan, Lab India, India
Raman spectroscopy	Bruker RFS 27 MultiRAM FT Raman Spectrophotometer, Switzerland
Field emission Scanning electron Microscopy	Jeol, Akishima, Tokyo, Japan

Transmission electron microscopy	JEM-2100 plus Electron microscope, Jeol Ltd., Japan
Tissue homogenizer	REMI RQ-1, India
Ultracentrifuge	REMI, RM-12C, REMI Elektrotechnik Ltd., India
UV Spectrophotometer	UV-1800, Shimadzu Co.Ltd., Kyoto, Japan
Stability chamber	REMI-WSC 100, India
X-Ray Diffraction	Bruker, Switzerland

4.Experimental work

4.1 Preformulation study of resveratrol

4.1.1 Melting point

The pharmacopeial approach was used to demonstrate the melting point of the active component in resveratrol in its bulk condition by using a glass capillary tube and the melting point equipment. The sample was moved from the capillary's open end to its closed end by tapping on the hard surface. The tapping procedure was repeated until the sample reached the appropriate capillary tube length. The melting point device was used to charge the sample that contained the capillary tube. The melting point device's temperature was gradually raised, and as the temperature changed, the sample's condition changed as well. The range of the temperature at which the solid state of the sample was transformed into the liquid state was recorded. The activity was performed in a triplicate manner. (Pharmacopeiaǁ, 2021)

4.1.2 UV calibration plot

4.1.2.1 Determination of absorption maxima

Precise 10 mg of resveratrol was added into 10 mL of volumetric flask containing methanol solvent with use of sonication, result in a solution namely stock solution I of 1000µg/mL. An aliquot of 1mL was obtained out of the stock solution and transferred to the 10mL volumetric flask to create a stock solution II concentration of 100 µg/mL. Sample was diluted employed methanol solvent as a diluent, until it reached the flask's mark. From stock solution II, a 0.5 mL aliquot was taken out and put into the 10 mL volumetric flask. The methanol solvent was used as a diluent to dilute the sample until it reached the flask's mark, producing a working solution of 5µg/mL. Solution was labeled and stored till further use. The activity was performed in a triplicate manner (Bancuta et al. 2015).

4.1.2.2 Preparation of standard plot in water

Precise 10 mg of resveratrol was added into 10 mL of volumetric flask containing methanol solvent with use of sonication, result in a solution namely stock solution I of 1000µg/mL. An aliquot of 1mL was obtained out of the stock solution and transferred to the 10mL volumetric flask to create a stock solution II concentration of 100 µg/mL. The sample was diluted employed methanol solvent as a diluent, until it reached the flask's mark. The standard calibration curve in the concentration range 1µg/mL to 4.0µg/mL was

prepared from the stock solution II of concentration 100µg/mL. A series of the aliquots 0.1mL, 0.15mL, 2.0mL, 2.5mL, 3.0mL, 3.5mL and 0.40 were withdrawn from the stock solution II and diluted up to 10mL separately. Each solution was diluted up to the mark of the flask using the water as diluent resulting in a series of the working solution 1µg/mL to 4.0µg/mL. Each working solution was scanned ranging 200-400nm using the UV spectrophotometer. The absorbance of each working solution was recorded at the absorption maxima of the resveratrol (Bancuta et al. 2015).

4.1.2.3 Preparation of standard plot in Phosphate Buffer Saline (PBS) 7.4

Precise 10 mg of resveratrol was added into 10 mL of volumetric flask containing methanol solvent with use of sonication, result in a solution namely stock solution I of 1000µg/mL. An aliquot of 1mL was obtained out of the stock solution and transferred to the 10mL volumetric flask to create a stock solution II concentration of 100 µg/mL. The sample was diluted employed methanol solvent as a diluent, until it reached the flask's mark. The standard calibration curve in the concentration range 1µg/mL to 8µg/mL was prepared from the stock solution II of concentration 100µg/mL. A series of the aliquots 0.1mL to 0.8 were withdrawn from the stock solution II and diluted up to 10mL separately. Each solution was diluted up to the mark of the flask using the phosphate buffer pH 7.4 as diluent resulting in a series of the working solution 1µg/mL to 8µg/mL. Each working solution was scanned ranging 200-400nm using the UV spectrophotometer. The absorbance of each working solution was recorded at the absorption maxima of the resveratrol (Bancuta et al. 2015).

4.1.3 Partition coefficient

The partition coefficient characteristic of the chemically active component resveratrol was evaluated in a 1:1 mixture of n-octanol and water using the shake flask method. The excess resveratrol drug was put in a glass tube with 20mL of a 1:1 mixture of n-octanol and water, and it was then stored in a water shaker set at 37°C and 100 rpm for a 24hr. After being taken out, the test samples were moved to the separating funnel and left there to separate the two layers. For fifteen minutes, each layer was centrifuged at 10,000 rpm. After being moved to the volumetric flask, the supernatant was diluted with methanol. Every sample was scanned with the UV spectrophotometer ranging 200- 400 nm. The

absorbance of each sample was recorded at the absorption maxima of the resveratrol and amount of resveratrol was determined using the standard calibration curve (Andrés et al. 2015).

$$Partition\ coefficent \frac{\text{Conc. of drug in Octanol}}{\text{Conc. of drug in water}} \ldots\ldots\ldots\ldots\ldots\ldots\ldots\ldots\ldots\ldots\ldots\ldots\ldots\ldots 4.1$$

4.1.4 Differential Scanning Calorimetry (DSC)

The resveratrol's DSC analysis was done to examine its thermal characteristics, such as its melting point. The sample's thermogram was recorded using a Perkin Elmer DSC 6000 DSC. The sample was moved to a DSC pan and put into the instrument's furnace. The sample was scanned in a nitrogen environment at temperatures between 20°C and 450°C at a scanning rate of 10°C/min (Zu et al. 2016).

4.1.5 Fourier Transform Infrared Spectroscopy (FTIR) spectra

FTIR, or Fourier Transform Infrared Spectroscopy, employed to examine the materials' distinctive functional group. The current work used a PerkinElmer 1750 FTIR (Beaconsfield, U.K.) to record the FTIR spectra of resveratrol. After the sample was combined with the dried KBr, it was shaped into a pellet. The test samples' pellets were scanned ranging 4000 and 400 cm^{-1} in order to gather the spectrum (KA et al. 2011).

4.1.6 Field Emission Scanning Electron Microscope (FE- SEM)

FE-SEM (JEOL JSM-7610F Plus) imaging employed to assess the topography of the resveratrol medication. A picture was taken from powders that were directly spread on conducting tape after a drop of an aqueous suspension of the test sample evaporated. Moreover, a uniform was produced by using ultrasonication to disperse the dried sample in water at a concentration of 2 mg/10 mL. With a few flakes precipitating, the prepared suspensions stayed stable for a longer amount of time. The material was examined at various magnifications and imaging resolutions (Shen et al. 2007).

4.1.7 X-Ray Diffraction (XRD)

An automatic Bruker D8 (Bruker Corporation, Billerica, MA, USA) Advance diffractometer was used to create X-ray diffraction patterns in reflection using nickel-filtered Cu–Kα 20 radiation in order to examine the crystalline characteristics. The scan range for the sample was 10–100° 2θ. Every sample's diffraction graph was captured (Dong et al. 2018).

4.1.8 Development of HPLC Methods

4.1.8.1 Chromatographic Conditions and Instrumentation

The HPLC (Waters, USA) instrument consists of a single pump 515, UV/Vis light detector 2489 along with a Rheodyne injector. The chromatographic procedure was separated using a Waters C18 column (250 mm × 4.6 mm I.D., 5 µm) at room temperature. Octadecylsilane, or C18, is made up of eighteen carbon atoms. Only eight carbon atoms make up Octylsilane (C8), which is bonded to silicon (Si) in the column parking. C18 has a higher resolution than C8. Software called Waters Empower 3 was used for the results' collecting and processing. Methanol to water ratios of 60:40, 50:50, 40:60, and 20:80 was among the several that were evaluated before the mobile ratio was finalised. The system flow rate was set at 0.8 mL/min, and the mobile phase ratio stayed at an isocratic 40% methanol to 60% water ratio. The analyses were performed at 308 nm and injection volume was set at 10 µL (Srivastava et al., 2024)

4.1.8.2 Safety measures

All studies were carried out in low light, and the samples were kept at room temperature with protection from the sun to avoid photochemical isomerisation from the trans- to cis-form.

4.1.8.3 Identification of retention time

A precise measurement of 10 mg of t-RES was carefully shifted to a 10 mL capacity volumetric flask. Initially, 2 mL methanol introduced and thoroughly agitated until the drug was completely dissolved after that solution was diluted up to 10 mL (stock solution I - 1000 µg/mL). Now withdraw 1 mL of stock solution and further diluted up to 10 mL (stock solution II-100 µg/mL). The working solution of concentration 2µg/mL prepared from the stock solution II of concentration 100µg/mL. An aliquot of 0.2mL removed from the sub stock solution II and diluted up to 10mL separately. The solution was diluted up to the mark of the flask using the methanol as diluent resulting in a working solution of concentration 2µg/mL was prepared. The working solution was filtered through the 0.2µ membrane filter paper and charges in the HPLC. The HPLC chromatogram of each working solution was recorded and determined the area (Chudoba et al., 2021).

4.1.8.3.1 Preparation stock solution

A stock solution I of concentration 1000µg/mL was get ready by solubilizing the amount 10mg of trans resveratrol in a 10mL volumetric flak containing 2mL of methanol as diluent solvent with aid of the sonication. A stock solution II concentration 100µg/mL was prepared by diluting the 1mL of stock solution I to the 10mL in a volumetric flask. The sample was diluted up to the mark of the flask using the methanol solvent as diluent.

4.1.8.3.2 Preparation working solution

The standard calibration curve in concentration range 2µg/mL to 10µg/mL was get ready from the sub stock solution II of concentration 100µg/mL. A series of the volumes 0.2mL, 0.4mL, 0.6mL, 0.8mL, to 1mL of sub stock solution II and diluted up to in 10mL volumetric flask separately. Each solution was diluted up to the mark of the flask using the methanol as diluent resulting in a series of the working solution 2µg/mL to 10µg/mL. Each working solution was filtered through the 0.2µ membrane filter paper and charges in the HPLC. The HPLC chromatogram of each working solution was recorded and determined the area (Chudoba et al., 2021).

4.1.8.4 Method Validation

The devised HPLC technique of resveratrol was validated to show that it was appropriate for its intended use. Following the ICH requirements, the HPLC method was validated. During the validation process, numerous criteria were reviewed and evaluated, including precision, accuracy, range, linearity, robustness, and limit of detection and quantification (LOD and LOQ) (Jain et al., 2007).

4.1.8.4.1 System Suitability

Six sequential injections of the working solution were used to test the system suitability parameters. Theoretical plates, retention time, mean, standard deviation (SD), and percentage relative standard deviation were calculated.

Process:

A stock solution I of concentration 1000µg/mL get ready by solubilizing the 10mg of trans resveratrol in a 10mL volumetric flak containing 2mL of methanol as diluent solvent with aid of the sonication. A stock solution II concentration 100µg/mL get ready from the stock solution I by withdrawing an aliquot of 1mL and transferred to the 10mL volumetric flask. The sample was diluted up to the mark of the flask using the methanol solvent as diluent.

The working solution of concentration 5µg/mL was prepared by withdrawing an aliquot 0.5mL from the sub stock solution II of concentration 100µg/mL and transferred to the 10mL volumetric flask separately. The solution was diluted up to the mark of the flask using the methanol as diluent. The working solution was filtered through the 0.2µ membrane filter paper and charges in the HPLC. The HPLC chromatogram of working solution was recorded and determined the area (Kowalska et al., 2020).

4.1.8.4.2 Limit of Detection and Limit of Quantification

The limit of quantification revealed as lowest quantity of drug that could be estimated, whereas the limit of detection (LOD) revealed as lowest quantity could be detected, separated from the background, and measured. The slope of the usual linear equation of resveratrol and its intercept was used to calculate the LOD and LOQ parameters. Equations such as these were used to establish the limits of quantitation (LOQ) and detection (LOD):

$$LOD=3.33\times\sigma/S \quad \ldots\ldots 4.2$$

$$LOQ=10\times\sigma/S \quad \ldots\ldots 4.3$$

where σ represents the standard deviation of the response, while S represents the slope of the calibration curve (Patel et al., 2021)

4.1.8.4.3 Range and Linearity

The linearity parameter of the resveratrol drug in methanol solvent was evaluated by analyzing five working solutions of concentration 2µg/mL to 10µg/mL. A stock solution I of concentration 1000µg/mL get ready by solubilizing the 10mg of trans resveratrol in a 10mL volumetric flak containing 2mL of methanol as diluent solvent with aid of the sonication. A stock solution II concentration 100µg/mL get ready by diluting 1mL of stock solution I to the 10mL in a volumetric flask. The sample was diluted up to the mark of the flask using the methanol solvent as diluent. The standard calibration curve in concentration range 2µg/mL to 10µg/mL get ready from the sub stock solution II of concentration 100µg/mL. A series of the volumes 0.2mL, 0.4mL, 0.6mL, 0.8mL, to 1.0mL pullout from the sub stock solution II and transferred to the 10mL volumetric flask separately. Each solution was diluted up to the mark of the flask using the methanol as diluent resulting in a series of the working solution 2µg/mL to 10µg/mL. Each working solution was filtered

through the 0.2µ membrane filter paper and charges in the HPLC. The HPLC chromatogram of each working solution was recorded and determined the area. The standard calibration curve was plotted and slope and intercept of the standard linear equation was determined. The acquired data were analysed using Microsoft Excel and the least squares approach for linear regression (Patel et al., 2021).

4.1.8.4.4 Accuracy

The proportion of the originally injected drug that was successfully retrieved from the processed samples was determined. Through the analysis of nine samples, the developed approach's accuracy was assessed. Three different levels of enrichment were applied to test samples (marketed tablet and Pure t-RES combined with t-RES loaded MWCNT formulation) with a reported concentration of 6 µg/mL: 80%, 100%, and 120%. Moreover, the recovery % was computed (Susmitha et al., 2022).

Process: A stock solution I of concentration 1000µg/mL get ready by solubilizing 10mg of trans resveratrol in a 10mL volumetric flak containing 2mL of methanol as diluent solvent with aid of the sonication. A stock solution II concentration 100µg/mL get ready from the stock solution I by withdrawing an aliquot of 1mL and transferred to the 10mL volumetric flask. The sample was diluted up to the mark of the flask using the methanol solvent as diluent. For accuracy parameters the working solution at three different level 80%, 100% and 120% or concentration 4.8µg/mL, 6µg/mL and 7.2µg/mL were prepared from the sub stock solution II of concentration 100µg/mL. Three different aliquots 0.48mL, 0.6mL, and 0.72mL from the sub stock solution II were added in volumetric flask containing test sample. Each solution was diluted up to the mark of the flask using the methanol as diluent. Each working solution was filtered through the 0.2µ membrane filter paper and charges in the HPLC. The HPLC chromatogram of each working solution was recorded and determined the area. The amount of resveratrol in each sample was determined using the standard linear equation.

4.1.8.4.5 Precision

Repeatability and intermediate precision are the components of the precision parameters. While six injections of the 6 µg/mL working solution were analysed in six different days for intermediate precision, the repeatability parameter was assessed by

analysing the six injections on the same day. Repeatability parameter was determined by estimating six injections of LQC, MQC, and HQC samples. The concepts of intraday, inter-day, and inter-analyst precision include the concept of intermediate precision. The inter-day experiments involved six injections of the LQC, MQC, and HQC samples over a three-day period. The intra-day analysis involves the assessment LQC, MQC, and HQC samples six times in a single day. Different analysts conducted inter-analyst analysis, injecting LQC, MQC, and HQC samples six-fold each. The experiments were conducted with precision under identical conditions on the same day (Khursheed et al., 2022).

$$\text{Absolute recovery } \frac{\text{Actual concentration recovered}}{\text{Theoretical concentration}} \times 100 \ldots\ldots\ldots\ldots\ldots\ldots\ldots 4.4$$

4.1.8.4.6 Robustness

The resilience parameters were assessed by implementing modifications to the experimental settings, including changes to the ratio of the mobile phase components (methanol: water) at different proportions (62:38, 60:40, and 58:42 v/v) and the flow rate (1.2, 1, and 0.8 mL/min). The procedure's intermediate concentration, 6 mg/mL, was administered six times in distinct runs, and the resulting recovery percentage, peak area, and retention length were recorded (Khursheed et al., 2022).

Process: A stock solution I of concentration 1000µg/mL get ready by solubilizing 10mg of trans resveratrol in a 10mL volumetric flak containing 2mL of methanol as diluent solvent with aid of the sonication. A stock solution II concentration 100µg/mL get ready from the stock solution I by withdrawing an aliquot of 1mL and transferred to the 10mL volumetric flask. The sample was diluted up to the mark of the flask using the methanol solvent as diluent. A working solution of concentration 6 µg/mL get ready from the sub stock solution II of concentration 100 µg/mL. An aliquot 0.6 mL was withdrawn from the sub stock solution II and relocated separately to the 10mL volumetric flask containing test sample. The solution was diluted up to the mark of the flask using the methanol as diluent. Each working solution was filtered through the 0.2µ membrane filter paper and analyzed using HPLC.

4.1.8.4.7 Force Degradation Studies

The method's specificity was assessed by subjecting a drug solution with a known concentration to a range of circumstances. These included being exposed to 1 mL of each

of the following: oxidising (30% H_2O_2 v/v for 24 hours), basic (0.1 M NaOH for 24 hours), acidic (0.1 M HCl for 24 hours), thermal stress (50°C for 24 hours), and photolytic degradation (for 24 hours). The solutions were diluted and properly treated before being tested to look for the drug peak and any degradation products (Susmitha et al., 2022).

4.2 Preformulation study of carbon nanotube

4.2.1 Physical appearance

The current study involves the investigation of the physical appearance parameters like colour, texture of the carbon nanotubes.

4.2.2 Fourier Transform Infrared Spectroscopy (FTIR) spectra

The distinctive functional group of the samples examined using Fourier Transform Infrared Spectroscopy (FTIR). The FTIR spectra of functionalised and plain multi-walled carbon nanotubes were obtained for the current investigation using a PerkinElmer 1750 FTIR (Beaconsfield, U.K.). The dried KBr was combined with the sample, which was then shaped into a pellet. The spectrum was obtained by scanning the test sample pellets between 4000 and 400 cm^{-1}. (Eren et al. 2016).

4.2.3 Field Emission Scanning Electron Microscope (FE- SEM)

FE-SEM imaging (JEOL JSM-7610F Plus) was engaged to compare the topography of functionalised amino multi-walled carbon nanotubes to that of pristine multi-walled carbon nanotubes. After a drop of the test sample's aqueous suspension evaporated, a picture of the powders spread out directly on conducting tape was taken. Additionally, using ultrasonication to disperse the dried sample in water at a concentration of 2 mg/10 mL produced a consistent. For extended periods of time, the prepared suspensions stayed stable, but some flakes did precipitate. Images were taken at various resolutions and the sample was examined at various magnifications. (Shen et al. 2007).

4.2.4 X-Ray Diffraction (XRD)

An automatic Bruker D8 (Bruker Corporation, Billerica, MA, USA) Advance diffractometer was used to create X-ray diffraction patterns in reflection using nickel-filtered Cu–Kα 20 radiation in order to examine the crystalline characteristics. The scan range for the sample was 10–100° 2θ. Every sample's diffraction graph was captured (Eren et al. 2016).

4.2.5 Zeta Size and Potential

The carbon nanotube test sample's size and surface charge were evaluated using photon correlation spectroscopy (Malvern Instruments, Nano ZS-90, U.K.). After the sample was moved to the volumetric flask, it was diluted with Demineralised DDW at 25°C until it reached the flask's mark with the help of a 40W sonicator for one minute. The polystyrene cuvettes were filled with the sonicated sample. The particle size analyser was filled with the cuvette-containing sample, and it was scanned at 25°C. A graph of the particle size distribution was captured. To determine the zeta potential, the sample was moved to the zeta cuvette and scanned to determine the sample's surface charges (Prajapati et al. 2019).

4.3 Formulation of Resveratrol loaded Carbon Nanotubes

250 mg of precisely weighed resveratrol was added to a beaker containing methanol solvent, and the mixture was sonicated for one minute to produce a clear solution. 250 mg of precisely weighed MWCNT was dissolved in the resveratrol alcoholic solution while being stirred at 150 rpm and room temperature. Stirring was continued for 48 hours in the dark until equilibrium was reached. The sample was subject to centrifugation for 40 minutes at 10,000 rpm. The produced pellet dried in a desiccator for 48 hours after being cleaned three times with distilled water. The sample was marked and kept in a container that was properly sealed (Amine-CNT, carboxylic acid-CNT). (Ali and Radwan 2021).

Table 4.3: Different parameter for drug optimization

Sr.No.	Formulation code	Drug amount (in mg)	Carrier Amount (in mg)	Carrier
1	RES-MWCNT 1	250	250	Amine-CNT
2	RES-MWCNT 2	250	250	Carboxylic Acid-CNT
3	RES-MWCNT 3	250	500	Amine-CNT
4	RES-MWCNT 4	250	500	Carboxylic Acid-CNT

4.4 Characterization of Resveratrol loaded Carbon Nanotubes

4.4.1 Uv spectroscopy

Each sample, which included pure resveratrol, carboxylic acid and amine functionalised carbon nanotubes, and the four formulations RES-MWCNT 1, RES-MWCNT 2, RES-MWCNT 3, and RES-MWCNT 4, was relocated to a beaker with 10 mL of methanolic solution while being stirred. The sample was scanned using the UV spectrophotometer, and the absorbance at 308 nm determined in comparison to the blank, methanol solvent.

4.4.2 Fourier Transform Infrared Spectroscopy (FTIR) spectra

Fourier Transform Infrared Spectroscopy (FTIR) engaged to examine the formulation's distinctive functional group and compare it to the FTIR spectra of the test sample. The PerkinElmer 1750 FTIR (Beaconsfield, U.K.) was used to record the FTIR spectra of the sample used in this investigation. After the sample was combined with the dried KBr, it was shaped into a pellet. The test samples' pellets were scanned at a signal resolution of 4 cm between 4000 and 400 cm^{-1} in order to gather the spectrum (KA et al. 2011).

4.4.3 X- Ray Diffraction (XRD)

The crystalline characteristics of the resveratrol medication in the carbon nanotube formulation were examined. By adopting an automatic Bruker D8 (Bruker Corporation, Billerica, MA, USA) Advance diffractometer to produce X-ray diffraction patterns in reflection using nickel-filtered Cu–Kα 20 radiation, the crystalline characteristics were examined. 10–100° 2θ was the range at which the sample was scanned. For each sample, the diffraction graph was captured (Dong et al. 2018).

4.4.4 Percentages entrapment of resveratrol to the carbon nanotube

500 mg of precisely weighed MWCNTs were relocated to 20mL capacity beaker with methanol using hand shaking. The nanotube alcoholic solution was continuously stirred while 500 mg of precisely weighed t-RES was added. In order to reduce light interference, the dispersion was stirred with magnetic stirring (Remi, India) at 150 rpm for 48 hours at 25±2 °C in a dark atmosphere. Following 48 hours, the dispersion was put into a tube and centrifuged for 30 minutes at 10,000 rpm. After being placed on top of the

bottom, the pellet was cleaned three times with deionised water and allowed to dry for 48 hours in a desiccator (Singh et al., 2012)

Percent drug entrapment efficiency was determined using following equation:

$$Percentage\ durg\ entrapment = \frac{\text{Amount of drug loaded into the carbon nanotube}}{\text{Total amount of formulation}} \times 100 \ldots\ldots 4.5$$

4.4.5 Particle size and Zeta Potential

The test sample's stability was evaluated by measuring the carbon nanotube's size and surface charge using photon correlation spectroscopy (Malvern Instruments, Nano ZS-90, U.K.). The sample was moved to a volumetric flask and diluted with demineralised DDW at 25°C until it reached the flask's mark, using a 40W sonicator for one minute. Transferring the sonicated material to the polystyrene cuvettes was done. After being placed in the particle size analyser, the cuvette containing the sample was scanned at 25°C. The distribution graph of particle sizes was captured. When measuring the zeta potential, the sample was moved to the zeta cuvette and scanned to determine the surface charges. (Singh et al. 2013).

4.4.6 ^{1}H and ^{13}CNMR NMR studies

The ^{1}H and ^{13}CNMR analysis of the test formulation, carbon nanotube, and resveratrol medication were ascertained using NMR spectroscopy. To solubilize the material, it was moved to a tube, the DMSO solvent was added, and it was agitated by hand. The solution was charged in the NMR device after being moved to the tube (Zhang et al., 2014).

4.4.7 Raman spectroscopy

A Raman spectrophotometer with an excitation wavelength of 532 nm is used to detect the Raman spectrum of the resveratrol drug, carbon nanotube, and test formulation. By comparing the sample's input and output wavelengths, the spectrophotometer determines the type of sample limits (Sharafi et al., 2024).

4.4.8 Differential Scanning Calorimetry (DSC)

The sample's thermal characteristics, such as its melting point and polymorphism, were examined using the DSC analysis. The sample's thermogram was recorded using a Perkin Elmer DSC 6000 DSC. The sample was moved to a DSC pan and put into the

instrument's furnace. The sample was scanned in a nitrogen environment at temperatures between 20°C and 450°C (Scanning rate of 10°C/min) (Ragab et al., 2019).

4.4.*9 In vitro* Release

In-vitro release profile of resveratrol from Test formulation t-RES-MWCNT 2 and bulk drug in vitro drug release profiles were assessed and compared utilising the dialysis membrane sac technique. The 25 mg of resveratrol drug and equivalent test formulation t-RES-MWCNT were transferred, individually shaken by hand, to a glass tube that held 5 mL of the appropriate solvent. The mixture was placed inside the dialysis membrane sac (weight cutoff of 8–10 kDa (Spectra/Por)). 50mL of drug release medium kept at 37 ºC and 100 rpm over a magnetic stirrer was placed in a beaker with the sample containing the dialysis membrane sac. Precisely measured samples 3mL were extracted at various intervals. Before being charged in the HPLC, the extracted sample was filtered using 0.22µ membrane filter paper. The HPLC chromatogram of the each was recorded and amount of the resveratrol in each sample was recorded (Singh et al., 2012)

4.5. Development of RES-CNT-CET formulation

A precise 50 mg dose of the RES-MWCNT 2 was transferred to a round-bottom flask. With constant stirring using a magnetic stirrer set at 150 rpm, a precisely measured cetuximab buffer solution of 10 mg/mL was introduced to the round-bottom flask. Continuous stirring was employed for 96 hours in order to allow the nanotube to swell and reach equilibrium. The activities took place in a dimly lit setting. Whatman filter paper was used to filter the mixture, which was then collected and kept for further examination at 2–8°C (Ali, and Radwan,2021; Kesharwani et al, 2015).

4.6. Characterization of RES-CNT-CET formulation

4.6.1 Raman spectroscopy

A Raman spectrophotometer with an excitation wavelength of 532 nm determines the Raman spectrum of the d test formulation. By measuring the sample's input and output wavelengths, the device determines the type of sample limits (Sharafi et al., 2024).

4.6.2 Particle size and Zeta Potential

The test sample's stability was evaluated by measuring the carbon nanotube's size and surface charge using photon correlation spectroscopy (Malvern Instruments, Nano ZS-90, U.K.). The sample was moved to a volumetric flask and diluted with demineralised

DDW at 25°C until it reached the flask's mark, using a 40W sonicator for one minute. Transferring the sonicated material to the polystyrene cuvettes was done. After being placed in the particle size analyser, the cuvette containing the sample was scanned at 25°C. The distribution graph of particle sizes was captured. When measuring the zeta potential, the sample was moved to the zeta cuvette and scanned to determine the surface charges. (Singh et al. 2013).

4.6.3 ^{1}H and ^{13}CNMR NMR studies

The ^{1}H and ^{13}CNMR analysis of the test formulation, carbon nanotube, and resveratrol medication were ascertained using NMR spectroscopy. To solubilize the material, it was moved to a tube, the DMSO solvent was added, and it was agitated by hand. The solution was charged in the NMR device after being moved to the tube (Zhang et al., 2014).

4.6.4 FTIR

Fourier Transform Infrared Spectroscopy (FTIR) was used to examine the formulation's distinctive functional group and compare it to the FTIR spectra of the test sample. The PerkinElmer 1750 FTIR (Beaconsfield, U.K.) was used to record the FTIR spectra of the sample used in this investigation. After the sample was combined with the dried KBr, it was shaped into a pellet. The test samples' pellets were scanned ranging 4000 and 400 cm^{-1} in order to gather the spectrum (Yu et al. 2023).

4.6.5 TEM

The transmission electron microscope (JEOL, JEM100CS, Japan) was used to assess the test formulation's surface morphology at 80KV. The test sample was attached to carbon-coated copper grids after being diluted ten times with distilled water. Subsequently, the grids were left to cure at ambient temperature. The transmission electron microscope charged the dried sample grid and took pictures at various magnifications (Salim et al, 2023).

4.6.6 Percentages entrapment of resveratrol to the carbon nanotube

A precisely weighed quantity of formulation was transferred to a beaker with 20 mL of methanol under continuous shaking. The dispersion was agitated with magnetic stirring (Remi, India) at 150 rpm for 48 h at 25±2°C under dark environment to minimize light interference. After 48 hours, the dispersion was subject to centrifugation for 30

minutes at 10,000 rpm. The pellet that was placed on top of the bottom was cleaned three times with deionised water before being dried for 48 hours in a desiccator (Pruthi et al., 2012). Percent drug loading efficiency was determined using following equation:

$$Percentage\ durg\ entrapment = \frac{\text{Amount of drug loaded into the carbon nanotube}}{\text{Total amount of formulation}} \times 100 \ldots\ldots 4.7$$

4.6.7 Drug Release

The in vitro drug release profile of RES-CNT-CET and resveratrol was established in a physiological setting to mimic the environment of cancer cells. In order to replicate the pH circumstances, the activity was carried out in both the cancer cell exposed environment and the normal conditions (pH 7.4). For the analysis, RES-CNT-CET and the resveratrol medication were utilised. Several time points were used to extract precisely measured 3mL of samples. After being filtered via 0.22µ membrane filter paper, the extracted material was charged in an HPLC. The amount of resveratrol in each sample was noted, as well as the HPLC chromatogram for each (Jawahar et al. 2020).

4.6.8 Release Kinetics

Drug release analyses obtained at pH 7.4 and pH 5 were examined using a number of kinetics equations, including zero-order kinetics, first-order kinetics, Korsmeyer-Peppas model, and Higuchi diffusion model, to examine drug release profile of the designed RES-CNT-CET formulation. The relationship between the release profile and the release exponent (n value) was examined. A value below 0.5 indicates diffusion through the Fickian mode. According to the Hixon Crowell model, modifications to the drug particles' total surface area or size were associated with the drug's release (Srivastava et al. 2024; Chudoba et al. 2021)

4.6.9 Stability study

Studies of stability aid in regulating the manufactured products' shelf life. It is the period during which the product maintains its pharmacokinetic, physical, and chemical attributes over the course of its pharmacological life. For the stability tests of the generated formulations, the ICH guideline of stability testing of new drug substances and products Q1A(R_2) was adhered to. Stability experiments were performed on the generated formulations to assess the product's stability over a period of six weeks. For six weeks, the produced RES-CNT-CET was maintained at 4±2 °C, room temperature (25±2 °C), and

accelerated temperature (40±2 °C), with seven-day intervals between studies. The test sample's colour, turbidity, precipitation, consistency, and percentage of drug entrapment were all assessed (Jose et al., 2016; Singh et al., 2016).

4.6.10 MTT Assay

The cytotoxicity against cancer cells was examined using the MTT assay, an in vitro test. For MTT assay HT-29 cell line was utilized. Cetuximab targets the epidermal growth factor receptor (EGFR), which is expressed by HT-29 cells (Human Colorectal Adenocarcinoma Cell Line). They are therefore perfect for assessing the effectiveness of cetuximab-anchored nanocarriers. The MTT test was used in the current investigation to examine the pure drugs resveratrol (RES), MWCNT, RES-MWCNT, CET, and RES-MWCNT-CET against the HT-29 cell line. In a 96-well plate, the cells cultivated at a density of 2×10^4 cells per well. DMEM-based culture mix was exposed to 10% FBS, 1% penicillin, and 1% streptomycin. 37 °C was the temperature at which the cells were incubated in a 5% CO_2 atmosphere. The wells were exposed with treatment in three times with differing concentrations (between 5 and 100, distributed in media) of all samples marked RES, MWCNT, RES-MWCNT, CET, and RES-MWCNT-CET following a 24-hour incubation period. The wells are rinsed with PBS and 200 µL of MTT (0.5 mg/mL) is added. After four hours, 200 µL of isopropanol was used to dissolve the formazan crystals. The optical absorbance at 570 nm was measured. The mean value and standard error (SE) of the data were given, and the proportion of surviving cells was quantified. The calculation was performed applying the following formula (Jain et al, 2007).

$$\% \text{ Cell survival} = \frac{\text{A570 nm of treated cells}}{\text{A570 nm of untreated control cells}} \times 100 \ldots\ldots\ldots\ldots 4.8$$

4.6.11 Cell Internalization

The cells were cultivated in 12-well plates at a density of approximately 1×10^5 cells per well. The cells were cultured at 37°C for 24 hours in a humid atmosphere with 5% CO_2. The cells were subsequently exposed with 30 µg doses of samples RES, MWCNT, RES-MWCNT, CET, and RES-MWCNT-CET (a formulation that contains rhodamine dye) and cultured for 24 hours. To determine the degree of cellular absorption, the cells were

treated with trypsin and then immersed in PBS. The flow cytometry method (BD FACS Canto-II, USA) was used to determine the quantity of RhB-positive cancer cells. For the qualitative study, the cells were first washed with PBS before being examined under a fluorescent microscope (Mishra et al., 2023).

4.6.12 *In-vivo* studies

The Central Animal House of the Lovely Professional University in Punjab, which is a division of the School of Pharmaceutical Sciences, provided 45 Wistar rats for the in vivo study. The rats weigh between 150 and 170 grams when they are all three to four weeks old. The animals were divided into five groups, with nine rats in each. They were required to fast all night after being fed a nutritious food for around a week before the trial began. The Institutional Animal Ethics Committee of LPU's School of Pharmaceutical Sciences granted approval for the in vivo inquiry experiment (LPU/IAEC/2023/Protocol No.42). The details of different animal groups required are as given below:

Table 4.4: Details of different animal groups

Group No.	**Sample code**	**Diet, dose, and route of drug treatment**	**No of animals**	**Time point**
Group 1	Vehicle control	Normal saline (Vehicle) + IP route (0.9% NaCl)	9	1h, 4h,8h.
Group 2	Drug - Resveratrol	RES + 1 mg/kg, single dose IP route	9	1h, 4h,8h.
Group 3	MWCNT	CNT+ 1 mg/kg, single dose IP route	9	1h, 4h,8h.
Group 4	RES-MWCNT2	RES + equivalent to 1 mg/kg, single dose IP route	9	1h, 4h,8h.
Group 5	RES-MWCNT-CET	RES- MWCNT-CET equivalent to 1 mg/kg, single dose IP route	9	1h, 4h,8h.

4.6.13.1 Development of Bio analytical method

The HPLC is made up of a rheodyne injector, a UV/Vis light detector, and a single pump (515). The chromatographic process was separated using a Waters C18 column (250 mm × 4.6 mm I.D., 10 µm) (Srivastava et al., 2024). Using the Waters Empower 3 program, the findings were gathered and combined. The mobile phase in isocratic mode was a mixture of methanol and water solvents. after several mobile phase ratios have been screened. The sample was detected at a wavelength of 308 nm using a 25 µL injection volume of the solvent, which was a 40:60 mixture of water and methanol. The solvent flowed at a rate of 0.8 mL/min.

4.6.13.2 Safety Measures

The drug resveratrol is sensitive to temperature and light, according to earlier research. When light is present, it isomerises from the trans to the cis form with ease. Consequently, the samples were stored at room temperature with light protection, and all investigations were conducted in low light.

4.6.13.3 Procurement of blood and separation of plasma

A capillary size glass tube was used to perform a retro-orbital puncture on the rat in order to extract its blood. The tube that was used to collect the blood for the radioimmunoassay (RIA) contained crystals of ethylene diamine tetra acetic acid (EDTA). They made the rat's eye protrude and immobilised it by gently compressing its neck. A capillary was inserted dorsally via the retro-orbital plexus of the eye", and blood was drawn from the capillary walls using a capillary tube and transferred into the EDTA vial. The blood samples were centrifuged for 15 minutes at 4932 g. Using a small pipette, the transparent liquid was extracted and placed in a freezer at -20 °C for further analysis.

4.6.13.4 Blank Plasma Sample Preparation

The plasma protein precipitated after a measured 1 mL of plasma was transferred to a tube with a 2 mL mixture of methanol: ACN in a 1:1 ratio and vortexed for 5 minutes. The mixture spent 15 minutes in a centrifuge set to 4932 g. They moved the supernatant to a 100 mL volumetric flask.

4.6.13.5 Standard Stock Solution Preparation

A stock solution of concentration 100µg/mL of resveratrol get ready in plasma. 10 mg of resveratrol was transferred was solubilized in the 2mL of plasma under gentle

agitation. The agitation was continuous for 10 min. Accurately measured mixture 2 mL of solvent methanol: ACN in 1:1 was mixed with the drug plasma mixture ratio, vortexed for 5 min resulting in the plasma protein got precipitated. The mixture was centrifuged at 10000 rpm at 4°C for 15 min. The supernatant was transferred to the 100 mL of volumetric flask. The volume of the flask was made using methanol solvent up to the mark of the flask resulting in solution of concentration 100 µg/mL. The solution was labelled as stock solution A.

Stock solution B concentration 10 µg/mL was prepared from the stock solution A by withdrawing an aliquot of 1mL and transferred to the 10 mL volumetric flask. The sample was diluted up to the mark of the flask using the methanol solvent as diluent.

4.6.13.6 Internal Standard (IS) Preparation

A stock solution of 100 µg/mL of caffeine get ready in methanol. 10 mg of drug was transferred to the 100 mL of volumetric flask containing 50 mL of methanol solvent and sonicated for the 5 min. to complete solubilization of the drug. The volume of the flask was made using methanol solvent up to the mark of the flask resulting in solution of concentration 100 µg/mL. The solution was labelled as stock solution. A working solution of concentration 10 µg/mL was prepared from the stock solution by withdrawing an aliquot of 1mL and transferred to the 10 mL volumetric flask. The sample was diluted up to the mark of the flask using the methanol solvent as diluent.

4.6.13.7 Method specificity

The specificity parameter was investigated to determine the interaction between the blank plasma peaks along with the drug spiked plasma peaks.

Process: A measured 1 mL Plasma was transferred to the tube containing 2 mL mixture of Methanol: ACN in 1:1 ratio. The solution was vortexed for 5 min, follow by centrifuged at 4932 g for 15 min. The supernatant was transferred to the 100 mL of volumetric and diluted up to the mark of the flask resulting in solution with a concentration of 100 µg/mL. The 100 µg/mL solution was diluted to the 2 µg/mL by withdrawing and transferred the 0.2 mL from the 100 µg/mL into the 10 mL volumetric flask. Furthermore the 2 mg/mL solution for RES was produced by diluting the stock solution with spiking matrix separately. Next, a solution of 2 µg/mL RES and 10 µg/mL caffeine was produced by adding 0.2 mL of a

100 µg/mL RES solution (stock solution A) and 1 mL of a 100 µg/mL caffeine solution (solution C) and diluted to 10 mL using methanol. The solution was filtered using the 0.22µ membrane filter paper and infected into the HPLC. After injecting 25 µL of both the blank plasma solution and the RES and IS solution into the HPLC system, the peak interaction at 308 nm was observed (Harish et al, 2022).

4.6.13.8 Standard calibration curve development

A stock solution of 100 µg/mL of resveratrol get ready in plasma. 10 mg of resveratrol was transferred was solubilized in the 2 mL of plasma under gentle agitation. The agitation was continuous for 10 min. Accurately measured mixture 2 mL of solvent methanol: ACN in 1:1 was mixed with the drug plasma mixture ratio, vortexed for 5 min and centrifuged at 10000 rpm at 4°C for 15min. The supernatant was transferred to the 100 mL of volumetric flask. The volume of the flask was made using methanol solvent up to the mark of the flask resulting in solution of concentration 100 µg/mL. The solution was labelled as stock solution A.

The standard linearity curve ranging 2-10 µg/mL was get ready from the stock solution A 100 µg/mL. A series of the aliquots ranging 0.2 mL to 1 mL were withdrawn from the stock solution A 100 µg/mL and transferred separately to the 10 mL of volumetric flask separately. In addition, 1mL of internal standard solution of caffeine of concentration 100 µg/mL was relocated to each working solution. Each working solution was diluted up to the mark of the volumetric flask using the methanol solvent. Each working solution filtered using the 0.22µ membrane filter paper and charges in the HPLC. The analysis was performed at the wavelength of 308 nm. The HPLC chromatogram of the each working solution was recorded and area of the resveratrol was determined. The standard linearity curve of the resveratrol was prepared using the excel sheet (Harish et al, 2022).

4.6.13.9 Accuracy

The investigation of the accuracy parameters involves the determination of the percentage recovery of the spiked standard resveratrol solution in the blank plasma samples or test samples.

Process: A stock solution of 100 µg/mL of resveratrol get ready in plasma. 10 mg of resveratrol was transferred was solubilized in the 2 mL of plasma under gentle agitation.

The agitation was continuous for 10min. Accurately measured mixture 2 mL of solvent methanol: ACN in 1:1 was mixed with the drug plasma mixture ratio, vortexed for 5 min centrifuged at 10000 rpm at 4°C for 15 min. The supernatant was transferred to the 100 mL of volumetric flask. The volume of the flask was made using methanol solvent up to the mark of the flask resulting in solution of concentration 100 µg/mL. The solution was labelled as stock solution A. The LQC at 80%, MQC at 100%, and HQC at 120% of the mid concentration, which is 6 µg/mL whereas, lower concentration is 4.8 µg/mL and higher concentration is 7.2 µg/mL get ready from the standard stock solution A. An aliquot 0.6 mL, 0.48mL and 0.72mL were withdrawn separately from the stock solution and transferred to the 10mL volumetric flaks. An internal standard solution of 10 µg/mL was added to each solution and diluted to the mark of the flask using the methanol solvent. Each solution was filtered using the 0.22µ membrane filter paper and charges in the HPLC. The analysis was performed at the wavelength of 308 nm. The HPLC chromatogram of the each working solution was recorded and area of the resveratrol was determined. The amount of the resveratrol was determined from the standard calibration curve (Le et al, 2019).

4.6.13.10 Precision

Repeatability, which describes measurements made within a single day (intraday), and intermediate precision, which relates to measurements made on various days (inter-day), were the two factors used to examine the precision parameters. Three levels of analysis were conducted on the parameter: LQC, MQC, and HQC. The standard stock solution A was used to prepare the lower quantified concentration at 80%, the medium quantified concentration at 100%, and the high quantified concentration at 120% of the mid concentration, or 6 µg/mL. The lower and higher concentration was 4.8 µg/mL and 7.2 µg/mL. The concentration of IS added to each of these solutions was 10 µg/mL. In repeatability parameter, inter day and intraday precision was performed. The experiments were conducted with precision under identical conditions on the same day (Kumar et al, 2020).

$$Absolute\ recovery = \frac{Actual\ concentration\ recovered}{Theoritical\ concentration} \times 100 \ldots\ldots\ldots\ldots\ldots 4.9$$

4.6.13.11 Limit of Detection and Quantification

The limit of quantification revealed as lowest quantity of drug that could be estimated, whereas the limit of detection (LOD) revealed as lowest quantity could be detected, separated from the background, and measured. The slope of the usual linear equation of resveratrol and its intercept was used to calculate the LOD and LOQ parameters. Equations such as these were used to establish the limits of quantitation (LOQ) and detection (LOD):

$$LOD=3.33\times\sigma/S \quad \ldots\ldots 4.10$$

$$LOQ=10\times\sigma/S \quad \ldots\ldots 4.11$$

where σ represents the standard deviation of the response, while S represents the slope of the calibration curve (Kurangi, B et al, 2022).

4.6.13.12 System Suitability

System suitability parameters were estimated by analysing the six consecutive injections of the working solution. Mean, standard deviation (SD), % relative standard deviation (%RSD), theoretical plates and of retention time were determined.

A stock solution of 100 µg/mL of resveratrol get ready in plasma. 10 mg of resveratrol was transferred was solubilized in the 2 mL of plasma under gentle agitation. The agitation was continuous for 10min. Accurately measured mixture 2 mL of solvent methanol: ACN in 1:1 was mixed with the drug plasma mixture ratio, vortexed for 5 and centrifuged at 10000 rpm at 4°C for 15 min. The supernatant was transferred to the 100 mL of volumetric flask. The volume of the flask was made using methanol solvent up to the mark of the flask resulting in solution of concentration 100 µg/mL. The solution was labelled as stock solution A.

A working solution of concentration 10µg/mL was prepared from the stock solution A by withdrawing an aliquot of 1mL and transferred to the 10 mL volumetric flask. Measured aliquots 1mL of the internal standard solution of concentration 100 µg/mL was added to the volumetric flask. The sample was diluted up to the mark of the flask using the methanol solvent as diluent resulting in solution with a concentration 10 µg/mL of resveratrol and 10 µg/mL of internal standard caffeine. The solution was filtered using the 0.22µ membrane filter paper and charged in the HPLC six time. The analysis was performed at the wavelength of 308 nm (Wu et al, 2022).

4.6.13.13 Stability studies

Plasma samples that had been injected with RES were freeze-thawed for three cycles as part of the stability experiment. The first cycle lasted three hours at ambient temperature, and the second cycle lasted three weeks -20 °C. 3 mL of plasma was relocated in RIA vial to evaluate freeze-thaw stability. A concentration of 1000 µg/mL was attained by adding 3 mg of RES to this vial. For five minutes, the resultant mixture was vortexed. The temperature of the test tube was kept at -20 °C in a deep freezer. The tube was pullout and kept and thawed at room temperature after the sample had been frozen. One millilitre of plasma (Cycle 1) was extracted from the thawed samples, and the other two millilitres of plasma were kept in a deep freezer for the next cycle. The samples were centrifuged. The supernatant was removed and diluted with 100 mL of methanol to achieve a concentration of 100 µg/mL. Additionally, dilutions were made to achieve concentrations of 7.2 µg/mL (HQC), 6 µg/mL (MQC), and 4.8 µg/mL (LQC). Likewise, 1 mL of the thawed sample was removed for cycles two and three. The entire procedure was repeated for cycles two and three's LOQ, MQC, and HQC. IS relocated to all of the aforementioned solutions and the concentration was maintained at 10 µg/mL. The samples were then evaluated at their respective retention times, with a wavelength of 308 nm (Khursheed et al, 2022).

In a similar manner, the short-term stability of plasma samples containing RES at room temperature was evaluated. One, two, and three hours before to the extraction, the stability was evaluated. Three millilitres of plasma were gathered and put in a single RIA vial for short-term stability. 3 mg of RES relocated to vials to reach a concentration of 1000 µg/mL, vortexed for five minutes, followed by kept at room temperature. At 1, 2, and 3 intervals, a 1 mL sample was taken and transformed in the LQC, MQC, and HQC working solution. An IS of 10 mg/mL was added following each interval. The dilutions were produced in triplicate and subsequently injected into the HPLC system. The samples were then evaluated at their respective retention times, with a wavelength of 308 nm (Reddy et al, 2019).

A volume of 1 mL plasma was gathered and put into each of the three RIA vials for long-term stability. 1mg of RES was added to this vial to reach a concentration of 1000

µg/mL, vortexed for five minutes, followed by kept at -20°C. The sample was withdrawn at different time interval 1, 2, and 3 weeks. After being separated from the plasma, the RES were ready for the LQC, MQC, and HQC. Following each interval, 10 mg/mL of IS was added. After being created in duplicate, the dilutions were then added to the HPLC apparatus. The samples were then assessed at a wavelength of 308 nm at their individual retention times (Khursheed et al, 2022).

4.6.14 Biodistribution studies

Biodistribution studies will be conducted using Wistar/Sprague-Dawley rats of both sexes. Five equal groups of rats will be present. In each group, there are nine rats (n=9). Animals will receive intraperitoneal administration of the medication, MWCNT, and formulation via the caudal tail vein (1 mg/kg resveratrol) after being dissolved in ordinary saline (0.9% w/v). When the colon, liver, kidney, lungs were carefully removed, they were cleaned twice to get rid of any tissues or adhering cell debris before being frozen and kept in storage. Following organ removal, ethanol will be added in the appropriate quantity, mixed with a tissue homogeniser or vortex, and centrifuged for 10 minutes at 3000 rpm. Using the 0.22 µ membrane filter paper, the material was filtered. The analysis was performed at the wavelength of 308 nm. Each sample's HPLC chromatogram was recorded and the resveratrol area was determined. The amount of the resveratrol was determined from the standard calibration curve (Prajapat et al, 2018, Jose et al, 2014).

Biodistribution investigations were subjected to statistical analysis via GraphPad Prism (11.0.2) to compute mean values, standard deviations, and to conduct comparative statistical assessments for a thorough evaluation of drug distribution throughout several organs. The software was utilized to provide clear graphical depictions of tissue uptake profiles, which were beneficial for visualizing and analysing organ-specific drug accumulation. PK Solver (version 2) was utilized for the organization and curve fitting of biodistribution data, but its use was confined to the systematic examination of drug distribution across different tissues and did not encompass the computation of pharmacokinetic parameters. The utilization of these analytical methods provided robust statistical confirmation and consistency of the biodistribution findings in accordance with

standard protocols for preclinical drug elimination studies (Zhang et al., 2010; Imlimthan et al., 2025).

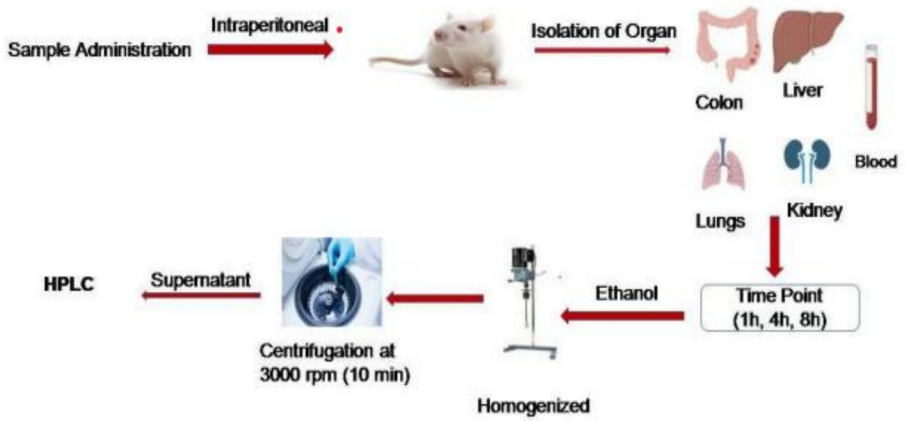


Figure 4.1: Process of the preparation of samples for biodistribution study.

4.6.15 Haematological studies

4.6.15.1 Hemolytic toxicity studies

The human blood was collected in anti-clot vials and spun for 15 minutes at 3000 rpm using a Remi centrifuge. Red blood cells (RBCs) will be separated, then cleaned, centrifuged, and resuspended in a 0.9% w/v saline solution. The RBCs solution (1 mL), 0.9% w/v normal saline (4.5 mL), and various samples (0.5 mL) will be combined and left to react for 60min. In order to quantify absorbance at 306 nm (Shimadzu 1601, Kyoto, Japan) as zero and complete haemolysis, the dilutions were prepared using deionised water and a 0.9% w/v NaCl solution. To calculate the percentage of haemolysis, the formula will be applied (Mishra et al, 2015, Singh et al, 2013).

$$Hemolysis\ (\%) = \frac{Abs - Abs0}{Abs100 - Abs0} \times 100 \quad \ldots\ldots 4.12$$

4.6.15.2 Haematological and Histopathological study

Haematological parameters were measured in healthy Wistar or Sprague-Dawley rats of both sexes that are uniformly sized and weighted. All animals shall be fed the same standard feed for no more than seven days. Equipped with equal doses of 1 mg/kg resveratrol and 2 mg/kg cetuximab, the medications, MWCNT, and formulations will be dissolved in ordinary saline (0.9% w/v) and given intravenously to animals via the caudal

tail vein. The blood samples collected after seven days will be analysed by a local pathology lab using the retro-orbital plexus method to determine the haematological parameters (Atmaca et al, 2014).

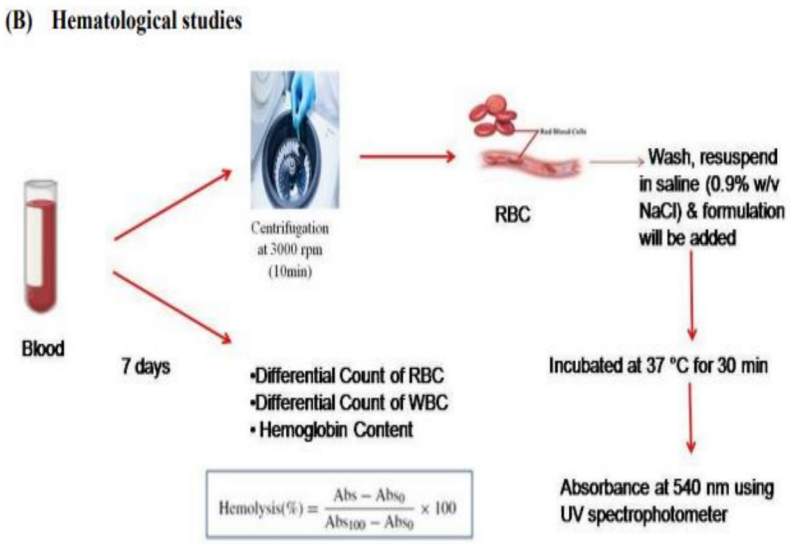


Figure 4.2: Process of the Haematological studies

5. Results and discussion

5.1 Preformulation study of t-RES

5.1.1 Melting point

Table 5.1 displays the observed value of the t-RES drug's melting point in bulk form. Table 5.1 revealed that the t-RES drug's melting point was 267±1.0-269.33±1.527 °C. The reference melting point value and the observed melting point value are extremely close.

Table 5.1: Melting Point of t-RES

Sr.No.	Drug	Reported Value	Observed value
1	t-RES	267°C (Zhou et al., 2021)	267±1.0-269.33±1.527 °C

Data has been expressed as Mean ± SD, n = 3

5.1.2 Establishment of UV standard linearity curve

5.1.2.1 Determination of the absorption maxima

Figure 5.1 displayed the spectrum for the working solution concentration of 5µg/mL of t-RES. The absorption maxima in t-RES at the wavelength of 308 nm (Yan et al., 2024) were verified by the UV spectrum to match the reference value.

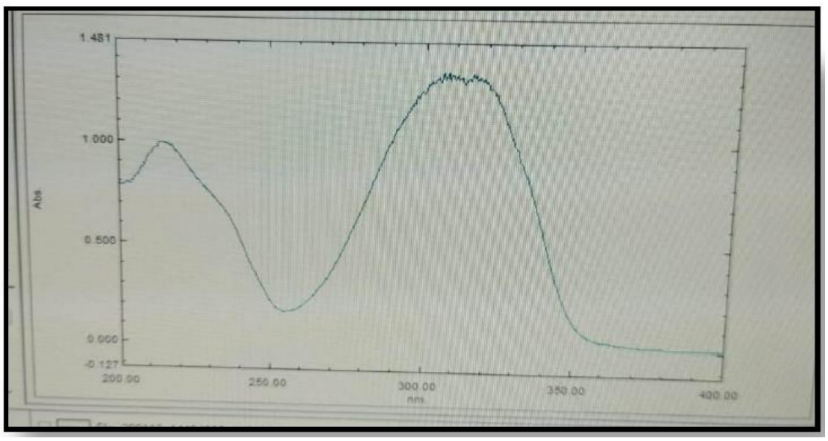


Figure 5.1: UV spectra of t-RES

5.1.2.2 Standard calibration curve in water solvent

A standard calibration curve ranged from 1µg/mL to 4µg/mL for the t-RES medication in water solvent. Figure 5.2 showed the linear curve with regression coefficient

0.995 and linear curve equation y = 0.230x + 0.011 within a concentration range of 1 µg/mL to 4 µg/mL.

Table 5.2: Standard calibration curve of t-RES in water

Sr.No.	Concentration (µg/mL)	Absorbance	Inference
1	1	0.246±0.013	Correlation coefficient=0.995
2	1.5	0.307±0.006	Linear regression equation
3	2	0.456±0.005	y = 0.230x + 0.011
4	2.5	0.552±0.042	
5	3	0.674±0.031	
6	3.5	0.800±0.020	
7	4	0.920±0.043	

Data has been expressed as Mean ± SD, n = 3

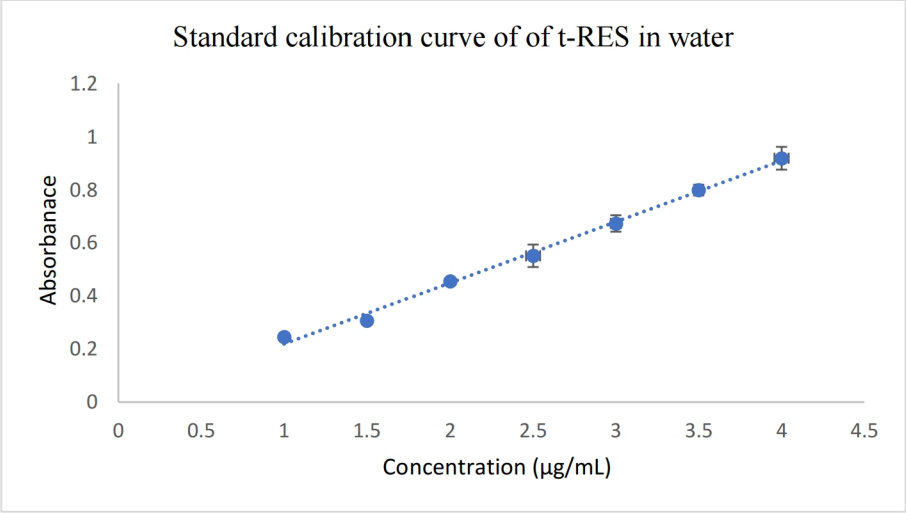


Figure 5.2: Standard calibration curve of t-RES in water

5.1.2.3 Linearity plot in Phosphate Buffer Saline (PBS) 7.4

A linearity plot ranged from 1µg/mL to 8µg/mL for the t-RES medication in Phosphate Buffer Saline (PBS) 7.4 solvent. Figure 5.2 showed the linear curve with regression coefficient 0.996 and linear curve equation y = 0.115x + 0.02 in the range of 1 µg/mL to 8 µg/mL.

Table 5.3: Standard calibration curve of t-RES in Phosphate Buffer Saline (PBS) 7.4

Sr.No.	Concentration (µg/mL)	Absorbance	Inferences
1	1	0.153±0.010	Correlation coefficient=0.996 Linear regression equation y = 0.115x + 0.02
2	2	0.236±0.013	
3	3	0.353±0.016	
4	4	0.473±0.016	
5	5	0.629±0.012	
6	6	0.699±0.013	
7	7	0.828±0.012	
8	8	0.945±0.022	

Data has been expressed as Mean ± SD, n = 3

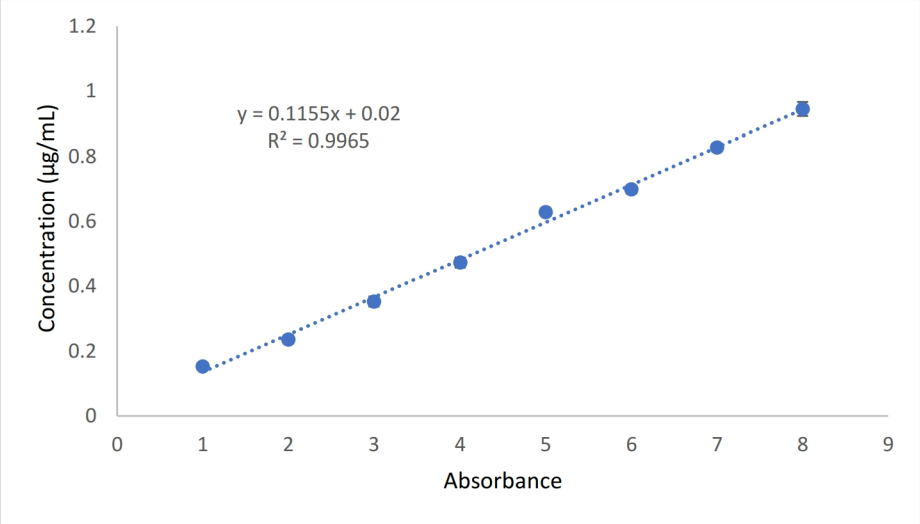


Figure 5.3: Standard calibration curve of drug in Phosphate Buffer Saline (PBS) 7.4

5.1.3 Partition coefficient

The observation of partition coefficient of t-RES is shown in Table 5.4-5.5

Table 5.4: Partition coefficient Absorbance of t-RES

Sr. No.	Solvent	Absorbance	Absorbance	Absorbance
1	Octanol	0.226	0.229	0.223
2	Water	0.990	0.996	0.995

Table 5.5: Partition coefficient of drug

Sr.No.	Reported value	Observed value
1	3.4 (www.drugbank.com)	3.372 ± 0.005

Data has been expressed as Mean ± SD, n = 3

In current activity the value of the t-RES was found to be 3.372 ± 0.005 close to the previous report value 3.4. The observation indicated the lipophilic nature of the t-RES drug.

5.1.4 Differential Scanning Calorimetry (DSC)

As shown in the Figure 5.4, namely DSC thermogram of the t-RES indicated a symmetric endothermic peak at 268.96°C, exploring the melting point if t-RES, similar to literature value of the melting point 268.4°C (Ainurofiq et al., 2022). Resveratrol displayed an exotherm at 267°C, according to Ansari and coworkers.

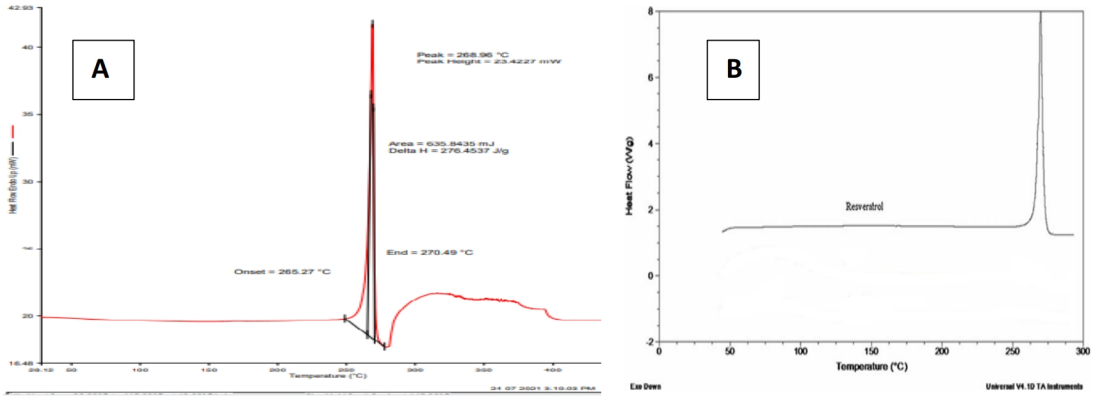


Figure 5.4: [A]: DSC thermogram of t-RES.**[B]** Reported DSC thermogram of t-RES (Ansari et al., 2011).

5.1.5 Fourier Transform Infrared Spectroscopy (FTIR) spectra

Fourier Transform Infrared Spectroscopy (FTIR) of t-RES drug in bulk form was shown in Figure 5.5 and characterises peaks were shown in Table 5.6

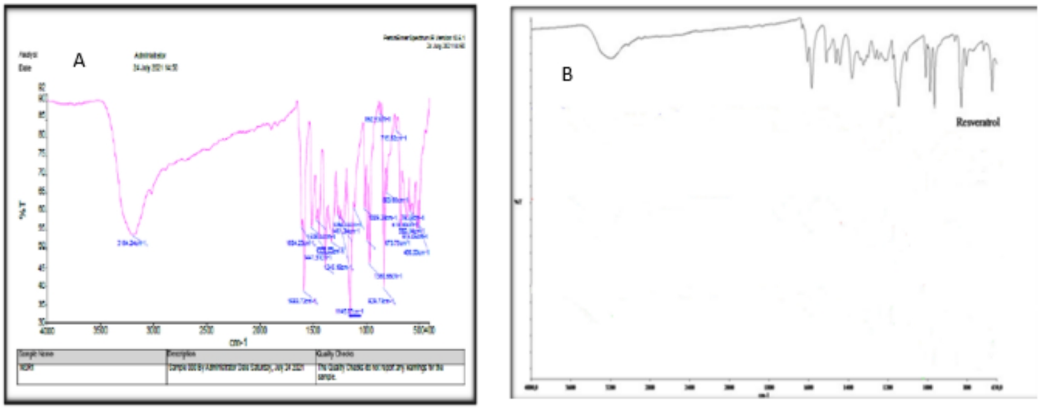


Figure 5.5: [A] FTIR spectra of t-RES. [B] Reported FTIR spectra of t-RES (KA et al. 2011).

Table 5.6: FTIR Peaks of t-RES

Sr No.	Peak Range (cm^{-1})	Observed Peak (cm^{-1})	Inference
1	3400–2400	3184.24	O-H stretch vibration
2	1300-1000	1380.68	C-O stretching
3	900-690	803.68	Aromatic (out-of-bend)
4	1650-2000	1604.23	Aromatic C=C stretch
5	1390-1310	1380.68	O-H bending Phenol
6	1500-1580	1508.44	C-C olefin stretches

FTIR measurements were performed for t-RES Figure 5.5 shown the results of the analysis reveal, that t-RES spectra were at 1508.44 and 1604.23 cm^{-1}; double peak which indicate C—C olefin stretches and aromatic C=C stretch, respectively another peak observed at 3184.24 cm^{-1} indicate the presence of free O—H stretch vibration. Additionally, O-H bending Phenol stretch vibrations occur at peak 1380 cm^{-1}. Ultimately,

peaks were identified at 803 cm^{-1} shown that C=C=H vibration due to bending indicate a Trans olefin group, confirm that compound exist in Trans form (Istenič et al. 2015).

5.1.6 Field Emission Scanning Electron Microscope (FE- SEM)

t-RES crystalline formations are depicted in Figure.5.6. Topographical data from samples can be displayed in high definition via the JEOL 3D. High-power optics, which is generally employed for high spatial resolution investigations, has two important features: high output and high efficiency. Additionally, the 'Gentle Beam mode' should have a tighter incident electron dispersion, allowing for the scrutiny of even weak materials. The photograph's morphological analysis reveals that the t-RES had a flat surface and a rod-like shape (Ainurofiq et al., 2018).

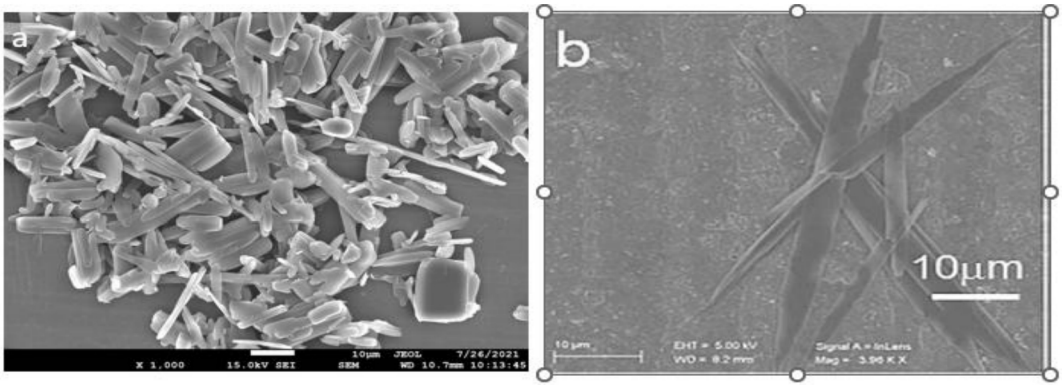


Figure 5.6: [a] FE-SEM of t-RES. [b] Reported FE-SEM of t-RES (Dong et al. 2018).

5.1.7 X-Ray Diffraction (XRD)

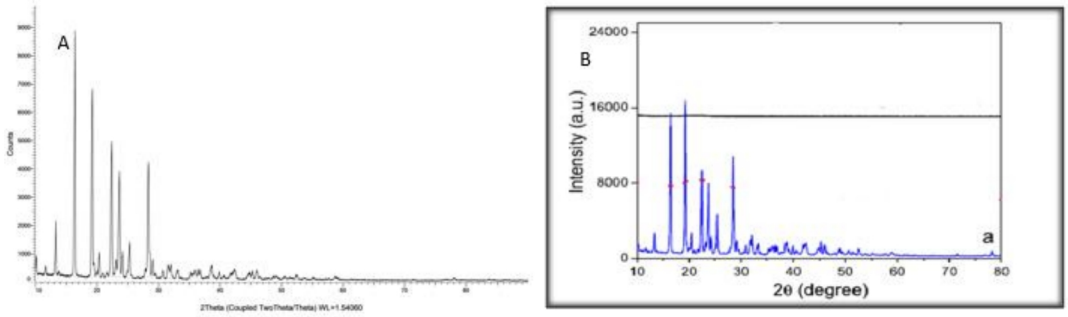


Figure 5.7: [A] XRD of t-RES. [B] Reported XRD patterns of t-RES (Dong et al. 2018).

The X-ray diffractogram of pure t-RES demonstrated several intense peaks, indicating its crystalline structure. The diffractogram (Figure 5.7) of pure t-RES demonstrated characteristics peaks at 2θ diffraction angles of 6.6, 16.4, 19.1, 22.3, and 28.3 (Sun et al., 2014).

5.1.8 Development of HPLC Methods

5.1.8.1 Identification of retention time

In accordance with Good Laboratory Practices (GLP), an HPLC method has been developed for the quantitative determination of t-RES in formulations based on MWCNTs. A Waters C18 column was used for the optimization trials, testing different methanol to water ratios. At a flow rate of 0.8 mL/min, the mobile phase was tuned to contain 60% water and 40% methanol. The HPLC was used to examine the working solution with a concentration of 2µg/mL. Table 5.7 displayed the theoretical plates, area, and retention time. The sample's HPLC chromatogram was displayed in Table 5.7. t-RES was found to elute with a retention time of 11.351 minutes under the experimental conditions (Figure 5.8).

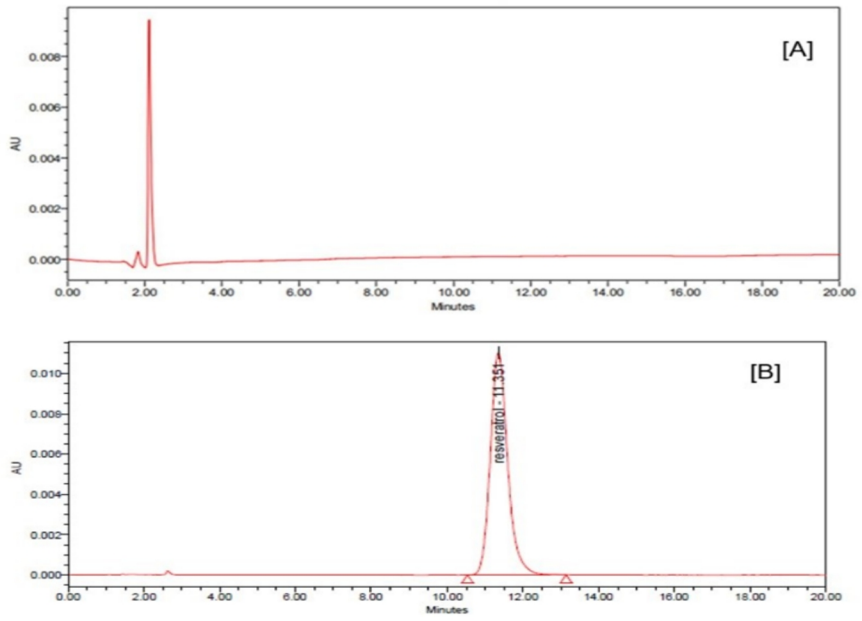


Figure 5.8: HPLC chromatogram of the A) Blank B) Sample working solution 2µg/mL

Table 5.7: Retention time, area and theoretical plates

Sr.No.	Sample	Retention time (min.)	Area	Theoretical plates
1	2.0 µg/mL	11.351	360586	3060.45

5.1.8.2 Method Validation

The proposed HPLC method of t-RES was validated to show that it was appropriate for its intended use. The ICH recommendations were followed in the process of validating the HPLC method. During the validation procedure, numerous criteria were analysed and evaluated, including precision, accuracy, range, linearity, robustness, and limit of detection and quantification (LOD and LOQ).

5.1.8.2.3 System Suitability

System suitability experiments were conducted to evaluate the column efficiency and chromatographic repeatability, as well as to make sure the proposed method for estimating t-RES in routine pharmaceutical applications is sufficient and feasible (Table 5.8). The percent relative standard deviation (%RSD) of peak regions following six consecutive injections was determined to be less than 2%, showing perfect chromatographic and environmental conditions as well as ideal injection repeatability. Ideal peak symmetry was indicated by the t-RES's tailing factor of 1.2 ± 0.026. There was satisfactory column efficiency in the measured values that matched the theoretical plate number.

Table 5.8. System suitability parameters

S. No	Parameter	Value
1	Theoretical plates	3060 ± 0.094
2	Retention time	11.351 ± 0.026 min
3	Tailing factor	1.2 ± 0.026

5.1.8.2.2 Limit of Detection (LOD) and Limit of Quantification (LOQ)

The calculated LOD for t-RES was found to be 1.6 µg/mL whereas, LOQ determined for t-RES was 4.8 μg/mL.

5.1.8.2.4 Range and Linearity

In the conc. ranges of 2 to 10 μg/mL, the linearity of t-RES was evaluated. In this assessment, the regression equation and its coefficient (r^2) were computed. The method of least squares was used to obtain the data (Figure 5.9). The R^2 score was 0.997, which generally indicates that the regression line was linear over the suggested concentration range and that the data fit the line well.

Table 5.9: Standard calibration curve

Con. (µg/mL)	Area 1	Area 2	Area 3	Area 4	Area 5	Area 6	Average Area	STD	% RSD
2	369668	363928	362168	360586	367168	352626	362690.67	5937.36	1.64
4	620505	624549	639963	612685	610376	626366	622407.33	10689.76	1.72
6	951864	964477	968711	966479	964906	963329	963294.33	5901.39	0.61
8	1297062	1296711	1293851	1294906	1292435	1281615	1292763.33	5731.14	0.44
10	1699816	1694818	1686987	1681910	1679499	1672259	1685881.50	10171.87	0.60

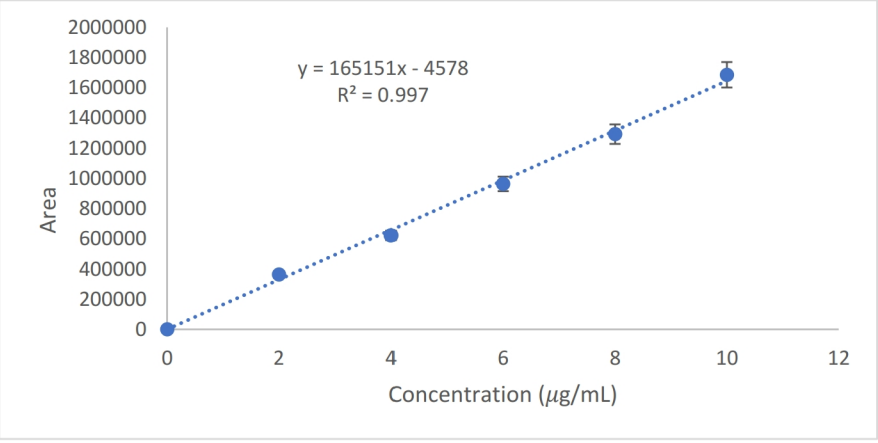


Figure 5.9: Calibration curve of t-RES

5.1.8.2.5 Accuracy

The average % recovery of the medication from the low-, medium-, and high-quality control (LQC, MQC, and HQC) samples was used to evaluate the accuracy of the procedure. According to the statistics, the mean percentage recovery for each of the three levels was between 95 and 105% (Table 5.10). This result implies that the created approach demonstrated a high degree of accuracy.

Table 5.10: Results of accuracy study

Dosage Form	**Level of addition (%)**	**% Recovery**
Bulk drug	80	101.71 ± 0.16
	100	103.42 ± 0.11
	120	99.34 ± 0.32
Marketed tablet	80	95.54 ± 0.14
	100	95.89 ± 0.15
	120	97.62 ± 0.17
t-RES-MWCNT	80	100.74 ± 0.42
	100	104.84 ± 0.56
	120	103.56 ± 0.21

5.1.8.2.6 Precision

The precision of the approach method was confirmed by evaluating the RSD using six replicate injections of three different levels of LQC, MQC, and HQC. Three distinct criteria—inter-analyst, intra-day, and inter-day—were taken into account for additional assessment. Under the same experimental setup, these parameters were estimated. According to the results of the experiment, the suggested method showed a significant level of accuracy, as seen by the percentage relative variance staying below 2%. Table 5.11.

Table 5.11: Results of precision

Intraday										
Level	**Standard Solution Conc. (µg/mL)**	**Area**						**Mean AUC (cm^2)**	**Std. Dev. (±)**	**% RSD**
		1	2	3	4	5	6			
LQC	4.8	812743	817568	815250	829176	817537	810423	817116.2	6530.3	0.79
MQC	6	961082	969475	968483	963820	961540	969029	965571.5	3876.7	0.40
HQC	7.2	1081414	1086429	1084470	1096246	1083629	1089818	1087001	5342.7	0.49
Intraday, Day 1										
LQC	4.8	825575	829865	829075	821964	827469	829116	827177.3	2980.4	0.36
MQC	6	966186	955361	958196	951945	959570	966969	959704.5	5935.5	0.61
HQC	7.2	1085706	1089133	1088209	1084569	1088767	1089649	1087672	2050.5	0.18
Day 2										
LQC	4.8	812719	815564	812299	813695	817469	819116	815143.7	2736.2	0.33
MQC	6	967324	969974	969974	966479	962992	965329	967012	2717.3	0.28
HQC	7.2	1080183	1084325	1081780	1088911	1084208	1085714	1084187	3049.4	0.28
Day 3										
LQC	4.8	813282	817956	817616	810070	815356	818153	815405.5	3222.4	0.39
MQC	6	967412	962065	965682	969643	962178	966969	965658.2	3023.1	0.31
HQC	7.2	1080317	1087255	1081766	1089814	1085623	1087541	1085386	3649.6	0.33
Intermediate Precision, Inter Analyst 1										
LQC	4.8	805648	804572	806650	802368	806954	807772	805660.7	1956.3	0.24
MQC	6	961427	961746	968058	965432	962914	960580	963359.5	2850.7	0.29
HQC	7.2	1085554	1082879	1087499	1085423	1088149	1087328	1086139	1938.3	0.18
Inter Analyst 2										
LQC	4.8	812258	817235	816521	818944	814540	819872	816561.7	2817.7	0.34
MQC	6	968769	962587	964723	961139	964765	966382	964727.5	2703.1	0.28

HQC	7.2	1082369	1086421	1083215	1089852	1086821	1086251	1085822	2701.9	0.25
Inter Analyst 3										
LQC	4.8	810208	818356	817456	812532	816892	819348	815798.7	3605.7	0.44
MQC	6	967894	968523	964221	962321	968998	961427	965564	3329.1	0.34
HQC	7.2	1082569	1085922	1087865	1086310	1089521	1086932	1086520	2323.7	0.21

5.1.8.2.7 Robustness

It was found that the results' RSD was less than 2% By slightly modifying the mobile phase ratio and flow rate. This indicates that the developed technique demonstrated a high degree of robustness (Table 5.12).

Table 5.12: Results of robustness study

Variable	**Value**	**Concentration (µg/mL)**	**Average AUC (Mean± SD)**	**% Recovery**	**RT (min)**	**% RSD**
Flow rate (mL/min)	0.8	6	965001.5±1764	97.7	11.024	0.45
	1.0	6	985803.3±3155	99.9	11.028	0.12
	1.2	6	994796.2±1389	100	10.566	0.32
Mobile phase (Methanol: Water)	42:58	6	947077.7±2457	97.8	11.023	0.16
	40: 60	6	965393.3±2670	96.03	11.042	0.13
	38:62	6	984381±2967	99.8	10.842	0.31
Column temperature (°C)	25	6	973924.7±1141	99.45	11.034	0.17
	30	6	990342.5±1034	98.67	11.543	0.19
	35	6	963346.6±1581	97.31	11.273	0.44
Mobile phase pH	2.8	6	985430.23±1432	99.53	11.023	0.25
	3.0	6	966643.65±1101	98.65	11.340	0.37
	3.2	6	995432.55±2910	99.78	11.072	0.29

(n=6); AUC: Area under the curve, RT: Retention time, RSD: Relative standard deviation

5.1.8.2.8 Force degradation Studies

The analysis showed that the developed method effectively separated the degradation products from the analyte result (Table 5.13). Both the analyte and the degradants had unique peaks in the chromatograms derived from the forced degradation investigation, which comprised exposing the sample to a variety of stress conditions,

including acid, base, light, oxidative, and thermal stress. This demonstrates the specificity and accuracy of the established method in distinguishing the analyte from its breakdown products. Although t-RES was more vulnerable to alkali treatment, it exhibited the strongest resilience to acid treatment (Figure 5.10).

Table 5.13: Results of stressed studies performed.

Stress applied	**% Mean Recovered ± SD**
Untreated sample	100±0.45
Acid treatment HCl (0.1M, 24 h)	97.23±0.66
Alkali treatment NaOH (0.1M, 24 h)	70.21± 0.26
Light exposure (24 h)	91.43±0.77
Treatment with H_2O_2 (30% v/v, 24 h)	85.53±0.85
Thermal treatment (50 °C, 24 h)	83.21±0.82

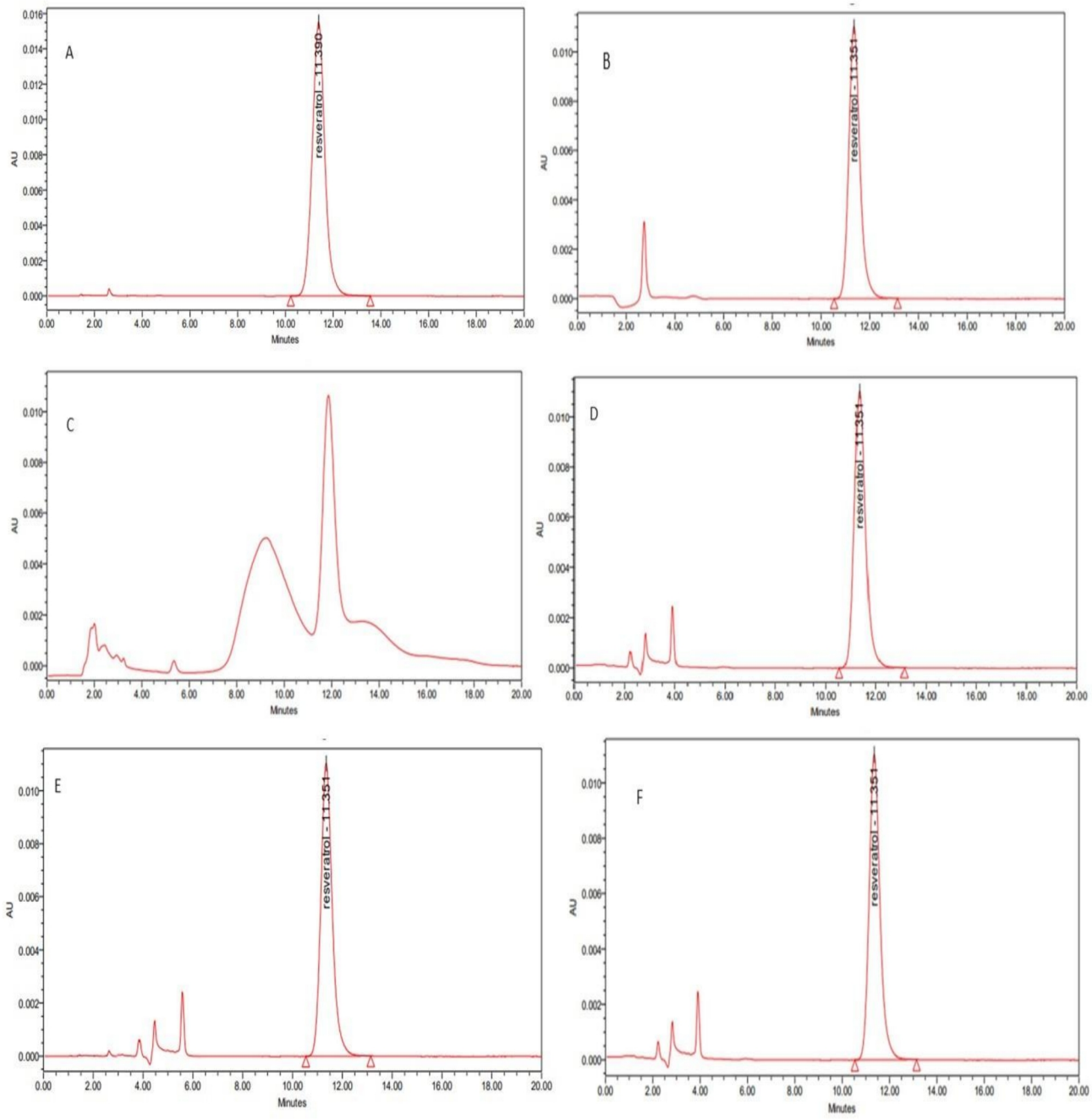


Figure 5.10: Chromatogram of (A) Untreated sample, (B) Acid treatment, (C) Alkali treatment, (D) Light exposure, (E) H2 O2 Treatment, and (F) Thermal treatment.

5.2 Preformulation study of carbon nanotube

5.2.1 Fourier Transform Infrared Spectroscopy (FTIR) spectra

The FTIR spectrum of the all-tested samples is shown in Figure 5.11 and 5.12.

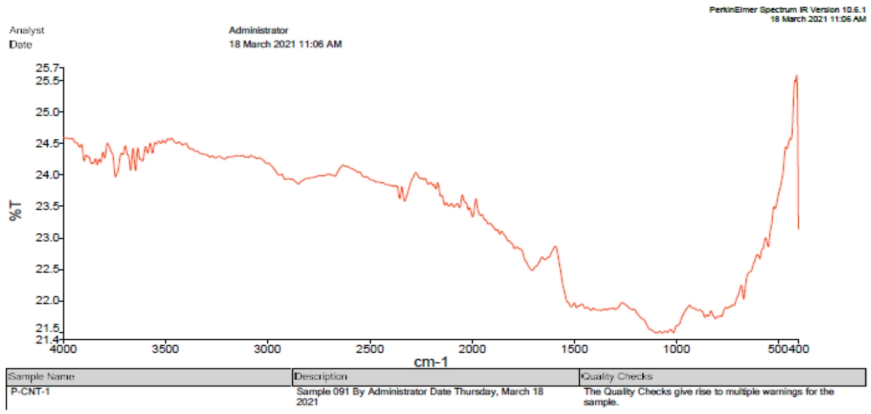


Figure 5.11: FTIR spectra of Pristine Multi-Wall Carbon Nanotubes.

It was noted that there are no noticeable bands in the line spectrum of clean MWCNTs. Nonetheless, the pure MWCNTs showed that the C=C groups in aromatic rings are responsible for the peak at 1640–1400 cm^{-1} range (Figure 5.11). (Chowdhry et al., 2019; Wang et al., 2013).

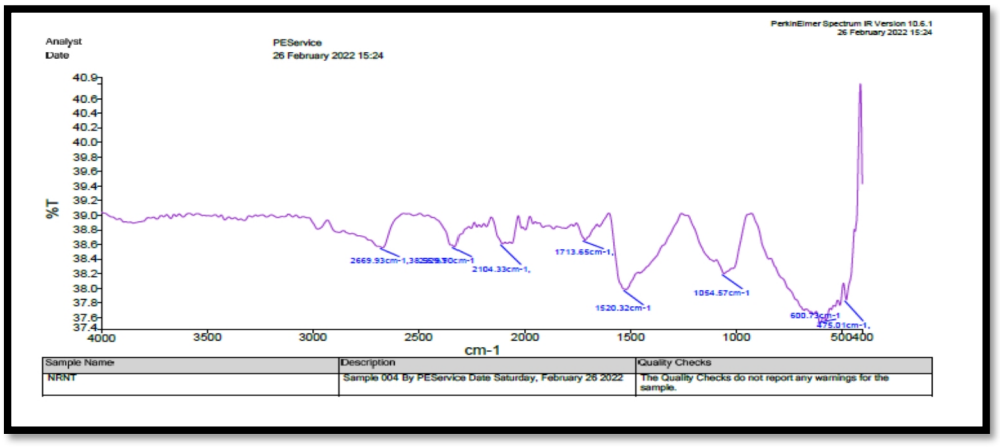


Figure 5.12: FTIR spectra of Amine-Functionalized Multi-Walled Carbon Nanotubes.

Table 5.14: FTIR spectra of amine-functionalized multi-walled carbon nanotubes.

Sr No.	Peak Range (Wavenumber cm^{-1})	Observed wavenumber cm^{-1}	Inference
1	3500–3400	3745.82cm	N-H (1° amine) and N-H (2° amine)
2	1550-1650	1630.57	C=C stretching of CNT structure
3	1000-1250	1101.96cm	C=N, and C–C stretching
4	1000-1250	1000.47cm	C-N stretching vibrations

FTIR analyses were used to find indications of amine attachments to multiwalled carbon nanotubes. The FTIR spectrum verified a modest variation in the availability of amine groups on the surface of the multiwalled carbon nanotubes. Pure multi-walled carbon nanotubes exhibited prominent peak at wavenumber 3745.82cm^{-1}, which is indicative of N-H (1° amine) and N-H (2° amine), then did amine multi-walled carbon nanotubes. A C=C stretching peak of the CNT structure is located at 1630.57 cm^{-1}, a C=N and C–C stretching peak is located at 1101.96 cm^{-1}, and a C-N stretching vibration peak is located at 1000.47 cm^{-1} (Eren et al. 2016).

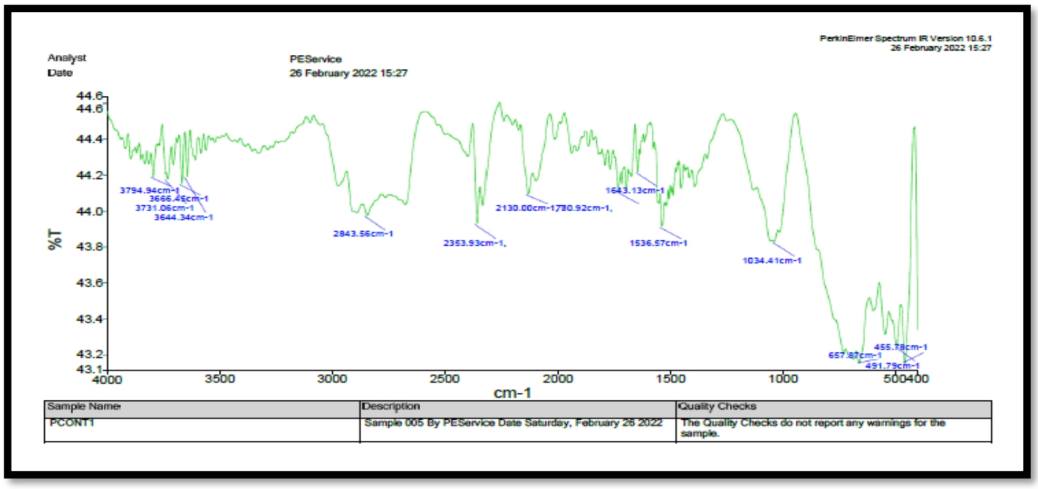


Figure 5.13: FTIR spectrum of COOH-MWCNT (Eren et al. 2016).

The spectra demonstrated peak at wavenumber of 3644.34 cm^{-1} corresponding to OH group (Stobinski et al., 2010). Both symmetric and asymmetric methylene stretching bands are seen at 2843.56 cm^{-1} in the MWCNT-COOH spectra. These groups are typically thought to be found at the sidewall surface defect areas (Scheibe et al., 2010). The MWCNT-COOH spectra display another noticeable peak at 1522 cm^{-1}, which is suggestive of a CO bond stretching frequency of the carboxylic group. These findings unequivocally show that the carboxyl group has been added to the CNT (Chowdhry et al., 2019).

5.2.2 Field Emission Scanning Electron Microscope (FE- SEM)

The FESEM captured images of the test samples are shown in Figure 5.14-5.16.

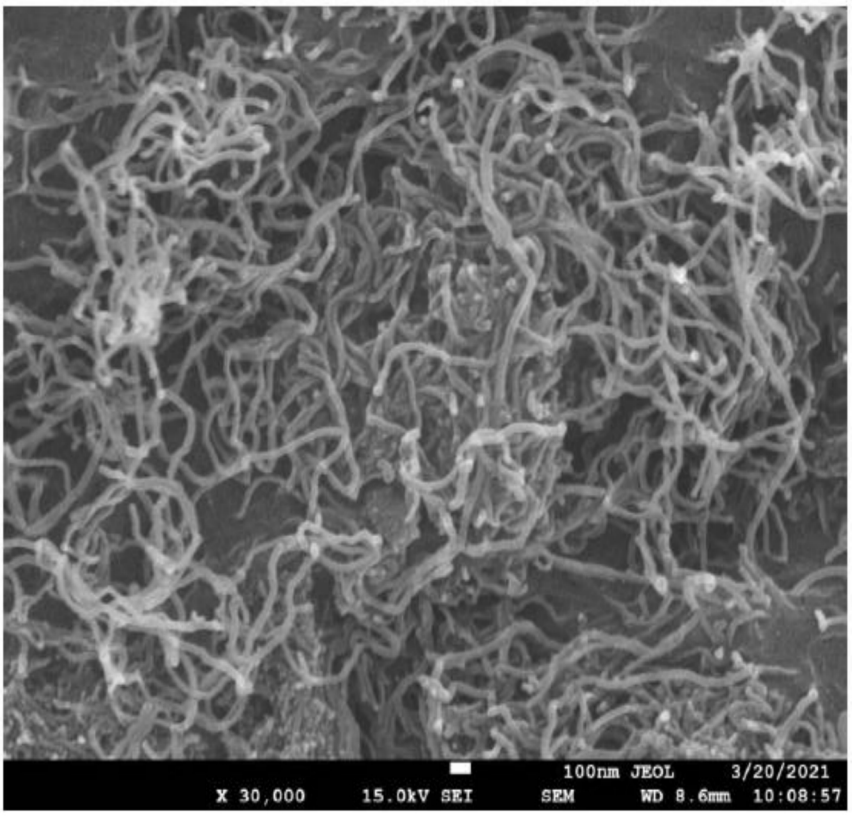


Figure 5.14: FE-SEM of Pristine Multi-Walled Carbon Nanotubes.

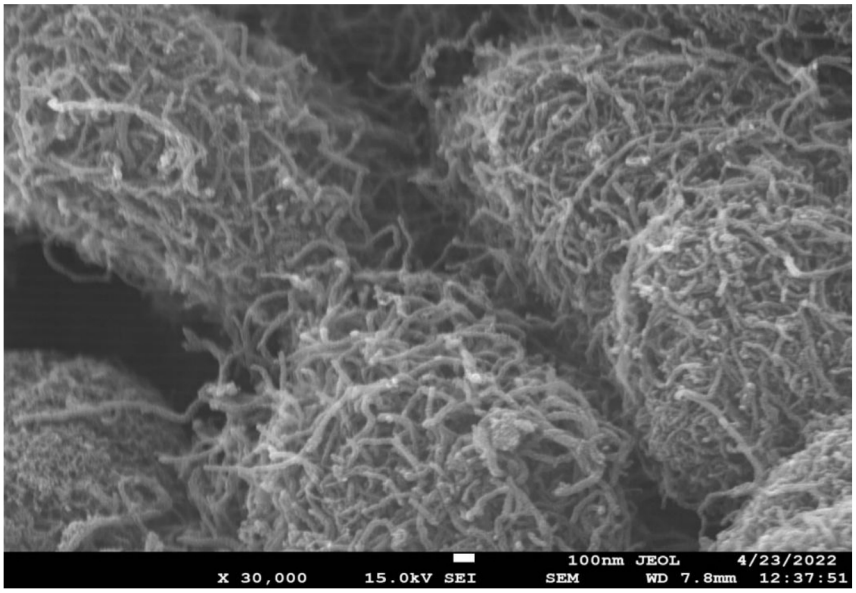


Figure 5.15: FE-SEM of NH_2-MWCNT

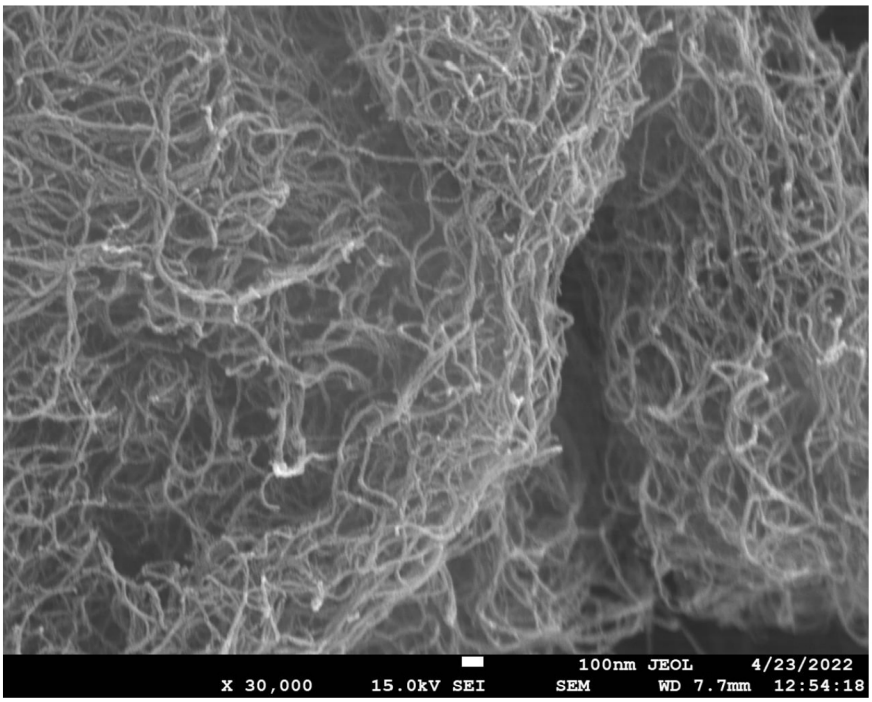


Figure 5.16: FE- SEM of COOH-MWCNT

The pristine MWCNTs' side walls were smooth, as seen in Figure 5.14, while the side walls of functionalised MWCNTs—whether MWCNT-COOH or MWCNT-NH_2—appeared to be rough with open cap structures. The emergence of disordered sites on the surface of MWCNTs is a sign of defect creation along their walls where additional functional groups (mostly carboxylic and amino) were introduced (Chowdhry et al., 2019).

5.2.3 X-Ray Diffraction (XRD)

The X-ray diffractogram of the test samples are shown in Figure 5.17-5.19.

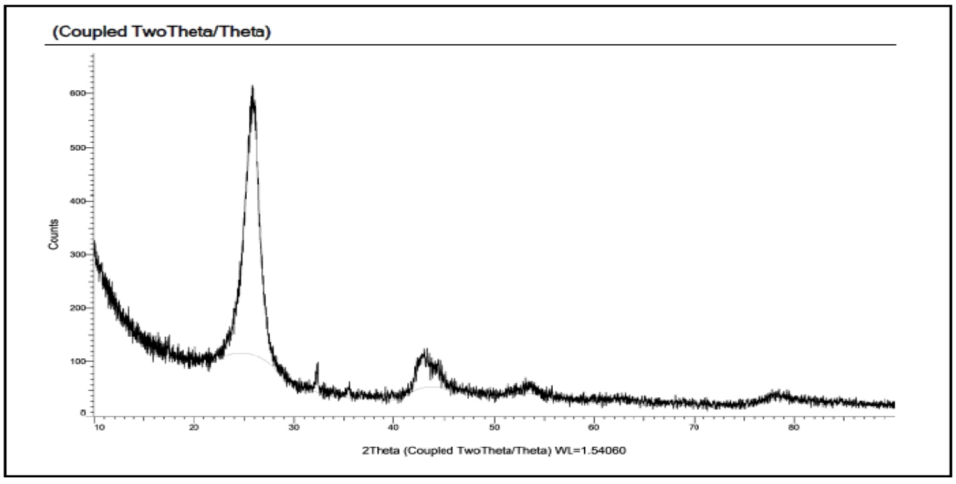


Figure 5.17: XRD of Pristine Multi-Walled Carbon Nanotubes

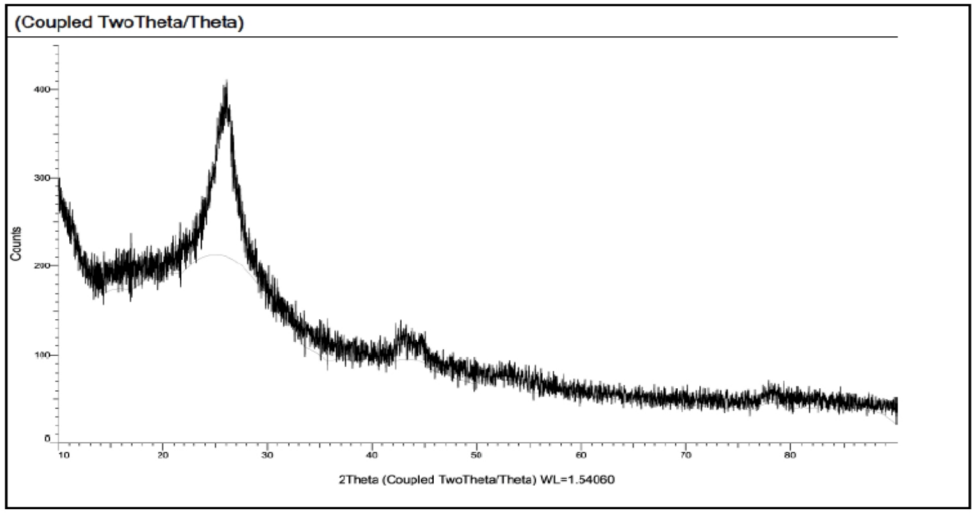


Figure 5.18: XRD of Amine-Functionalized Multi-Walled Carbon Nanotubes

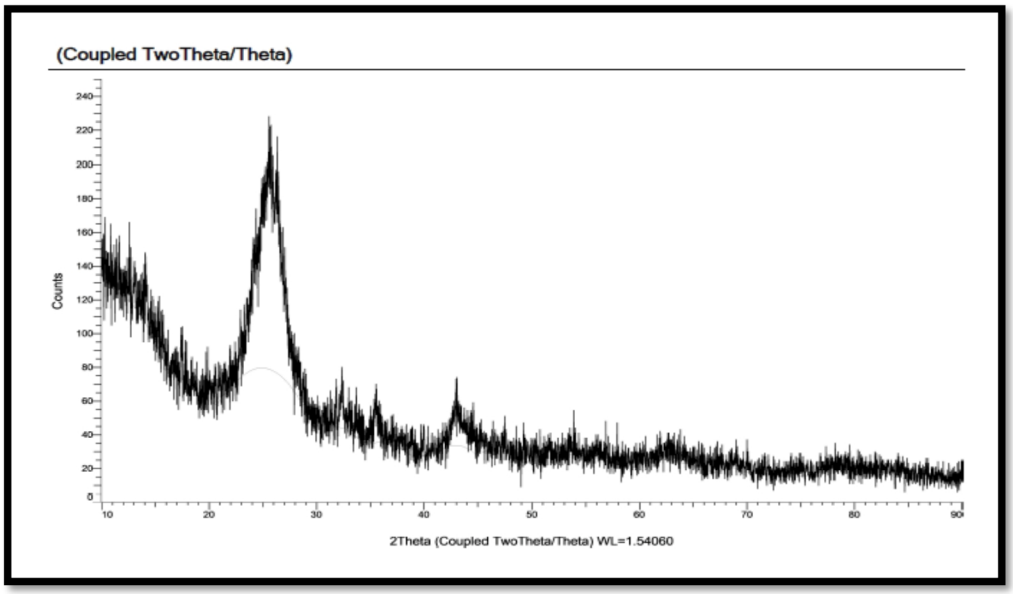


Figure 5.19: XRD pattern of COOH-MWCNT (Shen et al. 2007).

Figure 5.17-5.19 illustrates that the C (002) reflection of graphite may be identified by the XRD study of pristine, amino-functionalized, and COOH-MWCNT, which all have the same greatest and sharpest diffraction peak at about 2θ=26.3°. Since the C (002) peak is sharp, it can be concluded that MWCNTs' graphite structure was acid-oxidized without suffering any serious damage. The size of the crystal and the distance between layers were measured using XRD. Since the peaks of the carboxylic acid and amine-functionalized multi-walled carbon nanotubes are wider, it is likely that the degree of crystallinity was actually weakened by the treatment. However, there are extremely minor amounts of it (Khani et al., 2013).

5.2.4 Zeta Size and Potential

The size and surface charge density of the test samples are shown in Figure 5.20-5.25.

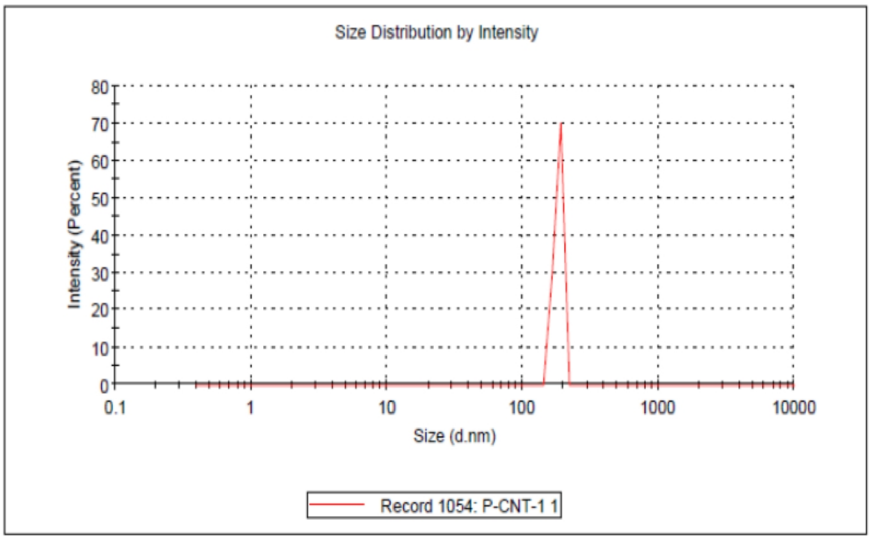


Figure 5.20: Zeta Size of Pristine Multi-Walled Carbon Nanotubes

		Mean (mV)	Area (%)	St Dev (mV)
Zeta Potential (mV): -8.02	Peak 1:	-8.02	100.0	5.72
Zeta Deviation (mV): 5.72	Peak 2:	0.00	0.0	0.00
Conductivity (mS/cm): 0.256	Peak 3:	0.00	0.0	0.00
Result quality Good				

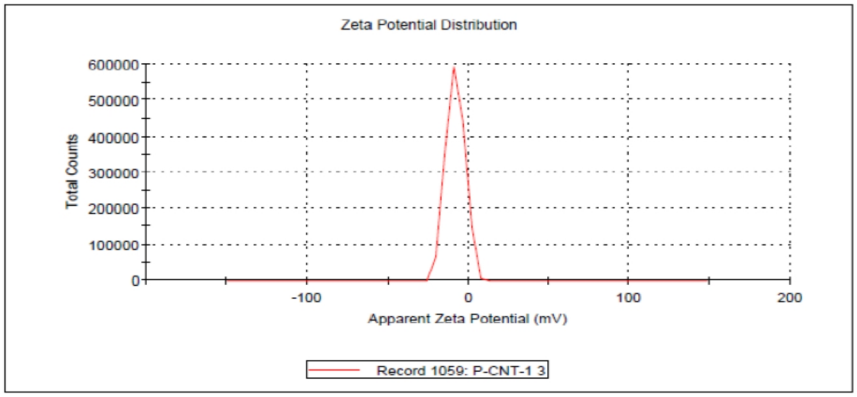


Figure 5.21: Zeta Potential of Pristine Multi-Walled Carbon Nanotubes

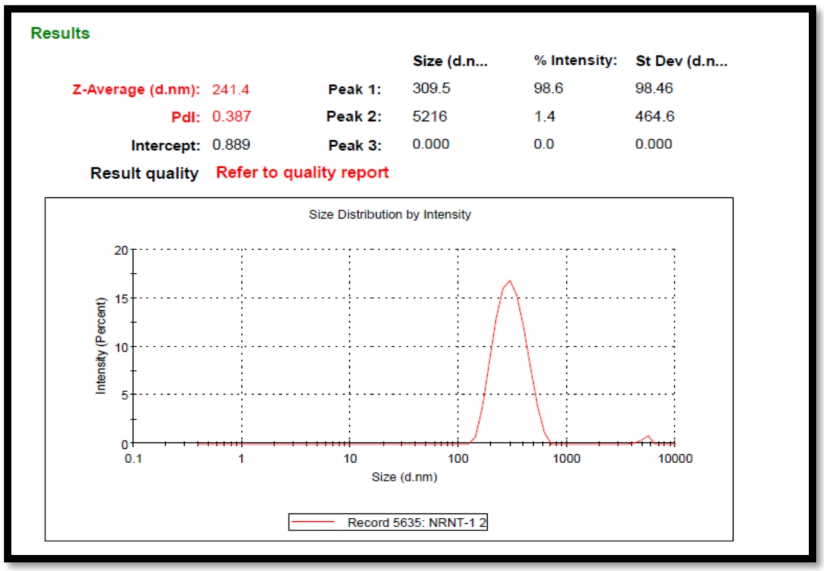


Figure 5.22: Zeta Size of Amine Multi-walled Carbon Nanotubes

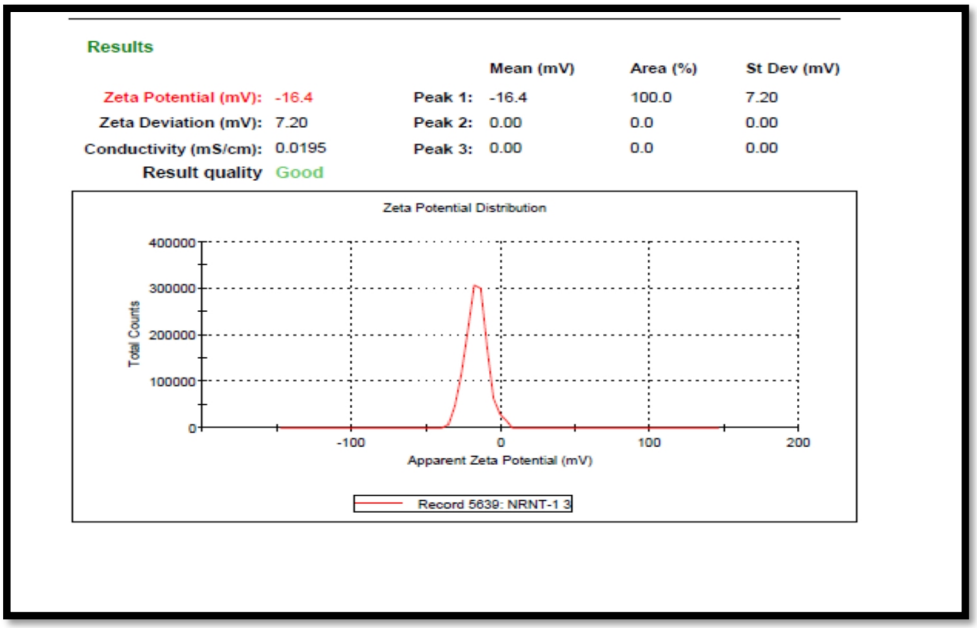


Figure 5.23: Zeta potential of Amine Multi-Walled Carbon Nanotubes.

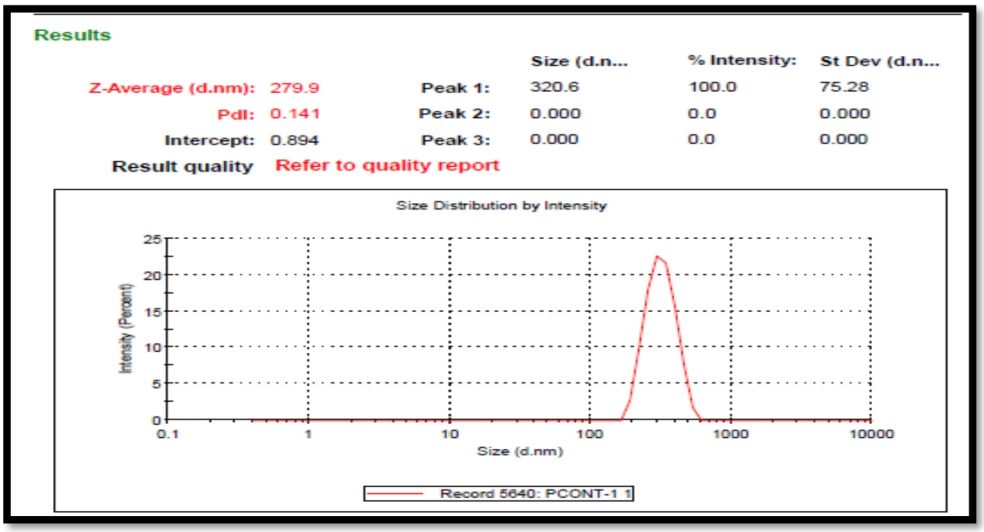


Figure 5.24: Zeta Size of Carboxylic Acid Multi-Walled Carbon Nanotubes

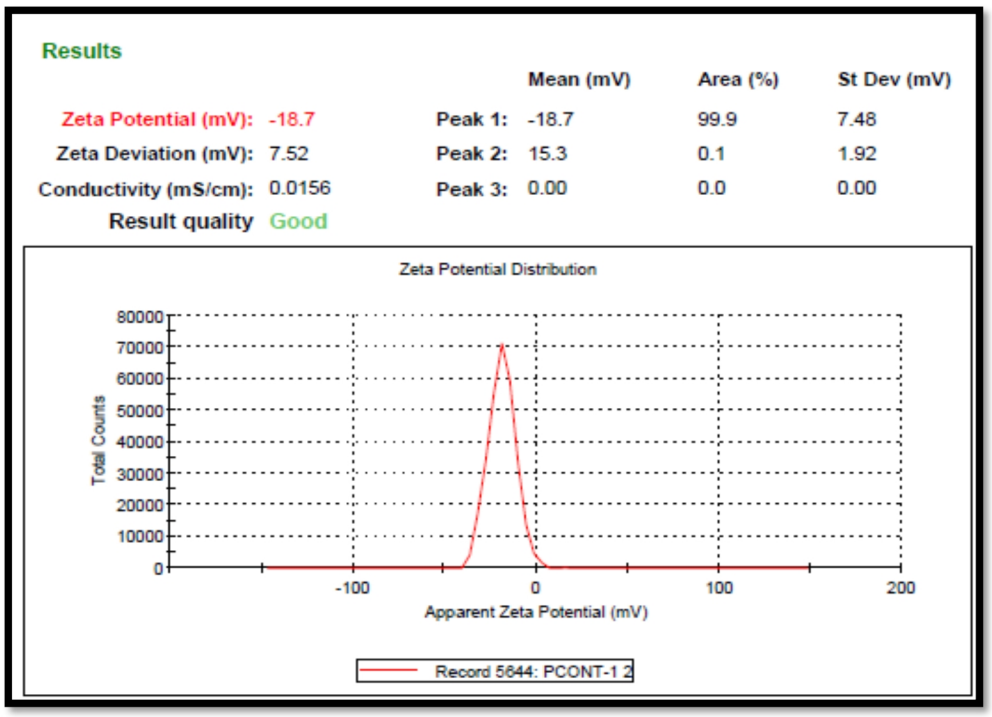


Figure 5.25: Zeta potential of Carboxylic Acid Multi-Walled Carbon Nanotubes

The particle sizes of pristine, amino-functionalized, and carboxylic acid-functionalized multi-walled carbon nanotubes were found to be 182.4 nm, 241.4 nm, and 279.9 nm, respectively, in Figure 5.20, 5.22, and 5.24. This suggests that the modification process was successful and that the size of the multi-walled carbon nanotubes increased (Parveen et al., 2017).

A common metric for assessing the colloidal stability of suspensions is their zeta potential. The zeta potential value of less than -15 mV or greater than +15 mV are regarded as stable. It shows the strength of the electrostatic contacts between the colloidal particles.

Zeta potential analysis provides quantitative information about created repulsion between particles with the aid of electrical double layers surrounding them, which in turn provides useful information about the stability of suspensions. This makes it a dependable technique for characterising stability. Furthermore, a reduced zeta potential results from the particles' increased bulk and slower motion when they are aggregated (Lee et al., 2005). As a result, zeta potential may also provide insight into aggregation; a higher zeta potential could indicate improved dispersion.

A zeta potential study was conducted to determine the charge to size ratio of the functionalised MWCNTs in distilled water in order to get insight into the outcomes of the agglomeration experiment. Following a 15-minute water bath sonication, the aqueous samples were run through the zeta potential analyser. The average readings for the Pristine carbon nanotube, MWCNT-NH_2, and MWCNT-COOH in distilled water were –8.04 mV, -16.4 mV, and -18.7 mV, as shown in mention Figure (Chowdhry et al., 2019).

5.3 Formulation of t-RES loaded Carbon Nanotubes

In the current activity, the two components were mixed in a 1:1 and 1:2 ratio to create the drug t-RES loaded carbon nanotube. Additionally, two distinct carbon nanotubes—Amine-CNT and Carboxylic Acid-CNT—were employed to load the t-RES. Zeta Potential, XRD, UV, and IR spectroscopy were used to characterise the prepared batches of the t-RES loaded carbon nanotube.

5.4 Characterization of t-RES loaded Carbon Nanotubes

5.4.1 Uv spectroscopy

As seen in Figure.5.26, the test samples Pure t-RES, RES-MWCNT-1(F1), RES-MWCNT-2(F2), RES-MWCNT-3(F5), and RES-MWCNT-4 (F6) were scanned using UV spectroscopy at wavelengths ranging from 200 to 400 nm. The overlay spectra verified that none of the samples' absorption maxima had changed.

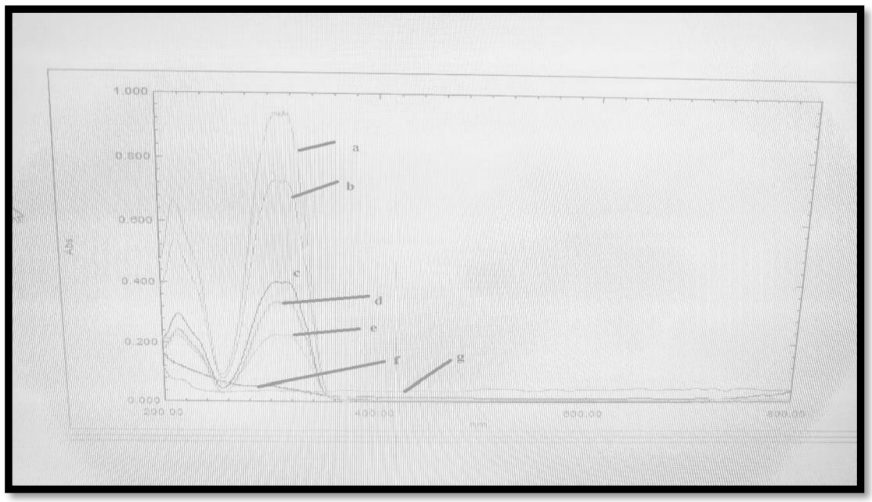


Figure 5.26: UV Spectroscopy of a) t-RES b) RES-MWCNT-4 c) RES-MWCNT-3 d) RES-MWCNT-2 e) RES-MWCNT-1 f) NH2-MWCNT 4 g) COOH-MWCNT

5.4.2 Fourier Transform Infrared Spectroscopy (FTIR) spectra

FTIR spectrum of RES-MWCNT 1, RES-MWCNT 2, RES-MWCNT 3, and RES-MWCNT 4 were shown in Figure 5.27-5.30.

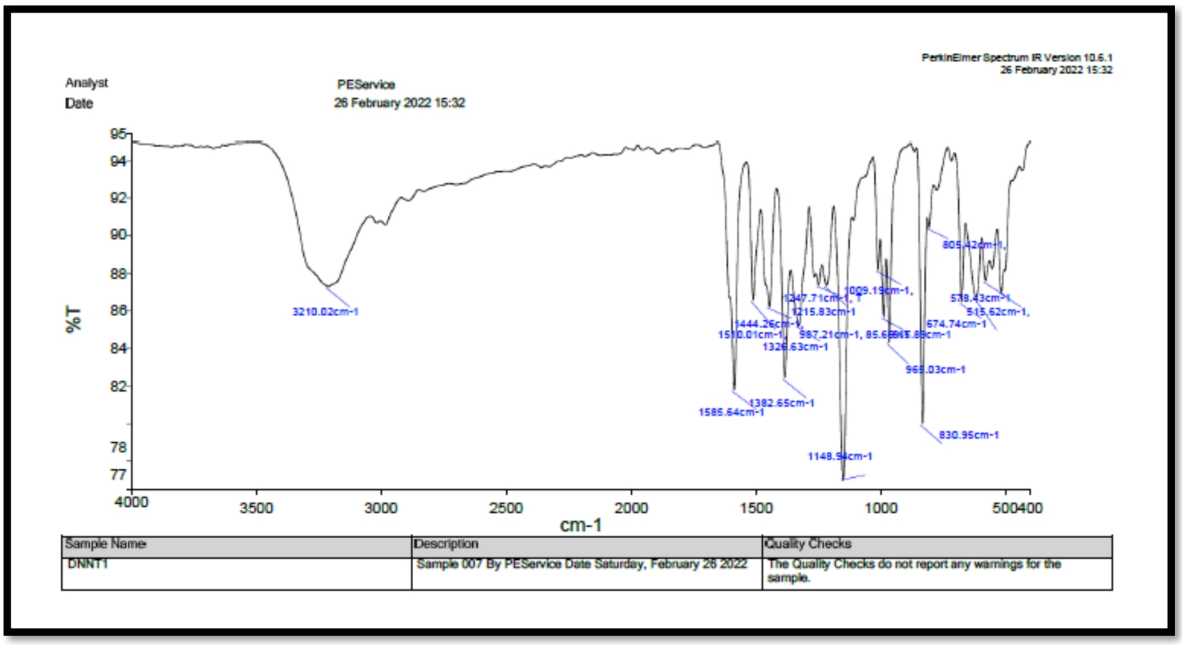


Figure 5.27: FTIR spectrum of Formulation RES-MWCNT 1.

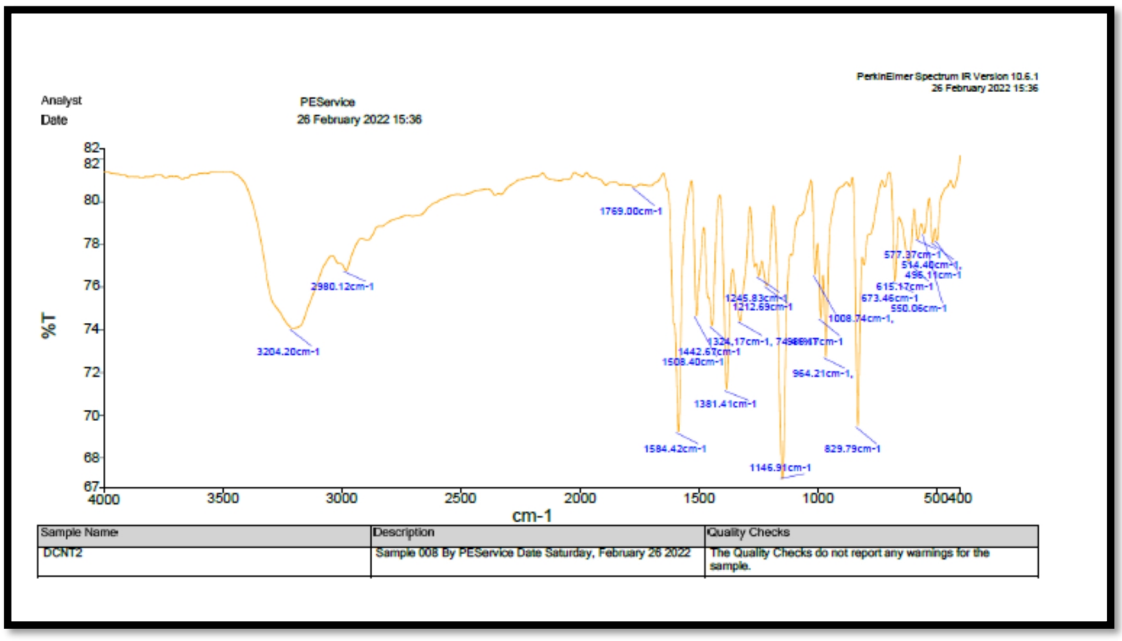


Figure 5.28: FTIR spectrum of Formulation RES-MWCNT 2.

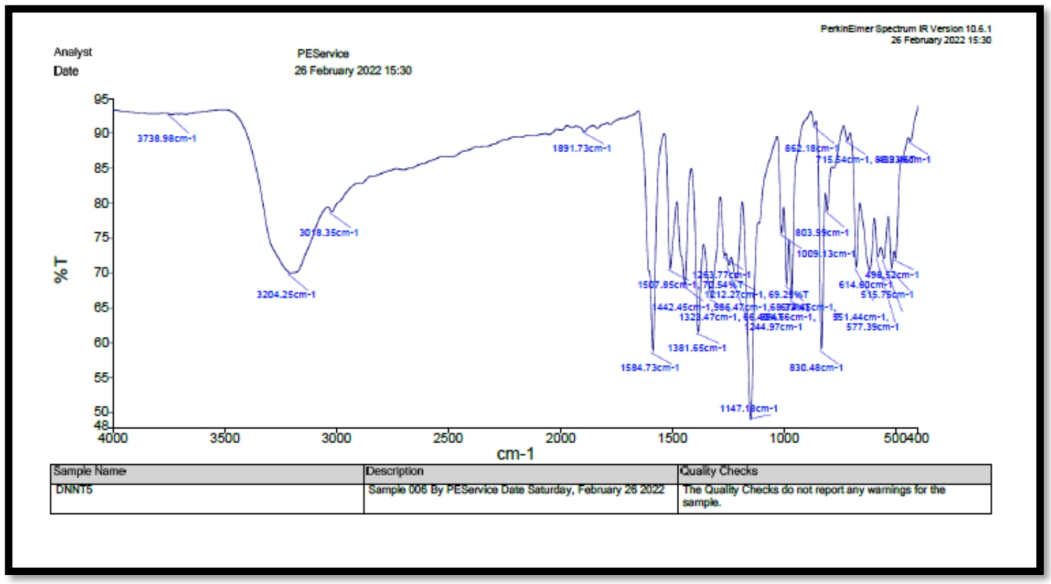


Figure 5.29: FTIR spectrum of Formulation RES-MWCNT 3.

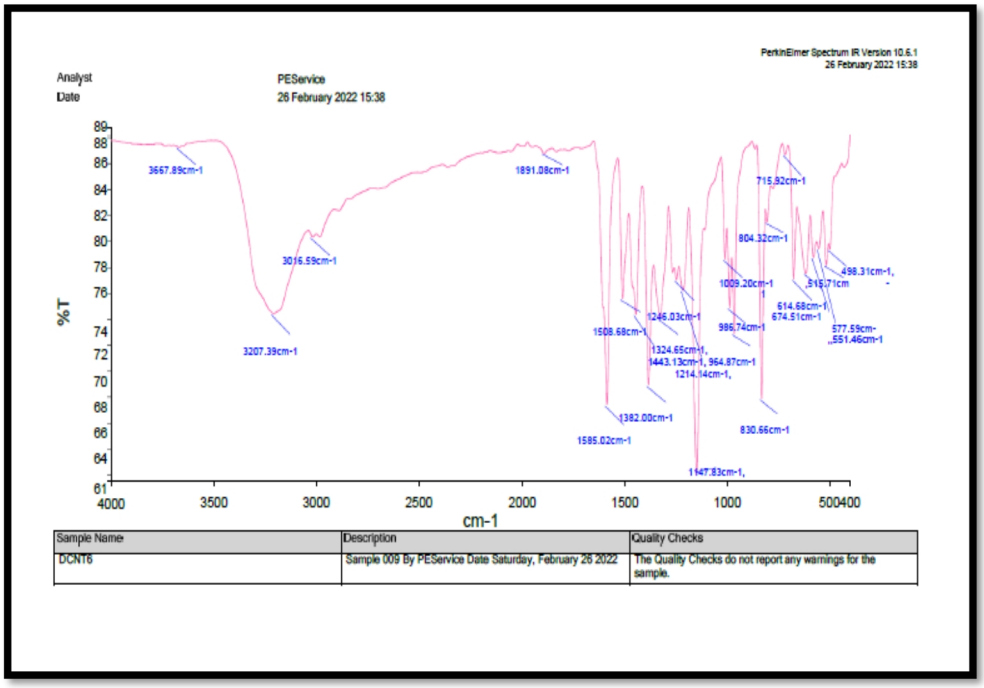


Figure 5.30: FTIR Spectrum of Formulation RES-MWCNT 4.

In this investigation, two distinct drug-to-CNT ratios (1:1 and 1:2) were used to load the t-RES drug over the amin-functionalized and COOH-functionalized CNTs. The chemical relationship between surface-modified CNT and t-RES was investigated using infrared spectral data. The peaks of t-RES 3680 to 3000, 1600 to 1300, and 950 cm^{-1} were found to be characteristic of each t-RES-loaded carbon nanotube. Similarly, the peaks of functionalised carbon nanotubes were found to show that there was no incompatibility between t-RES and CNT and that the t-RES drug was incorporated into the CNT's channel (Ali et al., 2021).

5.4.3 X- Ray Diffraction (XRD)

X-ray diffractogram of RES-MWCNT 1, RES-MWCNT 2, RES-MWCNT3, and RES-MWCNT4 ere shown in Figure 5.31-5.34.

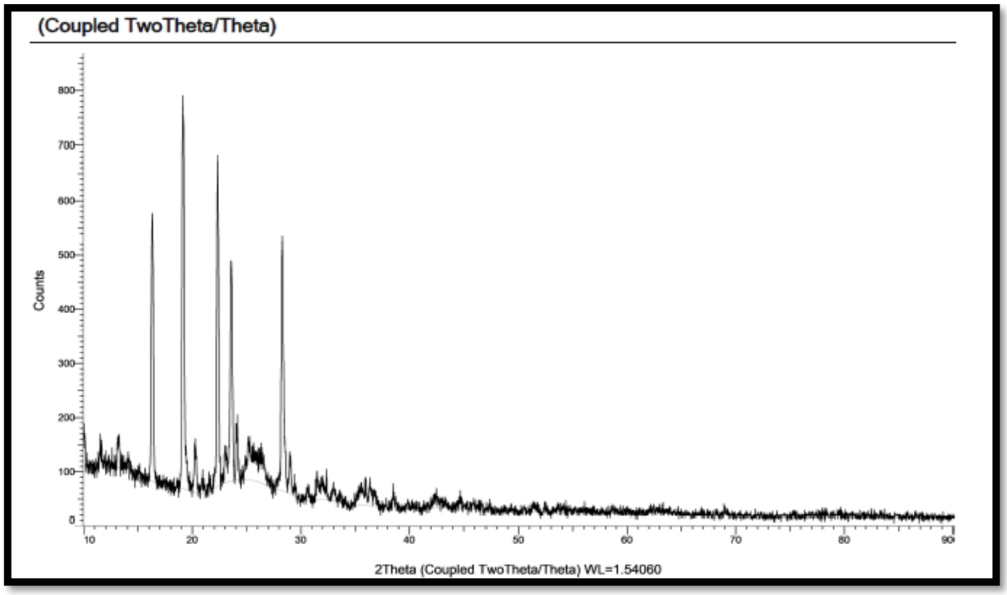


Figure 5.31: XRD pattern of RES-MWCNT 1.

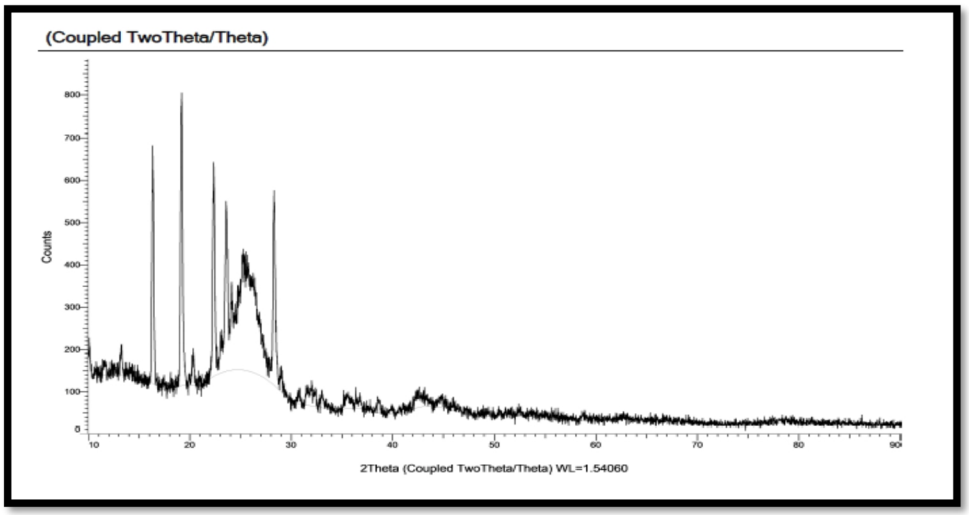


Figure 5.32: XRD pattern of RES-MWCNT 2

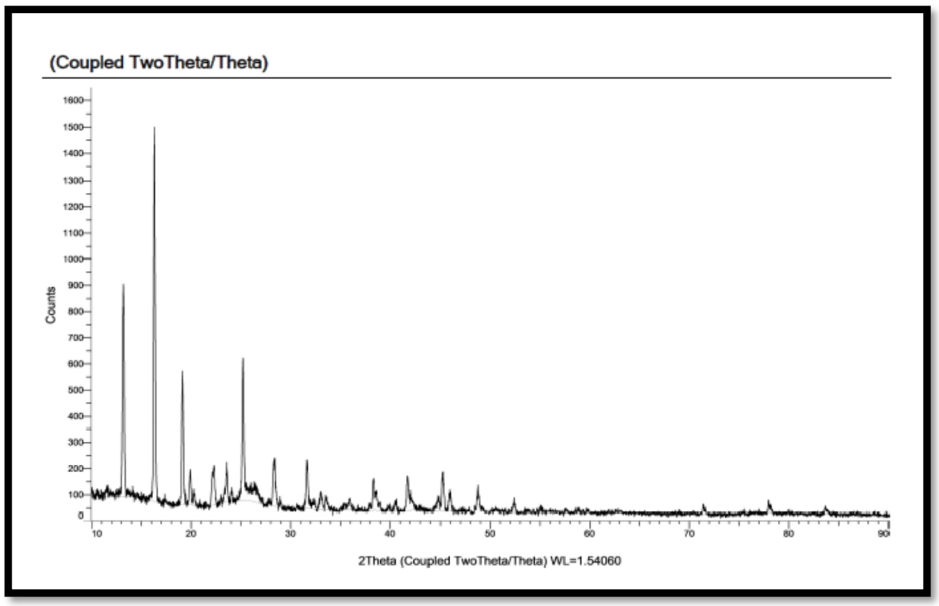


Figure 5.33: XRD pattern of RES-MWCNT 3

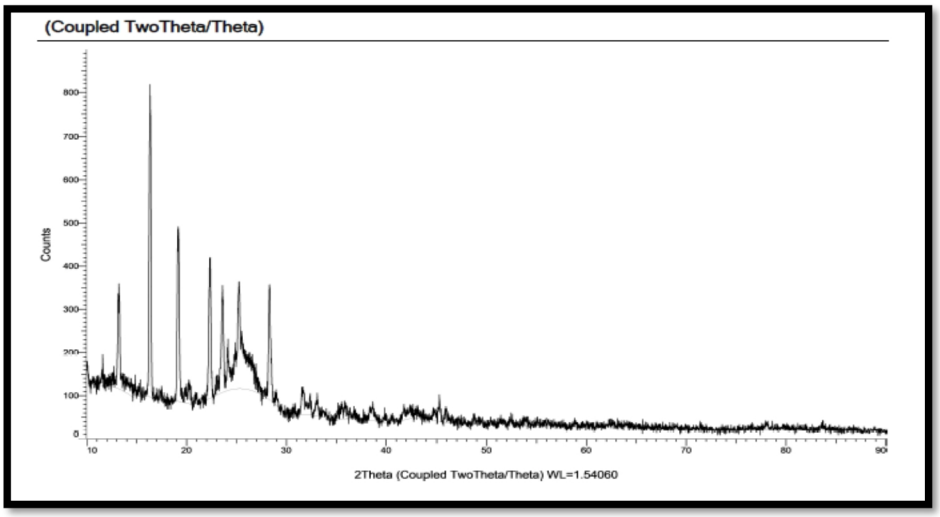


Figure 5.34: XRD pattern of RES-MWCNT-4.

The peaks of diffused intensity in the XRD diffractogram of carbon nanotubes functionalised with amines and carboxylic acids showed that the carbon nanotube was amorphous. On the other hand, the t-RES loaded carbon nanotube showed the distinctive peaks of the t-RES that indicated drug loading into the carrier in the X-ray diffractogram (Figure 5.31-5.34).

5.4.4 Percentage drug entrapment of t-RES to the carbon nanotube

The percentage entrapment of the t-RES into the carbon nanotube were shown in Table 5.15.

Table 5.15: Percentage drug loading of the t-RES in carbon nanotube

Sr.No.	Formulation code	Entrapment Efficiency (%)
1	RES-MWCNT 1	73.83 ± 0.023
2	RES-MWCNT2	96.29 ± 0.054
3	RES-MWCNT3	84.15 ± 0.076
4	RES-MWCNT4	80.68 ± 0.065

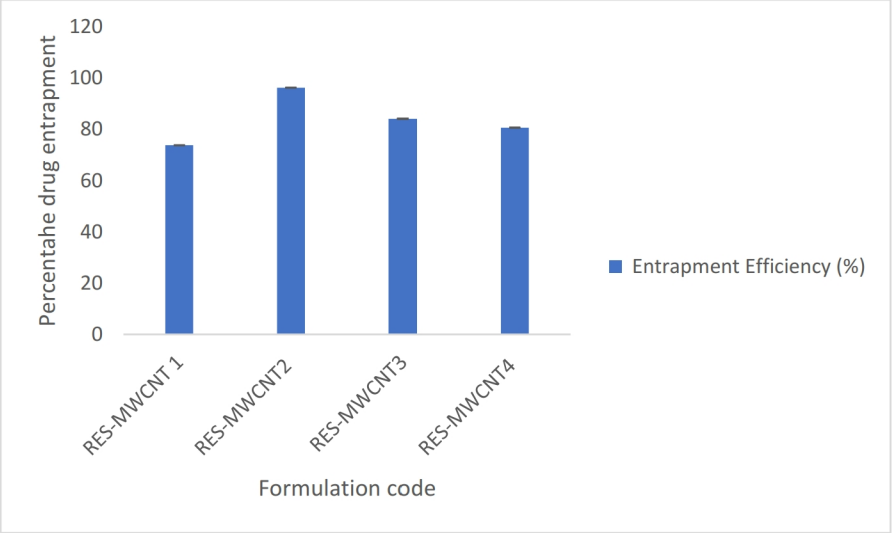


Figure 5.35: Percentage drug entrapment of t-RES in carbon nanotube

The drug t-RES loading in MWCNTs was ascertained using the established HPLC technique. In formulations RES-MWCNT 1, RES-MWCNT 2, RES-MWCNT 3, and RES-MWCNT 4, the percentage of t-RES drug entrapment was 73.83 ± 0.023%, 96.29 ± 0.054%, 84.15 ± 0.076%, and 80.68 ± 0.065%, respectively. The carbon nanotube functionalised with carboxylic acid has a greater t-RES entrapment. The carboxylic acid carbon nanotube's high degree of channel cross-linking may be the cause (Ali et al., 2024).

The t-RES loaded carbon nanotube formulation RES-MWCNT 2 was chosen for additional characterisation based on the percentage drug entrapment and the previously mentioned characterisation criteria.

5.4.5 Particle size and Zeta Potential

Figure 5.36 and 5.37 displayed the particle size and zeta potential of RES-MWCNT 2. Information on CNTs' hydrodynamic diameter (Z-average), which is correlated with the material's zeta potential and spherical particle diameter, is obtained using dynamic light-scattering measurements. Figure 5.36 displays the RES-MWCNT 2 hydrodynamic diameters. The hydrodynamic diameter of RES-MWCNT 2 was the smallest at 289.6 nm because to its greater zeta potential of -18.8 mv, which inhibited CNT aggregation. Given

that RES-MWCNT 2's PDI (0.070) was nearly 0.1, the system was regarded as monodispersed (Tsai et al., 2013).

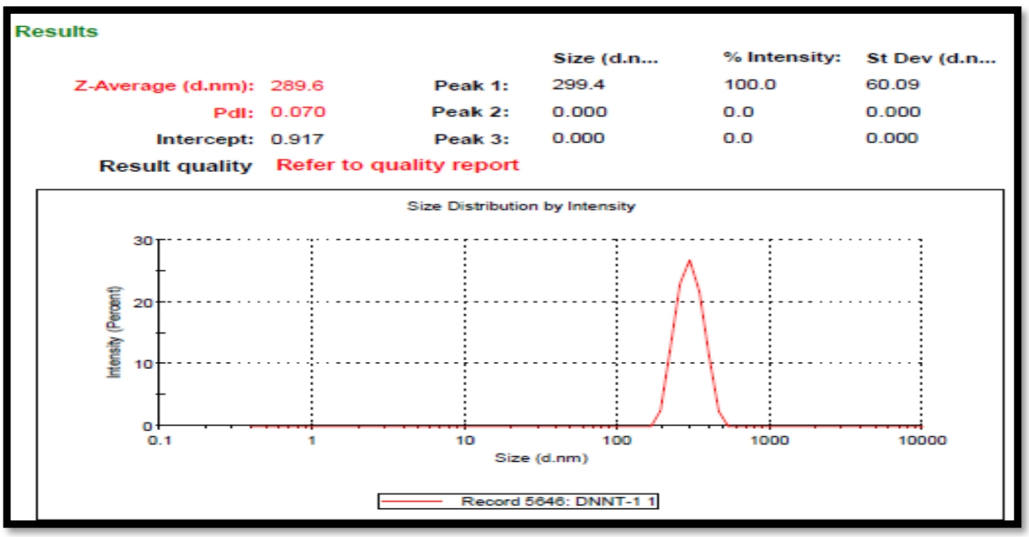


Figure 5.36: Particle size of RES-MWCNT 2

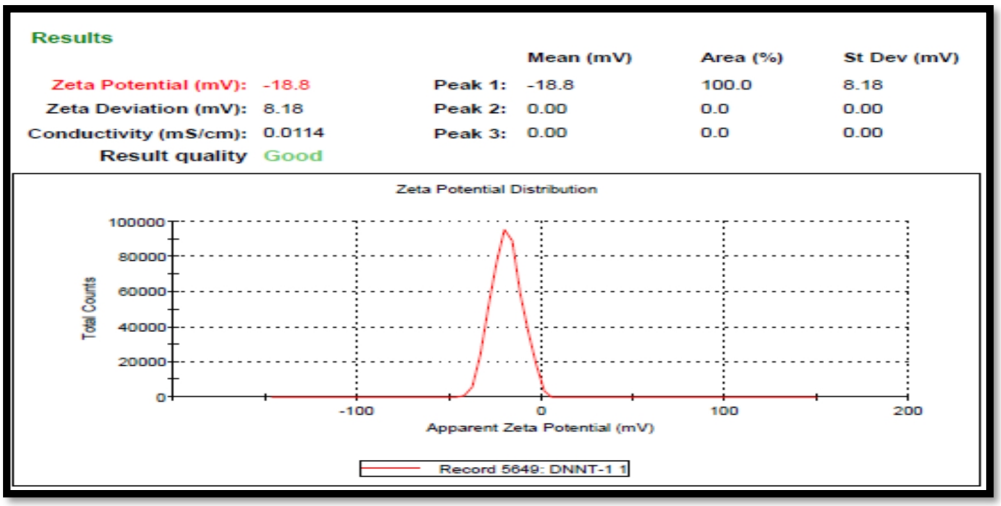


Figure 5.37: Zeta Potential of RES-MWCNT 2

5.4.6 ^{1}H and ^{13}CNMR NMR studies

Proton spectrum of pure drug t-RES, carboxylic CNT and RES-MWCNT 2 are shown in Figure 5.38-5.40.

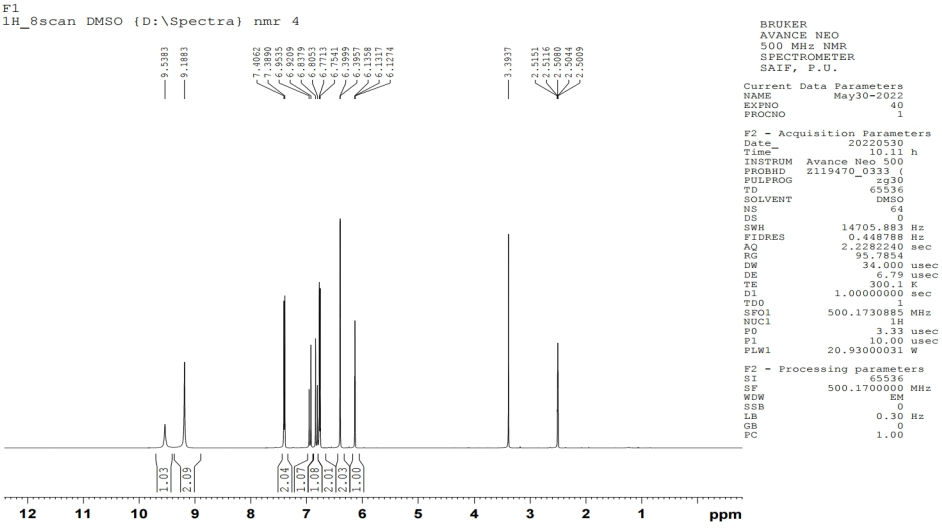


Figure 5.38: ^{1}H NMR spectra of t-RES

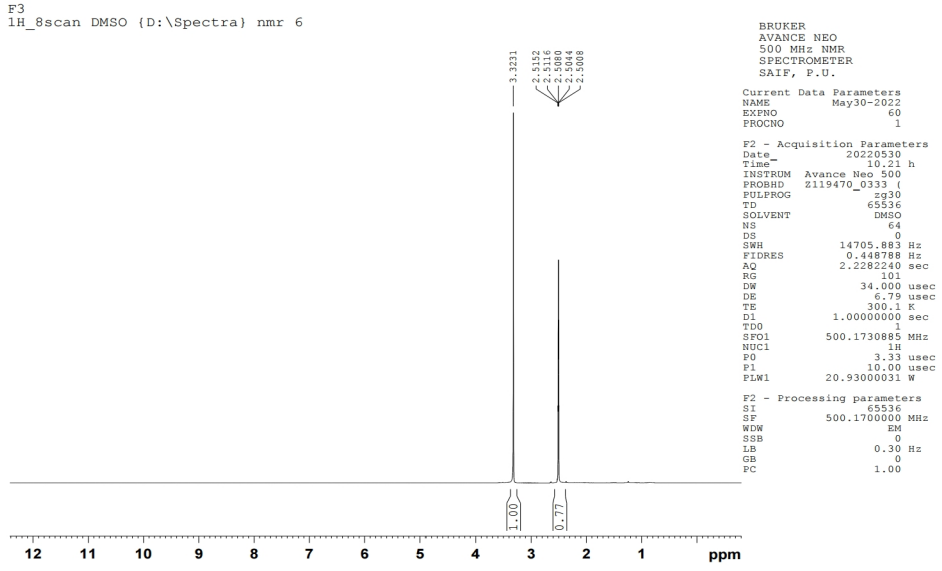


Figure 5.39: ^{1}H NMR spectra of carboxylic CNT

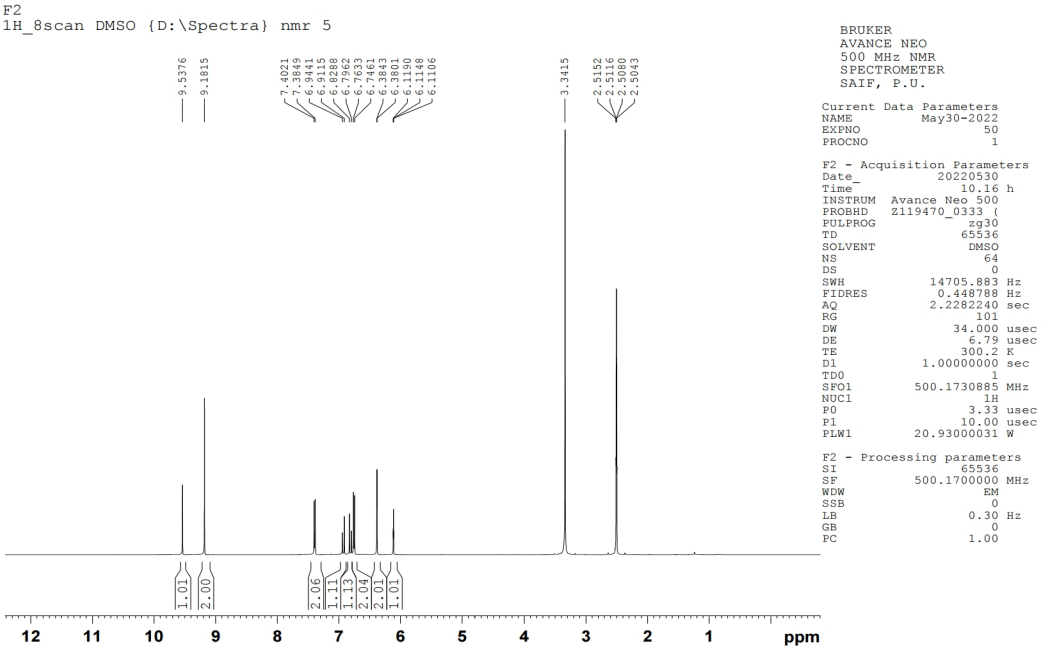


Figure 5.40: ^{1}H NMR spectra of RES-MWCNT 2

ChemNMR ^{1}H Estimation

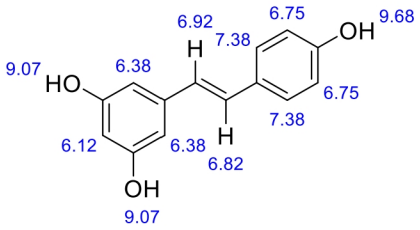


Figure 5.41: Chemical structure of t-RES

The following 1H NMR (500 MHz, DMSO-d6) peak is shown in Figure 5.37 graph: δ (ppm) 9.53 (s, 1H), 9.18 (s, 2H), 7.69 (d, J = 8Hz, 2H), 7.53 (d, J = 12 Hz, 1H), 7.42 (d, J = 12 Hz, 1H), 7.28 (d, J = 12 Hz, 2H), 6.95 (d, J = 1.68 Hz, 2H), and 6.30 (t, J = 4 Hz, 1H) confirm the structure of pure t-RES. The NMR spectra of carboxylic CNT in Figure 5.39 show peaks at 3.3415 ppm and 2.515, while RES-MWCNT 2 in Figure5.40 shows an extra MWCNT peak in addition to t-RES peaks.

[13] CNMR spectrum of pure drug t-RES, MWCNT and RES-MWCNT 2, RES-CNT-CET, RES-CNT-CET are shown in Figure 5.42-5.44.

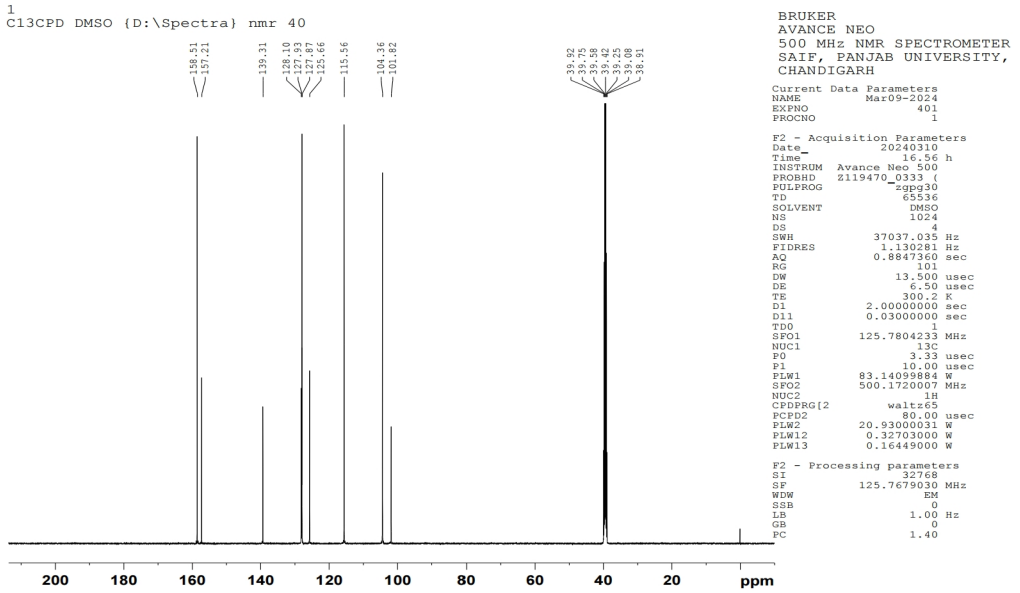


Figure 5.42: [13]C NMR spectra of pure drug

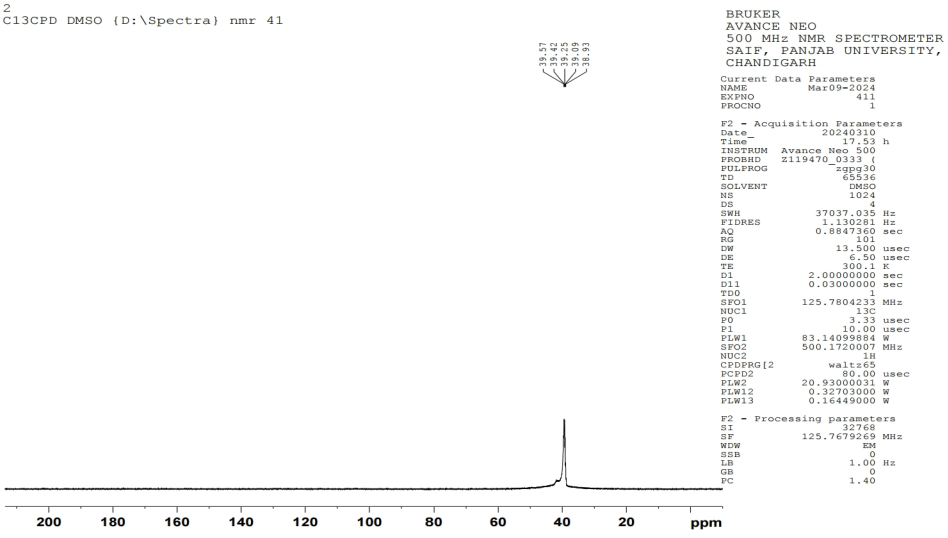


Figure 5.43: [13]C NMR spectra of MWCNT

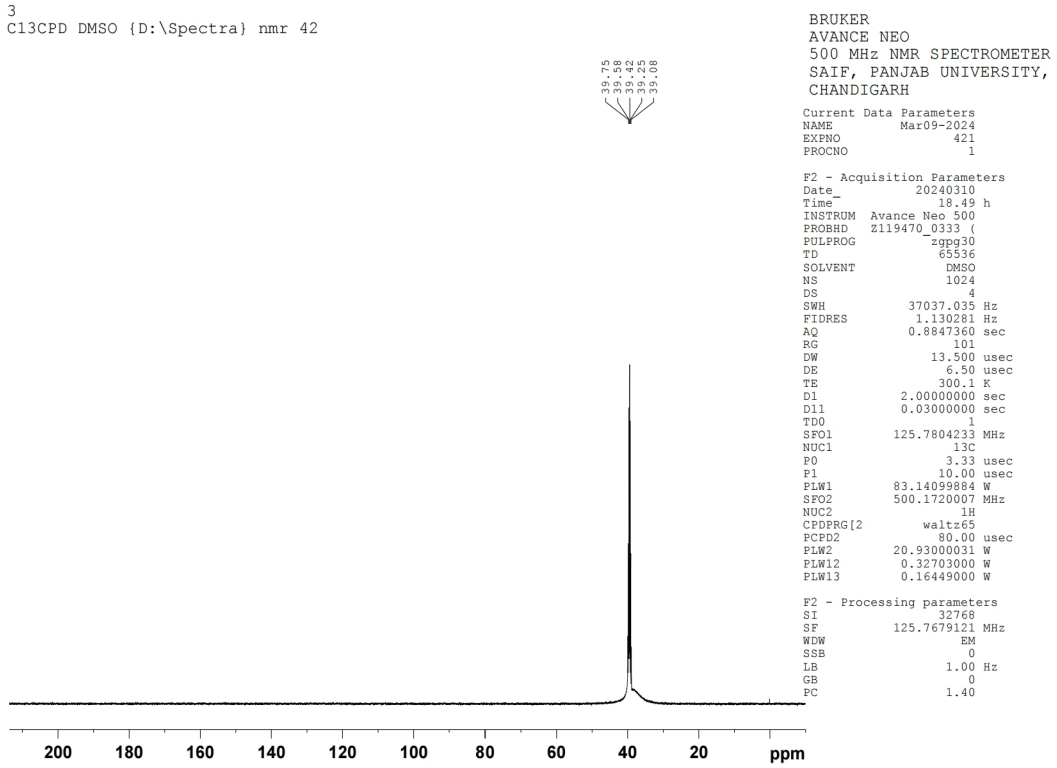
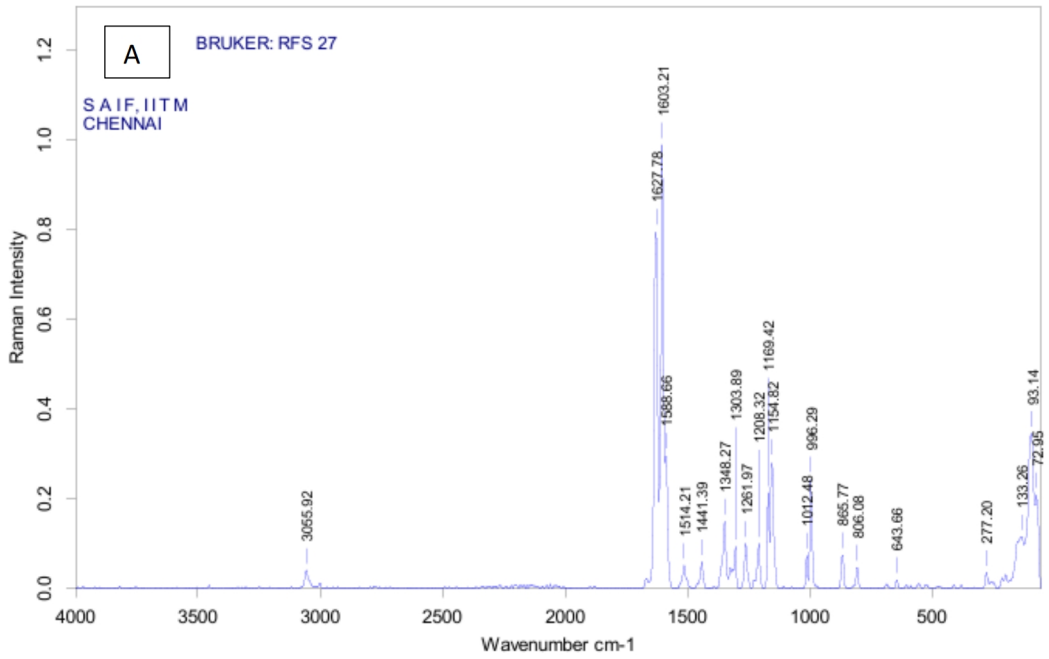


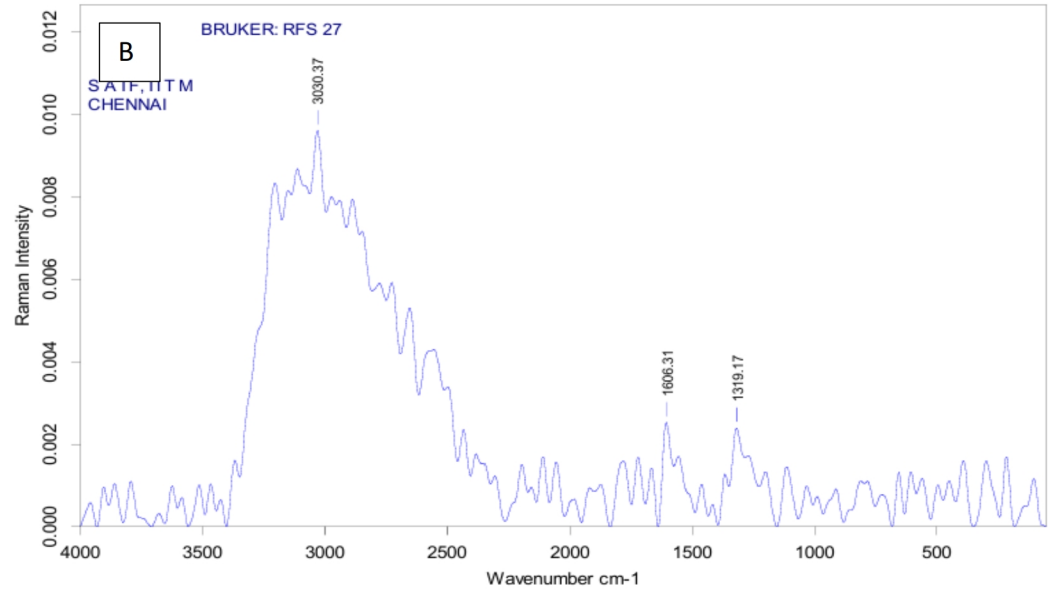
Figure 5.44: ^{13}C NMR spectra of RES-MWCNT 2

5.4.7 Raman spectroscopy

t-RES Raman Spectra are displayed in Figure. 5.45. It showed two significant bands at 1627 cm^{-1} and 1603 cm^{-1}, indicating exceptional property linked to t-RES. Together with v(C=C) vibrations connected to the phenyl rings, the two bands represent a configuration of v(C=C) and δ(C–H) vibrations connected to the trans-olefin carbons (Qin et al. 2020). In Figure 2(B), the distinctive peaks of the tangential modes of multi-walled carbon nanotubes (MWNT) are the D band, which is situated at about 1303 cm^{-1}, and the G band, which is about 1599 cm^{-1}, where ID/IG was 0.924.

The findings imply that a mild oxidation process produced a low ratio of structural flaws in the RES-MWCNT 2. According to the findings, the Raman spectrum's D band, which represents the hybridisation of some carbon atoms from sp^2 to sp^3, is linked to covalent sidewall functionalisation.


A
BRUKER: RFS 27
S A I F, I I T M
CHENNAI
Raman Intensity
Wavenumber cm-1
1603.21
1627.78
1588.66
3055.92
1514.21
1441.39
1348.27
1303.89
1261.97
1208.32
1154.82
1169.42
1012.48
996.29
865.77
806.08
643.66
277.20
133.26
93.14
72.95


B
BRUKER: RFS 27
S A I F, I I T M
CHENNAI
Raman Intensity
Wavenumber cm-1
3030.37
1606.31
1319.17

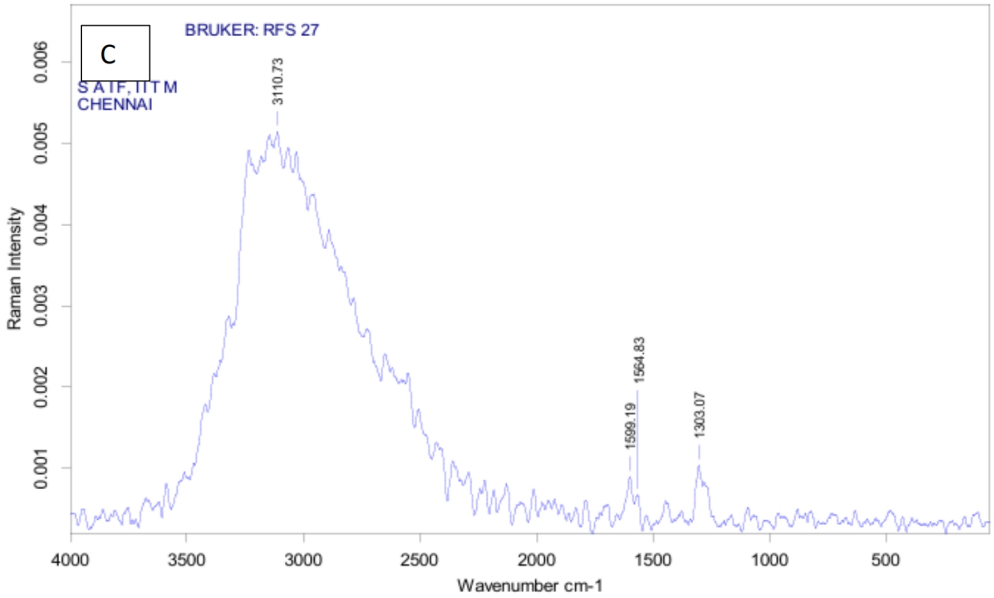
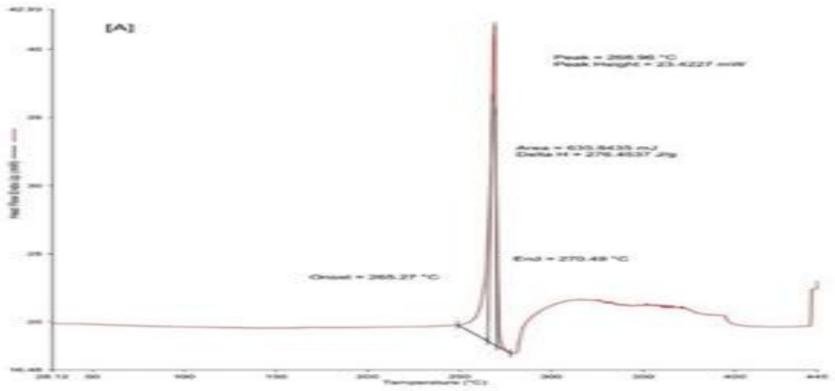


Figure 5.45: Raman spectra of (A) *t-RES* (B) COOH-MWCNT (C) RES-MWCNT 2

5.4.8 Differential scanning calorimetry (DSC)

The t-RES DSC thermogram is shown in Figure. 5.46A. When the temperature rose to 268.96 °C, which was quite near to the t-RES melting point, an endothermic peak appeared, signifying that the t-RES crystals had melted. The DSC patterns of RES-MWCNT 2 (Figure. 5.46C) and Carboxylated MWCNT (Figure. 5.46B) verify that the medication was successfully loaded into MWCNTs.



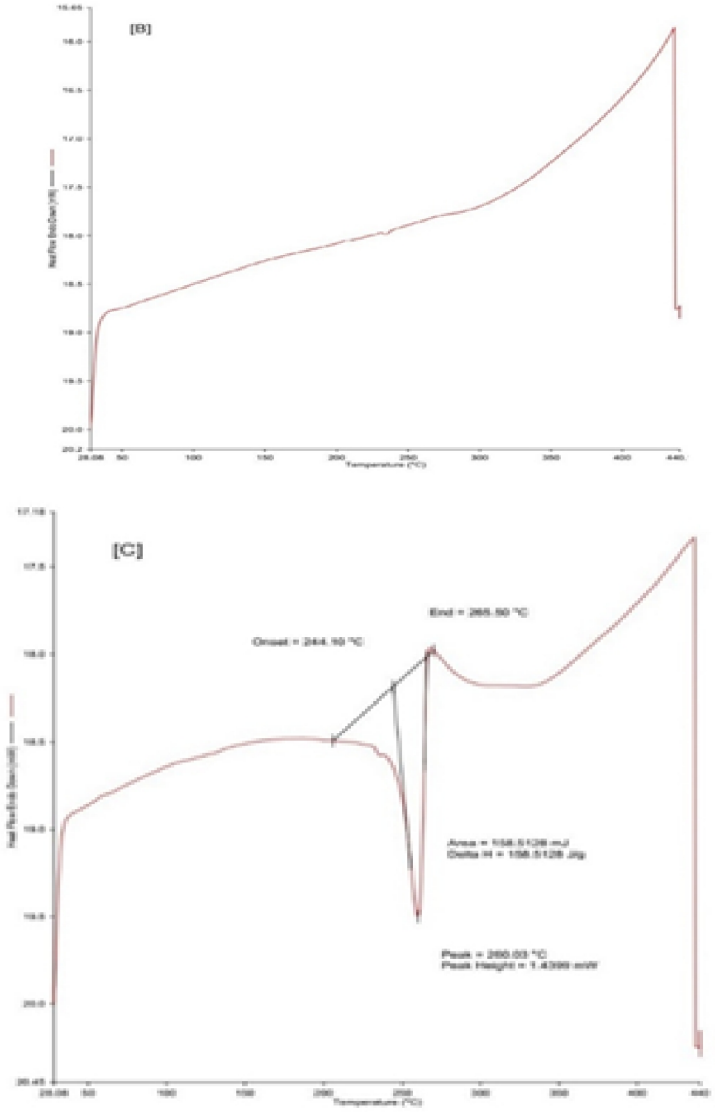


Figure 5.46: DSC thermogram of [A] *t-RES*, [B] Carboxylated MWCNTs, and [C] RES-MWCNT 2

5.4.*9 In vitro* Release

Colon cancer tumour microenvironments frequently display mild acidity (pH ~5.0–6.8). The formulation releases rapidly in acidic environments (pH 5), which can be beneficial for cancer cells indicates that RES-MWCNT might selectively release t-RES in tumour tissues, preserving healthy colon epithelium. This indicates that MWCNTs may

promote pH-sensitive diffusion or swelling, hence improving release in the simulate malignant cells environments. That enhance endocytosis-mediated uptake in cancer cells, hence boosting intracellular delivery of RES. This could cause high drug concentrations in the area, which would encourage apoptosis and stop cell division. The release profile lasts for 48 hours and goes from gradual to burst, which shows Initial release controlled by diffusion Then came matrix erosion or pore expansion. which facilitates the sustained maintenance of therapeutic t-RES levels, hence reducing the frequency of dose. The final cumulative release in Table 5.16 attains nearly 97.7% at pH 5 and approximately 93.6% at pH 7.4, indicating great drug Release. The presence of limited drugs residual is proof that effective encapsulation and relatively limited drug loss.

Table 5.16: % Cumulative drug release of t- RES from RES-MWCNT 2

Sr.No.	% Cumulative drug release of RES	
	Acetate Buffer pH 5	PBS pH 7.4
1	8.93 ± 0.05	12.20 ± 0.03
2	18.70 ± 0.03	14.49 ± 0.04
3	25.52 ± 0.09	21.02 ± 0.05
4	28.60 ± 0.04	26.32 ± 0.08
5	34.84 ± 0.02	29.90 ± 0.07
6	38.37 ± 0.03	33.91 ±0.05
8	45.32 ± 0.04	40.36 ± 0.03
9	79.78 ± 0.08	75.16 ± 0.06
10	83.51 ± 0.03	77.60 ± 0.04
11	86.26 ± 0.02	81.93 ± 0.06

12	91.50 ± 0.07	88.54 ± 0.09
24	95.50 ± 0.06	89.68 ± 0.04
48	97.73 ± 0.03	93.58 ± 0.06

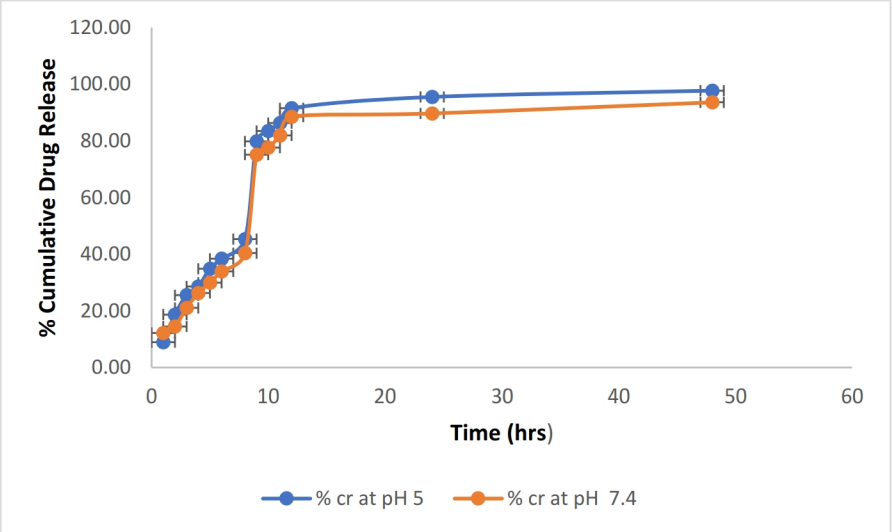


Figure 5.47: Percentage Cumulative drug release of RES from RES-MWCNT 2 at pH 5 and pH 7.4.

5.5 Development of RES-CNT-CET formulation

In order to create the cetuximab-containing t-RES loaded carbon nanotube (RES-MWCNT-CET), the antibodies were loaded via physical mixing. Cetuximab was physically added to the inner cavity of multi-walled nanotubes loaded with RES.

5.6 Characterization of RES-CNT-CET formulation

5.6.1 Raman Spectra

As shown in Figure.5.48, the RES-MWCNT-CET's ID/IG ratio was 1.621, indicating an increase in intensity ratios. Specifically, the inclusion of functional molecules

that disrupt the sp2 connecting network and break the π-conjugated configuration of the basic hexagonal carbon matrix (Muda et al. 2017).

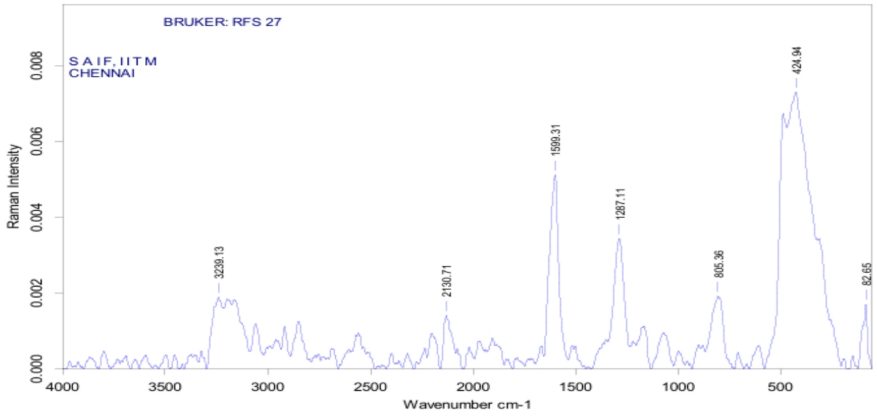


Figure 5.48: Raman spectra of RES-MWCNT-CET

5.6.2 Zeta potential and Particle size

The average size distribution investigations were carried out using a Malvern zeta sizer, which operates on the basis of dynamic light scattering. SDL can be used to efficiently examine non-spherical particles even though it is frequently used for analysing spherical particles. comparable to carbon nanotubes (CNTs), provided that they are functionalised adequately to guarantee adequate modification for assuring adequate dispersion in the solvent. Multi-walled carbon nanotubes with carboxylic functionalisation have zeta potentials of 279.9 and -18.7 mv, respectively. Zeta potential is thought to be negative because there aren't many free carboxylic groups present, which reduces the potential for aggregation.

It was found that the Z-average diameter of RES-MWCNT-CET was 730 nm. With a zeta potential of -11.9 mV, a shift to a positive scale is indicated. Despite the local neutral zeta potential, the RES-MWCNT-CET setup remained in an aggregated form. The significant changes in zeta potential show that RES and CET molecules have successfully conjugated onto functionalised MWCNTs.

RES-MWCNT-CET was found to have a hydrodynamic particle size of 728 nm. With a surface charge density of -11.9 mV, a shift to a positive scale is indicated. Despite

the local neutral zeta potential, the RES-MWCNT-CET setup remained in an aggregated form. The zeta value's notable variations indicate that the RES and CET molecules successfully attached to functionalised MWCNTs have done so.

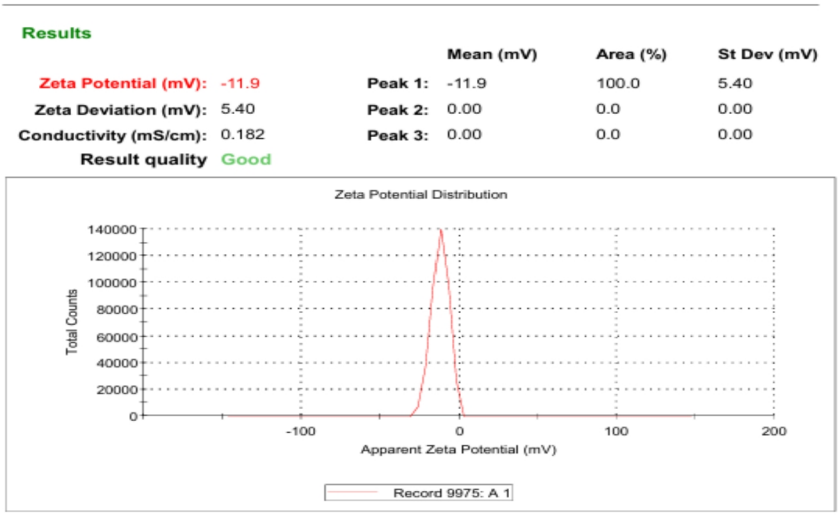


Figure 5.49: Zeta Potential of RES-MWCNT-CET

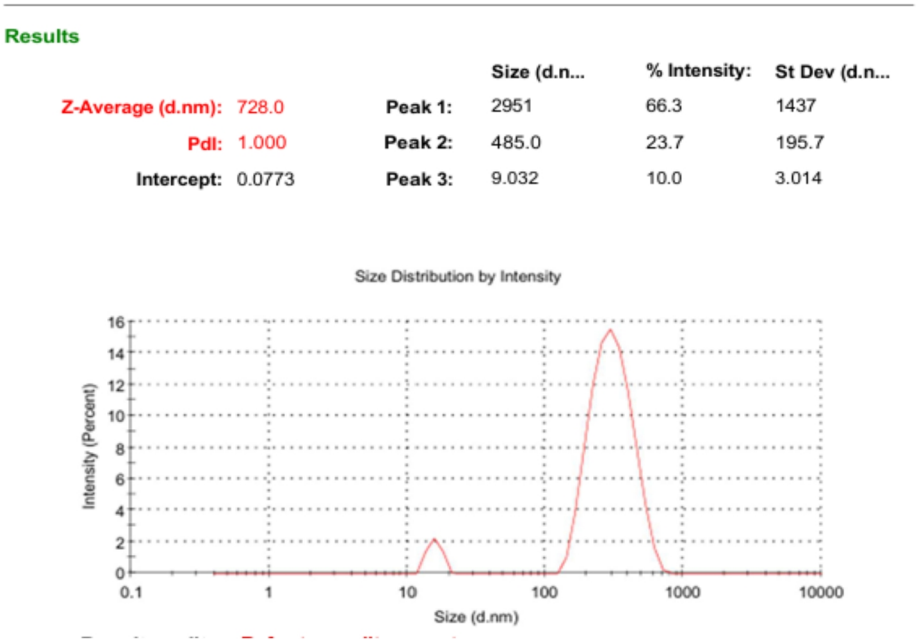


Figure 5.50: Particle Size of RES-MWCNT-CET

5.6.3 ^{1}HNMR and ^{13}CNMR studies

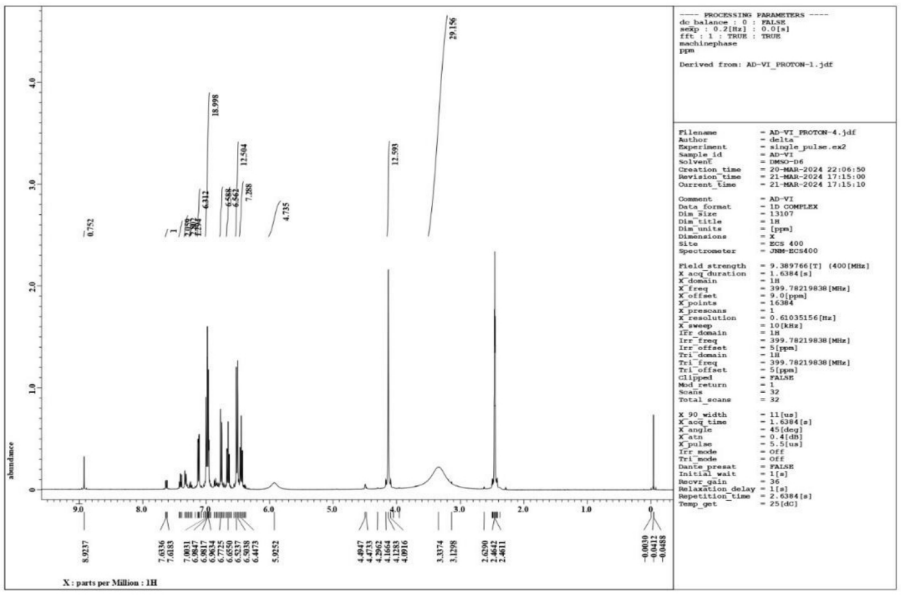


Figure 5.51: ^{1}HNMR spectra of RES-MWCNT-CET

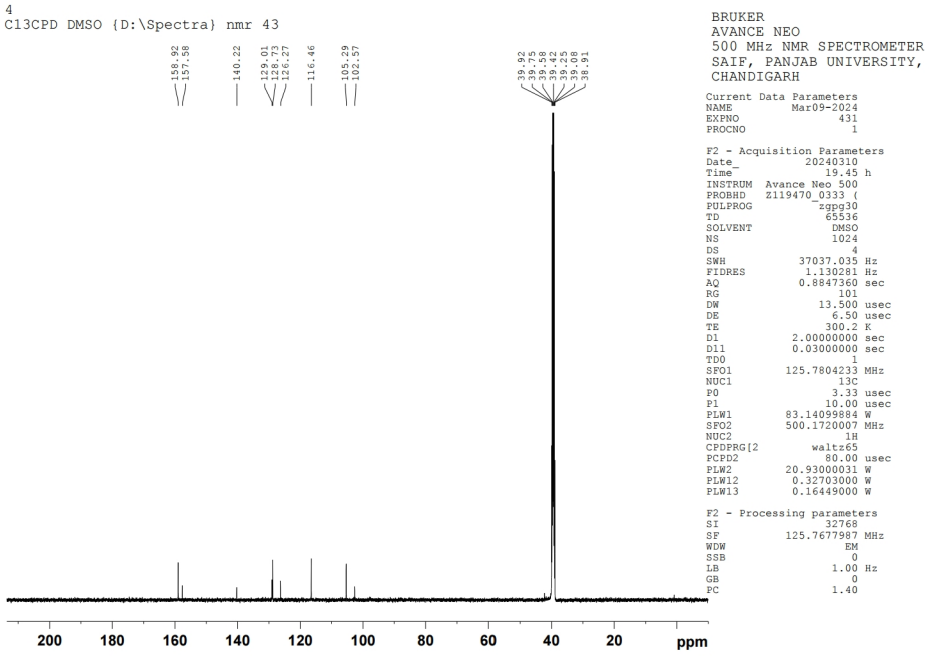


Figure 5.52: ^{13}C NMR spectra of RES-CNT-CET

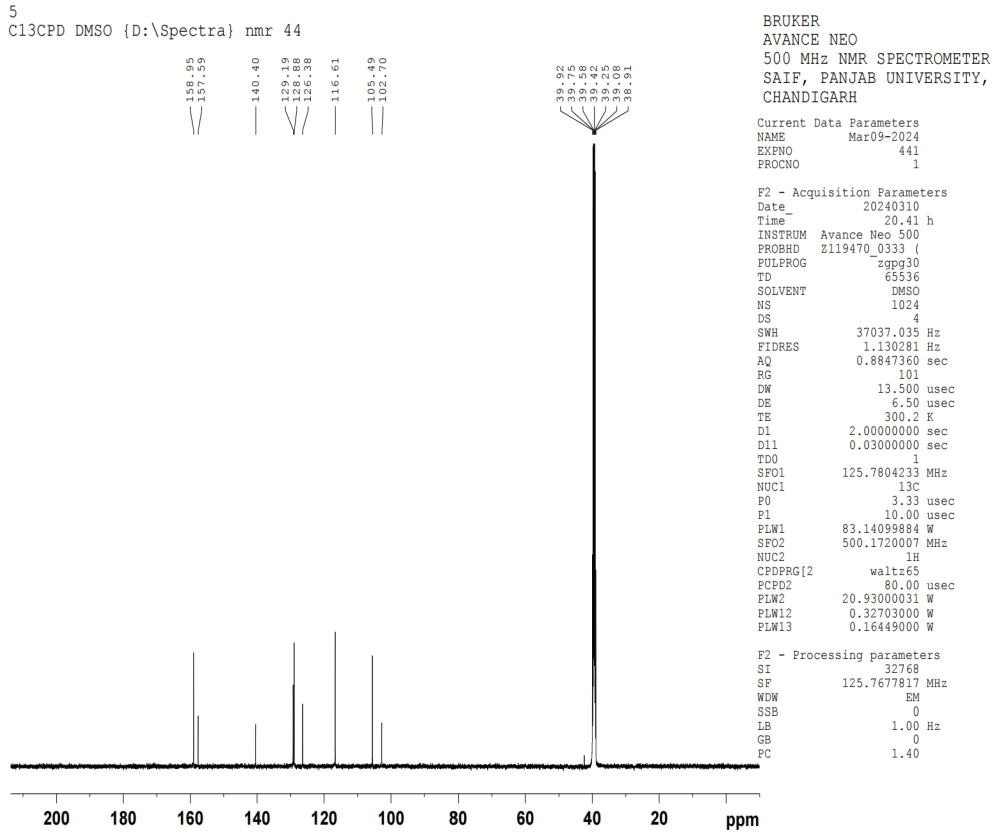


Figure 5.53: ^{13}C NMR spectra of RES-CNT-CET

In Figure 5.51–5.53, MWCNT loaded with t-RES displayed an extra MWCNT peak in addition to t-RES peaks, and the carboxylic CNT loaded with t-RES was anchored with cetuximab. After analysing all of the spectra, it was found that cetuximab was successfully attached and t-RES was successfully loaded onto the carbon nanotube.

5.6.4 FTIR

The FTIR spectra of RES-MWCNT-CET are shown in Figure 5.53.

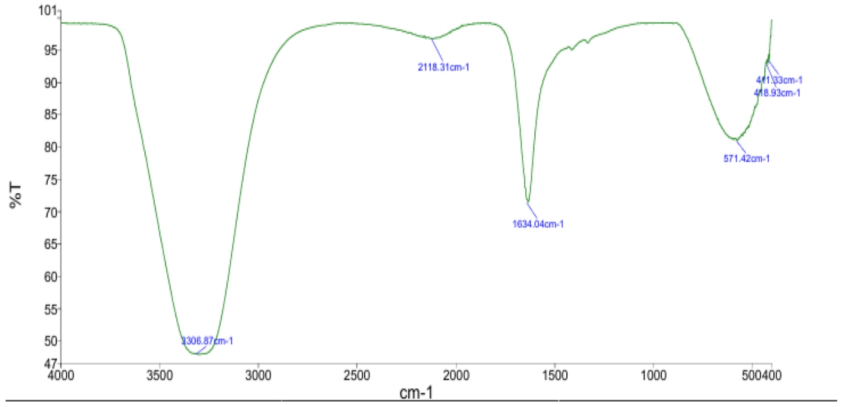


Figure 5.54: FTIR spectrum of CET

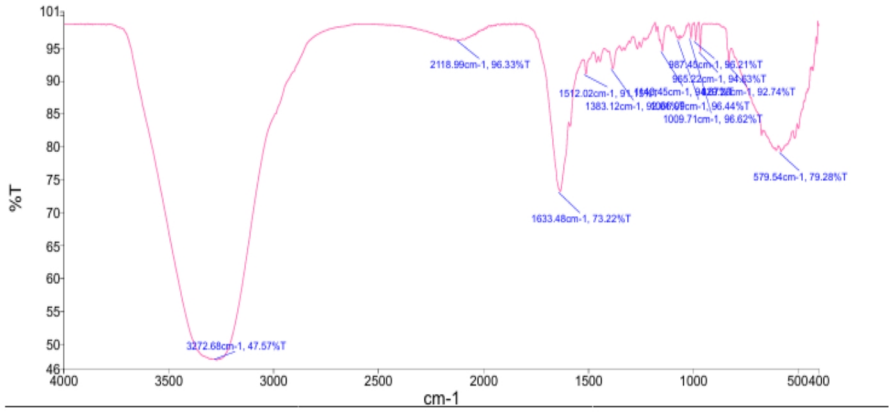


Figure 5.55: FTIR spectrum of RES-MWCNT-CET

In Figure 5.54 The distinctive protein amide peaks of cetuximab, located at 1634 cm-1 for amide I and 3306 cm-1 for amide II, respectively, represent the C=O stretching of amide I and the NH bending of amide II (Li. et al. 2017). A little peak shift from the basic structure was seen in Figure 5.55, indicating that the medication and ligand had successfully connected to the carrier.

5.6.5 TEM

Transmission electron microscopy (TEM) is distinguished by its propensity to reveal atomic structures in certain regions of substances. It provides a more thorough examination of the microstructure, namely the structural variations and interrelationships

between various regions. It was verified that carboxylate MWCNT had a tubular shape with open edges at the nanometric scale based on the TEM pictures of the material displayed in Figure. 5.56(A). Additionally, even after being CET attached, surface roughness was observed in the scans of Figure. 5.56 (B), (C), which showed no change in their tubular structure.

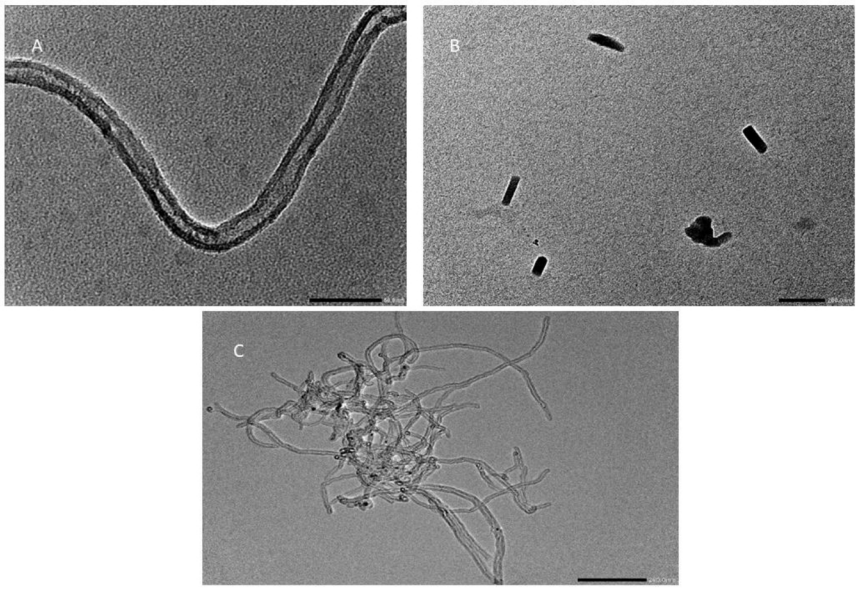


Figure 5.56: TEM image of (A) MWCNT, (B) RES- MWCNT (C) RES-MWCNT-CET.

5.6.6 Percentage drug entrapment

Percentage drug entrapment of the t-RES in RES-MWCNT-CET was observed to be 96.286 ± 0.021%.

5.6.7 Drug Release

The pattern and behaviour of a delivery system during the release of drugs must be observed in order to assess how successful it is. The toxicity of the medication can be reduced while its systemic effects are increased by employing a continuous release strategy. Apart from improving the drug's bioavailability and systemic concentration, a continuous release mechanism may also reduce the drug's toxicity. The rate of release was higher at pH 5 than at pH 7.4, which is because RES is more soluble at acidic pH. The hydrophilicity

and hydrogen bonding properties of carboxylate MWCNTs facilitated the faster and more controlled dissolution of t- RES.

t- RES 's poor water solubility was effectively overcome and therapeutic efficacy was increased by the drug-carrier conjugation method that used functionalised CNTs to assure stability and facilitate regulated release. The drug release was found to be 96.58 ±0.12% at pH 5 over 48 hours, while at pH 7.4 it was only 92.73 ±0.21%. A summary of the greater drug release that was observed at pH 5 as opposed to pH 7.4 is provided in Figure 5.57. RES's enhanced solubility at acidic pH has a greater impact on it instead. Targeted drug delivery applications are made possible by the pH-responsive actions of the developed system, which provide controlled and pH-dependent drug dissolution patterns that improve therapeutic efficacy.

Table 5.17: Cumulative drug release of t-RES from RES-MWCNT-CET

Time (Hr)	**% Cumulative drug release**	
	Acetate buffer pH 5	**PBS pH 7.4**
1	14.20 ± 0.04	6.93 ±0.05
2	16.49 ± 0.012	16.49 ± 0.09
3	19.02 ± 0.03	23.52 ± 0.02
4	24.32 ± 0.05	23.60 ± 0.08
5	26.90 ± 0.07	22.84 ± 0.04
6	32.91 ± 0.03	28.37 ± 0.06
8	34.36 ±0.06	23.32 ± 0.01
9	73.16 ± 0.09	30.78 ± 0.05
10	74.60 ± 0.02	31.51 ± 0.04

11	79.93 ± 0.05	34.26 ± 0.08
12	87.54 ± 0.09	45.50 ± 0.03
24	88.68 ± 0.05	61.50 ± 0.04
48	96.58 ± 0.08	92.73 ± 0.03

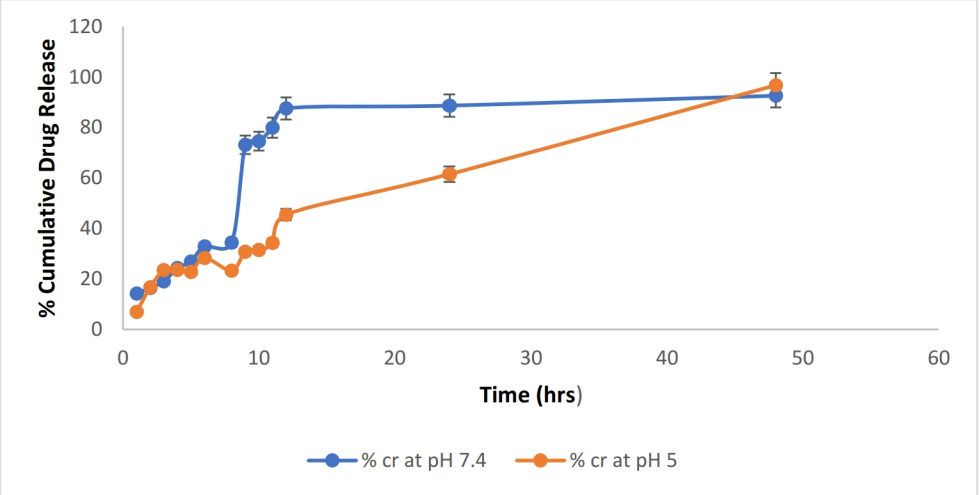


Figure 5.57: Percentage Cumulative drug release of RES from RES-MWCNT-CET at pH 5 and pH 7.4.

5.6.8 Drug release kinetics

Table 5.16 displays the findings of an investigation into drug release kinetics employing the RES-MWCNT-CET at different pH values, ranging from pH 5 to pH 7.4. The Hixon model was the best suitable model for both release profiles, with R^2 values of 0.9739 for the release profile data at pH 5 and 0.90302 for the release data at pH 7.4. With an R^2 of 0.9, the Hixon model was next in line. From an insoluble matrix, the Hixon model provides a better understanding of the Res release. A faster initial release was followed by a gradual decrease in release, according to the release pattern. In this approach, the concentration of the medication is much higher. After that, it releases and acts as a catalyst.

Gradient of concentration with time alterations lowering the diffusion, which in turn lowers the drug release.

Table 5.18: Drug release kinetics of RES showing R^2 value in RES-CNT-CET

Sr. No	Release	pH 5	pH 7.4
		R^2	R^2
1	First -order	0.9358	0.699
2	Zero-order	0.9388	0.5348
3	Korsmeyer-Peppas	0.7448	0.707
4	Higuchi	0.9551	0.7469
5	Hixon	0.9739	0.6353

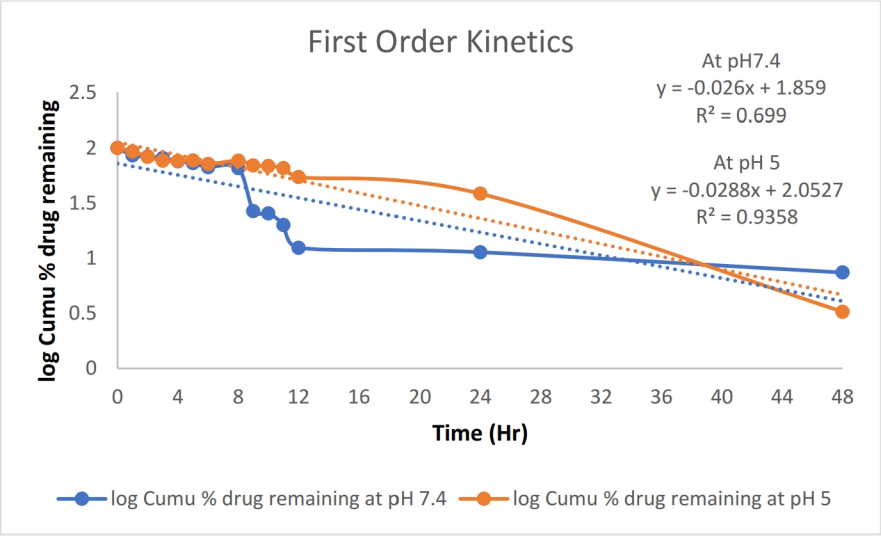


Figure 5.58: First Order Release kinetics

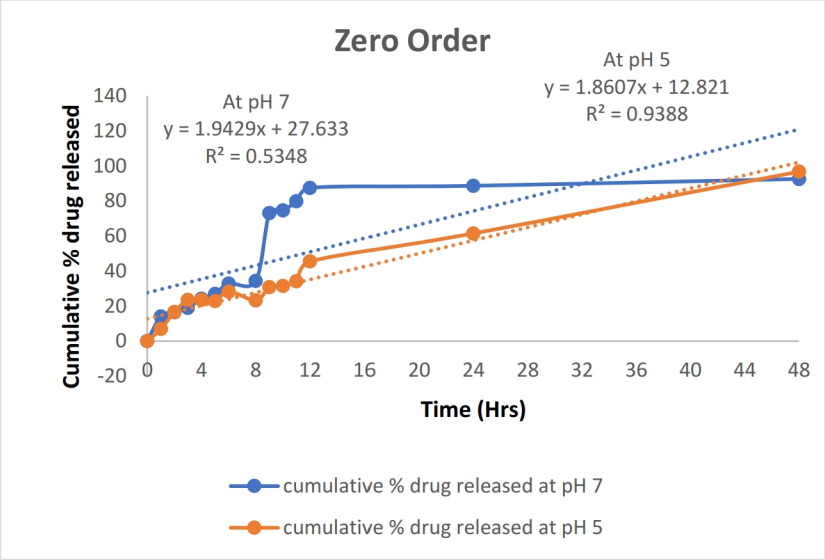


Figure 5.59: Zero Order Release kinetics

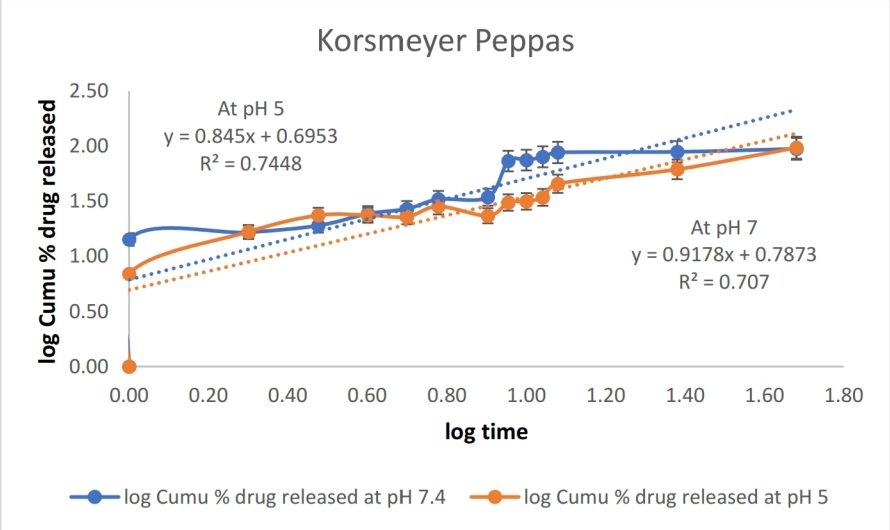


Figure 5.60: Korsmeyer Peppas release kinetics

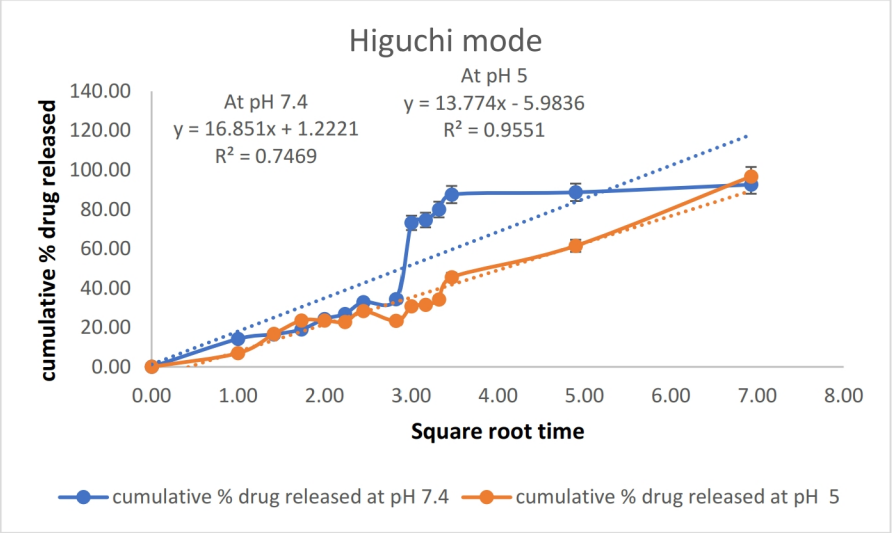


Figure 5.61: Higuchi release kinetics

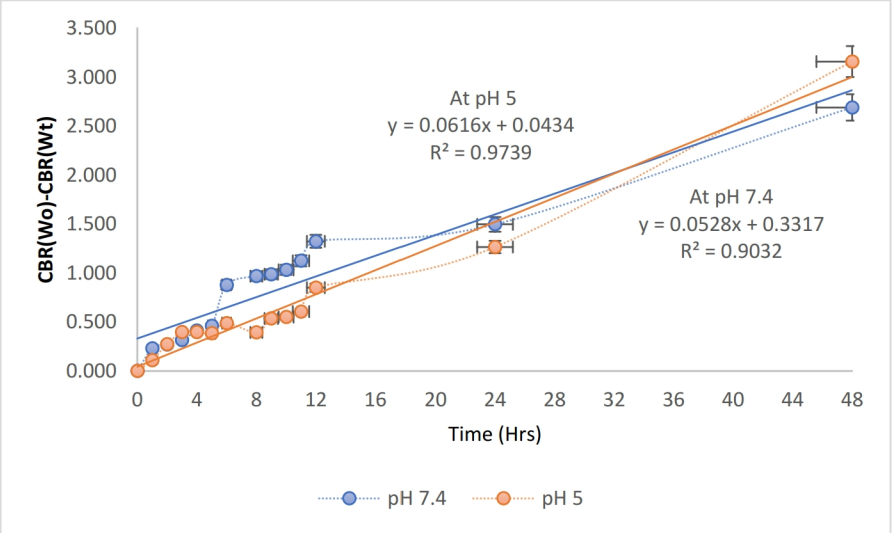


Figure 5.62: Hixson Crowell kinetics

5.6.9 Stability study

5.6.9.1 Physiochemical characterization

The purpose of the stability studies was to assess the drug's pharmacokinetic, chemical, and physical characteristics in the delivery system during the course of its shelf life. For six weeks, the produced RES-MWCNT-CET was exposed to 4±2°C, 25±2°C, and accelerated temperature 40±2°C. Changes in colour, precipitation, turbidity, and consistency were assessed at one-week intervals.

There is no discernible change in dark and light at 4°C, according to Table 5.17, which tabulates the colour change, precipitation, turbidity, and consistency of RES-MWCNT-CET. It was discovered that samples exposed to light had higher levels of turbidity and precipitation than samples stored in the dark at room temperature and at accelerated temperature.

The free functional group's polymerisation may be the reason of the increased turbidity at higher temperatures. The formulation proved to be more stable at chilly temperatures and in the dark (Soni et al., 2016).

Table 5.19: Physiochemical characterization of RES-MWCNT and RES-MWCNT-CET at different storage condition

Formulation code	**Parameter**	**Storage condition**					
		Light			**Dark**		
		4±2°C	**25±2°C**	**40±2°C**	**4±2°C**	**25±2°C**	**40±2°C**
RES-MWCNT-CET	Change in Colour	-	-	-	-	-	-
	Turbidity	+	+	+	+	+	+
	Precipitation	-	6th week	4th week	-	-	6th week
	Change in Consistency	-	-	+	-	-	+

5.6.9.2 Drug leakage

In order to assess whether the drugs were leaking from the RES-MWCNT-CET, a drug leakage test was conducted from the delivery system. Light and dark conditions were applied to RES-MWCNT-CET at 4±2°C, 25±2°C, and 40±2°C. It was shown in Table 5.18 that neither drug loss nor drug entrapment had changed significantly.

Table 5.20: % Drug leakage of RES-MWCNT and RES-MWCNT-CET at different storage condition

Formulation code	**Week**	**Percentage drug entrapment (%)**					
		Storage condition					
		Light			**Dark**		
		4±2°C	**25±2°C**	**40±2°C**	**4±2°C**	**25±2°C**	**40±2°C**
RES-MWCNT-CET	0 Days	96.89 ± 0.02	96.89 ± 0.02	96.89 ± 0.02	96.89 ± 0.02	96.89 ± 0.02	96.89 ± 0.02
	1st week	96.89 ± 0.02	96.86 ± 0.02	96.70± 0.27	96.66 ± 0.05	96.89 ± 0.02	96.89 ± 0.02
	3rd week	96.83 ± 0.01	96.82 ± 0.01	96.68 ± 0.08	96.57 ± 0.02	96.58 ± 0.02	96.55 ± 0.02
	6th week	96.80 ± 0.01	96.77 ± 0.02	96.66 ± 0.05	96.57± 0.02	96.53 ± 0.07	96.50± 0.08

5.6.10 MTT Assay

The in vitro toxicity of several nanotube formulations in HT-29 cells was assessed using the MTT test. The MTT assay, a simple colorimetric technique that does not use radiation to measure mitochondrial activity. deficiencies in metabolic processes as a result of the cells' role in cell survival or proliferation after treatment with the produced

formulation. In Table 5.19, the observed IC $_{50}$ value was displayed. MWCNT had a comparatively higher cytotoxicity than RES-MWCNT-CET. But when RES and RES-MWCNT-CET are compared, the cytotoxicity changes by 3.2 times. Cell viability was higher at lower concentrations, according to the data (Figure. 5.63), but cytotoxicity was striking as concentration rose (Prajapati et al. 2019)

Table 5.21: Evaluating the cytotoxicity of various formulations in HT-29 cancer cells using the MTT assay.

Sr. No	**Formulation code**	**IC_{50} (µg)**
1	RES	116.57±3.85
2	COOH-MWCNT	127.53±3.93
3	RES-MWCNT 2	112.90±2.88
4	CET	88.74±2.41
5	RES-MWCNT-CET	34.84±1.86

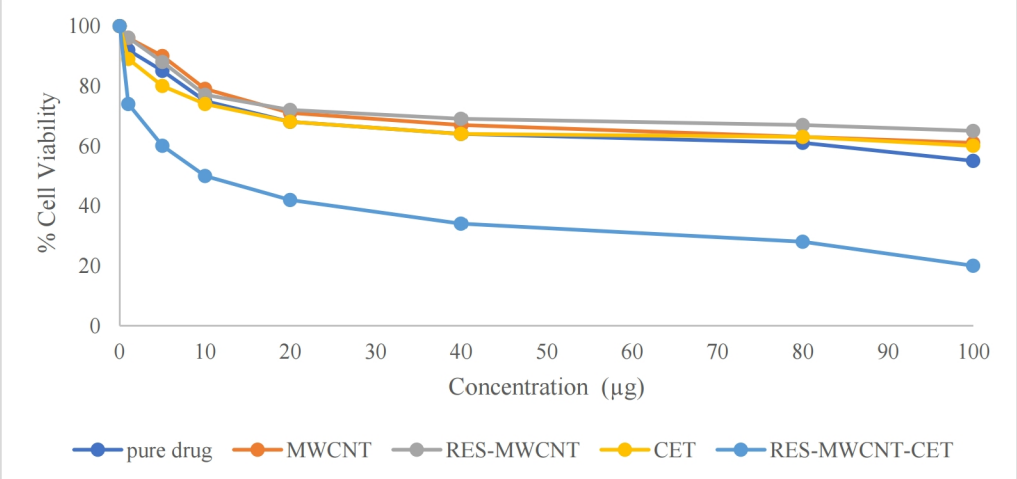


Figure 5.63: Percent cell growth inhibition by Free RES, COOH-MWCNTs, RES-MWCNT2, CET and RES-MWCNT-CET formulations.

5.6.11 Cell Internalization

Carbon nanotube-loaded formulations' intracellular fate was assessed using a cellular uptake assay. Results showed that cancer cells internalised the final formulations, with better absorption in the RES-MWCNT-CET setting. Table 5.20, Figure 5.64, and Figure 5.65 display the MIF values for Control, RES, MWCNT, RES-MWCNT2, CET, and RES-MWCNT-CET, which were 58.4,59.4, 93.4,2420, and 4571,5404 correspondingly. Uptake will be higher when the MIF value is higher. RES-MWCNT-CET has a higher cellular absorption than RES, according to the results mentioned above. MWCNT had the lowest cell uptake of any sample, though. In addition to an enhanced cytotoxicity against cancer cells and a better drug release profile, these investigations may support the therapeutic potential of produced nanoconjugates.

Table 5.22: Cell uptake studies by using FACS

Samples	Cell uptake (MFI)
Control	**58.4**
MWCNT	**59.4**
RES	**93.4**
RES-MWCNT2	**2420**
CET	**4571**
RES-MWCNT-CET	**5404**

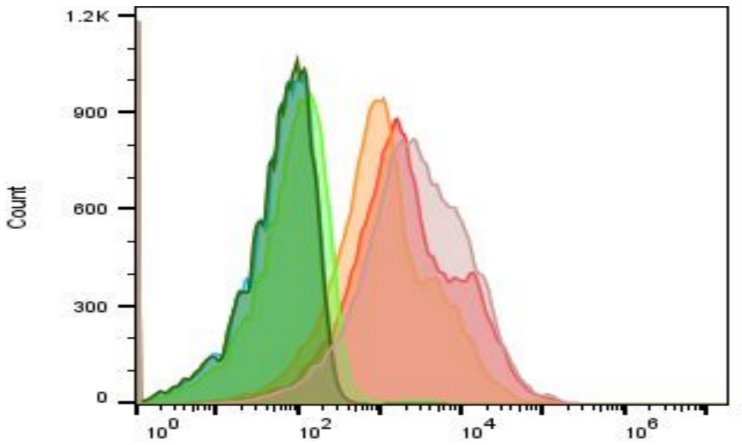


Figure 5.64: Combine cellular uptake studies graph by using FACS

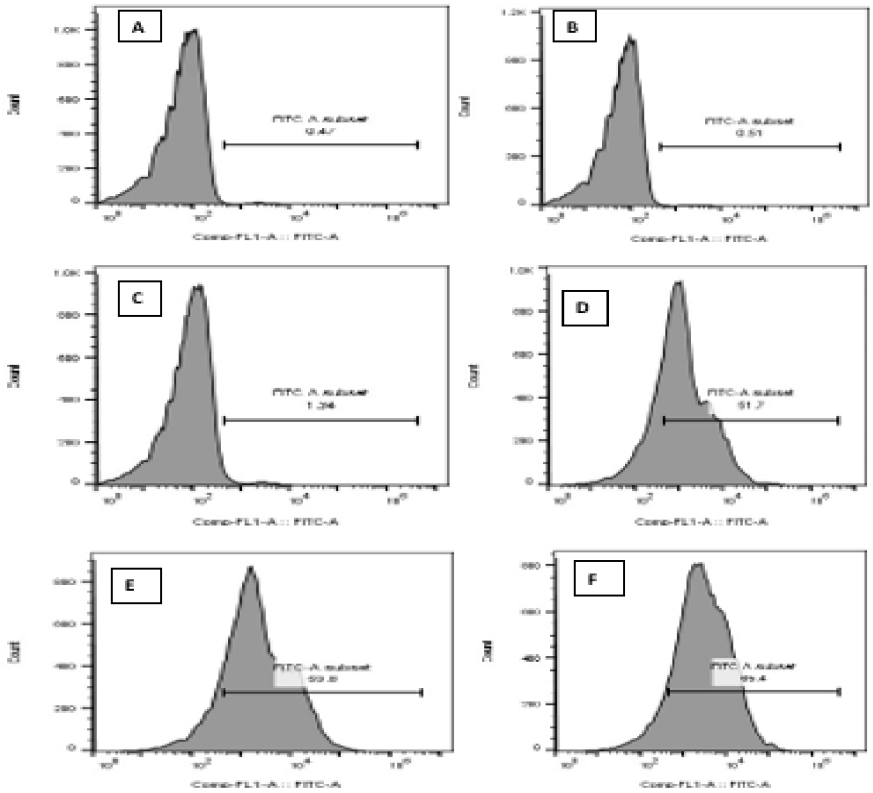


Figure 5.65: cellular uptake studies graph by using FACS

(A) control (B) RES (C) MWCNT (D) RES-MWCNT2 (E) CET (F) RES-MWCNT-CET

5.6.12 In-vivo studies

5.6.13 Development of Bio analytical method using HPLC

The chromatogram of RES and caffeine, which was generated in the mobile phase, is shown in Figure 5.66 (a and b). Caffeine had an RT of 5.70 minutes and a RES of 9.13 minutes, according to the results.

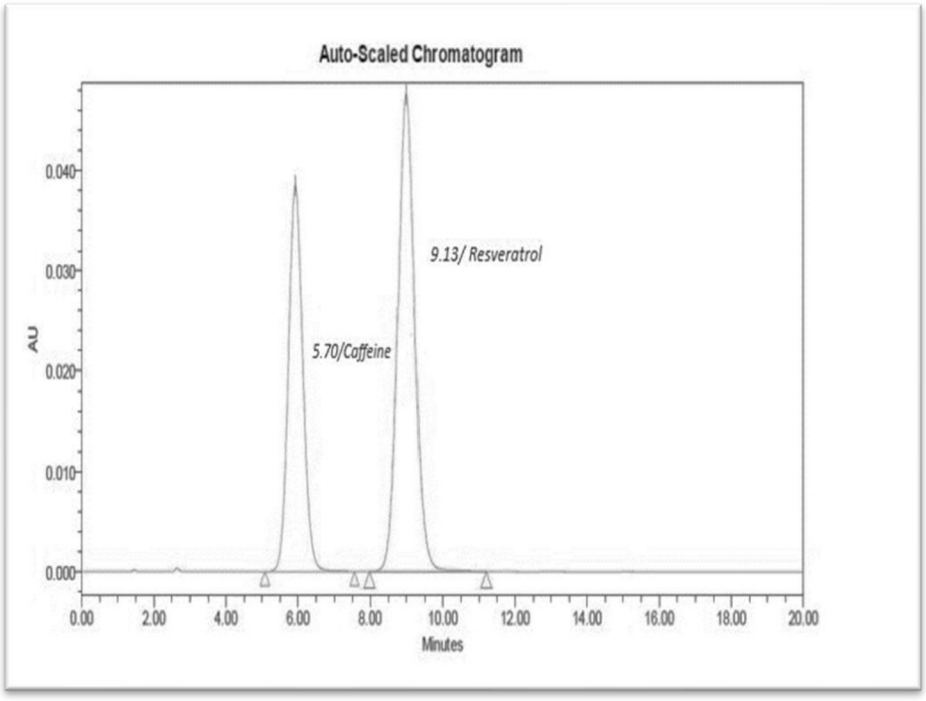


Figure 5.66: Chromatogram of RES and Caffeine in Mobile Phase

5.6.13.1 Specificity studies

Figure 5.68 shows the blank plasma chromatogram. Since neither drug showed a peak at the RT, it was concluded that the plasma matrix had no effect on the quantitative measurement of either RES or caffeine extracted from plasma. The addition of plasma to RES at a concentration of 2 µg/mL and caffeine at a concentration of 10 µg/mL had no effect on the retention durations of either substance (Figure. 5.69).

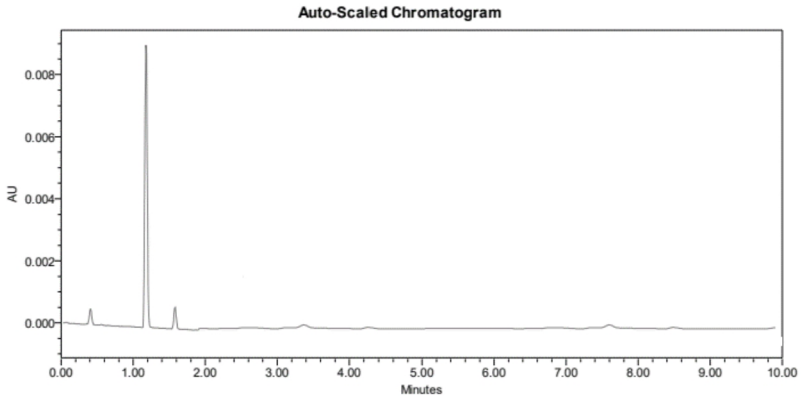


Figure 5.67: Chromatogram of Blank Plasma

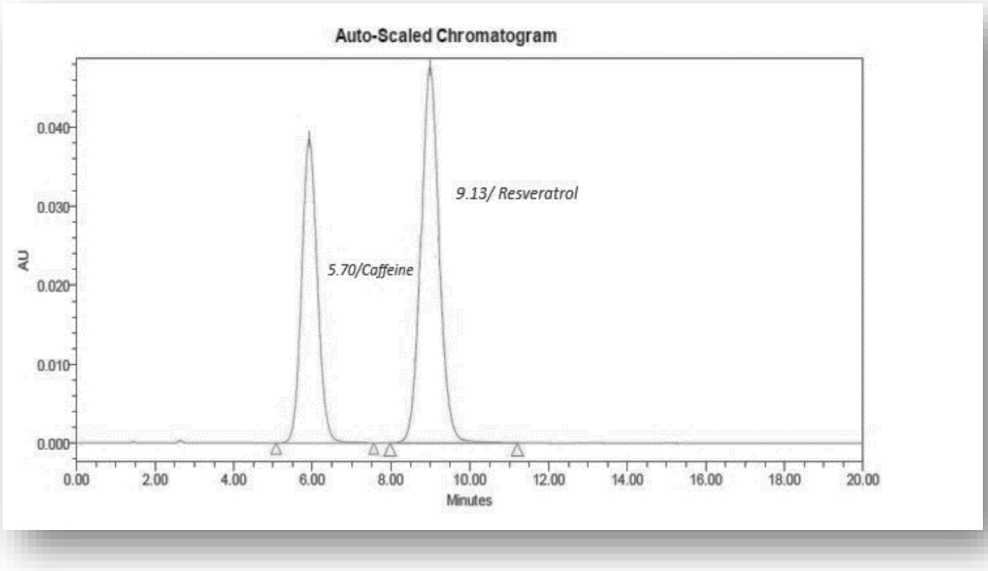


Figure 5.68: Chromatogram of t-RES and Caffeine in Plasma

5.6.13.2 Calibration curve Development

The regression equation Y= 73686x + 7764.9 (Figure. 5.70), as well as the R^2 values of 0.9989, show that the calibration curve of t- RES was generated in plasma and showed a notable degree of linearity.

Table 5.23: Standard calibration curve of t-RES in plasma

Sr.No.	Con.(µg/mL)	Area
1	0	0±0.0
2	2	144750.5±0.005
3	4	316654.5±0.005
4	6	474911.8±0.007
5	8	585114.8±0.007
6	10	735730.5±0.022

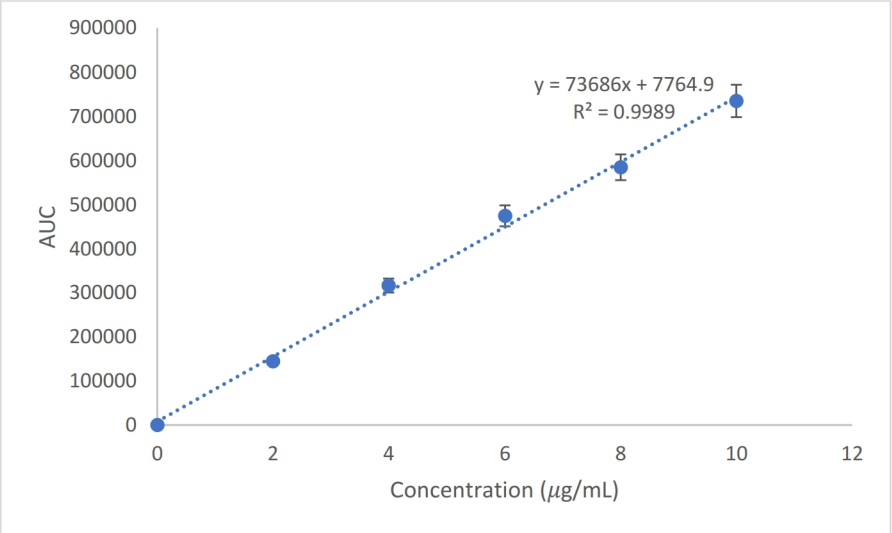


Figure 5.69: Calibration curve of t-RES in Plasma

5.6.13.3 Accuracy studies

The percentage recovery of t-RES in plasma was calculated to ascertain the accuracy. With at- RES recovery percentage in plasma over 95%, the developed approach

demonstrated great accuracy (Table 5.22). The fact that each example's percentage RSD was less than two is significant because it shows that the outcomes were repeatable.

Table 5.24: Accuracy Result of t-RES in plasma

Level	**Standard solution amount added (µg/mL)**	**Amount recovered (µg/mL)**	**Percentage recovery**	**Average Percentage recovery**	**STD**	**%RSD**
LQC	4.8	4.72	98.36	98.99	0.57	0.58
	4.8	4.77	99.48			
	4.8	4.76	99.14			
MQC	6	6.11	101.80	100.78	0.92	0.91
	6	6.03	100.51			
	6	6.00	100.03			
HQC	7.2	7.25	100.66	100.58	0.23	0.23
	7.2	7.25	100.76			
	7.2	7.22	100.32			

5.6.13.4 Precisions

The precision studies for RES in plasma and mobile phase, including intraday, interday, and interanalyst assessments, are shown in Table 5.23. For the LQC, MQC, and HQC samples, the reported regions' %RSD was less than 2, suggesting that the methodology was highly precise.

Table 5.25: Precision Result of t-RES in plasma

Intraday					
Level	**Conc.(µg/mL)**	**Amount recovered (µg/mL)**	**% Recovery**		
LQC	4.8	4.73	98.529	Average	98.328
		4.67	97.330	STD	0.779
		4.75	98.857	%RSD	0.792
		4.73	98.592		
		4.76	99.238		
		4.68	97.424		
MQC	6	5.94	99.052	Average	98.933
		6.00	99.919	STD	0.741
		5.87	97.898	%RSD	0.749
		5.94	98.991		
		5.90	98.289		
		5.97	99.450		
HQC	7.2	7.06	100.839	Average	100.493
		7.06	100.825	STD	0.496
		7.02	100.235	%RSD	0.494

		7.00	100.003		
		7.08	101.116		
		7.00	99.939		
Interday Day 1					
Level	**Conc.(µg/mL)**	**Amount recovered (µg/mL)**	**% Recovery**		
LQC	4.8	4.71	98.083	Average	98.052
		4.68	97.560	STD	0.418
		4.74	98.725	%RSD	0.426
		4.69	97.679		
		4.71	98.022		
		4.72	98.243		
MQC	6	5.90	98.276	Average	99.125
		5.95	99.114	STD	0.838
		5.88	98.027	%RSD	0.846
		6.00	100.016		
		6.00	99.995		
		5.96	99.324		
HQC	7.2	7.06	100.788	Average	100.393

		7.08	101.185	STD	0.647
		7.00	99.998	%RSD	0.645
		6.96	99.422		
		7.01	100.168		
		7.06	100.797		
Interday Day 2					
Level	**Conc.(µg/mL)**	**Amount recovered (µg/mL)**	**% Recovery**		
LQC	4.8	4.66	97.067	Average	98.431
		4.73	98.518	STD	0.781
		4.71	98.071	%RSD	0.793
		4.76	99.139		
		4.76	99.138		
		4.74	98.651		
MQC	6	5.99	99.882	Average	99.038
		5.90	98.253	STD	0.730
		5.91	98.538	%RSD	0.737
		5.99	99.871		
		5.91	98.446		
		5.95	99.240		

HQC	7.2	6.98	99.731	Average	100.475
		7.08	101.078	STD	0.481
		7.05	100.716	%RSD	0.479
		7.04	100.524		
		7.05	100.690		
		7.01	100.108		
Interday Day 3					
Level	**Conc.(µg/mL)**	**Amount recovered (µg/mL)**	**% Recovery**		
LQC	4.8	4.68	97.604	Average	98.473
		4.67	97.212	STD	0.845
		4.76	99.072	%RSD	0.858
		4.74	98.752		
		4.76	99.123		
		4.76	99.074		
MQC	6	5.97	99.446	Average	99.322
		5.94	99.064	STD	0.492
		6.00	99.974	%RSD	0.496
		5.91	98.508		
		5.97	99.466		

		5.97	99.471		
HQC	7.2	7.05	100.745	Average	100.405
		6.98	99.709	STD	0.586
		7.03	100.410	%RSD	0.584
		7.08	101.178		
		6.98	99.731		
		7.05	100.660		
Intermediate Precision, Inter Analyst 1					
Level	**Conc.(µg/mL)**	**Amount recovered (µg/mL)**	**% Recovery**		
LQC	4.8	4.78	99.487	Average	98.375
		4.71	98.087	STD	0.976
		4.75	98.956	%RSD	0.992
		4.67	97.364		
		4.76	99.181		
		4.66	97.176		
MQC	6	5.90	98.345	Average	98.590
		5.91	98.524	STD	0.619
		5.87	97.889	%RSD	0.628
		5.90	98.288		

		5.98	99.698		
		5.93	98.797		
HQC	7.2	6.99	99.918	Average	100.427
		7.06	100.904	STD	0.695
		7.05	100.663	%RSD	0.692
		7.04	100.535		
		6.95	99.319		
		7.09	101.223		
Intermediate Precision, Inter Analyst 2					
Level	**Conc.(µg/mL)**	**Amount recovered (µg/mL)**	**% Recovery**		
LQC	4.8	4.67	97.208	Average	98.364
		4.73	98.610	STD	0.631
		4.74	98.839	%RSD	0.641
		4.74	98.656		
		4.71	98.065		
		4.74	98.804		
MQC	6	5.92	98.697	Average	99.275
		5.95	99.242	STD	0.557
		5.98	99.723	%RSD	0.561

		5.91	98.538		
		5.99	99.906		
		5.97	99.544		
HQC	7.2	7.05	100.736	Average	100.557
		7.08	101.158	STD	0.516
		7.06	100.808	%RSD	0.513
		6.98	99.727		
		7.01	100.167		
		7.05	100.742		
Intermediate Precision, Inter Analyst 3					
Level	**Conc.(µg/mL)**	**Amount recovered (µg/mL)**	**% Recovery**		
LQC	4.8	4.71	98.136	Average	98.325
		4.74	98.811	STD	0.589
		4.71	98.193	%RSD	0.599
		4.76	99.201		
		4.71	98.060		
		4.68	97.546		
MQC	6	5.94	98.953	Average	99.526
		6.00	99.965	STD	0.624

		6.00	100.021	%RSD	0.627
		5.91	98.540		
		5.99	99.911		
		5.99	99.768		
HQC	7.2	7.05	100.712	Average	100.535
		7.04	100.564	STD	0.512
		7.08	101.171	%RSD	0.509
		6.98	99.765		
		7.01	100.126		
		7.06	100.869		

5.6.13.5 LOQ and LOD

It was shown that the limits of quantification (LOQ) and detection (LOD) for RES in the mobile phase and plasma were 2.45, 1.7, 2.3, and 1.54 respectively. These results imply that the method demonstrated significant sensitivity in RES detection at low concentrations.

5.6.13.6 System suitability

The system suitability includes the determination of parameters like column efficiency and chromatographic repeatability, as well as to guarantee the adequately of the proposed method for estimating t-RES (Table 5.24). After six consecutive injections, it was discovered that the RSD of peak regions was less than 2 percent, suggesting perfect injection repeatability as well as optimum chromatographic and environmental conditions.

With a tailing factor of 1.2, the t-RES demonstrated perfect peak symmetry. The column efficiency was adequate for the measured values that matched the theoretical plate number.

Table 5.26: System Suitability Parameter

Sr. No	**Parameter**	**Value**
1	Theoretical Plate	6450 ± 1.53
2	Retention Time (min.)	9.12 ±0.02
3	Tailing Factor	1.2 ± 0.10

5.6.13.7 Stabilities studies of plasma samples

Stability tests for RES-spiked plasma samples were conducted at three different time points: short-term, freeze-thaw cycles, and long-term stability studies for LQC, MQC, and HQC samples (Table 5.25). RES recovered over 95% of the time in all cases, according to the results, and the percentage RSD was less than 2. The findings of these studies demonstrated the stability of RES in plasma samples over time and under stress.

Table 5.27: Stability Studies

Level	**Conc.(µg/mL)**	**Amount recovered (µg/mL)**	**% Recovery**		
LQC	4.8	4.72	98.306	Average	98.777
		4.70	97.989	STD	0.522
		4.75	98.857	%RSD	0.529
		4.75	98.981		
		4.77	99.293		

		4.76	99.233		
MQC	6	5.94	99.043	Average	98.751
		5.89	98.241	STD	0.522
		5.97	99.444	%RSD	0.529
		5.95	99.111		
		5.91	98.501		
		5.89	98.164		
HQC	7.2	7.06	100.845	Average	100.419
		7.08	101.077	STD	0.452
		7.02	100.274	%RSD	0.450
		7.00	100.050		
		7.02	100.340		
		6.99	99.926		
2 Hrs					
Level	**Conc.(µg/mL)**	**Amount recovered (µg/mL)**	**% Recovery**		
LQC	4.8	4.65	96.839	Average	97.898
		4.68	97.594	STD	0.716
		4.75	98.979	%RSD	0.732
		4.69	97.693		

		4.71	98.028		
		4.72	98.252		
MQC	6	5.98	99.633	Average	99.538
		5.90	98.390	STD	0.622
		5.99	99.882	%RSD	0.625
		6.00	100.018		
		6.00	99.991		
		5.96	99.311		
HQC	7.2	6.97	99.586	Average	99.925
		6.97	99.614	STD	0.513
		7.00	100.017	%RSD	0.513
		6.96	99.380		
		7.01	100.170		
		7.05	100.784		
3hrs					
Level	**Conc.(µg/mL)**	**Amount recovered (µg/mL)**	**% Recovery**		
LQC	4.8	4.66	97.144	Average	98.688
		4.76	99.083	STD	0.890
		4.71	98.085	%RSD	0.902

		4.76	99.196		
		4.76	99.206		
		4.77	99.415		
MQC	6	6.13	102.234	Average	101.610
		6.06	101.012	STD	0.599
		6.13	102.111	%RSD	0.590
		6.13	102.111		
		6.06	101.004		
		6.07	101.185		
HQC	7.2	7.32	104.598	Average	104.249
		7.29	104.200	STD	0.391
		7.33	104.686	%RSD	0.375
		7.31	104.427		
		7.27	103.792		
		7.27	103.792		
Freez Thaw Stability Studies, Cycle 1					
Level	**Conc.(µg/mL)**	**Amount recovered (µg/mL)**	**% Recovery**		
LQC	4.8	4.68	97.457	Average	98.246
		4.73	98.597	STD	0.754

		4.70	97.828	%RSD	0.767
		4.73	98.554		
		4.77	99.434		
		4.68	97.604		
MQC	6	5.96	99.401	Average	99.397
		5.96	99.403	STD	0.339
		5.96	99.409	%RSD	0.341
		5.95	99.232		
		6.00	99.986		
		5.94	98.951		
HQC	7.2	7.03	100.396	Average	100.564
		7.02	100.232	STD	0.251
		7.07	100.934	%RSD	0.250
		7.05	100.732		
		7.04	100.623		
		7.03	100.466		
Cycle 2					
Level	**Conc.(µg/mL)**	**Amount recovered (µg/mL)**	**% Recovery**		
LQC	4.8	4.72	98.412	Average	98.060

		4.73	98.455	STD	0.515
		4.69	97.797	%RSD	0.525
		4.71	98.100		
		4.73	98.446		
		4.66	97.150		
MQC	6	5.95	99.091	Average	99.059
		5.91	98.576	STD	0.353
		5.95	99.087	%RSD	0.356
		5.95	99.193		
		5.98	99.608		
		5.93	98.799		
HQC	7.2	7.00	100.054	Average	100.275
		7.04	100.605	STD	0.533
		7.06	100.885	%RSD	0.532
		7.04	100.613		
		6.96	99.415		
		7.01	100.079		
Cycle 3					
Level	**Conc.(µg/mL)**	**Amount recovered (µg/mL)**	**% Recovery**		

LQC	4.8	4.71	98.085	Average	98.398
		4.73	98.568	STD	0.617
		4.77	99.405	%RSD	0.627
		4.73	98.593		
		4.68	97.584		
		4.71	98.154		
MQC	6	5.91	98.426	Average	99.152
		5.96	99.308	STD	0.552
		5.95	99.158	%RSD	0.557
		5.92	98.633		
		6.00	99.935		
		5.97	99.451		
HQC	7.2	7.06	100.827	Average	100.766
		7.05	100.732	STD	0.277
		7.07	100.944	%RSD	0.275
		7.07	100.929		
		7.02	100.227		
		7.07	100.936		
Long Term Stability Studies, week 1					

Level	**Conc.(µg/mL)**	**Amount recovered (µg/mL)**	**% Recovery**		
LQC	4.8	4.72	98.383	Average	98.787
		4.68	97.424	STD	0.766
		4.77	99.394	%RSD	0.775
		4.75	98.975		
		4.76	99.143		
		4.77	99.403		
MQC	6	5.99	99.857	Average	99.235
		5.97	99.512	STD	0.789
		5.90	98.407	%RSD	0.795
		5.99	99.880		
		5.98	99.679		
		5.88	98.073		
HQC	7.2	7.06	100.830	Average	100.436
		7.08	101.211	STD	0.488
		7.01	100.150	%RSD	0.486
		7.00	100.013		
		7.03	100.398		
		7.00	100.017		

Week 2					
Level	**Conc.(µg/mL)**	**Amount recovered (µg/mL)**	**% Recovery**		
LQC	4.8	4.66	97.001	Average	98.468
		4.77	99.290	STD	0.887
		4.75	98.923	%RSD	0.901
		4.70	97.817		
		4.76	99.131		
		4.74	98.648		
MQC	6	5.93	98.887	Average	99.400
		5.90	98.394	STD	0.655
		5.99	99.885	%RSD	0.659
		6.00	99.932		
		6.00	99.988		
		5.96	99.314		
HQC	7.2	7.08	101.145	Average	100.618
		7.08	101.158	STD	0.692
		7.00	100.024	%RSD	0.688
		6.96	99.494		
		7.07	100.946		

		7.07	100.939		
Week 3					
Level	**Conc.(µg/mL)**	**Amount recovered (µg/mL)**	**% Recovery**		
LQC	4.8	4.66	97.154	Average	98.412
		4.74	98.689	STD	0.832
		4.71	98.042	%RSD	0.846
		4.71	98.037		
		4.76	99.147		
		4.77	99.404		
MQC	6	6.00	99.974	Average	99.338
		5.93	98.759	STD	0.583
		6.00	99.990	%RSD	0.587
		5.97	99.577		
		5.92	98.744		
		5.94	98.985		
HQC	7.2	7.05	100.720	Average	100.477
		7.03	100.439	STD	0.404
		7.08	101.080	%RSD	0.402
		7.04	100.547		

		7.00	100.012		
		7.00	100.065		

5.6.14 Biodistribution studies

The percentage of the injected dose of various nanotube formulations that was recovered in different organs was ascertained using an analysis. The formulations Free RES, RES-MWCNT2, and RES-MWCNTs-CET were investigated at 1hr, 4hr, and 8hr intervals. At 1hr, the amount of RES extracted from RES-MWCNT and RES-MWCNT-CET and administered to the colon was substantially more than that of plain RES solution ($p<0.0001$). By contrast, the RES-MWCNT-CET significantly ($p<0.0001$) transported more t-RES to the colon (0.094±0.002µg) than the RES-MWCNT (0.054±0.003µg) at 1 hour.

t-RES was administered from the RES-MWCNT-CET in much smaller amounts than from the RES-MWCNT followed by pure drug solution in other organs such as the liver, kidney, lung, and plasma. Less t-RES was thus deposited in the kidney, liver, lungs, and plasma after an hour. Conversely, at 4 hours, the amount of RES extracted from RES-MWCNT and RES-MWCNT-CET and administered to the colon was substantially more ($p<0.0001$) than that of the simple RES solution. The RES-MWCNT-CET had a considerably ($p<0.0001$) larger level of t-RES (0.088±0.004µg) in the colon at 4 hours compared to the RES-MWCNT (0.063±0.003µg). The RES-MWCNT-CET delivered a much lower amount of t-RES to the liver, kidney, lung, and plasma than the RES-MWCNT followed by pure drug solution. As a result, by 4 hours, the liver, lungs, kidney, and plasma had less t-RES stored. Additionally, at 8 hours, the amount of RES that was extracted from RES-MWCNT and RES-MWCNT-CET and given to the colon was substantially larger than that of the simple RES solution ($p<0.0001$). The RES-MWCNT-CET provided the colon with a considerably ($p<0.0001$) greater amount of t-RES (0.106±0.002µg) at 8 hours than the RES-MWCNT (0.070±0.005µg).

The amount of t-RES supplied by the RES-MWCNT-CET was significantly less than that of the RES-MWCNT followed by pure drug solution at 8 hours in other organs such as the liver, kidney, lung, and plasma. As a result, by 4 hours, the liver, lungs, kidney, and plasma had less t-RES stored.

Table 5.28: Biodistribution studies of t-RES from pure drug, RES- MWCNT and RES-MWCNT-CET at 1hr

Sr.No.	**Name of Organ**	**Amount (µg) of t-RES at 1hr**					
		Pure Drug	**RES-MWCNT2**	**RES-MWCNT-CET**	**%age drug retention of Pure drug**	**%age drug retention of RES-MWCNT2**	**%age drug retention of RES-MWCNT-CET**
1	Colon	0.037±0.002	0.054±0.003	0.094±0.002	24.64±0.004	36.04±0.009	61.33±0.002
2	Plasma	0.039±0.005	0.038±0.005	0.034±±0.002	26.00±0.005	25.50±0.001	22.42±0.006
3	Kidney	0.029±0.001	0.028±0.002	0.025±0.005	19.58±0.008	18.67±0.004	16.75±0.007
4	Lungs	0.028±0.001	0.024±0.004	0.022±0.002	18.84±0.003	16.08±0.005	14.56±0.004
5	Liver	0.025±0.001	0.025±0.002	0.022±0.002	16.12±0.009	16.99±0.002	14.87±0.003

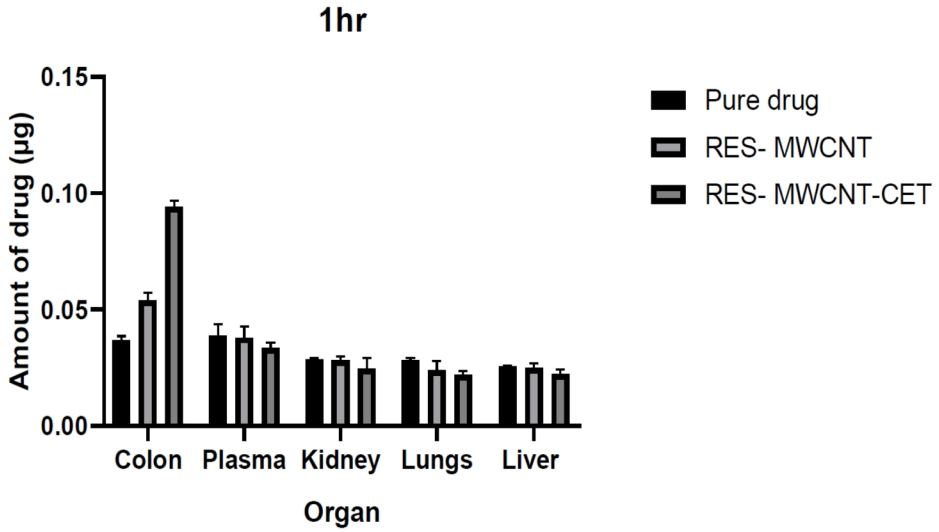


Figure 5.70: Amount of t-RES from pure drug, RES- MWCNT2 and RES- MWCNT-CET at 1h

Table 5.29: Biodistribution studies of t-RES from pure drug, RES- MWCNT2 and RES-MWCNT-CET at 4hr

Sr. No.	Name of Organ	Amount of t-RES in µg at 4hr					
		Pure Drug	RES-MWCNT2	RES-MWCNT-CET	%age drug retention of Pure drug	%age drug retention of RES-MWCNT2	%age drug retention of RES-MWCNT-CET
1	Colon	0.045±0.003	0.063±0.003	0.088±0.004	30.54±0.003	42.45±0.008	58.44±0.005
2	Plasma	0.042±0.002	0.035±0.005	0.034±0.002	28.61 ± 0.006	23.76 ±0.008	22.67±0.004
3	Kidney	0.029±0.001	0.025±0.004	0.023±0.002	19.65 ±0.003	16.63 ± 0.007	15.54 ± 0.009
4	Lungs	0.029±0.001	0.035±0.004	0.023±0.002	19.33 ± 0.004	23.65 ±0.007	15.43 ± 0.008
5	Liver	0.025±0.001	0.025±0.001	0.015±0.002	16.84 ±0.003	16.28±0.004	10.55 ±0.009

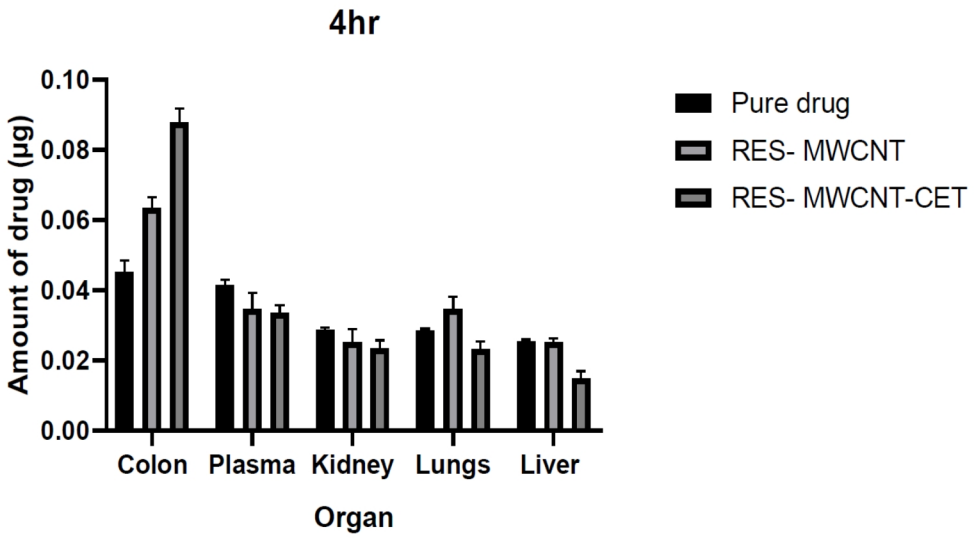


Figure 5.71: Amount of t-RES from pure drug, RES- MWCNT2 and RES- MWCNT-CET at 4h

Table 5.30: Biodistribution studies of t-RES from pure drug, RES- MWCNT2 and RES-MWCNT-CET at 8hr

Sr.No.	Name of Organ	Amount of t-RES in µg at 8hr					
		Pure Drug	RES- MWCNT2	RES-MWCNT-CET	%age drug retention of Pure drug	%age drug retention of RES-MWCNT2	%age drug retention of RES-MWCNT-CET
1	Colon	0.050±0.002	0.070±0.005	0.106±0.002	33.43 ±0.009	46.67 ±0.005	70.72±0.010
2	Plasma	0.036±0.003	0.037±0.001	0.035±0.002	24.64 ±0.011	24.92±0.06	23.33 ±0.004
3	Kidney	0.027±0.004	0.025±0.003	0.023±0.002	18.54 ±0.008	16.54 ±0.008	15.86 ±0.005
4	Lungs	0.026±0.002	0.030±0.004	0.026±0.003	17.27 ±0.005	20.29 ±0.009	17.31 ±0.001
5	Liver	0.023±0.002	0.025±0.001	0.024±0.003	15.44 ±0.009	16.67 ±0.002	16.00 ±0.007

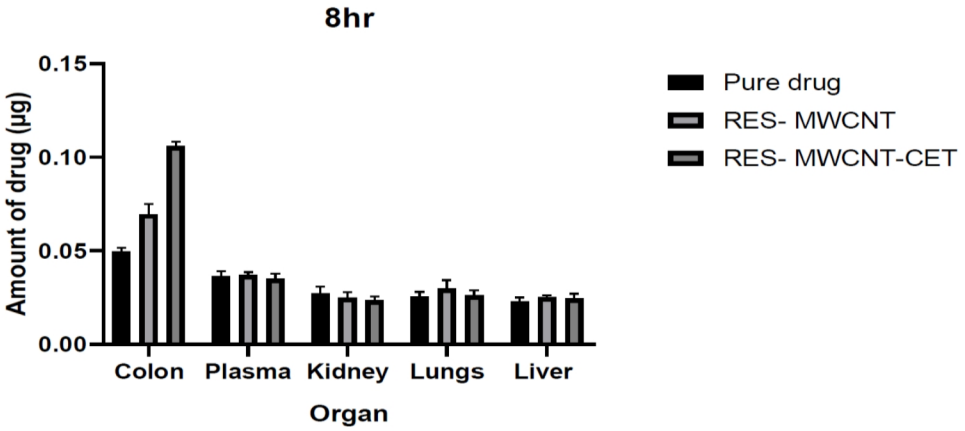


Figure 5.72: Amount of t-RES from pure drug, RES- MWCNT2 and RES- MWCNT-CET at 8hr

5.6.15 Hemolytic toxicity studies

The haemolytic toxicity of the amine MWCNTs was 10.25 ± 0.34%. The haemolysis rate of the medication RES (5 mg) was 30.75 ± 0.55%, which was 2.14 times greater than the haemolysis produced by RES-MWCNTs. The hemocompatibility of RES-MWCNT and RES-MWCNT-CET was found to be higher, with respective values of 14.92 ± 0.55% and 4.03 ± 0.43%. RES-MWCNT-CET reduces haemolysis by 7.5 times. Because the RES is protected in a milieu of biocompatible nanotubes, these formulations are less hazardous than the pure medications. When the CET ligand was attached to MWCNTs, the haemolysis of RBCs was significantly decreased. The conjugated MWCNTs' extended circulation time and the unconjugated MWCNTs' negatively charged amine groups' ability to keep RBCs from coming into contact with them are probably the causes of this effect. Procyk and Kutwin Reported the cutting edges and hydrophobic surfaces of raw carbon nanotubes (CNTs) make them highly hemolytic. By improving dispersion and minimizing membrane disruption, functionalization techniques like carboxylation and PEGylation can reduce hemolysis (Procyk and Kutwin 2025).

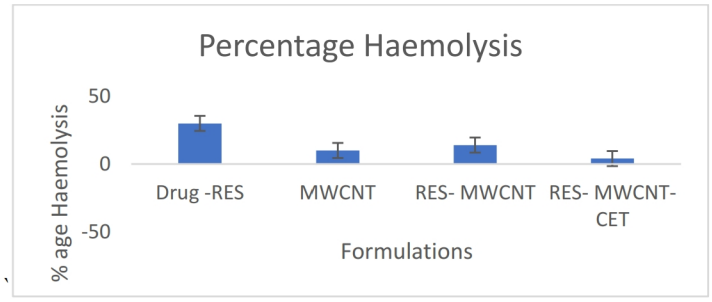


Figure 5.73: Hemolytic studies of different formulation

The RES-MWCNT-CET formulation's hemolytic research microscopic image provides important information on how it interacts with red blood cells (RBCs). Numerous spherical, undamaged erythrocytes with few lysis indicators are visible in the field, indicating that the formulation continues to maintain good hemocompatibility. Amorphous black particles and a few needle-like uric acid crystals are scattered throughout the cells; these could be metabolic byproducts or leftover formulation ingredients. Under the measured conditions, RES-MWCNT-CET does not cause appreciable hemolysis, as evidenced by the lack of ghost cells, broken membranes, or haemoglobin precipitates. In drug delivery systems where blood contact is unavoidable, this supports its possible safety profile for topical or systemic applications. The formulation's ability to maintain RBC integrity while maintaining biological activity is a potential feature for future pharmacological research.

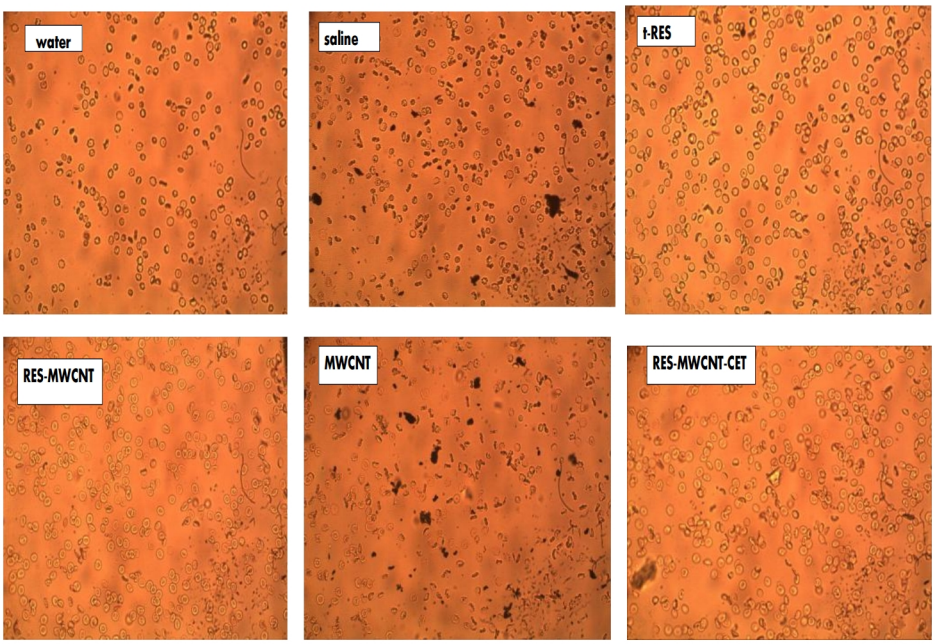


Figure 5.74: Homolysis of images of Water, Saline, t-RES, MWCNT, RES-MWCNT, RES-MWCNT-CET.

The hemolytic analysis of saline's microscopic picture shows an area dominated by spherical, undamaged white blood cells with granular interiors, indicating little hemolytic or cytotoxic activity. The reddish-orange background, which is probably the result of a staining method, makes cellular morphology more visible and makes it possible to clearly see the integrity of leukocytes. The lack of haemoglobin leakage, ghost forms, or broken cells shows that saline, as predicted, preserves cellular integrity and does not cause red blood cell lysis in a physiological setting. This validates its use as a biocompatible control in hemolytic tests, offering a standard against which test formulations can be compared. The image validates the continued use of saline in clinical and experimental contexts by demonstrating its inertness and safety in blood-contact applications.

The microscopic image, which was taken during hemolytic investigations with water, shows urine sediment that is full of red blood cells (RBCs), some of which have morphological changes including crenation, which is a condition in which the cell

membrane looks spiky or imperfect. These modifications raise the possibility that the RBCs were subjected to osmotic stress or a chemical imbalance, which could have been impacted by the composition or quality of the water. RBCs that are both intact and distorted in urine are clinically significant because they may be a symptom of haematuria associated with urinary tract or renal disease. Depending on its ionic strength, pH, or pollutants, water can alter erythrocyte integrity when added to biological systems. This graphic illustrates this point in the context of hemolytic analysis.

This microscopic image, which was taken during hemolytic investigations using multi-walled carbon nanotubes (MWCNTs), shows red blood cells (RBCs) with distinct central pallor and retained biconcave morphology, which are characteristics of healthy, non-lysed erythrocytes. Under the assessed conditions, the cells' homogeneity and intact structure suggest little to no hemolytic activity, suggesting that the MWCNTs utilized may be biocompatible at the concentration and exposure time studied. Such visual confirmation is essential in hemolytic experiments to evaluate the cytotoxic potential of nanomaterials. When MWCNTs are functionalized or purified appropriately, they may not jeopardize erythrocyte integrity, as seen by the lack of ghost cells or aggregation. This picture adds to a more comprehensive assessment of MWCNTs in biomedical applications, especially in drug delivery or biosensing, where hemocompatibility is a crucial safety factor.

This microscopic picture, which was taken during hemolytic investigations of t-RES-functionalized multi-walled carbon nanotubes (RES-MWCNTs), shows a field of urine sediment that is full of amorphous and granular particles in addition to a large number of red blood cells (RBCs). As evidenced by the presence of both intact and morphologically changed red blood cells, RES-MWCNTs may have mild to moderate hemolytic effects in some situations, depending on factors like concentration, exposure duration, or surface chemistry. The observed dark, asymmetrical formations and cellular debris may be signs of partial lysis or membrane tension, which would suggest a biological reaction to the nanomaterial. Even though t-RES is well-known for its preventive and antioxidant qualities, its coupling with MWCNTs might not completely eliminate harmful interactions in urine setting.

This microscopic image shows a field of red blood cells (RBCs) suspended in an orange-stained solution. It was taken during hemolytic experiments with t-RES (RES). Most RBCs still have the distinctive biconcave disc shape with a pale centre, which suggests minimal hemolytic damage and structural integrity. A small number of cells show minor morphological changes, like elongation or crenation, which could indicate modest oxidative or osmotic stress. The conclusion that RES does not cause appreciable hemolysis under the measured conditions is supported by the cells' uniform distribution and clarity, as well as the lack of ghost cells or lysed pieces. This picture highlights RES's potential as a safe bioactive substance in medicinal applications while reaffirming its hemocompatibility.

5.6.16 Haematological studies

Haematological parameters were measured in healthy Wistar or Sprague-Dawley rats of both sexes that are uniform in size and weight. All animals will be fed the same standard diet for a maximum of seven days. The drug, MWCNT, and formulations will be administered intraperitoneally (i.p.) to animals at a dose comparable to 1 mg/kg of t-RES after being dissolved in regular saline (0.9% w/v NaCl). Seven days later, the retro-orbital plexus technique will be used to obtain blood samples, which will then be examined at a local pathology lab to ascertain the haematological parameters (Atmaca et al, 2014

Table 5.31: Haematological parameters

Sr No.	**Sample code**	**Haemoglobin (g/dl)**	**RBC Count (10^6/ µL)**	**WBC count (× 10^3/µL)**	**Platelet count (×10^3/µL)**	**MCH (pg)**
1.	Vehicle control	15.5 ± 0.03	8.98 ± 0.03	40.2 ± 0.08	660 ± 0.11	17.3 ± 0.04
2.	Drug -RES	15.2 ± 0.05	8.60± 0.02	22.0 ± 0.03	612 ± 0.12	17.7 ± 0.07
3.	MWCNT	15.3 ±0.07	9.29 ± 0.01	22.9 ± 0.07	585 ± 0.04	16.5± 0.04

4.	RES- MWCNT	15.6 ± 0.04	8.88 ± 0.02	33.1 ± 0.05	581 ± 0.08	17.6 ± 0.08
5.	RES- MWCNT-CET	15.7 ± 0.04	8.69 ± 0.05	23.3 ± 0.03	383 ± 0.02	18.1 ± 0.04

In this investigation, blood was drawn for biochemical examination after administration. Table 5.29 displays the serum biochemistry data. The vehicle control and Drug-RES, MWCNT, RES-MWCNT, and RES-MWCNT-CET groups' serum levels of haemoglobin, RBC count, WBC count, platelet count, MCH, and other parameters were compared; only the platelet count and WBC count differed (Lacerda et al., 2008). According to haematological examination, haemoglobin levels in Wistar rats given the designated experimental circumstances ranged from 15.2 to 15.7 g/dL. The fact that this range is within the typical physiological bounds for adult Wistar rats in good health indicates that the medication did not significantly impair erythropoietic function or cause anaemia. An absence of acute hematotoxic effects is indicated by the maintenance of haemoglobin concentration, which also signifies steady oxygen-carrying capacity and systemic homeostasis. According to histological examinations, these results are consistent with retained organ integrity and support the intervention's haematological safety.

The haematological analysis of Wistar rats showed that their red blood cell (RBC) counts ranged from 8.6 to 9.29 million cells per microlitre, which is within the typical physiological range for this species. This consistent erythrocyte profile indicates that neither erythropoiesis nor circulatory health were negatively impacted by the experimental treatment. Hematotoxicity is further supported by the maintained RBC count, which indicates sufficient oxygen transport ability and systemic resilience. Together with stable haemoglobin levels, these results support the intervention's haematological safety and acceptability.

Wistar rats' haematological assessment showed white blood cell (WBC) counts ranging from 22 to 40.2 × 10^3/µL, which, depending on the treatment setting, may indicate a dynamic immunological response. Even though this range is within the normal range for

rodents, the higher readings might indicate moderate leucocytosis, which could be a sign of an immune system activation or a brief inflammatory response. Extreme WBC count increases or decreases suggest that the medication did not cause significant immunotoxicity or immunosuppression. Systemic tolerance and immunological balance in the treated Wistar rats are supported by these results when interpreted in conjunction with steady haemoglobin and RBC levels.

According to haematological study, the platelet counts of Wistar rats ranged from 383 to 660 per microlitre, which is within the physiological range that is typical for this species. Based on the stable thrombocyte profile, it appears that the experimental treatment did not cause thrombocytopenia or thrombocytosis or affect megakaryocyte function. Preserving adequate platelet levels signifies systemic compatibility and the lack of haematological toxicity. These levels are crucial for immunological modulation, vascular integrity, and haemostasis. These results support the intervention's general haematological safety and acceptability in Wistar rats when paired with stable haemoglobin, RBC, and WBC values.

A haematological analysis of Wistar rats revealed mean corpuscular haemoglobin (MCH) levels between 16.5 and 18.1 picogrammes, which is consistent with the physiological standards for this species. MCH is a crucial measure of a red blood cell's ability to carry oxygen and represents the average quantity of haemoglobin found in each cell. Since there were no symptoms of hypochromia or hyperchromia, the observed range implies that the erythrocyte haemoglobin content stayed constant, suggesting that erythropoietic function was sustained and that anemia-related pathology was absent. These results confirm the experimental settings' haematological safety and the intervention's systemic suitability.

5.6.17 Histopathology

Histopathological images of the various formulations Drug-RES, MWCNT, RES-MWCNT, RES- MWCNTCE treated groups were shown in Figure 5.76-5.80. Images of the liver, kidney, lungs, and colon were taken following the administration of the drug RES, MWCNT, RES-MWCNT, RES-MWCNTCE, and vehicle control. In this work, we tried to investigate any physio pathological effects of administering RES-MCNT-CET to animals

in comparison to vehicle control, Drug-RES, MWCNT, and RES-MWCNT. The findings showed that none of the various groups had experienced any tissue deterioration, inflammation, necrosis, or fibrosis. In contrast to the kidney, liver, and lungs, which showed no deposits, the colon showed an accumulation of RES-MWCNT and RES-MCNT-CET clusters (Lacerda et al., 2008).

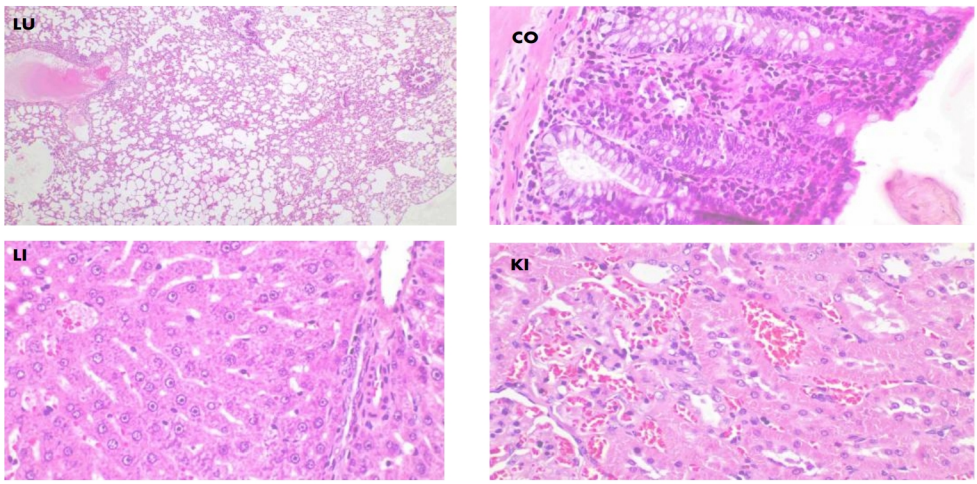


Figure 5.75: Histopathological images of vehicle control.

The tissue sections from the vehicle control group are represented by the histopathological slides with the labels LU (Lung), CO (Colon), LI (Liver), and KI (Kidney). These slides provide a reference point for comparison in experimental investigations. The LU slide displays a normal pulmonary architecture, with thin septa and intact alveolar spaces, suggesting that there are no fibrotic or inflammatory alterations and that respiratory function is retained. The CO slice has mucosal layers and glandular epithelium that are well-organised, which is indicative of healthy colonic tissue free of infiltration or dysplasia. There is no indication of necrosis, steatosis, or vascular congestion, and the hepatocytes are uniformly distributed in cords with nuclei in the centre of the slide, indicating normal liver morphology. The KI image demonstrates clean Bowman's gaps between separate renal tubules and glomeruli, indicating that the nephron structure is healthy and free of pathological changes.

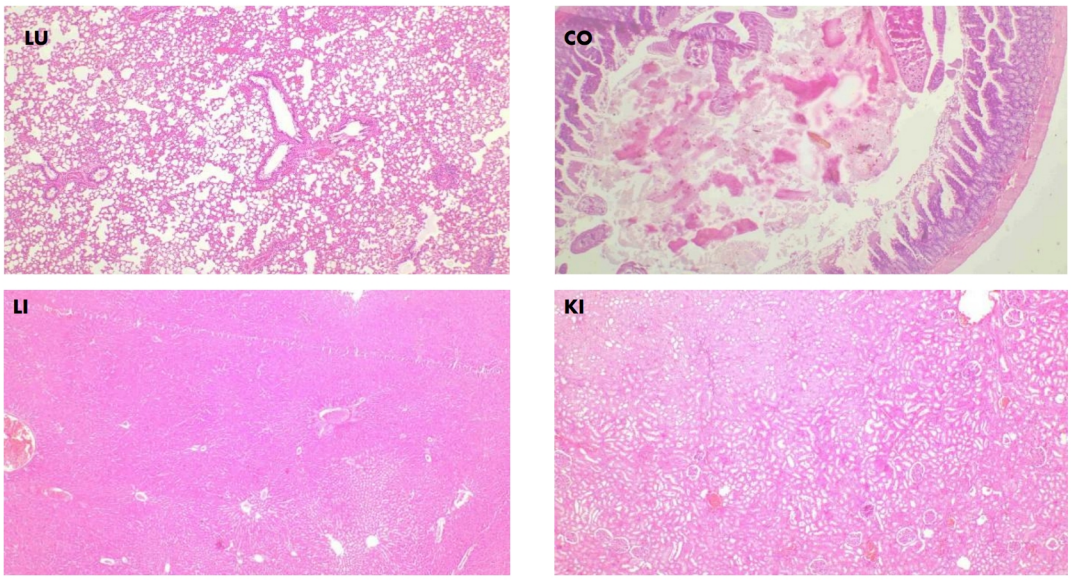


Figure 5.76: Histopathological images of t-RES treated group

The lung (LU), colon (CO), liver (LI), and kidney (KI) tissues represented by the histopathological slides from the t-RES treated group provide information about the tissue-level effects of trans-t-RES delivery. The LU slice demonstrates minimal thickening of the septal walls and intact alveolar architecture, indicating that t-RES may aid in preserving pulmonary integrity and lowering inflammatory infiltration. The colonic mucosa looks intact in the CO slide, with distinct crypts and epithelial lining, suggesting defence against oxidative stress or mucosal injury. With no obvious symptoms of necrosis, steatosis, or congestion, the LI picture shows hepatocytes organised in neat cords, suggesting hepatic stability and possible t-RES hepatoprotective benefits. The KI slice shows well-defined renal tubules and glomeruli, with no discernible interstitial inflammation or degeneration, indicating that the therapy has no effect on or may even support renal morphology. Overall, the histological profile of these slides is favourable throughout the major organs,

demonstrating the therapeutic potential of t-RES in maintaining tissue architecture and reducing degenerative alterations.

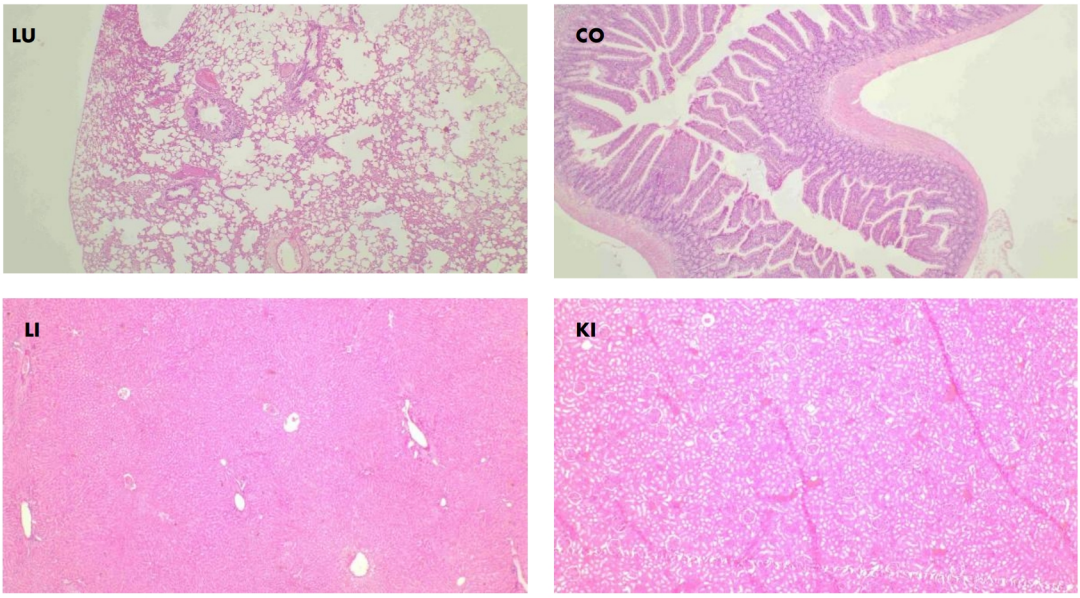


Figure 5.77: Histopathological images of MWCNT treated group

The lung (LU), colon (CO), liver (LI), and kidney (KI) tissues represented on the histopathology slides from the MWCNT-treated group show unique reactions to exposure to multi-walled carbon nanotubes. In the LU section, the alveolar architecture is changed, and there may be infiltration or thickening of the septal walls, which could indicate inflammation or pulmonary stress. A slight disturbance or the appearance of inflammatory cells in the colonic mucosa on the CO slide could suggest irritation or oxidative damage to the intestinal lining. Changes in hepatocyte density or organisation are visible in the LI picture, which may indicate early indications of hepatocellular stress, congestion, or mild degeneration. The KI section shows glomeruli and renal tubules with minor structural abnormalities that may indicate impaired renal function or nephrotoxicity. All of these findings point to the possibility that exposure to MWCNT may cause mild to moderate

histological changes in a number of important organs, necessitating more research into the material's systemic effects and biocompatibility.

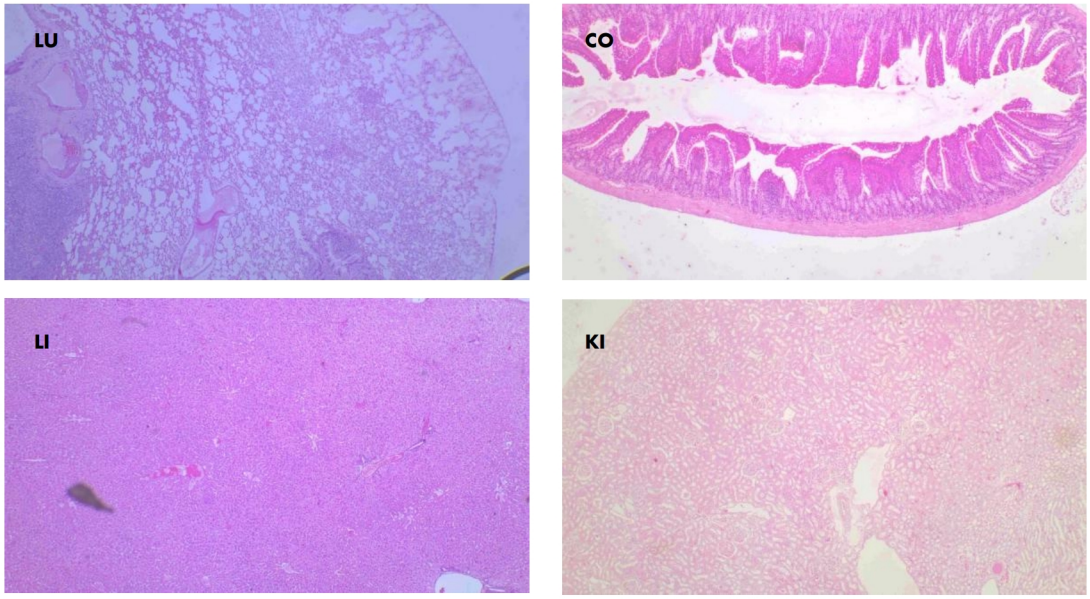


Figure 5.78: Histopathological images of RES-MWCNT treated group

The RES-MWCNT treated group's histopathological analysis shows organ-specific morphological characteristics that point to a regulated response to multi-walled carbon nanotubes functionalised with t-RES. A potentially protective or non-aggressive pulmonary interaction is indicated by the alveolar architecture seeming maintained with minimal structural distortion in the lung (LU) tissue. A limited inflammatory or cytotoxic effect on the intestinal epithelium is suggested by the colon (CO) section's intact mucosal layers and distinct glandular features. The histology of the liver (LI) shows clear sinusoidal gaps and well-organised hepatocyte cords, which indicate preserved hepatic integrity and fewer indications of congestion or degeneration. With no obvious indications of necrosis or tubular dilatation, kidney (KI) tissue exhibits well-preserved glomeruli and tubular forms, suggesting renal tolerance to the RES-MWCNT formulation. Overall, these findings imply

that RES-MWCNT treatment may have a biocompatible or even protective effect on key organs, which calls for more research into its safety profile and therapeutic potential.

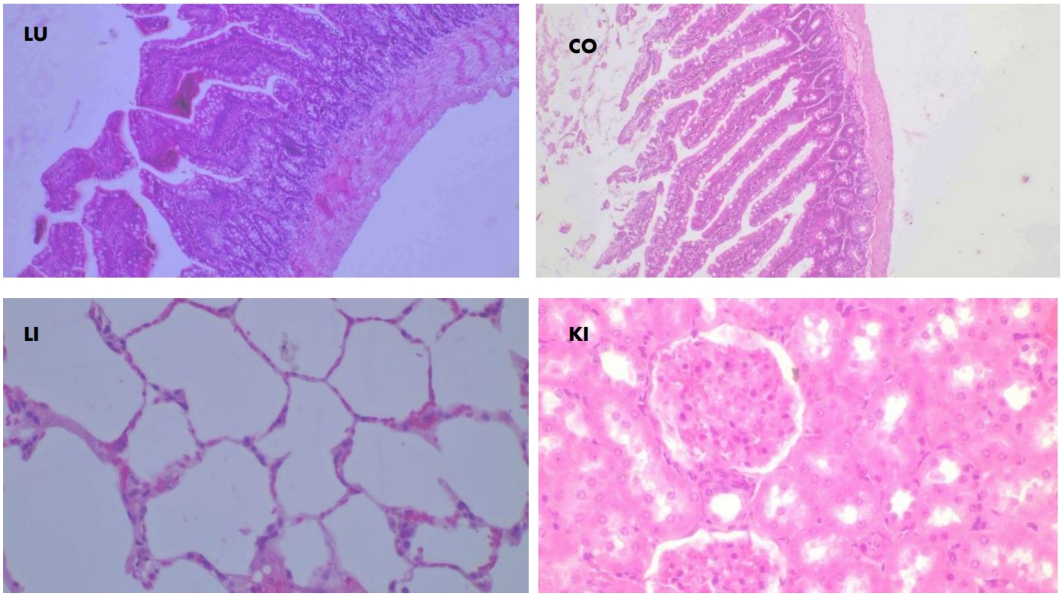


Figure 5.79: Histopathological images of RES-MWCNT-CET treated group

The lung (LU), colon (CO), liver (LI), and kidney (KI) tissues represented by the histopathology slides from the RES-MCNT-CET treated group show organ-specific morphological preservation, indicating a potentially positive biocompatibility profile of the RES-MCNT-CET formulation. With few indications of inflammatory infiltration or septal thickening, lung tissue (LU) maintains its alveolar architecture, suggesting low levels of pulmonary toxicity. With no obvious epithelial breakdown and intact mucosal layers and well-organised crypt structures, the colon (CO) slice indicates a steady gastrointestinal response. Hepatocytes in ordered cords with distinct sinusoidal gaps are shown in liver histology (LI), indicating little hepatocellular stress and sustained hepatic function. Renal tolerance is implied by kidney tissue (KI), which has distinct glomeruli and tubular structures free of necrosis or tubular degeneration. Overall, these results support the promise of RES-MCNT-CET as a safe and systemically compatible therapeutic candidate

by indicating that therapy does not result in severe histopathological damage across major organ.

Summary

The existing approaches for early detection and treatment of colorectal cancer (CRC) are imprecise, have side effects, and cause cancer cells to become resistant. CNTs are widely used in imaging, diagnostics, drug release monitoring, and the development of biosensors for associated medical applications. Targeted therapy for colorectal cancer may be possible with the coupling of a ligand, especially monoclonal antibody (mAb), to a drug delivery system. The Food and Drug Administration (FDA) approved cetuximab as an anticancer monoclonal antibody in 2004. The current formulation was development to enhance the therapeutic efficacy of the resveratrol in the treatment of colorectal cancer through the cetuximab conjugated carbon nanotubes. In Preformulation study resveratrol (t-RES) drug's melting point was 267±1.0-269.33±1.527 °C. In uv spectroscopy analysis the calibration of resveratrol in water was prepared with linear curve equation y = 0.230x + 0.011 within a concentration range of 1 µg/mL to 4 µg/mL.While in Phosphate Buffer Saline (PBS) 7.4 linearity plot was prepared ranged from 1µg/mL to 8µg/mL with linear curve equation y = 0.115x + 0.02. Partition coefficient was found to be 3.372 ± 0.005 indicated the lipophilic nature of the t-RES drug. DSC thermogram of the t-RES indicated a symmetric endothermic peak at 268.96°C, exploring the melting point if t-RES, FESEM images confirmed t-RES had a flat surface and a rod-like shape The X-ray diffractogram of pure t-RES demonstrated several intense peaks, indicating its crystalline structure. The diffractogram of pure t-RES demonstrated characteristics peaks at 2θ diffraction angles of 6.6, 16.4, 19.1, 22.3, and 28.3. Furthermore, in HPLC Analytical method validation includes the %RSD less than 2% for each parameter. The calculated LOD for t-RES was found to be 1.6 µg/mL whereas, LOQ determined for t-RES was 4.8 μg/mL. In HPLC, the linearity curve was prepared at conc. ranges of 2 to 10 μg/mL, The R^2 score was 0.997. Forced degradation study confirmed that t-RES was more vulnerable to alkali treatment, it exhibited the strongest resilience to acid treatment.

In Preformulation study of carbon nanotube, the pristine MWCNTs' side walls were smooth, as seen in Figure.5.14, while the side walls of functionalised MWCNTs—whether MWCNT-COOH or MWCNT-NH_2—appeared to be rough with open cap structures. The

emergence of disordered sites on the surface of MWCNTs is a sign of defect creation along their walls where additional functional groups (mostly carboxylic and amino) were introduced.

The particle sizes of pristine, amino-functionalized, and carboxylic acid-functionalized multi-walled carbon nanotubes were found to be 182.4 nm, 241.4 nm, and 279.9 nm, respectively. FTIR, XRD and DSC confirmed that no incompatibility between resveratrol and CNT and that the resveratrol drug was incorporated into the CNT's channel. In this investigation, distinct drug-to-CNT ratios were used to load the resveratrol drug over the amin-functionalized and COOH-functionalized CNTs namely RES-MWCNT 1, RES-MWCNT 2, RES-MWCNT 3, and RES-MWCNT 4. The drug t-RES loading in MWCNTs was ascertained using the established HPLC technique. In formulations RES-MWCNT 1, RES-MWCNT 2, RES-MWCNT 3, and RES-MWCNT 4, the percentage of resveratrol drug entrapment was 73.83 ± 0.023%, 96.29 ± 0.054%, 84.15 ± 0.076%, and 80.68 ± 0.065%, respectively. Among Four formulation RES-MWCNT 2 hydrodynamic diameters. The hydrodynamic diameter of RES-MWCNT 2 was the smallest at 289.6 nm because to its greater zeta potential of -18.8 mv, which inhibited CNT aggregation. Given that RES-MWCNT 2's PDI (0.070) was nearly 0.1, the system was regarded as monodispersed. The DSC patterns of RES-MWCNT 2 and Carboxylated MWCNT verify that the medication was successfully loaded into MWCNTs. In vitro release confirmed that the test samples displayed 97.7% at pH 5 and approximately 93.6% at pH 7.4, indicating great drug Release. The presence of limited drugs residual is proof that effective encapsulation and relatively limited drug loss. In order to create the cetuximab-containing t-RES loaded carbon nanotube (RES-MWCNT-CET), the antibodies were loaded via physical mixing. Cetuximab was physically added to the inner cavity of multi-walled nanotubes loaded with RES. It was found that the Z-average diameter of RES-MWCNT-CET was 730 nm. With a zeta potential of -11.9 mV, a shift to a positive scale is indicated. Despite the local neutral zeta potential, the RES-MWCNT-CET setup remained in an aggregated form. It was verified that carboxylate MWCNT had a tubular shape with open edges at the nanometric scale. Additionally, even after being CET attached, surface

roughness was observed in the scans of which showed no change in their tubular structure. The drug release was found to be 96.58 ±0.12% at pH 5 over 48 hours, while at pH 7.4 it was only 92.73 ±0.21%.

MWCNT had a comparatively higher cytotoxicity than RES-MWCNT-CET. But when RES and RES-MWCNT-CET are compared, the cytotoxicity changes by 3.2 times. Cell viability was higher at lower concentrations, The MIF values for Control, RES, MWCNT, RES-MWCNT2, CET, and RES-MWCNT-CET, which were 58.4,59.4, 93.4,2420, and 4571,5404 correspondingly. In plasma, the regression equation Y= 73686x + 7764.9 as well as the R^2 values of 0.9989, show that the calibration curve of RES was generated in plasma and showed a notable degree of linearity. RES recovered over 95% of the time in all cases, according to the results, and the percentage RSD was less than 2. At 1hr, the amount of RES extracted from RES-MWCNT and RES-MWCNT-CET and administered to the colon was substantially more than that of plain RES solution ($p<0.0001$). By contrast, the RES-MWCNT-CET significantly ($p<0.0001$) transported more resveratrol to the colon (0.094±0.002µg) than the RES-MWCNT (0.054±0.003µg) at 1hr, 4hr and 8hr. The RES-MWCNT-CET delivered a much lower amount of resveratrol to the liver, kidney, lung, and plasma than the RES-MWCNT followed by pure drug solution. The haemolytic toxicity of the amine MWCNTs was 10.25 ± 0.34%. The haemolysis rate of the medication RES (5 mg) was 30.75 ± 0.55%, which was 2.14 times greater than the haemolysis produced by RES-MWCNTs. The hemocompatibility of RES-MWCNT and RES-MWCNT-CET was found to be higher, with respective values of 14.92 ± 0.55% and 4.03 ± 0.43%. RES-MWCNT-CET reduces haemolysis by 7.5 times. The lung (LU), colon (CO), liver (LI), and kidney (KI) tissues represented on the histopathology slides from the MWCNT-treated group show unique reactions to exposure to multi-walled carbon nanotubes. Overall, the results support the promise of RES-MCNT-CET as a safe and systemically compatible therapeutic candidate by indicating that therapy does not result in severe histopathological damage across major organs.

Future Aspects

- To confirm safety and therapeutic effectiveness in animal models, in vivo research is required.
- Clinical translation will require thorough pharmacokinetic and toxicological characterization.
- Functionalizing MWCNTs with patient-specific biomarkers allows for integration into personalized medicine methodologies.
- This nanoplatform may be expanded to treat other tumours that overexpress EGFR, such as non-small cell lung cancer or head and neck cancer.

Bibliography

- Abdulkareem, A. S., Afolabi, A. S., Iyuke, S. E., & Vz Pienaar, H. C. (2007). Synthesis of carbon nanotubes by swirled floating catalyst chemical vapour deposition method. *Journal of nanoscience and nanotechnology*, *7*(9), 3233–3238. https://doi.org/10.1166/jnn.2007.685
- Adebayo, A. S., Agbaje, K., Adesina, S. K., & Olajubutu, O. (2023). Colorectal Cancer: Disease Process, Current Treatment Options, and Future Perspectives. *Pharmaceutics*, *15*(11),2620.https://doi.org/10.3390/pharmaceutics15112620
- Agarwal, V., Subash, A., Nayar, R. C., & Rao, V. (2019). Is EGFR really a therapeutic target in head and neck cancers? *Journal of surgical oncology*, *119*(6), 685–686. https://doi.org/10.1002/jso.25387
- Aggarwal, B. B., Bhardwaj, A., Aggarwal, R. S., Seeram, N. P., Shishodia, S., & Takada, Y. (2004). Role of resveratrol in prevention and therapy of cancer: preclinical and clinical studies. *Anticancer research*, *24*(5A), 2783–2840.
- Ahmed M. (2020). Colon Cancer: A Clinician's Perspective in 2019. *Gastroenterology research*, *13*(1), 1–10. https://doi.org/d10.14740/gr1239
- Ainurofiq, A., Hidayat, Y., Lestari, E. Y. P., Kumalasari, M. M. W., & Choiri, S. (2022). T-Res Nanocrystal Incorporated into Mesoporous Material: Rational Design and Screening through Quality-by-Design Approach. *Nanomaterials (Basel, Switzerland)*, *12*(2), 214. https://doi.org/10.3390/nano12020214
- Akinwumi, B. C., Bordun, K. M., & Anderson, H. D. (2018). Biological Activities of Stilbenoids. *International journal of molecular sciences*, *19*(3), 792. https://doi.org/10.3390/ijms19030792
- Albini, A., Cesana, E., & Noonan, D. M. (2011). Cancer stem cells and the tumor microenvironment: soloists or choral singers. *Current pharmaceutical biotechnology*, *12*(2), 171–181. https://doi.org/10.2174/138920111794295756
- Ali M., Ali S., Hosseini, M.S., Rezaeejam, H., Bagheri, F., Aghaei, A., Safari, H., and Hossein, D. (2024). Synthesis of curcumin loaded single walled carbon nanotubes: Characterization and anticancer effects in vitro. Results in Chemistry, 7;101370

- Ali, H. E., & Radwan, R. R. (2021). Synthesis, characterization and evaluation of resveratrol-loaded functionalized carbon nanotubes as a novel delivery system in radiation enteropathy. *European journal of pharmaceutical sciences: official journal of the European Federation for Pharmaceutical Sciences*, *167*, 106002. https://doi.org/10.1016/j.ejps.2021.106002
- Alhajj, O., Noor, D. M., & Md Hanafiah, N. H. (2024). Investigation on the cost–effectiveness of Cetuximab in treatment of colorectal cancer: a systematic review. *Colorectal Cancer*, *13*(1). https://doi.org/10.1080/1758194X.2024.2390822
- Al-Joufi, F. A., Setia, A., Salem-Bekhit, M. M., Sahu, R. K., Alqahtani, F. Y., Widyowati, R., & Aleanizy, F. S. (2022). Molecular Pathogenesis of Colorectal Cancer with an Emphasis on Recent Advances in Biomarkers, as Well as Nanotechnology-Based Diagnostic and Therapeutic Approaches. *Nanomaterials*, *12*(1), 169. https://doi.org/10.3390/nano12010169
- Ajayan, P.M., (2003). Bulk Metal and Ceramics Nanocomposites, Nanocomposite Science and Technology, Wiley-VCH Verlag GmbH & Co.,1–76.
- Amini, P., Moazamiyanfar, R., Dakkali, M. S., Khani, A., Jafarzadeh, E., Mouludi, K., Khodamoradi, E., Johari, R., Taeb, S., & Najafi, M. (2023). Resveratrol in Cancer Therapy: From Stimulation of Genomic Stability to Adjuvant Cancer Therapy: A Comprehensive Review. *Current topics in medicinal chemistry*, *23*(8), 629–648. https://doi.org/10.2174/1568026623666221014152759
- Ansari, K. A., Vavia, P. R., Trotta, F., & Cavalli, R. (2011). Cyclodextrin-Based Nanosponges for delivery of resveratrol: in vitro Characterisation, Stability, Cytotoxicity and Permeation study. *AAPS PharmSciTech*, *12*(1), 279–286. https://doi.org/10.1208/s12249-011-9584-3
- Anazawa, K., K. Shimotani, C. Manabe, H. Watanabe, & M. Shimizu, (2002). High purity carbon nanotube synthesis method. Applied Physics Letters, 81,739–741.
- Andrés, A., Rosés, M., Ràfols, C., Bosch, E., Espinosa, S., Segarra, V., & Huerta, J. M. (2015). Setup and validation of shake-flask procedures for the determination of

partition coefficients (logD) from low drug amounts. *European journal of pharmaceutical sciences : official journal of the European Federation for Pharmaceutical Sciences*, *76*, 181–191. https://doi.org/10.1016/j.ejps.2015.05.008

- Anisimova, N. Y., Kiselevsky, M. V., Sosnov, A. V., Sadovnikov, S. V., Stankov, I. N., & Gakh, A. A. (2011). Trans-, cis-, and dihydro-resveratrol: a comparative study. *Chemistry Central journal*, *5*, 88. https://doi.org/10.1186/1752-153X-5-88
- Anzar, N., Hasan, R., Tyagi, M., Yadav, N., & Narang, J. (2020). Carbon nanotube-A review on Synthesis, Properties and plethora of applications in the field of biomedical science, Sensors Inter, 1,100003.
- Aqel, A., El-Nour, K.M., Ammar, R.A., & Al-Warthan, A. (2012). Carbon nanotubes, science and technology part (I) structure, synthesis and characterization. *Arabian Journal of Chemistry,* 5,1–23.
- Arafat, Y., Loft, M., Cao, K., Reid, F., Kosmider, S., Lee, M., Gibbs, P., Faragher, I. G., & Yeung, J. M. (2022). Current colorectal cancer chemotherapy dosing limitations and novel assessments to personalize treatments. *ANZ journal of surgery*, *92*(11), 2784–2785. https://doi.org/10.1111/ans.18046
- Armaghany, T., Wilson, J.D., Chu, Q., & Mills, G. (2012). Genetic alterations in colorectal cancer. Gastrointest. *Cancer Research,* 5,19–27.
- Arshad, U., Sutton, P. A., Ashford, M. B., Treacher, K. E., Liptrott, N. J., Rannard, S. P., Goldring, C. E., & Owen, A. (2020). Critical considerations for targeting colorectal liver metastases with nanotechnology. *Wiley interdisciplinary reviews. Nanomedicine and nanobiotechnology*, *12*(2), e1588. https://doi.org/10.1002/wnan.1588
- Arteaga C. L. (2002). Epidermal growth factor receptor dependence in human tumors: more than just expression? *The oncologist*, *7 Suppl 4*, 31–39.
- https://doi.org/10.1634/theoncologist.7-suppl_4-31
- Aquina, C. T., Mohile, S. G., Tejani, M. A., Becerra, A. Z., Xu, Z., Hensley, B. J., Arsalani-Zadeh, R., Boscoe, F. P., Schymura, M. J., Noyes, K., Monson, J. R., & Fleming, F. J. (2017). The impact of age on complications, survival, and cause of death following colon cancer surgery. *British journal of cancer*, *116*(3), 389–397. https://doi.org/10.1038/bjc.2016.421

- Atmaca, N., Yıldırım, E., Güner, B., Kabakçı, R., & Bilmen, F. S. (2014). Effect of resveratrol on hematological and biochemical alterations in rats exposed to fluoride. *BioMed research international*, *2014*, 698628. https://doi.org/10.1155/2014/698628
- Balaji, S., Pandian, M. S., Kumar, M., & Chang, J. (2026). Carbon based Nanomaterials as Versatile Platforms for the Development of Drug Delivery Systems: Current Trends and Future Prospects. BioNanoScience, 16(7). https://doi.org/10.1007/s12668-026-02729-9
- Bancuta, O., Andrei, C., Iulian, B., Rodica, M., Radu, S., Tanta, S., Anca, G., & Marius L.. (2015). FT-IR and UV-VIS Characterization of Grape Extracts Used as Antioxidants in Polymers. *Revue Roumaine de Chimie,* 60 (5–6), 571–77.
- Bagnardi, V., Rota, M., Botteri, E., Tramacere, I., Islami, F., Fedirko, V., Scotti, L., Jenab, M., Turati, F., Pasquali, E., Pelucchi, C., Galeone, C., Bellocco, R., Negri, E., Corrao, G., Boffetta, P., & La Vecchia, C. (2015). Alcohol consumption and site-specific cancer risk: a comprehensive dose-response meta-analysis. *British journal of cancer*, *112*(3), 580–593. https://doi.org/10.1038/bjc.2014.579
- Baetke, S. C., Lammers, T., & Kiessling, F. (2015). Applications of nanoparticles for diagnosis and therapy of cancer. *The British journal of radiology*, *88*(1054), 20150207. https://doi.org/10.1259/bjr.20150207
- Bao, G., Mitragotri, S., & Tong, S. (2013). Multifunctional nanoparticles for drug delivery and molecular imaging. *Annual review of biomedical engineering*, *15*, 253–282. https://doi.org/10.1146/annurev-bioeng-071812-152409
- Bayat Mokhtari, R., Homayouni, T. S., Baluch, N., Morgatskaya, E., Kumar, S., Das, B., & Yeger, H. (2017). Combination therapy in combating cancer. *Oncotarget*, *8*(23), 38022–38043. https://doi.org/10.18632/oncotarget.16723
- Beg, S., Rizwan, M., Sheikh, A. M., Hasnain, M. S., Anwer, K., & Kohli, K. (2011). Advancement in carbon nanotubes: basics, biomedical applications and toxicity. *The Journal of pharmacy and pharmacology*, *63*(2), 141–163. https://doi.org/10.1111/j.2042-7158.2010.01167.x

- Benson, A. B., Venook, A. P., Al-Hawary, M. M., Arain, M. A., Chen, Y. J., Ciombor, K. K., Cohen, S., Cooper, H. S., Deming, D., Farkas, L., Garrido-Laguna, I., Grem, J. L., Gunn, A., Hecht, J. R., Hoffe, S., Hubbard, J., Hunt, S., Johung, K. L., Kirilcuk, N., Krishnamurthi, S., Gurski, L. A. (2021). Colon Cancer, Version 2.2021, NCCN Clinical Practice Guidelines in Oncology. *Journal of the National Comprehensive Cancer Network : JNCCN*, *19*(3), 329–359. https://doi.org/10.6004/jnccn.2021.0012
- Bhaskar, A.K., Deshmukh, V.N., & Prajapati, L. (2013). Carbon nanotube as a drug delivery system: a review. *International Journal of Pharmaceutical Technology and Biotechnology*, 5, 2695–2711.
- Bianco, A., Hoebeke, J., Kostarelos, K., Prato, M., & Partidos, C. D. (2005). Carbon nanotubes: on the road to deliver. *Current drug delivery*, *2*(3), 253–259. https://doi.org/10.2174/1567201054367959
- Boghossian, S., & Hawash, A. (2012). Chemoprevention in colorectal cancer--where we stand and what we have learned from twenty years' experience. *The surgeon: journal of the Royal Colleges of Surgeons of Edinburgh and Ireland*, *10*(1), 43–52. https://doi.org/10.1016/j.surge.2011.07.003.
- Bokey, E. L., Moore, J. W., Chapuis, P. H., & Newland, R. C. (1996). Morbidity and mortality following laparoscopic-assisted right hemicolectomy for cancer. *Diseases of the colon and rectum*, *39*(10 Suppl), S24–S28. https://doi.org/10.1007/BF02053802.
- Bomme, L., Heim, S., Bardi, G., Fenger, C., Kronborg, O., Brøgger, A., & Lothe, R. A. (1998). Allelic imbalance and cytogenetic deletion of 1p in colorectal adenomas: a target region identified between DIS199 and DIS234. *Genes, chromosomes & cancer*, *21*(3), 185–194. https://doi.org/10.1002/(sici)1098-2264(199803)21:3<185::aid-gcc2>3.0.co;2-w.
- Bomme, L., Lothe, R. A., Bardi, G., Fenger, C., Kronborg, O., & Heim, S. (2001). Assessments of clonal composition of colorectal adenomas by FISH analysis of chromosomes 1, 7, 13 and 20. *International journal of cancer*, *92*(6), 816–823. https://doi.org/10.1002/ijc.1275

- Botteri, E., Iodice, S., Bagnardi, V., Raimondi, S., Lowenfels, A. B., & Maisonneuve, P. (2008). Smoking and colorectal cancer: a meta-analysis. *JAMA*, *300*(23), 2765–2778. https://doi.org/10.1001/jama.2008.839.
- Boyle, T., Keegel, T., Bull, F., Heyworth, J., & Fritschi, L. (2012). Physical activity and risks of proximal and distal colon cancers: a systematic review and meta-analysis. *Journal of the National Cancer Institute*, *104*(20), 1548–1561. https://doi.org/10.1093/jnci/djs354.
- Bose, S., Panda, A. K., Mukherjee, S., & Sa, G. (2015). Curcumin and tumor immune-editing: resurrecting the immune system. *Cell division*, *10*, 6. https://doi.org/10.1186/s13008-015-0012-z.
- Brar, B., Ranjan, K., Palria, A., Kumar, R., Ghosh, M., Sihag, S., & Minakshi, P. (2021) Nanotechnology in Colorectal Cancer for Precision Diagnosis and Therapy. *Frontiers in Nanotechnology*, 3,699266. doi: 10.3389/fnano.2021.699266
- Bray, F., Ferlay, J., Soerjomataram, I., Siegel, R. L., Torre, L. A., & Jemal, A. (2018). Global cancer statistics 2018: GLOBOCAN estimates of incidence and mortality worldwide for 36 cancers in 185 countries. *CA: a cancer journal for clinicians*, *68*(6), 394–424. https://doi.org/10.3322/caac.21492.
- Brand, M., Gaylard, P., & Ramos, J. (2017). Colorectal cancer in South Africa: An assessment of disease presentation, treatment pathways and 5-year survival. *South African medical journal*, *108*(2), 118–122. https://doi.org/10.7196/SAMJ.2017.v108i2.12338
- Branca, C., Frusteri, F., Magazu, V., & Mangione, A. (2004). Characterization of carbon nanotubes by TEM and infrared spectroscopy. *The Journal of Physical Chemistry B*,108, 3469–3473.
- Brenner, H., Altenhofen, L., Stock, C., & Hoffmeister, M. (2013). Natural history of colorectal adenomas: birth cohort analysis among 3.6 million participants of screening colonoscopy. *Cancer epidemiology, biomarkers & prevention : a publication of the American Association for Cancer Research, cosponsored by the American Society of Preventive Oncology*, *22*(6), 1043–1051. https://doi.org/10.1158/1055-9965.EPI-13-0162.

- Brockmueller, A., Sajeev, A., Koklesova, L., Samuel, S. M., Kubatka, P., Büsselberg, D., Kunnumakkara, A. B., & Shakibaei, M. (2024). Resveratrol as sensitizer in colorectal cancer plasticity. *Cancer metastasis reviews*, *43*(1), 55–85. https://doi.org/10.1007/s10555-023-10126-x.
- Brockmueller, A., Girisa, S., Kunnumakkara, A. B., & Shakibaei, M. (2023). Resveratrol Modulates Chemosensitisation to 5-FU via β1-Integrin/HIF-1α Axis in CRC Tumor Microenvironment. *International journal of molecular sciences*, *24*(5), 4988. https://doi.org/10.3390/ijms24054988.

- Buhrmann, C., Shayan, P., Goel, A., & Shakibaei, M. (2017). Resveratrol Regulates Colorectal Cancer Cell Invasion by Modulation of Focal Adhesion Molecules. *Nutrients*, *9*(10), 1073. https://doi.org/10.3390/nu9101073.
- Buhrmann, C., Yazdi, M., Popper, B., Shayan, P., Goel, A., Aggarwal, B. B., & Shakibaei, M. (2018). Resveratrol Chemosensitizes TNF-β-Induced Survival of 5-FU-Treated Colorectal Cancer Cells. *Nutrients*, *10*(7), 888. https://doi.org/10.3390/nu10070888.
- Cai, J.-H., Tang, X.-H., Chen, X.-D., and Wang, M. (2021). Temperature and straininduced tunable electromagnetic interference shielding in polydimethylsiloxane/multiwalled carbon nanotube composites with temperature-sensitive microspheres. *Composites. Part A, Applied science and manufacturing,* 140, 106188. doi:10.1016/j.compositesa.2020.10618.
- Canavan, C., Abrams, K. R., & Mayberry, J. (2006). Meta-analysis: colorectal and small bowel cancer risk in patients with Crohn's disease. *Alimentary pharmacology & therapeutics*, *23*(8), 1097–1104. https://doi.org/10.1111/j.1365-2036.2006.02854.x.
- Cao, Y., Nishihara, R., Wu, K., Wang, M., Ogino, S., Willett, W. C., Spiegelman, D., Fuchs, C. S., Giovannucci, E. L., & Chan, A. T. (2016). Population-wide Impact of Long-term Use of Aspirin and the Risk for Cancer. *JAMA oncology*, *2*(6), 762–769. https://doi.org/10.1001/jamaoncol.2015.6396

- Chen,W., Shi,K., Yu, Y., Yang, P., Bei, Z., Mo, D., Yuan, L., Pan, M., Chen, Y., & Qian, Z. (2024). Drug delivery systems for colorectal cancer chemotherapy. *Chinese Chemical Letters,* 35(2), 109159 . https://doi.org/10.1016/j.cclet.2023.109159.
- Chang W. W. (1984). Histogenesis of colon cancer in experimental animals. *Scandinavian journal of gastroenterology. Supplement*, *104*, 27–43.
- Chen, J., & Gao, X. (2017). Recent advances in the flame synthesis of carbon nanotubes, Am. *Journal of Material Synthesis, Process*. 2, 71–89.
- Cheung, W., Pontoriero, F., Taratula, O., Chen, A. M., & He, H. (2010). DNA and carbon nanotubes as medicine. *Advanced drug delivery reviews*, *62*(6), 633–649. https://doi.org/10.1016/j.addr.2010.03.007.
- Chudoba, D., Jażdżewska, M., Łudzik, K., Wołoszczuk, S., Juszyńska-Gałązka, E., & Kościński, M. (2021). Description of Release Process of Doxorubicin from Modified Carbon Nanotubes. *International journal of molecular sciences*, *22*(21), 12003. https://doi.org/10.3390/ijms222112003.
- Coleman, J. N., Khan, U., & Gun'ko, Y. K. (2006). Mechanical reinforcement of polymers using carbon nanotubes. *Advanced Material*. 18, 689–706.
- Camont, L., Cottart, C. H., Rhayem, Y., Nivet-Antoine, V., Djelidi, R., Collin, F., Beaudeux, J. L., & Bonnefont-Rousselot, D. (2008). Simple spectrophotometric assessment of the trans-/cis-resveratrol ratio in aqueous solutions. *Analytica chimica acta*, *634*(1), 121–128. https://doi.org/10.1016/j.aca.2008.12.003.
- Chowdhry, A., Kaur, J., Khatri, M., Puri, V., Tuli, R., & Puri, S. (2019). Characterization of functionalized multiwalled carbon nanotubes and comparison of their cellular toxicity between HEK 293 cells and zebra fish in vivo. *Heliyon*, *5*(10), e02605. https://doi.org/10.1016/j.heliyon.2019.e02605.
- Chow, H. H., Garland, L. L., Hsu, C. H., Vining, D. R., Chew, W. M., Miller, J. A., Perloff, M., Crowell, J. A., & Alberts, D. S. (2010). Resveratrol modulates drug- and carcinogen-metabolizing enzymes in a healthy volunteer study. *Cancer prevention research (Philadelphia, Pa.)*, *3*(9), 1168–1175. https://doi.org/10.1158/1940-6207.CAPR-09-0155.

- Cianchi, F., Cortesini, C., Fantappiè, O., Messerini, L., Schiavone, N., Vannacci, A., Nistri, S., Sardi, I., Baroni, G., Marzocca, C., Perna, F., Mazzanti, R., Bechi, P., & Masini, E. (2003). Inducible nitric oxide synthase expression in human colorectal cancer: correlation with tumor angiogenesis. *The American journal of pathology*, *162*(3), 793–801. https://doi.org/10.1016/S0002-9440(10)63876-X.
- Corley, D. A., Jensen, C. D., Marks, A. R., Zhao, W. K., de Boer, J., Levin, T. R., Doubeni, C., Fireman, B. H., & Quesenberry, C. P. (2013). Variation of adenoma prevalence by age, sex, race, and colon location in a large population: implications for screening and quality programs. *Clinical gastroenterology and hepatology : the official clinical practice journal of the American Gastroenterological Association*, *11*(2), 172–180. https://doi.org/10.1016/j.cgh.2012.09.010.
- Correale, P., Botta, C., Cusi, M. G., Del Vecchio, M. T., De Santi, M. M., Gori Savellini, G., Bestoso, E., Apollinari, S., Mannucci, S., Marra, M., Abbruzzese, A., Aquino, A., Turriziani, M., Bonmassar, L., Caraglia, M., & Tagliaferri, P. (2011). Cetuximab ± chemotherapy enhances dendritic cell-mediated phagocytosis of colon cancer cells and ignites a highly efficient colon cancer antigen-specific cytotoxic T-cell response in vitro. *International journal of cancer*, *130*(7), 1577–1589. https://doi.org/10.1002/ijc.26181
- Cottart, C. H., Nivet-Antoine, V., Laguillier-Morizot, C., & Beaudeux, J. L. (2010). Resveratrol bioavailability and toxicity in humans. *Molecular nutrition & food research*, *54*(1), 7–16. https://doi.org/10.1002/mnfr.200900437.
- Crockett, S. D., & Nagtegaal, I. D. (2019). Terminology, Molecular Features, Epidemiology, and Management of Serrated Colorectal Neoplasia. *Gastroenterology*, *157*(4), 949–966.e4. https://doi.org/10.1053/j.gastro.2019.06.041.
- Crozier, A., Jaganath, I. B., & Clifford, M. N. (2009). Dietary phenolics: chemistry, bioavailability and effects on health. *Natural product reports*, *26*(8), 1001–1043. https://doi.org/10.1039/b802662a.
- Cronin, K. A., Krebs-Smith, S. M., Feuer, E. J., Troiano, R. P., & Ballard-Barbash, R. (2001). Evaluating the impact of population changes in diet, physical activity, and

weight status on population risk for colon cancer (United States). *Cancer causes & control : CCC*, *12*(4), 305–316. https://doi.org/10.1023/a:1011244700531.

- Cui, X., Zheng, X., Ren, J., Liu, H., Jia, Y., Wu, A., & Han, X. (2023). Development and validation of two bioanalysis methods for the determination of etimicin in human serum and urine by liquid chromatography-tandem mass spectrometry: Applications to a human pharmacokinetic and breakpoint study. *Frontiers in pharmacology*, *14*, 1076046. https://doi.org/10.3389/fphar.2023.1076046.
- Cui, L., Liu, W., Liu, H., Qin, Q., Wu, S., He, S., Pang, X., Zhu, C., & Shen, P. (2019). pH-Triggered Charge-Reversal Mesoporous Silica Nanoparticles Stabilized by Chitosan Oligosaccharide/Carboxymethyl Chitosan Hybrids for Effective Intracellular Delivery of Doxorubicin. *ACS applied bio materials*, *2*(5), 1907–1919. https://doi.org/10.1021/acsabm.8b00830.
- Dai, H., (2002). Carbon nanotubes: opportunities and challenges. *Surface Science,* 500,218–241. https://doi.org/10.1016/S0039-6028(01)01558-8.
- Determination of Melting Points According to Pharmacopeia." n.d. Accessed September 23, 2021. www.thinkSRS.com
- Ding, S., Hu, C., Fang, J., & Liu, G. (2020). The Protective Role of Probiotics against Colorectal Cancer. *Oxidative medicine and cellular longevity*, *2020*, 8884583. https://doi.org/10.1155/2020/8884583.
- Ding, R. G., Lu, G. Q., Yan, Z. F., & Wilson, M. A. (2001). Recent advances in the preparation and utilization of carbon nanotubes for hydrogen storage. *Journal of nanoscience and nanotechnology*, *1*(1), 7–29. https://doi.org/10.1166/jnn.2001.012.
- Dinicola, S., Morini, V., Coluccia, P., Proietti, S., D'Anselmi, F., Pasqualato, A., Masiello, M. G., Palombo, A., De Toma, G., Bizzarri, M., & Cucina, A. (2013). Nicotine increases survival in human colon cancer cells treated with chemotherapeutic drugs. *Toxicology in vitro : an international journal published in association with BIBRA*, *27*(8), 2256–2263. https://doi.org/10.1016/j.tiv.2013.09.020.
- Dolan, J. W., Snyder, L. R., Blanc, T., & Van Heukelem, L. (2000). Selectivity differences for C18 and C8 reversed-phase columns as a function of temperature and

gradient steepness. I. Optimizing selectivity and resolution. *Journal of chromatography. A*, *897*(1-2), 37–50. https://doi.org/10.1016/s0021-9673(00)00851-7.

- Dong, Q, Hui Ling Yuan, Jia Jia Qian, Cai Yun Zhang, and Wei Dong Chen. (2018). Preparation and in Vitro-in Vivo Characterization of Trans-Resveratrol Nanosuspensions. *Bio-Medical Materials and Engineering,* 29 (3),333–45. https://doi.org/10.3233/BME-181729.
- Dong, Z., Cui, M. Y., Peng, Z., Li, Y., Wang, X., Fang, Z., Jiang, M., Xu, L., Luo, Y., Li, Z. P., & Feng, S. T. (2016). Nanoparticles for Colorectal Cancer Targeted Drug Delivery and MR Imaging: Current Situation and Perspectives. *Current cancer drug targets*, *16*(6), 536–550. https://doi.org/10.2174/1568009616666151130214442.
- Downs-Canner, S., Magge, D., Ravindranathan, R., O'Malley, M. E., Francis, L., Liu, Z., Sheng Guo, Z., Obermajer, N., & Bartlett, D. L. (2016). Complement Inhibition: A Novel Form of Immunotherapy for Colon Cancer. *Annals of surgical oncology*, *23*(2), 655–662. https://doi.org/10.1245/s10434-015-4778-7.
- Drago L. (2019). Probiotics and Colon Cancer. *Microorganisms*, *7*(3), 66. https://doi.org/10.3390/microorganisms7030066
- Dresselhaus, M. S., Dresselhaus, G., Charlier, J. C., & Hernández, E. (2004). Electronic, thermal and mechanical properties of carbon nanotubes. *Philosophical transactions. Series A, Mathematical, physical, and engineering sciences*, *362*(1823), 2065–2098. https://doi.org/10.1098/rsta.2004.1430.
- Eaden, J. A., Abrams, K. R., & Mayberry, J. F. (2001). The risk of colorectal cancer in ulcerative colitis: a meta-analysis. *Gut*, *48*(4), 526–535. https://doi.org/10.1136/gut.48.4.526.
- Eklund, P.C., Holden, & J.M., Jishi, R.A. (1995). Vibrational modes of carbon nanotubes; spectroscopy and theory. Carbon, 33, 959–972. https://doi.org/10.1016/0008-6223(95)00035-C.
- Ebbesen, T.W., & Ajayan, P.M. (1992). Large-scale synthesis of carbon nanotubes. Nature, 358,220.
- Entezar-Almahdi, E., Mohammadi-Samani, S., Tayebi, L., & Farjadian, F. (2020). Recent Advances in Designing 5-Fluorouracil Delivery Systems: A Stepping Stone in

the Safe Treatment of Colorectal Cancer. *International journal of nanomedicine*, *15*, 5445–5458. https://doi.org/10.2147/IJN.S257700

- Eren, O., Ucar, N., Onen, A ., Kızıldag, N., Vurur, O. F., Demirsoy, N., & Karacan. I. (2014). Effect of Amine-Functionalized Carbon Nanotubes on the Properties of CNT-PAN Composite Nanofibers. *International Journal of Chemical, Molecular, Nuclear, Materials and Metallurgical Engineering,* 8 (8), 726–28.
- Fadlallah, H., El Masri, J., Fakhereddine, H., Youssef, J., Chemaly, C., Doughan, S., & Abou-Kheir, W. (2024). Colorectal cancer: Recent advances in management and treatment. *World journal of clinical oncology*, *15*(9), 1136–1156. https://doi.org/10.5306/wjco.v15.i9.1136.
- Falahzadeh, K., Esmaeili, F., Nematollahi, L., Bayat, E., Khoobi, M., Mazloomi, M., Jalalvand, M., Majidi, R.F., & Negahdari, B., (2024). Oxaliplatin-Loaded Chitosan Nanoparticles Decorated with Cetuximab Single-Chain Variable Fragment for Human Colorectal Cancer Treatment. Cell Journal, 26(9), 530-542.
- Fabregas, J. C., Ramnaraign, B., & George, T. J. (2022). Clinical Updates for Colon Cancer Care in 2022. Clinical colorectal cancer, 21(3), 198–203. https://doi.org/10.1016/j.clcc.2022.05.006.
- Fan, Z., Shang, B. Y., Lu, Y., Chou, J. L., & Mendelsohn, J. (1997). Reciprocal changes in p27(Kip1) and p21(Cip1) in growth inhibition mediated by blockade or overstimulation of epidermal growth factor receptors. *Clinical cancer research : an official journal of the American Association for Cancer Research*, *3*(11), 1943–1948.
- Farani, R.M., Lak, M., C. Cho, W., Kang, H., Azarian, M., Yazdian, F., Sharareh H., Khoshmaram, K., Alipourfard, I., Hushmandi, K., Hwang, S. & Huh Y. (2024). Carbon nanomaterials: a promising avenue in colorectal cancer treatment. *Carbon Letters.* 34, 2035–2053 (2024). https://doi.org/10.1007/s42823-024-00805-2.
- Farjami, A., Siahi-Shadbad, M., Akbarzadehlaleh, P., Roshanzamir, K., & Molavi, O. (2019). Evaluation of the Physicochemical and Biological Stability of Cetuximab under Various Stress Condition. *Journal of pharmacy & pharmaceutical sciences: a publication of the Canadian Society for Pharmaceutical Sciences, Societe canadienne des sciences pharmaceutiques, 22*(1), 171–190. https://doi.org/10.18433/jpps30427.

- Fearon, E. R., & Vogelstein, B. (1990). A genetic model for colorectal tumorigenesis. Cell, 61(5), 759–767. https://doi.org/10.1016/0092-8674(90)90186-i.
- Ferri, V., Vicente, E., Quijano, Y., Duran, H., Diaz, E., Fabra, I., Malave, L., Agresott, R., Isernia, R., Cardinal-Fernandez, P., Ruiz, P., Nola, V., de Nobili, G., Ielpo, B., & Caruso, R. (2021). Right-side colectomy with complete mesocolic excision vs conventional right-side colectomy in the treatment of colon cancer: a systematic review and meta-analysis. *International journal of colorectal disease*, *36*(9), 1885–1904. https://doi.org/10.1007/s00384-021-03951-5.
- Firouzpour, H., Najafi, F., Mohammadgholi, A., Alizadegan, D., Beram, F. M., Akhtari, N., Zoghi, M., Ansar, N., Tavakkoli Yaraki, M., (2026). Nanoparticle-based drug delivery systems for effective cancer treatment: Mechanisms and applications. *Next Nanotechnology*, *9*, 100372. https://doi.org/10.1016/j.nxnano.2026.100372
- Figarol, A., Pourchez, J., Boudard, D., Forest, V., Tulliani, J.M., Lecompte, J.P., Cottier, M., Bernache-Assollant, D., & Grosseau, P. (2014). Biological response to purification and acid functionalization of carbon nanotubes. Journal of Nano Research, 16, 1–12.
- Fong, L., Hou, Y., Rivas, A., Benike, C., Yuen, A., Fisher, G. A., Davis, M. M., & Engleman, E. G. (2001). Altered peptide ligand vaccination with Flt3 ligand expanded dendritic cells for tumor immunotherapy. *Proceedings of the National Academy of Sciences of the United States of America*, *98*(15), 8809–8814. https://doi.org/10.1073/pnas.141226398.
- Fortina, P., Kricka, L. J., Graves, D. J., Park, J., Hyslop, T., Tam, F., Halas, N., Surrey, S., & Waldman, S. A. (2007). Applications of nanoparticles to diagnostics and therapeutics in colorectal cancer. *Trends in biotechnology*, *25*(4), 145–152. https://doi.org/10.1016/j.tibtech.2007.02.005.
- Freisling, H., Arnold, M., Soerjomataram, I., O'Doherty, M. G., Ordóñez-Mena, J. M., Bamia, C., Kampman, E., Leitzmann, M., Romieu, I., Kee, F., Tsilidis, K., Tjønneland, A., Trichopoulou, A., Boffetta, P., Benetou, V., Bueno-de-Mesquita, H. B. A., Huerta, J. M., Brenner, H., Wilsgaard, T., & Jenab, M. (2017). Comparison of general obesity and measures of body fat distribution in older adults in relation to cancer risk: meta-

analysis of individual participant data of seven prospective cohorts in Europe. *British journal of cancer*, *116*(11), 1486–1497. https://doi.org/10.1038/bjc.2017.106.

- Fukuhara, H., Ino, Y., & Todo, T. (2016). Oncolytic virus therapy: A new era of cancer treatment at dawn. *Cancer science*, *107*(10), 1373–1379. https://doi.org/10.1111/cas.13027 .
- Gmeiner W. H. (2024). Recent Advances in Therapeutic Strategies to Improve Colorectal Cancer Treatment. *Cancers*, *16*(5), 1029. https://doi.org/10.3390/cancers16051029.
- Fukuoka, N., Ishida, T., Ishii, K., Sato, A., Dagli, M. L. Z., Virgona, N., & Yano, T. (2023). Resveratrol can induce differentiating phenotypes in canine oral mucosal melanoma cells. *The Journal of veterinary medical science*, *85*(7), 721–726. https://doi.org/10.1292/jvms.22-0446 .
- Freitas, S. C., Sanderson, D., Caspani, S., Magalhães, R., Cortés-Llanos, B., Granja, A., Reis, S., Belo, J. H., Azevedo, J., Gómez-Gaviro, M. V., & Sousa, C. T. (2023). New Frontiers in Colorectal Cancer Treatment Combining Nanotechnology with Photo- and Radiotherapy. *Cancers*, *15*(2), 383. https://doi.org/10.3390/cancers15020383 .
- Gogoi, P., Kaur, G., & Singh, N. K. (2022). Nanotechnology for colorectal cancer detection and treatment. *World journal of gastroenterology*, *28*(46), 6497–6511. https://doi.org/10.3748/wjg.v28.i46.6497.
- Gadag, S., Narayan, R., Nayak, Y., & Nayak, U. Y. (2022). Bioanalytical RP-HPLC method validation for resveratrol and its application to pharmacokinetic and drug distribution studies. *Journal of Applied Pharmaceutical Science*, *12*(2), 158-164.
- Gajendran, M., Loganathan, P., Jimenez, G., Catinella, A. P., Ng, N., Umapathy, C., Ziade, N., & Hashash, J. G. (2019). A comprehensive review and update on ulcerative colitis. *Disease-a-month:DM*, *65*(12),100851. https://doi.org/10.1016/j.disamonth.2019.02.004.
- Gambini, J., Inglés, M., Olaso, G., Lopez-Grueso, R., Bonet-Costa, V., Gimeno-Mallench, L., Mas-Bargues, C., Abdelaziz, K. M., Gomez-Cabrera, M. C., Vina, J., & Borras, C. (2015). Properties of Resveratrol: In Vitro and In Vivo Studies about

Metabolism, Bioavailability, and Biological Effects in Animal Models and Humans. *Oxidative medicine and cellular longevity*, *2015*, 837042. https://doi.org/10.1155/2015/837042.

- Gao, S., Xu, B., Sun, J., & Zhang, Z. (2024). Nanotechnological advances in cancer: therapy a comprehensive review of carbon nanotube applications. *Frontiers in bioengineering and biotechnology*, *12*, 1351787. https://doi.org/10.3389/fbioe.2024.1351787.
- Gao, W., Zhang, W., Yu, H., Xing, W., Yang, X., Zhang, Y., & Liang, C. (2022). 3D CNT/MXene microspheres for combined photothermal/photodynamic/chemo for cancer treatment. *Frontiers in bioengineering and biotechnology*, *10*, 996177. https://doi.org/10.3389/fbioe.2022.996177 .
- Ge, M. H., Cao, J., Wang, J. Y., Huang, Y. Q., Lan, X. B., Yu, B., Wen, Q. L., & Cai, X. J. (2017). Nomograms predicting disease-specific regional recurrence and distant recurrence of papillary thyroid carcinoma following partial or total thyroidectomy. *Medicine*, *96*(30), e7575. https://doi.org/10.1097/MD.0000000000007575.
- Ge, L., Wang, Y. F., Tian, J. H., Mao, L., Zhang, J., Zhang, J. H., Shen, X. P., & Yang, K. H. (2016). Network meta-analysis of Chinese herb injections combined with FOLFOX chemotherapy in the treatment of advanced colorectal cancer. *Journal of clinical pharmacy and therapeutics*, *41*(4), 383–391. https://doi.org/10.1111/jcpt.12410.
- Geng, W., Guo, X., Zhang, L., Ma, Y., Wang, L., Liu, Z., Ji, H., & Xiong, Y. (2018). Resveratrol inhibits proliferation, migration and invasion of multiple myeloma cells via NEAT1-mediated Wnt/β-catenin signaling pathway. *Biomedicine & pharmacotherapy = Biomedecine & pharmacotherapie*, *107*, 484–494. https://doi.org/10.1016/j.biopha.2018.08.003.
- Gielecińska, A., Kciuk, M., Mujwar, S., Celik, I., Kołat, D., Kałuzińska-Kołat, Ż., & Kontek, R. (2023). Substances of Natural Origin in Medicine: Plants vs. Cancer. *Cells*, *12*(7), 986. https://doi.org/10.3390/cells12070986.

- Ginghină, O., Hudiță, A., Zaharia, C., Tsatsakis, A., Mezhuev, Y., Costache, M., & Gălățeanu, B. (2021). Current Landscape in Organic Nanosized Materials Advances for Improved Management of Colorectal Cancer Patients. *Materials (Basel, Switzerland)*, *14*(9), 2440. https://doi.org/10.3390/ma14092440.
- Goku, P.E., Orman, E., Quartey, A.N.K., Adu, J.K., & Adosraku, R.K. (2020). A simple RP-HPLC method to simultaneously assay the contents of lamivudine, tenofovir, and nevirapine in fixed dose combined oral antiviral medicines. *Journal of Chemistry*. 4618360,1–9, https://doi.org/10.1155/2020/4618360.
- Goldstein, N. I., Prewett, M., Zuklys, K., Rockwell, P., & Mendelsohn, J. (1995). Biological efficacy of a chimeric antibody to the epidermal growth factor receptor in a human tumor xenograft model. *Clinical cancer research: an official journal of the American Association for Cancer Research*, *1*(11), 1311–1318.
- Goldstein, D.A., Chen, Q., & Ayer, T. (2017). Bevacizumab for metastatic colorectal cancer: a global cost–effectiveness analysis. Oncologist. 2, 22, 694–699.doi:10.1634/theoncologist.2016-0455.
- Gong, H., Peng, R., & Liu, Z. (2013). Carbon nanotubes for biomedical imaging: the recent advances. *Advanced drug delivery reviews*, *65*(15), 1951–1963. https://doi.org/10.1016/j.addr.2013.10.002
- Green, J., Czanner, G., Reeves, G., Watson, J., Wise, L., Roddam, A., & Beral, V. (2012). Menopausal hormone therapy and risk of gastrointestinal cancer: nested case-control study within a prospective cohort, and meta-analysis. *International journal of cancer*, *130*(10), 2387–2396. https://doi.org/10.1002/ijc.26236 .
- Guan, X., Zhao, Z., Yang, M., Chen, H., Chen, W., Liu, Z., Jiang, Z., Chen, Y., Wang, G., & Wang, X. (2017). Whether partial colectomy is oncologically safe for patients with transverse colon cancer: a large population-based study. *Oncotarget*, *8*(54), 93236–93244. https://doi.org/10.18632/oncotarget.21275.
- Güller, U., Zettl, A., Worni, M., Langer, I., Cabalzar-Wondberg, D., Viehl, C. T., Demartines, N., & Zuber, M. (2012). Molecular investigation of lymph nodes in colon cancer patients using one-step nucleic acid amplification (OSNA): a new road to better staging?. *Cancer*, *118*(24), 6039–6045. https://doi.org/10.1002/cncr.27667 .

- Gurdal, H., Tuglu, M. M., Bostanabad, S. Y., & Dalkiliç, B. (2019). Partial agonistic effect of cetuximab on epidermal growth factor receptor and Src kinase activation in triple-negative breast cancer cell lines. *International journal of oncology*, *54*(4), 1345–1356. https://doi.org/10.3892/ijo.2019.4697.
- Harish, V., Almalki, W. H., Alshehri, A., Alzahrani, A., Alzarea, S. I., Kazmi, I., Gulati, M., Tewari, D., Chellappan, D. K., Gupta, G., Dua, K., & Singh, S. K. (2022). Bioanalytical Method Development, Validation and Stability Assessment of Xanthohumol in Rat Plasma. *Molecules (Basel, Switzerland)*, *27*(20), 7117. https://doi.org/10.3390/molecules27207117.
- Ha, E. S., Park, H., Lee, S. K., Sim, W. Y., Jeong, J. S., Baek, I. H., & Kim, M. S. (2020). Pure *Trans*-Resveratrol Nanoparticles Prepared by A Supercritical Antisolvent Process Using Alcohol and Dichloromethane Mixtures: Effect of Particle Size on Dissolution and Bioavailability in Rats. *Antioxidants (Basel, Switzerland)*, *9*(4), 342. https://doi.org/10.3390/antiox9040342.
- He, M., Zhang, S., & Zhang, J. (2020). Horizontal Single-Walled Carbon Nanotube Arrays: Controlled Synthesis, Characterizations, and Applications. *Chemical reviews*, *120*(22), 12592–12684. https://doi.org/10.1021/acs.chemrev.0c00395.
- Hiller, J. G., Perry, N. J., Poulogiannis, G., Riedel, B., & Sloan, E. K. (2018). Perioperative events influence cancer recurrence risk after surgery. *Nature reviews. Clinical oncology*, *15*(4), 205–218. https://doi.org/10.1038/nrclinonc.2017.194.
- Hirsch A. (2002). Functionalization of single-walled carbon nanotubes. *Angewandte Chemie (International ed. in English)*, *41*(11), 1853–1859. https://doi.org/10.1002/1521-3773(20020603)41:11<1853::aid-anie1853>3.0.co;2-n .
- Hossain, M. S., Karuniawati, H., Jairoun, A. A., Urbi, Z., Ooi, J., John, A., Lim, Y. C., Kibria, K. M. K., Mohiuddin, A. K. M., Ming, L. C., Goh, K. W., & Hadi, M. A. (2022). Colorectal Cancer: A Review of Carcinogenesis, Global Epidemiology, Current Challenges, Risk Factors, Preventive and Treatment Strategies. *Cancers*, *14*(7), 1732. https://doi.org/10.3390/cancers14071732.
- Hossain M.S., & Urbi, Z. (2016). Effect of Naphthalene Acetic Acid on the Adventitious Rooting in Shoot Cuttings ofAndrographis paniculata(Burm.f.) Wall. ex

Nees: An Important Therapeutical Herb. *International Journal of Agronomy,* 1617543. https://doi.org/10.1155/2016/1617543.

- Hossain, M. S., Urbi, Z., Sule, A., & Hafizur Rahman, K. M. (2014). Andrographis paniculata (Burm. f.) Wall. ex Nees: a review of ethnobotany, phytochemistry, and pharmacology. *TheScientificWorldJournal*, *2014*, 274905. https://doi.org/10.1155/2014/274905.
- Hossain M.S., Urbi Z., & Phang I.C. (2021). Auxin increased adventitious root development in the medicinal plant Andrographis paniculata (Burm. f.) Wall. ex Nees. Agronomy Journal, 113,3222–3231. https://doi.org/10.1002/agj2.20745
- Honari, M., Shafabakhsh, R., Reiter, R. J., Mirzaei, H., & Asemi, Z. (2019). Resveratrol is a promising agent for colorectal cancer prevention and treatment: focus on molecular mechanisms. *Cancer cell international*, 19, 180. https://doi.org/10.1186/s12935-019-0906-y.
- Howlader, N., A. M. Noone, M. Krapcho (2009). Eds., SEER Cancer Statistics Review, 1975–2009, National Cancer Institute, Bethesda, Md, USA, 2012, http://seer.cancer.gov/csr/1975 2009 pops09/.
- Hu, Z., Ott, P. A., & Wu, C. J. (2018). Towards personalized, tumour-specific, therapeutic vaccines for cancer. *Nature reviews. Immunology*, *18*(3), 168–182. https://doi.org/10.1038/nri.2017.131
- Huang, L., Zhang, S., Zhou, J., & Li, X. (2019). Effect of resveratrol on drug resistance in colon cancer chemotherapy. *RSC advances*, *9*(5), 2572–2580. https://doi.org/10.1039/c8ra08364a.
- Huyghe, N., Baldin, P., & Van den Eynde, M. (2020). Immunotherapy with immune checkpoint inhibitors in colorectal cancer: what is the future beyond deficient mismatch-repair tumours?. *Gastroenterology report*, *8*(1), 11–24. https://doi.org/10.1093/gastro/goz061.
- Hynes R. O. (2002). Integrins: bidirectional, allosteric signaling machines. *Cell*, *110*(6), 673–687. https://doi.org/10.1016/s0092-8674(02)00971-6.
- https://www.who.int/news-room/fact-sheets/detail/colorectal-cancera 2023.

- Iannone, A., Losurdo, G., Pricci, M., Girardi, B., Massaro, A., Principi, M., Barone, M., Ierardi, E., & Di Leo, A. (2016). Stool Investigations for Colorectal Cancer Screening: From Occult Blood Test to DNA Analysis. *Journal of gastrointestinal cancer*, *47*(2), 143–151. https://doi.org/10.1007/s12029-016-9810-z.
- Ishigami, M., Cumings, J., Zettl, A., & Chen, S. (2000). A simple method for the continuous production of carbon nanotubes, *Chemical Physics Letters*, 319,457–459. https://doi.org/10.1016/S0009-2614(00)00151-2.
- Itkis, M. E., Perea, D. E., Jung, R., Niyogi, S., & Haddon, R. C. (2005). Comparison of analytical techniques for purity evaluation of single-walled carbon nanotubes. *Journal of the American Chemical Society*, *127*(10), 3439–3448. https://doi.org/10.1021/ja043061w.
- Ijaz, H., Mahmood, A., Abdel-Daim,M.M., Sarfraz, R. M., Zaman, M., Zafar, N., Alshehery, S., Salem-Bekhit, M.M., Ali, M.A., Eltayeb, L.B., Benguerba, Y. (2023). Review on carbon nanotubes (CNTs) and their chemical and physical characteristics, with particular emphasis on potential applications in biomedicine. *Inorganic Chemistry Communications*, 111020. https://doi.org/10.1016/j.inoche.2023.111020.
- Jain, A. K., Kumar Mehra, N., Lodhi, N., Dubey, V., Mishra, D. K., Jain, P. K., & Jain, N. K. (2007). Carbon nanotubes and their toxicity. *Nanotoxicology*, *1*(3), 167–197. https://doi.org/10.1080/17435390701639688.
- Jain, N. K., Tare, M. S., Mishra, V., & Tripathi, P. K. (2015). The development, characterization and in vivo anti-ovarian cancer activity of poly(propylene imine) (PPI)-antibody conjugates containing encapsulated paclitaxel. *Nanomedicine : nanotechnology, biology, and medicine*, *11*(1), 207–218. https://doi.org/10.1016/j.nano.2014.09.006.
- Jawahar, N., De, A., Jubee, S., & Reddy, E. S. (2020). Folic acid-conjugated raloxifene hydrochloride carbon nanotube for targeting breast cancer cells. *Drug development research*, *81*(3), 305–314. https://doi.org/10.1002/ddr.21620.
- Jin, H., Gao, S., Song, D., Liu, Y., & Chen, X. (2021). Intratumorally CpG immunotherapy with carbon nanotubes inhibits local tumor growth and liver metastasis

by suppressing the epithelial-mesenchymal transition of colon cancer cells. *Anti-cancer drugs*, *32*(3), 278–285. https://doi.org/10.1097/CAD.0000000000001000.

- Jones, H. J. S., Al-Najami, I., Baatrup, G., & Cunningham, C. (2021). Local excision after polypectomy for rectal polyp cancer: when is it worthwhile?. *Colorectal disease : the official journal of the Association of Coloproctology of Great Britain and Ireland*, *23*(4), 868–874. https://doi.org/10.1111/codi.15480.
- Johns, L. E., & Houlston, R. S. (2001). A systematic review and meta-analysis of familial colorectal cancer risk. *The American journal of gastroenterology*, *96*(10), 2992–3003. https://doi.org/10.1111/j.1572-0241.2001.04677.x .
- Journet, C., & Bernier, P., (1998). Production of carbon nanotubes. Applied Physics A: Materials Science and Processing, 67,1–9.
- Jorio, A., Pimenta, M.A., Souza Filho, A.G., Saito, R., Dresselhaus, G., & Dresselhaus, M.S. (2003). Characterizing carbon nanotube samples with resonance Raman scattering, New Journal of Physics, 5,139.
- Jose, J., & Charyulu, R. N. (2016). Prolonged drug delivery system of an antifungal drug by association with polyamidoamine dendrimers. *International journal of pharmaceutical investigation*, *6*(2), 123–127. https://doi.org/10.4103/2230-973X.177833.
- Jose, S., Anju, S. S., Cinu, T. A., Aleykutty, N. A., Thomas, S., & Souto, E. B. (2014). In vivo pharmacokinetics and biodistribution of resveratrol-loaded solid lipid nanoparticles for brain delivery. *International journal of pharmaceutics*, *474*(1-2), 6–13. https://doi.org/10.1016/j.ijpharm.2014.08.003.
- Kamal, R., Awasthi, A., Paul, P., Mir, M. S., Singh, S. K., & Dua, K. (2024). Novel drug delivery systems in colorectal cancer: Advances and future prospects. *Pathology, research and practice*, *262*, 155546. https://doi.org/10.1016/j.prp.2024.155546.
- Kang, M. S., Lee, H., Jeong, S. J., Eom, T. J., Kim, J., & Han, D. W. (2022). State of the Art in Carbon Nanomaterials for Photoacoustic Imaging. *Biomedicines*, *10*(6), 1374. https://doi.org/10.3390/biomedicines10061374.
- Karkon-Shayan, S., Aliashrafzadeh, H., Dianat-Moghadam, H., Rastegar-Pouyani, N., Majidi, M., Zarei, M., Moradi-Vastegani, S., Bahramvand, Y., Babaniamansour, S., &

Jafarzadeh, E. (2023). Resveratrol as an antitumor agent for glioblastoma multiforme: Targeting resistance and promoting apoptotic cell deaths. *Acta histochemica*, *125*(6), 152058. https://doi.org/10.1016/j.acthis.2023.152058.

- Kaushik, B.K., & Majumder, M.K. (2015). Carbon Nanotube: Properties and Applications, 86 57.
- Sinnott, S. B., & Andrews, R. (2001). Carbon Nanotubes: Synthesis, Properties, and Applications. *Critical Reviews in Solid State and Materials Sciences*, *26*(3), 145–249. https://doi.org/10.1080/20014091104189.
- Kesharwani, P., Mishra, V., & Jain, N. K. (2015). Validating the anticancer potential of carbon nanotube-based therapeutics through cell line testing. *Drug discovery today*, *20*(9), 1049–1060. https://doi.org/10.1016/j.drudis.2015.05.004.
- Keum, N., & Giovannucci, E. (2019). Global burden of colorectal cancer: emerging trends, risk factors and prevention strategies. *Nature reviews. Gastroenterology & hepatology*, *16*(12), 713–732. https://doi.org/10.1038/s41575-019-0189-8 .
- Khabashesku, V.N., Peng, H., Billups, W.E., Ying, Y., Margrave, J.L. (2006). William Marsh Rice University, 1–26.
- Khani, H., & Moradi, O. (2013). Influence of surface oxidation on the morphological and crystallographic structure of multi-walled carbon nanotubes via different oxidants. *Journal Of Nanostructure in Chemistry*, 3,73
- Kowalska, M., Woźniak, M., Kijek, M., Mitrosz, P., Szakiel, J., & Turek, P. (2022). Management of validation of HPLC method for determination of acetylsalicylic acid impurities in a new pharmaceutical product. *Scientific reports*, *12*(1), 1. https://doi.org/10.1038/s41598-021-99269-x.
- Khursheed, R., Wadhwa, S., Kumar, B., Gulati, M., Gupta, S., Chaitanya, M. V. N. L., Kumar, D., Jha, N.K., Gupta, G., Prasher, P., Chellappan, D.K. & Singh, S. K. (2022). Development and validation of RP-HPLC based bioanalytical method for simultaneous estimation of curcumin and quercetin in rat's plasma. *South African Journal of Botany*, *149*, 870-877.

- Kim, E. S., Khuri, F. R., & Herbst, R. S. (2001). Epidermal growth factor receptor biology (IMC-C225). *Current opinion in oncology*, *13*(6), 506–513. https://doi.org/10.1097/00001622-200111000-00014.
- Kim, J.H., & Min, B.G. (2010). Functionalization of multi-walled carbon nanotube by treatment with dry ozone gas for the enhanced dispersion and adhesion in polymeric composites. *Carbon Letter,* 11, 298-303.
- Kimura, Y., Sumiyoshi, M., & Baba, K. (2008). Antitumor activities of synthetic and natural stilbenes through antiangiogenic action. *Cancer science*, *99*(10), 2083–2096. https://doi.org/10.1111/j.1349-7006.2008.00948.x .
- Kumar, R., Kumar, R., Khursheed, R., Awasthi, A., Ramanunny, A. K., Kaur, J., Khurana, N., Singh, S. K., Khurana, S., Pandey, N. K., Kapoor, B., & Sharma, N. (2020). Validated Reverse Phase-High-Performance Liquid Chromatography Method for Estimation of Fisetin in Self-Nanoemulsifying Drug Delivery System. *Assay and drug development technologies*, *18*(6), 274–281. https://doi.org/10.1089/adt.2020.983.
- Kumar, A., Gautam, V., Sandhu, A., Rawat, K., Sharma, A., & Saha, L. (2023). Current and emerging therapeutic approaches for colorectal cancer: A comprehensive review. World journal of gastrointestinal surgery, 15(4), 495–519. https://doi.org/10.4240/wjgs.v15.i4.495.
- Kumar, S., Ansari, A., Basu, M., Ghosh, S., Begam, S. and Ghosh, M.K. (2025) Carbon Nanotubes in Cancer Diagnosis and Treatment: Current Trends and Future Perspectives. *Advanced Therapeutics*, 8.
- https://doi.org/10.1002/adtp.202400283
- Kumar, A., Kurmi, B. D., Singh, A., & Singh, D. (2022). Potential role of resveratrol and its nano-formulation as anti-cancer agent. *Exploration of targeted anti-tumor therapy*, *3*(5), 643–658. https://doi.org/10.37349/etat.2022.00105.
- Kumari, A., Yadav, S. K., & Yadav, S. C. (2010). Biodegradable polymeric nanoparticles based drug delivery systems. *Colloids and surfaces. B, Biointerfaces*, *75*(1), 1–18. https://doi.org/10.1016/j.colsurfb.2009.09.001.
- Kurai, J., Chikumi, H., Hashimoto, K., Yamaguchi, K., Yamasaki, A., Sako, T., Touge, H., Makino, H., Takata, M., Miyata, M., Nakamoto, M., Burioka, N., & Shimizu, E.

(2007). Antibody-dependent cellular cytotoxicity mediated by cetuximab against lung cancer cell lines. *Clinical cancer research : an official journal of the American Association for Cancer Research*, *13*(5), 1552–1561. https://doi.org/10.1158/1078-0432.CCR-06-1726.

- Lee, S. C., Srivastava, R. M., López-Albaitero, A., Ferrone, S., & Ferris, R. L. (2011). Natural killer (NK): dendritic cell (DC) cross talk induced by therapeutic monoclonal antibody triggers tumor antigen-specific T cell immunity. *Immunologic research*, *50*(2-3), 248–254. https://doi.org/10.1007/s12026-011-8231-0.
- Labianca, R., & Merelli, B. (2010). Screening and diagnosis for colorectal cancer: present and future. *Tumori*, *96*(6), 889–901.
- Lacerda, L., Ali-Boucetta, H., Herrero, M. A., Pastorin, G., Bianco, A., Prato, M., & Kostarelos, K. (2008). Tissue histology and physiology following intravenous administration of different types of functionalized multiwalled carbon nanotubes. *Nanomedicine (London, England)*, *3*(2), 149–161. https://doi.org/10.2217/17435889.3.2.149.
- Lacerda, L., Bianco, A., Prato, M., & Kostarelos, K. (2006). Carbon nanotubes as nanomedicines: from toxicology to pharmacology. *Advanced drug delivery reviews*, *58*(14), 1460–1470. https://doi.org/10.1016/j.addr.2006.09.015 .
- Lanç, A., Delmas, D., Osman, H., Thénot, J. P., Jannin, B., & Latruffe, N. (2005). Human hepatic cell uptake of resveratrol: involvement of both passive diffusion and carrier-mediated process. *Biochemical and biophysical research communications*, *316*(4), 1132–1137. https://doi.org/10.1016/j.bbrc.2004.02.164.
- Laroui, H., Rakhya, P., Xiao, B., Viennois, E., & Merlin, D. (2013). Nanotechnology in diagnostics and therapeutics for gastrointestinal disorders. *Digestive and liver disease : official journal of the Italian Society of Gastroenterology and the Italian Association for the Study of the Liver*, *45*(12), 995–1002. https://doi.org/10.1016/j.dld.2013.03.019.
- Levin, B., Lieberman, D. A., McFarland, B., Andrews, K. S., Brooks, D., Bond, J., Dash, C., Giardiello, F. M., Glick, S., Johnson, D., Johnson, C. D., Levin, T. R., Pickhardt, P. J., Rex, D. K., Smith, R. A., Thorson, A., Winawer, S. J., American Cancer

Society Colorectal Cancer Advisory Group, US Multi-Society Task Force, & American College of Radiology Colon Cancer Committee (2008). Screening and surveillance for the early detection of colorectal cancer and adenomatous polyps, 2008: a joint guideline from the American Cancer Society, the US Multi-Society Task Force on Colorectal Cancer, and the American College of Radiology. *Gastroenterology*, *134*(5), 1570–1595. https://doi.org/10.1053/j.gastro.2008.02.002'

- Lee, K. M., Li, L., & Dai, L. (2005). Asymmetric end-functionalization of multi-walled carbon nanotubes. *Journal of the American Chemical Society*, *127*(12), 4122–4123. https://doi.org/10.1021/ja0423670 .
- Lee, J. Y., Kim, J. S., An, K. H., Lee, K., Kim, D. Y., Bae, D. J., & Lee, Y. H. (2005). Electrophoretic and dynamic light scattering in evaluating dispersion and size distribution of single-walled carbon nanotubes. *Journal of nanoscience and nanotechnology*, *5*(7), 1045–1049. https://doi.org/10.1166/jnn.2005.160.
- Lécuyer, T., Teston, E., Ramirez-Garcia, G., Maldiney, T., Viana, B., Seguin, J., Mignet, N., Scherman, D., & Richard, C. (2016). Chemically engineered persistent luminescence nanoprobes for bioimaging. *Theranostics*, *6*(13), 2488–2524. https://doi.org/10.7150/thno.16589.
- Liang, Y. C., Huang, Y. T., Tsai, S. H., Lin-Shiau, S. Y., Chen, C. F., & Lin, J. K. (1999). Suppression of inducible cyclooxygenase and inducible nitric oxide synthase by apigenin and related flavonoids in mouse macrophages. *Carcinogenesis*, *20*(10), 1945–1952. https://doi.org/10.1093/carcin/20.10.1945 .
- Liu, J., & Guo, B. (2020). RNA-based therapeutics for colorectal cancer: Updates and future directions. *Pharmacological research*, *152*, 104550. https://doi.org/10.1016/j.phrs.2019.104550.
- Liu, J., Lécuyer, T., Seguin, J., Mignet, N., Scherman, D., Viana, B., & Richard, C. (2019). Imaging and therapeutic applications of persistent luminescence nanomaterials. *Advanced drug delivery reviews*, *138*, 193–210. https://doi.org/10.1016/j.addr.2018.10.015.
- Li, Q., Geng, S., Luo, H., Wang, W., Mo, Y. Q., Luo, Q., Wang, L., Song, G. B., Sheng, J. P., & Xu, B. (2024). Signaling pathways involved in colorectal cancer: pathogenesis

and targeted therapy. *Signal transduction and targeted therapy*, *9*(1), 266. https://doi.org/10.1038/s41392-024-01953-7 .

- Li, F., Lin, Y., Li, R., Shen, X., Xiang, M., Xiong, G., Zhang, K., Xia, T., Guo, J., Miao, Z., Liao, Y., Zhang, X., & Xie, L. (2023). Molecular targeted therapy for metastatic colorectal cancer: current and evolving approaches. *Frontiers in pharmacology*, *14*, 1165666. https://doi.org/10.3389/fphar.2023.1165666.
- Li, Y.., Mann, D., Rolandi, M., Kim, W., Ural, A., Hung, S., Javey, A., Cao, J., Wang, D., Yenilmez, E., & Wang, Q. (2004). Preferential growth of semiconducting single-walled carbon nanotubes by a plasma enhanced CVD method. Nano Letters, 4, 317–321.
- Lynch, H. T., & de la Chapelle, A. (2003). Hereditary colorectal cancer. *The New England journal of medicine*, *348*(10), 919–932. https://doi.org/10.1056/NEJMra012242.
- Ma, J., Wang, G., Ding, X., Wang, F., Zhu, C., & Rong, Y. (2023). Carbon-Based Nanomaterials as Drug Delivery Agents for Colorectal Cancer: Clinical Preface to Colorectal Cancer Citing Their Markers and Existing Theranostic Approaches. *ACS omega*, *8*(12), 10656–10668. https://doi.org/10.1021/acsomega.2c06242.
- Mamalis, A.G., Vogtlander, L.O.G., & Markopoulos, A. (2004). Nanotechnology and nanostructured materials: trends in carbon nanotubes, Precision Engineering, 28,16–30.
- Mallakpour, S., & Soltanian, S. (2016). Surface functionalization of carbon nanotubes: fabrication and applications, RSC Advances. 6,109916–109935.
- Malki, A., ElRuz, R. A., Gupta, I., Allouch, A., Vranic, S., & Al Moustafa, A. E. (2020). Molecular Mechanisms of Colon Cancer Progression and Metastasis: Recent Insights and Advancements. *International journal of molecular sciences*, *22*(1), 130. https://doi.org/10.3390/ijms22010130 .
- Marsh, P. J., James, R. D., & Schofield, P. F. (1995). Definition of local recurrence after surgery for rectal carcinoma. *The British journal of surgery*, *82*(4), 465–468. https://doi.org/10.1002/bjs.1800820412 .

- Matos, A. I., Carreira, B., Peres, C., Moura, L. I. F., Conniot, J., Fourniols, T., Scomparin, A., Martínez-Barriocanal, Á., Arango, D., Conde, J. P., Préat, V., Satchi-Fainaro, R., & Florindo, H. F. (2019). Nanotechnology is an important strategy for combinational innovative chemo-immunotherapies against colorectal cancer. *Journal of controlled release : official journal of the Controlled Release Society*, *307*, 108–138. https://doi.org/10.1016/j.jconrel.2019.06.017.
- Matsuda, T., Yamashita, K., Hasegawa, H., Utsumi, M., & Kakeji, Y. (2020). Current status and trend of laparoscopic right hemicolectomy for colon cancer. *Annals of gastroenterological surgery*, *4*(5), 521–527. https://doi.org/10.1002/ags3.12373.
- Moutabian, H., Majdaeen, M., Ghahramani-Asl, R., Yadollahi, M., Gharepapagh, E., Ataei, G., Falahatpour, Z., Bagheri, H., & Farhood, B. (2022). A systematic review of the therapeutic effects of resveratrol in combination with 5-fluorouracil during colorectal cancer treatment: with a special focus on the oxidant, apoptotic, and anti-inflammatory activities. *Cancer cell international*, *22*(1), 142. https://doi.org/10.1186/s12935-022-02561-7.
- Mello, M. R. S. P., Moura, S. F., Muzi, C. D., & GuimarÃes, R. M. (2020). Clinical Evaluation and Pattern of Symptoms in Colorectal Cancer Patients. *Arquivos de gastroenterologia*, *57*(2), 131–136. https://doi.org/10.1590/s0004-2803.202000000-24.
- Meenakshi, D. U., Narde, G. K., Khan, S. A., & Ahuja, A. (2026). Formulation, Characterization, and In Vitro Biological Evaluation of a Triple-Phytochemical Nano Delivery System for Colon Cancer Therapy—A Preliminary Feasibility Study. *Pharmaceutics*, *18*(2), 277. https://doi.org/10.3390/pharmaceutics18020277
- Mendelsohn J. (2001). The epidermal growth factor receptor as a target for cancer therapy. *Endocrine-related cancer*, *8*(1), 3–9. https://doi.org/10.1677/erc.0.0080003.
- Mendelsohn, J., & Baselga, J. (2003). Status of epidermal growth factor receptor antagonists in the biology and treatment of cancer. *Journal of clinical oncology : official journal of the American Society of Clinical Oncology*, *21*(14), 2787–2799. https://doi.org/10.1200/JCO.2003.01.504.

- Messersmith W. A. (2019). NCCN Guidelines Updates: Management of Metastatic Colorectal Cancer. *Journal of the National Comprehensive Cancer Network : JNCCN*, *17*(5.5), 599–601. https://doi.org/10.6004/jnccn.2019.5014
- Mishra, L., Bhowmik, S., Singh, R., Patel, P., Gupta, G. D., & Kurmi, B. D. (2023). Quality by design-assisted development of D-α-tocopherol polyethylene glycol 1000 succinate-incorporated gefitinib-loaded cationic liposome(s). *Therapeutic delivery*, *14*(12), 745–761. https://doi.org/10.4155/tde-2023-0075.
- Moghaddam, M.J., Taylor, S., Gao, M., Huang, S., Dai, L., & McCall, M.J. (2004). Highly efficient binding of DNA on the sidewalls and tips of carbon nanotubes using photochemistry. *Nano Letters*, 4, 89–93.
- Montalesi, E., Cracco, P., Acconcia, F., Fiocchetti, M., Iucci, G., Battocchio, C., Orlandini, E., Ciccone, L., Nencetti, S., Muzzi, M., Moreno, S., Venditti, I., & Marino, M. (2023). Resveratrol Analogs and Prodrugs Differently Affect the Survival of Breast Cancer Cells Impairing Estrogen/Estrogen Receptor α/Neuroglobin Pathway. *International journal of molecular sciences*, *24*(3), 2148. https://doi.org/10.3390/ijms24032148
- Moradi-Marjaneh, R., Paseban, M., & Moradi Marjaneh, M. (2019). Hsp70 inhibitors: Implications for the treatment of colorectal cancer. *IUBMB life*, *71*(12), 1834–1845. https://doi.org/10.1002/iub.2157.
- Mutsaers, A. J., Francia, G., Man, S., Lee, C. R., Ebos, J. M., Wu, Y., Witte, L., Berry, S., Moore, M., & Kerbel, R. S. (2009). Dose-dependent increases in circulating TGF-alpha and other EGFR ligands act as pharmacodynamic markers for optimal biological dosing of cetuximab and are tumor independent. *Clinical cancer research : an official journal of the American Association for Cancer Research*, *15*(7), 2397–2405. https://doi.org/10.1158/1078-0432.CCR-08-1627.
- Naief, M.F., Mohammed, S.M., Mayouf, H.J., Mohammed, A.M. (2023). A review of the role of carbon nanotubes for cancer treatment based on photothermal and photodynamic therapy techniques. *Journal of Organometallic Chemistry*, 122819.
- Naik, S. S., Lee, S. J., Theerthagiri, J., Yu, Y., & Choi, M. Y. (2021). Rapid and highly selective electrochemical sensor based on ZnS/Au-decorated f-multi-walled carbon

nanotube nanocomposites produced via pulsed laser technique for detection of toxic nitro compounds. *Journal of hazardous materials*, *418*, 126269. https://doi.org/10.1016/j.jhazmat.2021.126269.

- Namdeo, J., Shah, M.D., Karthik, N., S. Pramod, N., & Bhatia, N.M. (2007). Methods of carbon nanotube and nanohorn synthesis: a review, RGO Journal, 5.
- Nguyen, H. T., & Duong, H. Q. (2018). The molecular characteristics of colorectal cancer: Implications for diagnosis and therapy. *Oncology letters*, *16*(1), 9–18. https://doi.org/10.3892/ol.2018.8679.
- Nguyen, H. T., & Duong, H. Q. (2018). The molecular characteristics of colorectal cancer: Implications for diagnosis and therapy. *Oncology letters*, *16*(1), 9–18. https://doi.org/10.3892/ol.2018.8679
- Nicholson, R. I., Gee, J. M., & Harper, M. E. (2001). EGFR and cancer prognosis. *European journal of cancer (Oxford, England : 1990)*, *37 Suppl 4*, S9–S15. https://doi.org/10.1016/s0959-8049(01)00231-3.
- Norizan, M. N., Moklis, M. H., Ngah Demon, S. Z., Halim, N. A., Samsuri, A., Mohamad, I. S., Knight, V. F., & Abdullah, N. (2020). Carbon nanotubes: functionalisation and their application in chemical sensors. *RSC advances*, *10*(71), 43704–43732. https://doi.org/10.1039/d0ra09438b.
- Oh, S., Hyon, C., Sull, S., Hwang, S., and Park, Y. (2003). Detection and volume estimation of semiconductor quantum dots from atomic force microscope images, *Review of Scientific Instrument*. 74,4687–4695. https://doi.org/10.1063/1.1618015.
- Orallo, F. (2006). Comparative studies of the antioxidant effects of cis- and trans-resveratrol. *Current medicinal chemistry*, *13*(1), 87–98. 10.2174/092986706775197962
- Ordóñez-Mena, J. M., Walter, V., Schöttker, B., Jenab, M., O'Doherty, M. G., Kee, F., Bueno-de-Mesquita, B., Peeters, P. H. M., Stricker, B. H., Ruiter, R., Hofman, A., Söderberg, S., Jousilahti, P., Kuulasmaa, K., Freedman, N. D., Wilsgaard, T., Wolk, A., Nilsson, L. M., Tjønneland, A., & Quirós, J. R., Consortium on Health and Ageing: Network of Cohorts in Europe and the United States (CHANCES) (2018). Impact of prediagnostic smoking and smoking cessation on colorectal cancer prognosis: a meta-

analysis of individual patient data from cohorts within the CHANCES consortium. *Annals of oncology : official journal of the European Society for Medical Oncology*, *29*(2), 472–483. https://doi.org/10.1093/annonc/mdx761.

- Orsini, G., Legitimo, A., Failli, A., Ferrari, P., Nicolini, A., Spisni, R., Miccoli, P., & Consolini, R. (2013). Defective generation and maturation of dendritic cells from monocytes in colorectal cancer patients during the course of disease. International journal of molecular sciences, 14(11), 22022–22041. https://doi.org/10.3390/ijms141122022 .
- Paloniemi, H., Aäritalo, T., Laiho, T., Liuke, H., Kocharova, N., Haapakka, K., Terzi, F., Seeber, R., & Lukkari, J. (2005). Water-soluble full-length single-wall carbon nanotube polyelectrolytes: preparation and characterization. *The journal of physical chemistry. B*, *109*(18), 8634–8642. https://doi.org/10.1021/jp0443097.
- Park, S. M., Hwang, C. Y., Cho, S. H., Lee, D., Gong, J. R., Lee, S., Nam, S., & Cho, K. H. (2019). Systems analysis identifies potential target genes to overcome cetuximab resistance in colorectal cancer cells. *The FEBS journal*, *286*(7), 1305–1318. https://doi.org/10.1111/febs.14773 .
- Parveen, S, Rana, S., Fangueiroa, R., & Paiv, M.C. (2017). Characterizing dispersion and long term stability of concentrated carbon nanotube aqueous suspensions for fabricating ductile cementitious composites. *Powder Technology,* 307,1–9, https://doi.org/10.1016/j.powtec.2016.11.010.
- Peate, I., (2018). Anatomy and physiology, The gastrointestinal system. *British Journal of Healthcare Assistants*, *12*(3), 110-114.
- Pentek, T., Newenhouse, E., O'Brien, B., & Chauhan, A. S. (2017). Development of a Topical Resveratrol Formulation for Commercial Applications Using Dendrimer Nanotechnology. *Molecules (Basel, Switzerland)*, *22*(1), 137. https://doi.org/10.3390/molecules22010137.
- Patel, K.Y., Dedania, Z.R., Dedania, R.R. & Patel, U. (2021). QbD approach to HPLC method development and validation of ceftriaxone sodium. *Future Journal of Pharmaceutical Sciences,*7, 141 https://doi.org/10.1186/s43094-021-00286-4

- Patel, K. R., Scott, E., Brown, V. A., Gescher, A. J., Steward, W. P., & Brown, K. (2011). Clinical trials of resveratrol. *Annals of the New York Academy of Sciences*, *1215*, 161–169. https://doi.org/10.1111/j.1749-6632.2010.05853.x.
- Maurya, P.K., & Mani. A. (2024). Current Perspective and Treatment Strategies in Targeted Therapy for Colorectal Cancer. Clinical Cancer Drugs. 10.
- 10.2174/012212697X308365240529100442
- Prajapati, S. K., Jain, A., Shrivastava, C., & Jain, A. K. (2019). Hyaluronic acid conjugated multi-walled carbon nanotubes for colon cancer targeting. *International journal of biological macromolecules*, *123*, 691–703. https://doi.org/10.1016/j.ijbiomac.2018.11.116.
- Prewett, M., Rockwell, P., Rockwell, R. F., Giorgio, N. A., Mendelsohn, J., Scher, H. I., & Goldstein, N. I. (1996). The biologic effects of C225, a chimeric monoclonal antibody to the EGFR, on human prostate carcinoma. *Journal of immunotherapy with emphasis on tumor immunology : official journal of the Society for Biological Therapy*, *19*(6), 419–427. https://doi.org/10.1097/00002371-199611000-00006.
- Pathak, P. S., Chan, G., Deming, D. A., & Chee, C. E. (2024). State-of-the-Art Management of Colorectal Cancer: Treatment Advances and Innovation. *American Society of Clinical Oncology educational book. American Society of Clinical Oncology. Annual Meeting*, *44*(3), e438466. https://doi.org/10.1200/EDBK_438466
- Procyk, M., & Kutwin, M. (2025). Evaluation of the hemolytic properties of carbon nanomaterials. *Polskie Stowarzyszenie Biomateriałów*. https://doi.org/10.34821/eng.biomat.173.2025.13
- Pruthi, J., Mehra, N. K., & Jain, N. K. (2012). Macrophages targeting of amphotericin B through mannosylated multiwalled carbon nanotubes. *Journal of drug targeting*, *20*(7), 593–604. https://doi.org/10.3109/1061186X.2012.697168.
- Qiu, W., Zhang, C., Wang, S., Yu, X., Wang, Q., Zeng, D., Du, P., Ma, J., Zheng, Y., Pang, B., Yu, Y., Long, F., Pang, X., & Sun, Z. (2019). A Novel Anti-EGFR mAb Ame55 with Lower Toxicity and Better Efficacy than Cetuximab When Combined with

Irinotecan. *Journal of immunology research*, *2019*, 3017360. https://doi.org/10.1155/2019/3017360

- Ragab, G. H., & Bahgat, E. A. (2019). Development of bioanalytical HPLC method for simultaneous determination of the antialzhiemer, donepezil hydrochloride and the antidepressant, citalopram hydrobromide in raw materials, spiked human plasma and tablets dosage form. *Annales pharmaceutiques francaises*, *77*(2), 112–120. https://doi.org/10.1016/j.pharma.2018.09.004.
- Rahman, G., Najaf, Z., Mehmood, A., Bilal, S., Shah, A. u. H. A., Mian, S. A., & Ali, G. (2019). An Overview of the Recent Progress in the Synthesis and Applications of Carbon Nanotubes. *C*, *5*(1), 3. https://doi.org/10.3390/c5010003.
- Randive, D.S., Shejawal, K.P., Bhinge, S.D., Bhutkar, M.A., Jadhav, N.R.,. Patil, S.B. & Nadaf, S.N. (2023). Efficient in vitro oxaliplatin delivery with functionalized single-walled carbon nanotube for enhanced colon cancer treatment. *Future Journal of Pharmaceutical Sciences,* 9, 91.https://doi.org/10.1186/s43094-023-00543-8
- Rastin, F., Javid, H., Oryani, M. A., Rezagholinejad, N., Afshari, A. R., & Karimi-Shahri, M. (2024). Immunotherapy for colorectal cancer: Rational strategies and novel therapeutic progress. *International immunopharmacology*, *126*, 111055. https://doi.org/10.1016/j.intimp.2023.111055.
- Rathod, V., Tripathi, R., Joshi, P., Jha, P. K., Bahadur, P., & Tiwari, S. (2019). Paclitaxel Encapsulation into Dual-Functionalized Multi-Walled Carbon Nanotubes. *AAPS PharmSciTech*, *20*(2), 51. https://doi.org/10.1208/s12249-018-1218-6.
- Reddy B. S. (2007). Strategies for colon cancer prevention: combination of chemopreventive agents. *Sub-cellular biochemistry*, *42*, 213–225. https://doi.org/10.1007/1-4020-5688-5_10 .
- Reddy, V. K., Swamy, N., Rathod, R., & Sengupta, P. (2019). A Bioanalytical Method for Eliglustat Quantification in Rat Plasma. *Journal of chromatographic science*, *57*(7), 600–605. https://doi.org/10.1093/chromsci/bmz033.
- Ren, B., Kwah, M. X., Liu, C., Ma, Z., Shanmugam, M. K., Ding, L., Xiang, X., Ho, P. C., Wang, L., Ong, P. S., & Goh, B. C. (2021). Resveratrol for cancer therapy:

Challenges and future perspectives. *Cancer letters*, *515*, 63–72. https://doi.org/10.1016/j.canlet.2021.05.001.

- Rezaee, M., Behnam, B., Banach, M., & Sahebkar, A. (2018). The Yin and Yang of carbon nanomaterials in atherosclerosis. *Biotechnology advances*, *36*(8), 2232–2247. https://doi.org/10.1016/j.biotechadv.2018.10.010.
- Ried, T., Knutzen, R., Steinbeck, R., Blegen, H., Schröck, E., Heselmeyer, K., du Manoir, S., & Auer, G. (1996). Comparative genomic hybridization reveals a specific pattern of chromosomal gains and losses during the genesis of colorectal tumors. *Genes, chromosomes & cancer*, *15*(4), 234–245. https://doi.org/10.1002/(SICI)1098-2264(199604)15:4<234::AID-GCC5>3.0.CO;2-2.
- Roshandel, G., Ghasemi-Kebria, F., & Malekzadeh, R. (2024). Colorectal Cancer: Epidemiology, Risk Factors, and Prevention. *Cancers*, *16*(8), 1530. https://doi.org/10.3390/cancers16081530
- Robertson, D.J. (2012). ABC of colorectal cancer. Gastroenterology, 143, 868–869.
- Rosado-de-Castro, P. H., Morales, M. D. P., Pimentel-Coelho, P. M., Mendez-Otero, R., & Herranz, F. (2018). Development and Application of Nanoparticles in Biomedical Imaging. *Contrast media & molecular imaging*, *2018*, 1403826. https://doi.org/10.1155/2018/1403826.
- Rotelli, M. T., Bocale, D., De Fazio, M., Ancona, P., Scalera, I., Memeo, R., Travaglio, E., Zbar, A. P., & Altomare, D. F. (2015). IN-VITRO evidence for the protective properties of the main components of the Mediterranean diet against colorectal cancer: A systematic review. *Surgical oncology*, *24*(3), 145–152. https://doi.org/10.1016/j.suronc.2015.08.001 .
- Salim, E.I., Mosbah, A.M., Elhussiny, F.A., Hanafy, N.A.N., & Abdou, Y. (2023). Preparation and characterization of cetuximab-loaded egg serum albumin nanoparticles and their uses as a drug delivery system against Caco-2 colon cancer cells. *Cancer Nanotechnol* , 14(1).. http://dx.doi.org/10.1186/s12645-022-00153-8
- Saoudi González, N., Ros, J., Baraibar, I., Salvà, F., Rodríguez-Castells, M., Alcaraz, A., García, A., Tabernero, J., & Élez, E. (2024). Cetuximab as a Key Partner in

Personalized Targeted Therapy for Metastatic Colorectal Cancer. *Cancers*, *16*(2), 412. https://doi.org/10.3390/cancers16020412.

- Sharafi, A.M.A. Hosseini, M.S., Rezaeejam, H., Bagheri, F., Aghaei, A., Safari, H., Danafar, H. (2024). Synthesis of curcumin loaded single walled carbon nanotubes: Characterization and anticancer effects in vitro. Results in Chemistry, 7,101370
- Sathishbabu, P., Hani, U., Shakeela, C., Hemanth Vikram, P. R., Ghazwani, M., Osmani, R. A. M., Gurupadayya, B. M., & Gowda, D. V. (2022). A novel RP-HPLC method development and validation for simultaneous quantification of gefitinib and resveratrol in polymeric hybrid lipid nanoparticles and glioma cells. *Journal of chromatography. B, Analytical technologies in the biomedical and life sciences*, *1212*, 123483. https://doi.org/10.1016/j.jchromb.2022.123483.
- Sawicki, T., Ruszkowska, M., Danielewicz, A., Niedźwiedzka, E., Arłukowicz, T., & Przybyłowicz, K. E. (2021). A Review of Colorectal Cancer in Terms of Epidemiology, Risk Factors, Development, Symptoms and Diagnosis. *Cancers*, *13*(9), 2025. https://doi.org/10.3390/cancers13092025.
- Schipper, M. L., Nakayama-Ratchford, N., Davis, C. R., Kam, N. W., Chu, P., Liu, Z., Sun, X., Dai, H., & Gambhir, S. S. (2008). A pilot toxicology study of single-walled carbon nanotubes in a small sample of mice. *Nature nanotechnology*, *3*(4), 216–221. https://doi.org/10.1038/nnano.2008.68 .
- Scheibe, B., Borowiak-Palen, E., & Kalenczuk, R.J. (2010). Oxidation and reduction of multiwalled carbon nanotubes - preparation and characterization. Materials Characterization, 61, 185. https://doi.org/10.1016/j.matchar.2009.11.008.
- Schuell, B., Gruenberger, T., Kornek, G. V., Dworan, N., Depisch, D., Lang, F., Schneeweiss, B., & Scheithauer, W. (2005). Side effects during chemotherapy predict tumour response in advanced colorectal cancer. *British journal of cancer*, *93*(7), 744–748. https://doi.org/10.1038/sj.bjc.6602783.
- Shankar, S., Singh, G., & Srivastava, R. K. (2007). Chemoprevention by resveratrol: molecular mechanisms and therapeutic potential. Frontiers in bioscience : a journal and virtual library, 12, 4839–4854. https://doi.org/10.2741/2432.

- Sharma, A., Deeb, A. P., Iannuzzi, J. C., Rickles, A. S., Monson, J. R., & Fleming, F. J. (2013). Tobacco smoking and postoperative outcomes after colorectal surgery. *Annals of surgery*, *258*(2), 296–300. https://doi.org/10.1097/SLA.0b013e3182708cc5 .
- Shejawal, K.P., Randive, D.S., Bhinge, S.D. (2021). Functionalized carbon nanotube for colon-targeted delivery of isolated lycopene in colorectal cancer: *In vitro* cytotoxicity and *in vivo* roentgenographic study. *Journal of Materials Research* 36, 4894–4907, https://doi.org/10.1557/s43578-021-00431-y
- Shen, J., Huang, W., Wu, L., Hu, Y., & Ye, M. (2007). Study on amino-functionalized multiwalled carbon nanotubes. *Materials Science and Engineering: A*, *464*(1-2), 151-156. https://doi.org/10.1016/j.msea.2007.02.091.
- Shinji, S., Yamada, T., Matsuda, A., Sonoda, H., Ohta, R., Iwai, T., Takeda, K., Yonaga, K., Masuda, Y. and Yoshida, H., (2022). Recent advances in the treatment of colorectal cancer: a review. *Journal of Nippon Medical School*, *89*(3), 246-254.
- Siddique, S., and Chow, J. C. L. (2020). Application of Nanomaterials in Biomedical Imaging and Cancer Therapy. Nanomaterials 10 (9), 1700. doi:10.3390/ nano10091700
- Siddique, S., and Chow, J. C. L. (2020). Gold Nanoparticles for Drug Delivery and Cancer Applied Sciences,10, 3824. doi:10.3390/app10113824
- Siegel, R. L., Giaquinto, A. N., & Jemal, A. (2024). Cancer statistics, 2024. *CA: a cancer journal for clinicians*, *74*(1), 12–49. https://doi.org/10.3322/caac.21820 .
- Singh, R., Mehra, N. K., Jain, V., & Jain, N. K. (2013). Gemcitabine-loaded smart carbon nanotubes for effective targeting to cancer cells. *Journal of drug targeting*, *21*(6), 581–592. https://doi.org/10.3109/1061186X.2013.778264 .
- Singh, G., Pai, R. S., & Pandit, V. (2012). Development and validation of a HPLC method for the determination of trans-resveratrol in spiked human plasma. *Journal of advanced pharmaceutical technology & research*, *3*(2), 130–135. https://doi.org/10.4103/2231-4040.97296 .
- Singh, R. P., Sharma, G., Sonali, Singh, S., Patne, S. C. U., Pandey, B. L., Koch, B., & Muthu, M. S. (2016). Effects of transferrin conjugated multi-walled carbon nanotubes in lung cancer delivery. *Materials science & engineering. C, Materials for biological applications*, *67*, 313–325. https://doi.org/10.1016/j.msec.2016.05.013.

- Singh, S.K., Solanki, R., & Patel, S. (2024). Nano pharmaceutical delivery in combating colorectal cancer. Medicine in Drug Discovery, 21,100173. https://doi.org/10.1016/j.medidd.2023.100173
- Song, P., Song, J., and Zhang, Y. (2020). Stretchable conductor based on carbon nanotube/carbon black silicone rubber nanocomposites with highly mechanical, electrical properties and strain sensitivity. *Composites Part B: Engineering*, 191, 107979. doi:10. 1016/j.compositesb.2020.107979
- Song, B., Wang, W., Tang, X., Goh, R. M. W., Thuya, W. L., Ho, P. C. L., Chen, L., & Wang, L. (2023). Inhibitory Potential of Resveratrol in Cancer Metastasis: From Biology to Therapy. *Cancers*, *15*(10), 2758. https://doi.org/10.3390/cancers15102758.
- Sordelett, S. (1982). Gastrointestinal system. in Broadwell D, Jackson B (eds): Principles of Ostomy Care. St Loui\. Hlosby, 23-43
- Sahoo, N.G., Rana, S., Cho, J.W., Li, L., & Chan, S.H.(2010). Polymer nanocomposites based on functionalized carbon nanotubes. Progress in Polymer Science, 35, 837–867. https://doi.org/10.1016/j.progpolymsci.2010.03.002.
- Smith, R. A., Andrews, K. S., Brooks, D., Fedewa, S. A., Manassaram-Baptiste, D., Saslow, D., Brawley, O. W., & Wender, R. C. (2019). Cancer screening in the United States, 2019: A review of current American Cancer Society guidelines and current issues in cancer screening. *CA: a cancer journal for clinicians*, *67*(2), 100–121. https://doi.org/10.3322/caac.21392
- Sokic-Milutinovic A. (2019). Appropriate Management of Attenuated Familial Adenomatous Polyposis: Report of a Case and Review of the Literature. *Digestive diseases (Basel, Switzerland)*, *37*(5), 400–405. https://doi.org/10.1159/000497207.
- Srivastava, N., Mishra, V., Mishra, Y., Ranjan, A., Aljabali, A. A. A., El-Tanani, M., Alfagih, I. M., & Tambuwala, M. M. (2024). Development and evaluation of a protease inhibitor antiretroviral drug-loaded carbon nanotube delivery system for enhanced efficacy in HIV treatment. *International journal of pharmaceutics*, *650*, 123678. https://doi.org/10.1016/j.ijpharm.2023.123678 .
- Stobinski, L., Lesiak, B., Kövér, L., Tóth, J., Biniak, S., Trykowski, G., & Judek, J. (2010). Multiwall carbon nanotubes purification and oxidation by nitric acid studied

by the FTIR and electron spectroscopy methods. Journal of Alloys and Compounds, 501, 77 https://doi.org/10.1016/j.jallcom.2010.04.032.

- Stoffel, E. M., & Kastrinos, F. (2014). Familial colorectal cancer, beyond Lynch syndrome. *Clinical gastroenterology and hepatology : the official clinical practice journal of the American Gastroenterological Association*, *12*(7), 1059–1068. https://doi.org/10.1016/j.cgh.2013.08.015.
- Stoffel, E. M., & Murphy, C. C. (2020). Epidemiology and Mechanisms of the Increasing Incidence of Colon and Rectal Cancers in Young Adults. *Gastroenterology*, *158*(2), 341–353. https://doi.org/10.1053/j.gastro.2019.07.055 .
- Sung, H., Ferlay, J., Siegel, R. L., Laversanne, M., Soerjomataram, I., Jemal, A., & Bray, F. (2021). Global Cancer Statistics 2020: GLOBOCAN Estimates of Incidence and Mortality Worldwide for 36 Cancers in 185 Countries. *CA: a cancer journal for clinicians*, *71*(3), 209–249. https://doi.org/10.3322/caac.21660.
- Sudha, T., El-Far, A. H., Mousa, D. S., & Mousa, S. A. (2020). Resveratrol and Its Nanoformulation Attenuate Growth and the Angiogenesis of Xenograft and Orthotopic Colon Cancer Models. *Molecules (Basel, Switzerland)*, *25*(6), 1412. https://doi.org/10.3390/molecules25061412 .
- Susmitha, K., & Menaka, M. (2022). LC-ESI-MS/MS method for the fosamprenavir quantification bioanalytical method development and validation for the quantification fosamprenavir in human plasma by LC-ESI-MS/MS, IJPER, 56 (3), S599–S604, https://doi.org/10.5530/ijper.56.3s.168.
- Sun, R., Zhao, G., Ni, S., and Xia. Q. (2014). Lipid based nanocarriers with different lipid compositions for topical delivery of t-Res: comparative analysis of characteristics and performance. Journal of Drug Delivery Science and Technology, 24 (6) 591-600. https://doi.org/10.1016/S1773-2247(14)50124-4
- Symeonidis, D., Christodoulidis, G., Koukoulis, G., Spyridakis, M., & Tepetes, K. (2011). Colorectal cancer surgery in the elderly: limitations and drawbacks. *Techniques in coloproctology*, *15 Suppl 1*, S47–S50. https://doi.org/10.1007/s10151-011-0751-z.

- Takakura, A., Beppu, K., Nishihara, T., Fukui, A., Kozeki, T., Namazu, T., Miyauchi, Y., & Itami, K. (2019). Strength of carbon nanotubes depends on their chemical structures. *Nature communications*, *10*(1), 3040. https://doi.org/10.1038/s41467-019-10959-7.
- Talib, W. H., Alsayed, A. R., Farhan, F., & Al Kury, L. T. (2020). Resveratrol and Tumor Microenvironment: Mechanistic Basis and Therapeutic Targets. *Molecules (Basel, Switzerland)*, *25*(18), 4282. https://doi.org/10.3390/molecules25184282.
- Tang, Z. K., Zhang, L., Wang, N., Zhang, X. X., Wen, G. H., Li, G. D., Wang, J. N., Chan, C. T., & Sheng, P. (2001). Superconductivity in 4 angstrom single-walled carbon nanotubes. *Science (New York, N.Y.)*, *292*(5526), 2462–2465. https://doi.org/10.1126/science.1060470.
- Tariq, M., Thomas, S., Singh, A., and Talegaonkar, S. (2019). Developed and validated stability indicating HPLC method for the determination of epirubicin in bulk drug, marketed injection and polymeric nanoparticles. Brazilian Journal of Pharmaceutical Sciences, 54(04), e17515.
- Testa, U., Pelosi, E., & Castelli, G. (2018). Colorectal cancer: genetic abnormalities, tumor progression, tumor heterogeneity, clonal evolution and tumor-initiating cells. *Medical sciences (Basel, Switzerland)*, *6*(2), 31. https://doi.org/10.3390/medsci6020031 .
- Tagmatarchis, N., & Prato, M. (2004). Functionalization of carbon nanotubes via 1, 3dipolar cycloadditions, Journal of Material Chemistry, 14, 437–439.
- Thakur, C. K., Karthikeyan, C., Abou-Dahech, M. S., Altabakha, M. M. a. M., Shahwan, M. J. S. A., Ashby, C. R., Tiwari, A. K., Babu, R. J., & Moorthy, N. S. H. N. (2023). Microwave-Assisted functionalization of Multi-Walled carbon nanotubes for biosensor and drug delivery applications. *Pharmaceutics*, *15*(2), 335. https://doi.org/10.3390/pharmaceutics15020335.
- Thess, A., Lee, R., Nikolaev, P., Dai, H., Petit, P., Robert, J., Xu, C., Lee, Y. H., Kim, S. G., Rinzler, A. G., Colbert, D. T., Scuseria, G. E., Tomanek, D., Fischer, J. E., &

Smalley, R. E. (1996). Crystalline Ropes of Metallic Carbon Nanotubes. *Science (New York, N.Y.)*, *273*(5274), 483–487. https://doi.org/10.1126/science.273.5274.483.

- Thirumalaisamy, R., Nimithap, S., Selvankumar, T., Manikandan, R., & Vadivel, P. (2026). Emerging roles of carbon nanotubes in cancer therapy, diagnosis and targeted drug delivery: Current insights and toxicity considerations. *Chemical Physics Impact*, *12*, 101003. https://doi.org/10.1016/j.chphi.2026.101003
- Toi, M., Sperinde, J., Huang, W., Saji, S., Winslow, J., Jin, X., Tan, Y., Ohno, S., Nakamura, S., Iwata, H., Masuda, N., Aogi, K., Morita, S., Petropoulos, C., & Bates, M. (2010). Differential survival following trastuzumab treatment based on quantitative HER2 expression and HER2 homodimers in a clinic-based cohort of patients with metastatic breast cancer. *BMC cancer*, *10*, 56. https://doi.org/10.1186/1471-2407-10-56.
- Tour, J., Hudson, J., Dyke, C., Stephenson, J. (2007). Functionalization of Carbon Nanotubes in Acidic Media, William Marsh Rice University, U.S. Patent Application 10/ 593,918.
- Trung, L. Q., & An, D. T. T. (2018). Is Resveratrol a Cancer Immunomodulatory Molecule?. *Frontiers in pharmacology*, *9*, 1255. https://doi.org/10.3389/fphar.2018.01255 Tsai, H. C., Lin, J. Y., Maryani, F., Huang, C. C., & Imae, T. (2013). Drug-loading capacity and nuclear targeting of multiwalled carbon nanotubes grafted with anionic amphiphilic copolymers. *International journal of nanomedicine*, *8*, 4427–4440. https://doi.org/10.2147/IJN.S53636.
- Urbi Z., & Zainuddin Z. (2015). Standardization of surface sterilization protocol of field grown Stevia rebaudiana prior to in vitro clonal propagation. Jurnal Teknologi 77(24). 10.11113/jt.v77.6722.
- Umar, A., Boland, C. R., Terdiman, J. P., Syngal, S., de la Chapelle, A., Rüschoff, J., Fishel, R., Lindor, N. M., Burgart, L. J., Hamelin, R., Hamilton, S. R., Hiatt, R. A., Jass, J., Lindblom, A., Lynch, H. T., Peltomaki, P., Ramsey, S. D., Rodriguez-Bigas, M. A., Vasen, H. F., Hawk, E. T., & Srivastava, S. (2004). Revised Bethesda Guidelines

for hereditary nonpolyposis colorectal cancer (Lynch syndrome) and microsatellite instability. *Journal of the National Cancer Institute*, *96*(4), 261–268. https://doi.org/10.1093/jnci/djh034.

- Umeyama,T., Tezuka, N., Fujita, M., Matano, Y., Takeda, N., Murakoshi, K., Yoshida, K., Isoda, S., Imahori, H., (2007). Retention of intrinsic electronic properties of soluble single-walled carbon nanotubes after a significant degree of sidewall functionalization by the Bingel reaction. The Journal of Physical Chemistry C,111, 9734–9741. https://doi.org/10.1021/jp071604t.
- Upendra, L., Minakshi, P., Brar, B., Guray, M., and Ranjan, K. (2016). Nanodiagnostics: a New Frontier for Veterinary and Medical Sciences. Journal of Experimental Biology and Agricultural Sciences, 4 (3S), 307–318.
- Beljanski, V. (2007). Cetuximab. xPharm: The Comprehensive Pharmacology Reference,1-4
- Vander Wal, L.R., & Thomas M.T. (2001). Flame and furnace synthesis of SingleWalled and multi-walled carbon nanotubes and nanofibers, The Journal of Physical Chemistry B, 105, 10249–10256. https://doi.org/10.1021/jp012838u.
- Georgakilas, V., Kordatos, K., Prato, M., Guldi, D.M., Holzinger, M., Hirsch, A. (2002). Organic functionalization of carbon nanotubes, Journal of the American Chemical Society,124, 760–761. https://doi.org/10.1021/ja016954m.
- Varshney, K. (2014). Carbon nanotubes: a review on synthesis, properties and applications. International Journal of Engineering Research and General Science, 2, 2091–2730.
- Ven Fong, Z., Chang, D. C., Lillemoe, K. D., Nipp, R. D., Tanabe, K. K., & Qadan, M. (2019). Contemporary Opportunity for Prehabilitation as Part of an Enhanced Recovery after Surgery Pathway in Colorectal Surgery. *Clinics in colon and rectal surgery*, *32*(2), 95–101. https://doi.org/10.1055/s-0038-1676473.
- Vieira, A. R., Abar, L., Chan, D. S. M., Vingeliene, S., Polemiti, E., Stevens, C., Greenwood, D., & Norat, T. (2017). Foods and beverages and colorectal cancer risk: a systematic review and meta-analysis of cohort studies, an update of the evidence of the WCRF-AICR Continuous Update Project. *Annals of oncology : official journal of the*

European Society for Medical Oncology, *28*(8), 1788–1802. https://doi.org/10.1093/annonc/mdx171 .

- Verkuijl, S. J., Jonker, J. E., Trzpis, M., Burgerhof, J. G. M., Broens, P. M. A., & Furnée, E. J. B. (2021). Functional outcomes of surgery for colon cancer: A systematic review and meta-analysis. *European journal of surgical oncology : the journal of the European Society of Surgical Oncology and the British Association of Surgical Oncology*, *47*(5), 960–969. https://doi.org/10.1016/j.ejso.2020.11.136 .
- Vitaglione, P., Sforza, S., Galaverna, G., Ghidini, C., Caporaso, N., Vescovi, P. P., Fogliano, V., & Marchelli, R. (2005). Bioavailability of trans-resveratrol from red wine in humans. *Molecular nutrition & food research*, *49*(5), 495–504. https://doi.org/10.1002/mnfr.200500002.
- Vogelstein, B., Fearon, E. R., Hamilton, S. R., Kern, S. E., Preisinger, A. C., Leppert, M., Nakamura, Y., White, R., Smits, A. M., & Bos, J. L. (1988). Genetic alterations during colorectal-tumor development. *The New England journal of medicine*, *319*(9), 525–532. https://doi.org/10.1056/NEJM198809013190901 .
- Wang H., Li, J., Zhang, X., Ouyang, Z., Li, Q., Su, Z. and Wei, G. (2013). Synthesis, characterization and drug release application of carbon nanotube-polymer nanosphere composites. RSC Advances, 3, 9304–9310
- Wang, L. X., Heredia, A., Song, H., Zhang, Z., Yu, B., Davis, C., & Redfield, R. (2004). Resveratrol glucuronides as the metabolites of resveratrol in humans: characterization, synthesis, and anti-HIV activity. *Journal of pharmaceutical sciences*, *93*(10), 2448–2457. https://doi.org/10.1002/jps.20156 .
- Walle, T., Hsieh, F., DeLegge, M. H., Oatis, J. E., Jr, & Walle, U. K. (2004). High absorption but very low bioavailability of oral resveratrol in humans. *Drug metabolism and disposition: the biological fate of chemicals*, *32*(12), 1377–1382. https://doi.org/10.1124/dmd.104.000885.
- Walter, V., Jansen, L., Ulrich, A., Roth, W., Bläker, H., Chang-Claude, J., Hoffmeister, M., & Brenner, H. (2016). Alcohol consumption and survival of colorectal cancer patients: a population-based study from Germany. *The American journal of clinical nutrition*, *103*(6), 1497–1506. https://doi.org/10.3945/ajcn.115.127092.

- Walter, F. M., Emery, J. D., Mendonca, S., Hall, N., Morris, H. C., Mills, K., Dobson, C., Bankhead, C., Johnson, M., Abel, G. A., Rutter, M. D., Hamilton, W., & Rubin, G. P. (2016). Symptoms and patient factors associated with longer time to diagnosis for colorectal cancer: results from a prospective cohort study. British journal of cancer, 115(5), 533–541. https://doi.org/10.1038/bjc.2016.221.
- Walter, V., Jansen, L., Hoffmeister, M., Ulrich, A., Chang-Claude, J., & Brenner, H. (2015). Smoking and survival of colorectal cancer patients: population-based study from Germany. *International Journal of cancer*, *137*(6), 1433–1445. https://doi.org/10.1002/ijc.29511.
- Wang, N., Chen, L., Huang, W., Gao, Z., & Jin, M. (2024). Current Advances of Nanomaterial-Based Oral Drug Delivery for Colorectal Cancer Treatment. *Nanomaterials (Basel, Switzerland)*, *14*(7), 557. https://doi.org/10.3390/nano14070557.
- Wang, J., Li, J., Cao, N., Li, Z., Han, J., & Li, L. (2018). Resveratrol, an activator of SIRT1, induces protective autophagy in non-small-cell lung cancer via inhibiting Akt/mTOR and activating p38-MAPK. *OncoTargets and therapy*, *11*, 7777–7786. https://doi.org/10.2147/OTT.S159095.
- Wang, Y., Wang, W., Wu, X., Li, C., Huang, Y., Zhou, H., & Cui, Y. (2020). Resveratrol sensitizes colorectal cancer cells to cetuximab by connexin 43 Upregulation-Induced AKT inhibition. *Frontiers in Oncology*, *10*, 383. https://doi.org/10.3389/fonc.2020.00383
- Weiser, M. R., Gönen, M., Chou, J. F., Kattan, M. W., & Schrag, D. (2011). Predicting survival after curative colectomy for cancer: individualizing colon cancer staging. *Journal of clinical oncology : official journal of the American Society of Clinical Oncology*, *29*(36), 4796–4802. https://doi.org/10.1200/JCO.2011.36.5080.
- West, N. R., McCuaig, S., Franchini, F., & Powrie, F. (2015). Emerging cytokine networks in colorectal cancer. *Nature reviews. Immunology*, *15*(10), 615–629. https://doi.org/10.1038/nri3896 .
- Wu, P., Chen, X., Hu, N., Tam, U. C., Blixt, O., Zettl, A., & Bertozzi, C. R. (2008). Biocompatible carbon nanotubes generated by functionalization with

glycodendrimers. *Angewandte Chemie (International ed. in English)*, *47*(27), 5022–5025. https://doi.org/10.1002/anie.200705363.

- Wu, D., Wu, P., Wu, X., Ye, J., Wang, Z., Zhao, S., Ni, C., Hu, G., Xu, J., Han, Y., Zhang, T., Qiu, F., Yan, J., & Huang, J. (2015). *Ex vivo* expanded human circulating Vδ1 γδT cells exhibit favorable therapeutic potential for colon cancer. *Oncoimmunology*, *4*(3), e992749. https://doi.org/10.4161/2162402X.2014.992749 .
- Xia, L., Tan, S., Zhou, Y., Lin, J., Wang, H., Oyang, L., Tian, Y., Liu, L., Su, M., Wang, H., Cao, D., & Liao, Q. (2018). Role of the NFκB-signaling pathway in cancer. *OncoTargets and therapy*, *11*, 2063–2073. https://doi.org/10.2147/OTT.S161109.
- Xiao, J. B., Leng, A. M., Zhang, Y. Q., Wen, Z., He, J., & Ye, G. N. (2019). CUEDC2: multifunctional roles in carcinogenesis. *Frontiers in bioscience (Landmark edition)*, *24*(5), Xie, Y. H., Chen, Y. X., & Fang, J. Y. (2020). Comprehensive review of targeted therapy for colorectal cancer. *Signal transduction and targeted therapy*, *5*(1), 22. https://doi.org/10.1038/s41392-020-0116-z.
- Xie, J., Li, D., Niu, S., Sheng, Y., Shen, R., He, Y., Xu, C., Zhang, Y., Wang, T., & Xue, Y. (2024). Nano-Titanium Oxide-Coated Carbon Nanotubes for Photothermal Therapy in the Treatment of Colorectal Cancer. *Advanced healthcare materials*, *13*(23), e2401009. https://doi.org/10.1002/adhm.202401009.
- Yaghoubi, A., & Ramazani, A. (2020). Anticancer DOX delivery system based on CNTs: Functionalization, targeting and novel technologies. Journal of controlled release: official journal of the Controlled Release Society, 327, 198–224. https://doi.org/10.1016/j.jconrel.2020.08.001.
- Yang, C., Fang, H., Gong, X., Wang, J., & Zou, T. (2026). Nanoparticles for colorectal cancer therapy: A review. *Biomaterials Advances*, *186*, 214926. https://doi.org/10.1016/j.bioadv.2026.214926
- Yan, M., Wang, Y., Wang, C., Feng, S., & Zhang, T. (2024). Whey protein isolate-resveratrol complex as a radical scavenging foaming ingredient with increased

ultraviolet stability. *Food chemistry*, *434*, 137519. https://doi.org/10.1016/j.foodchem.2023.137519

- Yang, W., Thordarson, P., Gooding, J.J., Ringer, S.P., & Braet, F. (2007).Carbon nanotubes for biological and biomedical applications. *Nanotechnology*,18, 41.
- Yadav, S., van Vlerken, L. E., Little, S. R., & Amiji, M. M. (2009). Evaluations of combination MDR-1 gene silencing and paclitaxel administration in biodegradable polymeric nanoparticle formulations to overcome multidrug resistance in cancer cells. *Cancer chemotherapy and pharmacology*, *63*(4), 711–722. https://doi.org/10.1007/s00280-008-0790-y.
- Yallapu, M. M., Nagesh, P. K., Jaggi, M., & Chauhan, S. C. (2015). Therapeutic Applications of Curcumin Nanoformulations. *The AAPS journal*, *17*(6), 1341–1356. https://doi.org/10.1208/s12248-015-9811-z.
- Yinghuai, Z., Peng, A. T., Carpenter, K., Maguire, J. A., Hosmane, N. S., & Takagaki, M. (2005). Substituted carborane-appended water-soluble single-wall carbon nanotubes: new approach to boron neutron capture therapy drug delivery. *Journal of the American Chemical Society*, *127*(27), 9875–9880. https://doi.org/10.1021/ja0517116 .
- Yu, C., Zhang, C., Guan, X., & Yuan, D. (2023). The solid dispersion of resveratrol with enhanced dissolution and good system physical stability. Journal of Drug Delivery Science and Technology, 184,104507. http://dx.doi.org/10.1016/j.jddst.2023.104507
- Yu, B., Huang, A., Chen, D., Srinivas, K., Zhang, X., Wang, X., Wang, B., Ma, F., Liu, C., Zhang, W., He, J., Wang, Z., & Chen, Y. (2021). In Situ Construction of Mo_2C Quantum Dots-Decorated CNT Networks as a Multifunctional Electrocatalyst for Advanced Lithium-Sulfur Batteries. *Small (Weinheim an der Bergstrasse, Germany)*, *17*(23), e2100460. https://doi.org/10.1002/smll.202100460.
- Zahavi D., & Weiner, L. (2020). Monoclonal Antibodies in Cancer Therapy. Antibodies, 9,34.
- Zhang, X., Ma, J., Tennent, H., & Hoch, R (2011). Hyperion Catalysis International Inc, assignee. Method for preparing single walled carbon nanotubes.

- Zhang, X., Zhou, W., Wu, C., Jiang, J., Guo, Q., Feng, L., Cheng, X., & Zhang, X. (2024). Cetuximab inhibits colorectal cancer development through inactivating the Wnt/β-catenin pathway and modulating PLCB3 expression. *Scientific reports*, *14*(1), 10642. https://doi.org/10.1038/s41598-024-59676-2 .
- Zhang, Y., Li, Y., & Zhang, P. (2014). De novo growth of poly(amidoamine) dendrimers on the surface of multi-walled carbon nanotubes. Journal of Material Science, 49,3469–3477
- Zhang, H., Li, H. X., & Cheng, H. M. (2006). Water-soluble multiwalled carbon nanotubes functionalized with sulfonated polyaniline. *The journal of physical chemistry. B*, *110*(18), 9095–9099. https://doi.org/10.1021/jp060193y .
- Zhang, F., Feng, Y., Qin, M., Gao, L., Li, Z., Zhao, F., et al. (2019a). Stress controllability in thermal and electrical conductivity of 3D elastic graphenecrosslinked carbon nanotube sponge/polyimide nanocomposite. Advance Functional Material. 29, 1901383. doi:10.1002/adfm.201901383
- Zenda, S., Ota, Y., Kiyota, N., Okano, S., Fujii, M., Kitamura, M., Takahashi, S., Ueda, T., Monden, N., Yamanaka, T., & Tahara, M. (2019). A Multicenter Phase II Trial of Docetaxel, Cisplatin, and Cetuximab (TPEx) Followed by Cetuximab and Concurrent Radiotherapy for Patients With Local Advanced Squamous Cell Carcinoma of the Head and Neck (CSPOR HN01: ECRIPS Study). Frontiers in oncology, 9, 6. https://doi.org/10.3389/fonc.2019.00006
- Zeng, L., Alemany, L.B., Edwards, C.L., Barron, A.R. (2008). Demonstration of covalent sidewall functionalization of single wall carbon nanotubes by NMR spectroscopy: side chain length dependence on the observation of the sidewall sp3 carbons. Nano Resreach, 1,72–88.
- Zhou, J., Ji, Q., & Li, Q. (2021). Resistance to anti-EGFR therapies in metastatic colorectal cancer: underlying mechanisms and reversal strategies. *Journal of experimental & clinical cancer research : CR*, *40*(1), 328. https://doi.org/10.1186/s13046-021-02130-2

- Zhou, H., Wang, Y., Li, S., & Lu, M. (2021). Improving chemical stability of resveratrol in hot melt extrusion based on formation of eutectic with nicotinamide. *International journal of pharmaceutics*, *607*, 121042. https://doi.org/10.1016/j.ijpharm.2021.121042
- Zhou, J., & Jokerst, J. V. (2020). Photoacoustic imaging with fiber optic technology: A review. *Photoacoustics*, *20*, 100211. https://doi.org/10.1016/j.pacs.2020.100211 .
- Zhou, J., Ji, Q., & Li, Q. (2021). Resistance to anti-EGFR therapies in metastatic colorectal cancer: underlying mechanisms and reversal strategies. *Journal of experimental & clinical cancer research: CR*, *40*(1), 328. https://doi.org/10.1186/s13046-021-02130-2 .
- Zu, Y., Zhang, Y., Wang, W., Zhao, X., Han, X., Wang, K., & Ge, Y. (2016). Preparation and in vitro/in vivo evaluation of resveratrol-loaded carboxymethyl chitosan nanoparticles. *Drug delivery*, 23(3), 981–991. https://doi.org/10.3109/10717544.2014.924167

长沙市惠瑞生物科技有限公司
CHANGSHA HUIR BIOLOGICAL-TECH CO.,LTD

Certificate of Analysis

Product Name:	**Grape Skin Extract**	Latin Name:	***Vitis vinifera L.***
Part Used:	**Skin**	Extract Solvent:	**Ethanol &Water**
Country of Origin:	**China**	Extract Ratio:	/
Batch Number:	**19081012**	Manufacture Date:	**Aug. 10th 2019**
Representative Qty.:	**1000kg**	Expiry Date:	**Aug. 09th 2022**

Report Date: Aug. 18th 2019

ITEM		SPECIFICATION	RESULT	STANDARD REFERENCED
Physical	Appearance	Off white powder	Complies	Visual
	Odor	Characteristic	Complies	Sensory
	Taste	Characteristic	Complies	Sensory
	Loss on drying	≤2.0%	0.41%	2g/105℃/5hrs
	Residue on Ignition	≤1.0%	0.08%	2g/800℃/5hrs
	Particle size	98% pass 80 mesh	Complies	Sieve
Chemical	Heavy metals	≤20ppm	Complies	Colorimetric Method
	Arsenic(As)	≤2ppm	Complies	Atomic Absorption
	Lead(Pb)	≤2ppm	Complies	Atomic Absorption
	Cadmium(Cd)	≤1ppm	Complies	Atomic Absorption
	Mercury(Hg)	≤0.1ppm	Complies	Atomic Absorption
	Solvent residual	≤5000ppm	Complies	Gas Chromatography
Assay	Resveratrol	≥98.0%	98.31%	HPLC
Microbial	Total microbacterial count	≤1000CFU/g	Complies	CP2015
	Yeast & Mould	≤100CFU/g	Complies	CP2015
	Escherichia Coli presence	Negative	Negative	CP2015
	Salmonella	Negative	Negative	CP2015
Else	Packing	Pack in paper-drums and two food grade poly bags inside. Net weight: 25kg/drum		
	Storage condition	Store in a well closed place with constant low temperature and no direct sun light		
	Shelf life	Three years when properly stored.		

Tel: +86-731-84680108 Fax: +86-731-84152788 Email:info@phyhuir.com HTTP://WWW.PHYHUIR.COM
Add: Jindan Bldg. B, 5th Floor, Longping High-Tech Park, Furong, Changsha, China

THINK INDIA Journal

ISSN:0971-1260
Vol-22-Issue-16-August-2019

Carbon nanotubes in delivery of curcumin: An overview

Neha Sharma[1], Vijay Mishra[1]*, Manvendra Singh[1], Pallavi Nayak[1]

[1]School of Pharmaceutical Sciences, Lovely Professional University, Phagwara (Punjab), India- 144411

***Corresponding author**

Dr. Vijay Mishra

School of Pharmaceutical Sciences,

Lovely Professional University, Phagwara, (Punjab), India

Email: vijaymishra2@gmail.com

Abstract

From the hour of Ayurveda Curcumin (diferuloylmethane) got from the Curcuma longa plant, generally known as turmeric is outstanding for its nontoxic and restorative properties including against oxidant, pain-relieving, calming germ-free action and hostile to malignant growth. Clinically confine the utilization because of its poor water dissolvability, fast digestion and quick end which bring about poor oral bioavailability. To upgrade the bioavailability curcumin will be conveyed via carbon nanotubes. Carbon nanotubes (CNTs) have risen as enamoring assets, promising to focus on tranquilizing conveyance inferable from their one of kind physicochemical properties like cell layer entrance, high surface territory and medication payload, biocompatibility, simple surface adjustment. It was first proved a splendid vehicle for the transmission of sedates into cells without digestion by the body. In this way utilization of CNTs gives diverse methodology towards expanded bioavailability of curcumin.

Keywords: Carbon nanotubes, Curcumin, Targeted drug delivery, Bioavailability.

Copyright © 2019Authors

CHAPTER 1

An Overview of Biomaterial Toxicity and Excretion

Srijana Sharma[1], Yachana Mishra[2], Shubham Bisht[1], Neha Sharma[1,3] and Vijay Mishra[1,*]

[1] *School of Pharmaceutical Sciences, Lovely Professional University, Phagwara (Punjab), India*

[2] *Department of Zoology, Shri Shakti Degree College, Sankhahari, Ghatampur, Kanpur Nagar (Uttar Pradesh), India*

[3] *Rayat Institute of Pharmacy, Railmajra, Shaheed Bhagat Singh Nagar, (Punjab), India*

Abstract: Biomaterial is a growing family of materials with specific physicochemical properties. Significant studies have been made to characterize the potential *in vivo* and *in vitro* toxicity of biomaterials. The cytotoxicity may be attributed to variations in the physicochemical properties, target cell types, particle dispersion methods, *etc*. The reported cytotoxicity effects mainly include the impact on the biological system and organ-specific toxicity such as CNS toxicity, lung toxicity, cardiac toxicity, dermal toxicity, gastrointestinal toxicity, *etc*. Despite cellular toxicity, the immunological effects of biomaterials, such as the activation of pulmonary macrophages and associated inflammation, have been extensively studied. In this chapter, the latest research results on the toxicological profiles of nanomaterials, highlighting both the cellular toxicities and the immunological effects, have been incorporated. This analysis also offers details on the overall status, patterns, and research needs for dealing with the toxicological behavior of biomaterials.

Keywords: Biomaterials, Cytotoxicity, Nanocarriers, Toxicity.

INTRODUCTION

With the development of human civilization, biomaterials evolved by incorporating various materials on various lengths from nano- to micro- to macro level with a simple focus on extending human life and improving quality of life. More than 1000 years ago, silver, in various ways, was used as an antimicrobial agent to prevent infection. Different surgical procedures can be found at the very beginning of civilization. However, perhaps the most significant development took place in biomaterials in 1901-2000. Over the past 60 years, the quality of life

* **Corresponding author Vijay Mishra:** School of Pharmaceutical Sciences, Lovely Professional University, Phagwara (Punjab), 144411, India E-mail: vijaymishra2@gmail.com

Alaa A. Aljabali and Kaushik Pal (Eds.)
All rights reserved-© 2022 Bentham Science Publishers

International Journal of Applied Pharmaceutics

ISSN- 0975-7058 Vol 17, Issue 6, 2025

Original Article

DEVELOPMENT AND VALIDATION OF HPLC METHOD FOR THE DETERMINATION OF RESVERATROL IN BULK DOSAGE FORM, COMMERCIAL TABLET, AND MULTIWALLED CARBON NANOTUBES-BASED FORMULATION

NEHA SHARMA[1,2], YACHANA MISHRA[3], NEELAM SHARMA[2], VIJAY MISHRA[1]

[1]School of Pharmaceutical Sciences, Lovely Professional University, Phagwara (Punjab)-144411, India. [2]ISBA[S]M College of Pharmacy Bela, Ropar-140111, India. [3]School of Bioengineering and Biosciences, Lovely Professional University, Phagwara (Punjab)-144411, India *Corresponding author: Vijay Mishra; *Email: vijaymishra2@gmail.com

Received: 09 May 2025, Revised and Accepted: 28 Aug 2025

ABSTRACT

Objective: Resveratrol (RES), a polyphenol, is a promising option to treat multiple diseases due to its anticancer, cardioprotective, anti-inflammatory, and antioxidant activities. The present study was designed to develop and validate a simple, precise, rapid and reproducible analytical method for the detection of RES in different formulations.

Methods: A novel analytical technique was developed and validated for the detection of RES via ultrafast liquid chromatography utilizing C$_{18}$ column. Methanol along with high-performance liquid chromatography (HPLC) grade water (40:60) was used as a mobile phase with a rate of flow of 0.8 ml/min. This technique has been validated following the International Conference for Harmonization (ICH) Q2 (R1) guidelines. The method's accuracy was determined through the percent recovery within the limit of 95 to 105%.

Results: The method demonstrated linearity within the 2- 30 µg/ml range, exhibiting a regression coefficient of 0.997. The precision of the method was indicated by the percentage RSD, which was recorded to be less than 2%. Limit of detection (LOD), and limit of quantification (LOQ) were found to be 1.6 µg/ml and 4.8 µg/ml, respectively. The proposed approach has been proved to be robust because the response did not significantly change due to a change in the rate of flow, along with the composition of the mobile phase.

Conclusion: The results of the study demonstrated that the developed method has passed all the validation test parameters and can be applied for the estimation of RES in bulk dosage form, commercial tablet, and developed multiwalled carbon nanotube (MWCNTs)-based formulations.

Keywords: Resveratrol, Multiwalled carbon nanotubes, HPLC, Validation

© 2025 The Authors. Published by Innovare Academic Sciences Pvt Ltd. This is an open access article under the CC BY license (https://creativecommons.org/licenses/by/4.0/)
DOI: https://dx.doi.org/10.22159/ijap.2025v17i6.99503 Journal homepage: https://innovareacademics.in/journals/index.php/ijap

INTRODUCTION

Resveratrol (RES), specifically trans-3,4′,5-trihydroxystilbene, is an inherent poly-phenolic compound that can be found in various food sources, predominantly in red grapes (fig. 1). Resveratrol, a highly effective antioxidant, is primarily found in the skin of the grape [1, 2]. A minor quantity of trans-RES can also be found within the seed and core of grapes. The trans-RES is derived from Polygonum cuspidatum, a botanical species indigenous to China and Japan [3-5]. In recent years, there has been a notable increase in the interest and focus of health professionals, diet nutritionists, and medical chemists on trans-RES primarily due to the numerous advantageous outcomes associated with it, such as its ability to inhibit the formation of new blood vessels, modulate the immune system, combat microbial infections, affect the nervous system, prevent the development of cancer, regulate blood sugar levels, and mitigate the risk of cardiovascular diseases, reduce inflammation, works against free radicals [6-13].

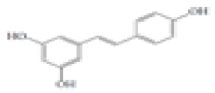


Fig. 1: Chemical structure of trans-RES [3]

RES is present in both cis-and trans-isomeric forms, but the trans-isomer is a predominant and physiologically active variant. The compound undergoes rapid metabolism by phase II enzymes in the gastrointestinal tract and hepatic tissues [14, 15]. The poor solubility of the RES (less than 0.05 mg/ml) in aqueous medium can be attributed to its enzymatic structure, potentially impacting its consumption [16, 17]. The excretion of total urinary metabolites following the administration of ^{14}C labeled RES demonstrated that RES was given either orally or intravenously, resulting in an increased rate of absorption of approximately 70%. However, it exhibited significant metabolic activity, leading to the accumulation of sulphate glucuronides [18]. A scientific framework called the biopharmaceutics classification system (BCS) is used for categorizing the drugs according to their permeability and solubility [19, 20]. Regardless of its limited aqueous solubility, RES demonstrates significant permeability across membranes and can be classified under BCS Class-II drugs [16, 17]. The plasma half-life of RES is relatively brief, estimated to be approximately 8-14 min. The quick and extensive presystemic metabolism of this compound results in a significantly low oral bioavailability [3, 18]. The utilization of multi-walled carbon nanotubes (MWCNTs) in the context of targeted drug delivery has emerged as a highly promising approach [21-23].

Carbon nanotubes (CNTs) have garnered considerable interest owing to their distinctive mechanical, electrical, and thermal characteristics. The remarkable characteristics of CNTs render them effective in several applications, including electronics, optics, and medicines. CNTs demonstrate toxicity via various pathways, impacting allergies, fibrosis, organ dysfunction, neurological damage, liver toxicity, renal toxicity, and lungs toxicity. Nonetheless, apprehensions regarding the possible toxicity of carbon nanotubes have. Furthermore, concerns have been elevated, necessitating thorough studies to elucidate their impacts on people's health along with the ecosystem. Numerous research has examined the toxicity of CNTs, with results varying based on aspects like as surface chemistry, shape, size, and exposure route [24-27]. Mohammadi and co-worker studied the toxicological parameter of CNTs and suggested that due to lipophilic nature, the pristine CNTs are more susceptible for agglomeration and issues in dispersibility when exposed to biological systems, so they are more toxic. Functionalized



ICRAHS

LOVELY PROFESSIONAL UNIVERSITY
Transforming Education Transforming India

Certificate No. 265881

Certificate of Participation

This is to certify that **Prof./Dr./Mr./Ms. Neha Sharma** has successfully participated as "**Delegate and Oral Presenter**" in the International Conference on **"Recent Advances in Health Sciences" (ICRAHS-2023)** on the Theme of "Interdisciplinary Research: A key to transform Health care." from 14th April, 2023 to 15th April, 2023 organized by School of Pharmaceutical Sciences in association with Komar University of Sciences and Technology at Lovely Professional University, Punjab.

Date of Issue : 01-05-2023
Place : Phagwara (Punjab), India

Prepared by
(Administrative Officer-Records)

Dr. M Vijay Kumar
General Chair

Prof. Dr. Kawis Aziz Faraj
Conference Co-Chair

Dr. Monica Gulati
Conference Chair

CHANDIGARH GROUP OF COLLEGES
Building Careers. Transforming Lives.

Certificate of Participation

This is to certify that Prof./Dr./Mr./Ms. Neha Sharma has participated in the Oral Presentation / ~~Poster Presentation~~ /Delegate / Member of LOC / Student Coordinator at the International Conference on "INDUSTRY DRIVEN PHARMACEUTICAL EDUCATION AND RESEARCH: CURRENT TRENDS AND FUTURE PROSPECTS" IDPER-2023 on 27th & 28th April, 2023.

Prof. (Dr.) Supriya Agnihotri
Organizing Secretary
HOD CCP

Prof. (Dr.) Saurabh Sharma
Convener
Director-Principal CCP

INTELLECTUAL PROPERTY INDIA
PATENTS | DESIGNS | TRADE MARKS
GEOGRAPHICAL INDICATIONS

सत्यमेव जयते

प्रमाणपत्र सं. / Certificate No.:
LD-20260183106

प्रतिलिप्याधिकार कार्यालय, भारत सरकार | Copyright Office, Government Of India

प्रतिलिप्यधिकार प्रमाणपत्र | Copyright Certificate

प्रतिलिप्यधिकार नियम का नियम 70 | Rule 70 of The Copyright Rules

प्रतिलिप्यधिकार रजिस्टर से उद्धरण | Extracts from the Register of Copyrights

आवेदन सं. / Application No.: LD-52820/2025-CO **दाखिल करने की तिथि/ Date of Filing:** 18/12/2025

एतद्वारा यह प्रमाणित किया जाता है कि प्रतिलिप्यधिकार अधिनियम, 1957 के प्रावधानों के अनुसार, उपर्युक्त आवेदन में प्रकट किए गए "Development and Evaluation of Cetuximab Anchored Resveratrol Loaded Multiwalled Carbon Nanotubes for the Treatment of Colorectal Cancer" नामक कार्य के लिए प्रतिलिप्यधिकार प्रदान किया गया है।

This is to certify that a copyright has been registered for the work titled "Development and Evaluation of Cetuximab Anchored Resveratrol Loaded Multiwalled Carbon Nanotubes for the Treatment of Colorectal Cancer" as disclosed in the below mentioned application in accordance with the provisions of the Copyright Act,1957.

रचयिता / Authors:

सं. / SNO.	नाम / Name	पता / Address
1	NEHA SHARMA	LOVELY PROFESSIONAL UNIVERSITY, JALANDHAR, DELHI-GT ROAD, PHAGWARA PUNJAB-144411
2	DR. VIJAY MISHRA	LOVELY PROFESSIONAL UNIVERSITY, JALANDHAR, DELHI-GT ROAD, PHAGWARA PUNJAB-144411
3	DR. YACHANA MISHRA	LOVELY PROFESSIONAL UNIVERSITY, JALANDHAR, DELHI-GT ROAD, PHAGWARA PUNJAB-144411

स्वामी / Owners:

सं. / SNO.	नाम / Name	पता / Address
1	LOVELY PROFESSIONAL UNIVERSITY	LOVELY PROFESSIONAL UNIVERSITY, JALANDHAR, DELHI-GT ROAD, PHAGWARA PUNJAB-144411

प्रकाशक विवरण / Publisher Details:	N.A.
कार्य की भाषा / Language of the Work:	English
कार्य का विवरण / Description of the Work:	N.A.
(शर्तें / टिप्पणियाँ, यदि कोई हो) / (Conditions/ Remarks, if any):	N.A.

आर. ओ. सी. जारी होने की तिथि / Date of ROC: 03/03/2026

उमा शंकर पांडेय

Registrar of Copyrights